STUDIES ON THE ANTI-CANCER PROPERTIES OF ARTESUNATE: ANTI-PROLIFERATIVE AND CYTOTOXIC EFFECTS ON BREAST AND OVARIAN CANCER CELLS

by

Anna L. Greenshields

Submitted in partial fulfilment of the requirements
for the degree of Doctor of Philosophy

at

Dalhousie University
Halifax, Nova Scotia
January 2014

Table of Contents

List of Tables ..... **viii**

List of Figures ..... **ix**

Abstract ..... **xi**

List of Abbreviations Used ..... **xii**

Acknowledgements ..... **xvii**

CHAPTER 1: INTRODUCTION **1**

1.1 Cancer Overview **1**

1.2 Ovarian Cancer **1**

1.2.1 Epithelial Ovarian Carcinoma 2

1.2.1.1 Serous EOC 2

1.2.1.2 Mucinous EOC 3

1.2.1.3 Endometrioid EOC 3

1.2.1.4 Clear Cell EOC 3

1.2.2 EOC Staging and Treatment 4

1.2.3 Limitations of Current Cancer Therapies 7

1.3 Breast Cancer **7**

1.3.1 Breast Cancer Subtypes 7

1.3.1.1 Tumour Stage and Grade 7

1.3.1.2 Breast Cancer Histology 8

1.3.1.3 Molecular Characterisation 8

1.3.2 Breast Cancer Treatment 9

1.3.3 Limitations of Current Therapeutic Agents 10

1.4 Therapeutic Targets **11**

1.4.1 Cell Proliferation 11

1.4.1.1 The Cell Cycle and Cancer 13

1.4.2 Cell Death Pathways 15

1.4.2.1 Apoptosis 15

1.4.2.1.2 The Intrinsic / Mitochondrial Pathway 16

1.4.2.1.3 The Extrinsic / Death Receptor Pathway 17

1.4.2.2 Necrosis 17
1.4.2.2.1 Necroptosis 18
1.4.3 Oxidative Stress 18
1.4.3.1 ROS as Second Messengers 19
1.4.3.2 Cytotoxic Effects of ROS 21
1.5 Artesunate (ART) 22
1.5.1 Basic Pharmacokinetic Properties of ART 22
1.5.2 Anti-malarial Properties of ART 25
1.5.3 Anti-cancer Properties of ART 25
1.5.3.1 Anti-cancer Activity of ART *in vivo* 27
1.5.3.2 Anti-ovarian Cancer Activity of ART 28
1.5.3.3 Anti-breast Cancer Activity of ART 30
1.5.4 Safety of ART 33
1.6 Research Rationale and Objectives 34
CHAPTER 2.0: MATERIALS AND METHODS 35
2.1 Reagents. 35
2.2 Antibodies. 36
2.3 Cell Culture. 36
2.3.1 Culture of Cancer Cell Lines 36
2.3.2 Ovarian Cancer Spheroid Culture 37
2.3.3 Breast Cancer Spheroid Culture. 37
2.4 Breast and Ovarian Cell Seeding and Harvesting. 37
2.4.1 Human Ovarian Cancer Cell Line Seeding. 38
2.4.2 Murine Ovarian Cancer Cell Line Seeding 38
2.4.3 Breast Cancer Cell Line Seeding 38
2.4.4 Cell Harvesting. 38
2.5 Flow cytometry. 39
2.6 MTT Assay. 39
2.6.1 Pre-treatment with holo-transferrin. 40
2.6.2 Combined Modality Treatments. 40
2.6.3 Combined Treatment of ART and Ionizing Radiation. 40
2.7 Acid Phosphatase Assay. 40
2.8 Acid Phosphatase Assay of Spheroids. 41

2.9 Annexin-V-FLUOS/PI Flow Cytometric Analysis. 41
2.9.1 Importance of Iron on ART-induced Cell Death. 42
2.9.1.1 Effect of Increased Iron on ART-induced Cancer Cell Death. 42
2.9.1.2 Effect of Decreased Iron Availability on ART-induced Cancer Cell Death. 42
2.9.2 Importance of Caspase Activity on ART-induced Cytotoxicity. 42
2.9.3 Importance of The Necroptotic Pathway in ART-induced Cytotoxicity. 42
2.9.4 Importance of ROS in ART-induced Cancer Cell Death. 42
2.9.5 Oxygen Requirement for ART-induced Cancer Cell Death. 43
2.10 Detection of ART-induced Caspase Activation. 43
2.11 Determination of Changes in Mitochondrial Membrane Stability. 43
2.11.1 Importance of ROS in ART-induced Changes in Mitochondrial Membrane Stability. 43
2.12 Detection of Intracellular ROS production. 44
2.12.1 Effect of Increased Iron on ROS Production. 44
2.13 Cell Proliferation Assay. 45
2.13.1 Importance of ROS in the Anti-proliferative Activity of ART. 45
2.13.2 Importance of Iron in the Anti-proliferative Activity of ART. 45
2.14 ART Wash-out MTT Assay. 45
2.15 Cell Cycle Analysis. 46
2.16 Analysis of CD71 Surface Expression. 46
2.17 Colony Forming Assay. 47
2.17.1 Combined Modality Colony Forming Assay 47
2.18 SDS-PAGE and Western Blotting. 47
2.19 Statistical Analysis. 48
CHAPTER 3: RESULTS 49
3.1 Results: Investigation of the Anti-ovarian Cancer Activity of ART. 49
3.1.1 ART Inhibits the Growth of a Panel of Ovarian Cancer Cell Lines in a Dose- and Time-dependent Manner. 49
3.1.2 ART is Cytotoxic to Ovarian Cancer Cell Spheroids. 52
3.1.3 Ovarian Cancer Cells Treated with Low Doses of ART Regrow Following ART Removal. 52
3.1.4 ART Causes Dose-dependent Cell Death in Ovarian Cancer Cell Lines. 55
3.1.5 The ID8 Murine Ovarian Cancer Cell Line is Killed by ART. 55

3.1.6 RIPK1 Inhibition Decreases ART-induced Cell Death in HEY1 and HEY2 Ovarian Cancer Cells. 58
3.1.7 ART Induces ROS Production in Ovarian Cancer Cell Lines. 58
3.1.8 ART Causes ROS-dependent Cell Death in Ovarian Cancer Cell Lines. 61
3.1.9 ART-induced Ovarian Cancer Cell Death Requires Iron and is Enhanced by HT Treatment. 61
3.1.10 Caspases are Involved but are Not Essential for ART-induced Cancer Cell Death. 64
3.1.11 ART Does Not Affect Surface CD71 Expression in Ovarian Cancer Cells 64
3.1.12 ART has an Anti-proliferative Effect on Ovarian Cancer Cells 67
3.1.13 ART Induces Cell Cycle Arrest in Ovarian Cancer Cells 67
3.1.14 ART Affects the Expression of Cell Cycle Regulatory Proteins in Ovarian Cancer Cells. 70
3.1.15 ART-induced G2/M Cell Cycle Arrest in Ovarian Cancer Cells is ROS-dependent. 70
3.1.16 ART-induces ROS-dependent DNA Damage 73
3.1.17 ART-induced ROS Production Regulates the Expression of CDC25C and Cyclin B. 73
3.2 Results: Investigation of the Anti-breast Cancer Activity of ART 75
3.2.1 ART Inhibits the Growth of a Panel of Breast Cancer Cells Including a Paclitaxel-resistant Cell Line. 75
3.2.2 ART Maintains its Anti-breast Cancer Activity in 3D Cultures 77
3.2.3 The Colony-forming Capacity of MDA-MB-468 Breast Cancer Cells is Reduced Following ART Treatment. 77
3.2.4 ART Induces Apoptosis in MDA-MB-468 and SK-BR-3 Breast Cancer Cells 80
3.2.5 RIPK1 Activity Does Not Significantly Contribute to the Cytotoxic Effects of ART Against Breast Cancer Cells. 80
3.2.6 ART-induced Apoptosis in Breast Cancer Cells is Caspase-dependent and Characterised by PARP-1 Cleavage. 83
3.2.7 ART Induces the Production of ROS which is Required for ART-mediated MDA-MB-468 and SK-BR-3 Breast Cancer Cell Apoptosis. 85
3.2.8 ART-induced Apoptosis is Iron-dependent 85
3.2.9 ART-induced ROS-dependent DNA Damage 88
3.2.10 Oxygen is Required for ART-induced Apoptosis. 88
3.2.11 ART Induces Dose-dependent Mitochondrial Membrane Destabilization in Breast Cancer Cells. 88

3.2.12 ART-induced Mitochondrial Membrane Destabilization is Characterised by the Release of Cytochrome c and Smac/DIABLO. 92
3.2.13 ART Induces ROS-dependent Mitochondrial Membrane Destabilization in MDA-MB-468 and SK-BR-3 Breast Cancer Cell Lines. 92
3.2.14 ART-treatment of MDA-MB-468 and SK-BR-3 Breast Cancer Cells Leads to a Decrease in the Surface Expression of CD71. 92
3.2.15 ART Inhibits MDA-MB-468 and SK-BR-3 Breast Cancer Cell Proliferation. 96
3.2.16 ART Alters the Expression of Key Cell Cycle Regulatory Proteins in Breast Cancer Cells. 96
3.2.17 MDA-MB-468 and SK-BR-3 Breast Cancer Cells Treated with ART Arrest in the G2/M and G1 Phases of the Cell Cycle, Respectively. 99
3.2.18 ART-induced MDA-MB-468 G2/M Cell Cycle Arrest is ROS-dependent 99
3.2.19 Low Doses of ART Enhance the Effect of Radiation Therapy on MDA-MB-468 Breast Cancer Cells 102
3.2.20 Low Doses of ART Sensitises MDA-MB-468 Breast Cancer Cells to Chemotherapeutic Agents. 102
3.2.21 Treatment of MDA-MB-468 with a Sub-cytotoxic Level of ART Sensitises Breast Cancer Cells to Cisplatin. 102
CHAPTER 4: DISCUSSION 107
4.1 ART Inhibits the Growth of Ovarian and Breast Cancer Cell Lines 107
4.2 ART Maintains its Inhibitory Activity in Ovarian and Breast Cancer Spheroid Cultures 109
4.3 ART is Cytotoxic to Breast and Ovarian Cancer Cells. 110
4.3.1 ART is Cytotoxic to Ovarian Cancer Cell Lines 111
4.3.2 ART induces breast cancer cell apoptosis 114
4.4 ART-mediated Cell Death is ROS and Iron-dependent 115
4.5 Oxygen is Required for ART-induced Breast Cancer Cell Death. 118
4.6 ART Causes Decreased Ovarian Cancer Cell Proliferation. 119
4.7 ART-Treatment Causes Cell Cycle Arrest. 121
4.8 ART-mediated G2/M Cell Cycle Arrest is ROS-dependent. 124
4.9 ART Enhances The Inhibitory Effects of Ionizing Radiation and Established Chemotherapeutic Agents on the Growth of Breast Cancer Cells. 125
4.10 Advantages and Limitations of ART as an Anti-Cancer Agent 128
4.11 Study Limitations and Future Directions 129
4.11.1 *In vivo* studies 129
4.11.2 Continued Investigation of ART-mediated Anti-cancer Mechanisms 130

4.11.3 Novel Drug Delivery Platforms 130
4.11.4 Combined Modality Treatments 131
4.11.5 Continued Studies of Ovarian Tumour Spheroids 131
4.12 Conclusions 132
REFERENCES 135
APPENDIX 160

List of Tables

Table 1.1 Federation Internationale de Gynecologie et d'Obstetrique (FIGO) staging for ovarian carcinoma (adapted from(29)) 6

Table 3.1 Ovarian Cell Line Characteristics and ART IC_{50} 50

Table 4.1 Summary of ART Activity in Breast and Ovarian Cancer Cell Lines. 134

List of Figures

Figure 1.4.1 Overview of Some Important Regulators of the Cell Cycle..... 14

Figure 3.1.1 ART has a Potent Dose-dependent Inhibitory Effect on the Growth of Ovarian Cancer Cells. 51

Figure 3.1.2 ART Maintains its Anti-cancer Activity in 3D Ovarian Cancer Cell Spheroids..... 53

Figure 3.1.3 Ovarian Cancer Cells Treated with a Low Dose of ART Regain their Proliferative Capacity Following ART Removal. 54

Figure 3.1.4 ART Induces Dose-dependent Cell Death in Ovarian Cancer Cell Lines.... 56

Figure 3.1.5 Murine Ovarian Cancer Cells are Sensitive to ART 57

Figure 3.1.6 Inhibition of RIP1 Kinase Activity by Nec-1 Decreases ART-mediated Cytotoxicity in HEY1 and HEY2 Ovarian Cancer Cell Lines. 59

Figure 3.1.7 ART Treatment Induces Dose-dependent ROS Production in Ovarian Cancer Cells. 60

Figure 3.1.8 ART Induces ROS-dependent Cell Death in Ovarian Cancer Cell Lines. ... 62

Figure 3.1.9 Iron is Involved in ART-mediated Cytotoxicity in Ovarian Cancer Cells... 63

Figure 3.1.10 Caspases are Involved but are Not Essential for the Majority of ART-mediated Ovarian Cancer Cell Death. 65

Figure 3.1.11 ART Does Not Affect Surface Expression of CD71 on HEY1 or HEY2 Cells. 66

Figure 3.1.12 The Anti-proliferative Activity of ART is Not ROS-dependent. 68

Figure 3.1.13 ART Induces Dose-dependent G2/M Cell Cycle Arrest in Ovarian Cancer Cells. 69

Figure 3.1.14 ART Treatment Alters the Expression of Cell Cycle Regulatory Proteins. 71

Figure 3.1.15 ART-induced G2/M Cell Cycle Arrest is ROS-dependent in Ovarian Cancer Cells. 72

Figure 3.1.16 ART-induced ROS Production Causes DNA Damage and Modulates the Expression of CDC25C and Cyclin B Cell Cycle Regulatory Proteins. 74

Figure 3.2.1 ART has a Potent Dose-dependent Inhibitory Effect on Breast Cancer Cell Growth..... 76

Figure 3.2.2 ART has an Anti-cancer Effect on MCF-7 Breast Cancer Spheroids. 78

Figure 3.2.3 ART Inhibits the Colony-forming Capacity of MDA-MB-468 Breast Cancer Cells. 79

Figure 3.2.4 ART Causes Dose- and Time-dependent Apoptosis in Breast Cancer Cells. 81

Figure 3.2.5 ART Fails to Cause Necroptotic Cell Death in MDA-MB-468 Breast Cancer Cells. 82

Figure 3.2.6 ART-induced Breast Cancer Cell Apoptosis is Caspase-dependent. 84

Figure 3.2.7 ART-induced ROS Production is Involved in Apoptosis Induction in Breast Cancer Cells. 86

Figure 3.2.8 Iron is Required for ART-induced Apoptosis and Iron Pre-treatment Enhances ROS Production and Sensitises Breast Cancer Cells to ART. 87

Figure 3.2.9 ART Induces ROS-dependent DNA Damage in Breast Cancer Cells. 89

Figure 3.2.10 Oxygen is Required for ART-mediated Apoptosis in MDA-MB-468 Breast Cancer Cells. 90

Figure 3.2.11 ART-induced Apoptosis is Characterised by Mitochondrial Membrane Destabilisation. 91

Figure 3.2.12 ART-mediated Mitochondrial Membrane Destabilisation is Characterised by the Release of Cytochrome c and Smac/DIABLO. 93

Figure 3.2.13 ART-mediated Mitochondrial Membrane Destabilisation is ROS-dependent. 94

Figure 3.2.14 ART Decreases Surface Expression of CD71 in Breast Cancer Cells. 95

Figure 3.2.15 ART has a ROS-independent Anti-proliferative Effect on MDA-MB-468 and SK-BR-3 Breast Cancer Cells. 97

Figure 3.2.16 ART Modulates the Expression of Key Cell Cycle Regulatory Proteins in Breast Cancer Cells. 98

Figure 3.2.17 ART Induces G2/M Cell Cycle Arrest in MDA-MB-468 Breast Cancer Cells and G1 and G2/M Arrest in SK-BR-3 Cells. 100

Figure 3.2.18 ART-induced G2/M Cell Cycle Arrest is ROS-dependent. 101

Figure 3.2.19 Low Doses of ART Enhances the Effect of Radiation Treatment on MDA-MB-468 Breast Cancer Cells. 103

Figure 3.2.20 ART Enhances MDA-MB-468 Breast Cancer Cell Growth Inhibition by a Panel of Chemotherapeutic Agents. 105

Figure 3.2.21 ART Enhances the Inhibitory Effects of Cisplatin on the Clonogenic Survival of MDA-MB-468 Breast Cancer Cells. 106

Appendix 1 Confirmation of TX400 MCF-7 Paclitaxel-resistance. 160

Abstract

In women, breast cancer is the most prevalent cancer diagnosis while ovarian cancer represents the most lethal gynecological neoplasm. The high incidence and mortality of these cancer types, in addition to the emergence of multi-drug resistant clones, highlights the need to develop novel therapeutic agents. Artesunate (ART) is a semi-synthetic derivative of artemisinin, a natural compound derived from the Chinese herb *Artemisia annua L*. ART is a potent anti-malarial agent that also possesses anti-cancer activity. Since the use of ART as an anti-malarial agent is associated with few adverse effects, ART may represent a less toxic alternative to conventional chemotherapy. This study investigates the cytotoxic effects of ART on breast and ovarian cancer cell lines and the mechanism(s) underlying its activity. ART exhibited a potent growth-inhibitory effect on a panel of breast and ovarian cancer cell lines. Anti-cancer activity was also observed in 3D cultures of both cancer cell types. Oregon Green488 and propidium iodide (PI) staining of cancer cells revealed that ART strongly inhibited cancer cell proliferation and, depending on the cell type, arrested cells in the G1 or G2/M phases of the cell cycle. Arrest in the G2/M phase was dependent on reactive oxygen species (ROS) production. The anti-proliferative effect of ART was associated with altered expression of several cell cycle regulatory proteins in both breast and ovarian cancer cell lines, including cyclin D3, E2F-1, and CDC25C. Annexin-V-FLUOS/PI staining of ART-treated cancer cells revealed cytotoxicity against breast and ovarian cancer cell. ART-induced cell death was iron- and ROS-dependent. Pre-treatment of cancer cells with a pan-caspase inhibitor decreased but did not eliminate ART-induced cancer cell death, suggesting that caspase-dependent apoptosis is involved in ART-mediated cancer cell killing. ART induced ROS-dependent DNA damage as indicated by the presence of γH2AX, which implicated the DNA damage pathway in ART-induced cancer cell death. These data show that ART has a potent anti-proliferative and cytotoxic effect on both breast and ovarian cancer cells. The cytotoxic activity of ART and its excellent safety record in malaria patients make ART a worthy candidate for further investigation as a possible treatment for breast and ovarian cancer.

List of Abbreviations Used

4HC	4-hydroxycyclophosphamide
x *g*	Times gravity
Ab	Antibody
ABC	ATP-binding cassette
ACT	Artemisinin-based combination therapies
AJCC	American Joint Committee on Cancer
AIF	Apoptosis-inducing factor
ANOVA	Analysis of variance
AP-1	Activation protein 1
Apaf-1	Apoptosis-protease activating factor 1
ART	Artesunate
ATP	Adenosine triphosphate
ATR	Ataxia telangiectasia and Rad3-related protein
ATM	Ataxia telangiectasia mutated
Bak	Bcl-2 homologous antagonist killer
Bax	Bcl-2-associated X protein
Bcl-2	B-cell leukemia/lymphoma 2
Bcl-X_L	B-cell lymphoma-extra large
BH	Bcl-2 homology domain
Bim	Bcl-2-like protein 11
β-ME	Beta-mercaptoethanol
BRCA1	Breast cancer gene 1
BRCA2	Breast cancer gene 2
BSA	Bovine serum albumin
BCRP	Breast cancer resistance protein
C	Cytokinesis checkpoint
°C	Degrees Celsius
CAD	Caspase-Activated Deoxyribonuclease
$CaCl_2$	Calcium chloride
CAM	Complementary and alternative medicine
CAK	CDK activating proteins
CARD	Caspase recruitment domain
Caspase	Cysteine aspartate-specific protein
CD71	Transferrin 1 receptor
CDC	Cell division cycle
CDK	Cyclin-dependent kinase
CDMEM	Complete Dulbecco's Modified Eagle's Medium
CKI	Cyclin-dependent kinase inhibitor
CM-H_2DCFDA	5-(and-6)-chloromethyl-2',7'-dichlorodihydrofluorescein diacetate, acetyl ester
CO_2	Carbon dioxide
Cu	Copper
CYP	Cytochrome P450
DD	Death domain
dd$H_2$0	Distilled, deionized water

DFE	Deferiprone
DFO	Deferoxamine
DHA	Dihydroartemesinin
DIABLO	Direct inhibitor of apoptosis-binding protein with low pI
DiOC6	3,3'-dihexyloxacarbocyanine iodide
DMEM	Dulbecco's Modified Eagle's Medium
DMSO	Dimethylsulphoxide
DMT1	Divalent metal transporter 1
DNA	Deoxyribonucleic acid
DNase	Deoxyribonuclease
DR	Death receptor pathway
DTT	Dithiothreitol
EC_{50}	Half Maximal Effective Concentration
EDTA	Ethylene diamine tetraacetic acid
EGTA	Ethylene glycol tetraacetic acid
ENDOG	Endonuclease G
EOC	Epithelial ovarian cancer
ER	Endoplasmic Reticulum
ER+	Estrogen receptor positive
EtOH	Ethanol
FACS	Fluorescence-activated cell sorting
FADD	Fas-associated death domain
FGF	Fibroblast Growth Factor
FBS	Fetal bovine serum
Fe	Iron
FGM-2	Fibroblast growth
FISH	Fluorescence in situ hybridization
FNA	Fine needle aspiration
FU	Fluorouracil
g	gram
G_0	Quiescent phase
G_1	Gap phase 1
G_2	Gap phase 2
GSH	Reduced glutathione
GSSG	Oxidised glutathione
Gy	Gray
h	Hours
H_2O_2	Hydrogen peroxide
HEPES	5 mM N-2-hydroxyethylpiperazine-N-2ethanesulfonic acid
HER2	Human epidermal growth factor receptor 2
HGSC	High grade serous carcinoma
HIF1α	Hypoxia-inducible factor 1α
HI-FBS	Heat-inactivated FBS
HRP	Horseradish peroxidase
HT	Holo-transferrin
IAP	Inhibitor of apoptosis protein

IC_{50}	Inhibitory concentration 50
ICAD	CADs inhibitor
IDC-NST	Invasive ductal carcinomas (no special type)
IgG	Immunoglobulin G
i.p.	Intraperitoneal
IL-1β	Interleukin 1β
IRE1	Inositol-requiring 1 protein
i.v.	Intravenous
J	Joules
JNK	c-Jun N-terminal kinase
kDa	KiloDalton
KCl	Potassium chloride
kg	Kilogram
Kip	Kinase inhibitory protein
L	Liters
LCIS	Lobular carcinoma *in situ*
LD50	Lethal Dose 50
M	Molar
M phase	Mitotic Phase
MAb	Monoclonal antibody
MAPK	Mitogen-activated protein kinase
MCF	Mean channel fluorescence
MDM2	Murine double minute2
MDR	Multiple drug resistance
mg	Milligram
$MgSO_4$	Magnesium sulphate
min	Minute
mL	Millilitre
mm^2	Millimetre squared
mM	Millimolar
MOMP	Mitochondrial membrane pemiabilisation
mTOR	Mammalian target of rapamycin
MTT	3-(4,5-Dimethylthiazol-2-yl)-2,5-diphenyltetrazolium bromide
NaCl	Sodium chloride
NaF	Sodium fluoride
NaOH	Sodium hydroxide
NADPH	Nicotinamide Adenine Dinucleotide Phosphate
NaH_2PO_4	Sodium dihydrogen phosphate
Na_2HPO_4	Disodium hydrogen phosphate
Na_3VO_4	Sodium orthovanadate
NCI	National Cancer Institute
NOX	Nicotine adenine dinucleotide phosphate oxidases
nM	Nanomolar
NFκB	Nuclear factor kappa light chain enhancer of activated B cells

NS	Non-significant
O_2	Oxygen
$O_2^{\bullet-}$	Superoxide anion
OD	Optical density
•OH	Hydroxyl radical
4-OH	4 hydroperoxy cyclophosphamide
OOR	Peroxy radical
p21	21 kDa Cyclin-dependent kinase inhibitor
p27	27 kDa Cyclin-dependent kinase inhibitor
p53	53 kDa tumour suppressor protein
pAb	Polyclonal antibody
PARP-1	Poly (ADP-ribose) polymerase-1
PBS	Phosphate buffered saline
PFA	Paraformaldehyde
pH	Power of hydrogen
PI	Propidium iodide
PI3K	Phosphatidylinositol-3-kinase
PMSF	Phenylmethyl sulfonyl fluoride
PR	Progesterone receptor
PS	Phosphotidylserine
PTEN	Phosphatase and tensin homolog
PTP	Protein tyrosine phosphatase
PTPC	Permeability transition pore complexes
PTU	Propylenethiourea
PUMA	p53 upregulated modulator of apoptosis
R	Restriction point
Rb	Retinoblastoma protein
RIP1	Receptor-interacting protein 1
RNA	Ribonucleic acid
RNase	Ribonuclease
ROS	Reactive oxygen species
S phase	Synthesis phase
SEM	Stand error of the mean
SERM	Selective estrogen receptor modulator
SD	Standard deviation
SDS	Sodium dodecylsulphate
Smac	Second mitochondria-derived activator of caspases
SOD	Super oxide dismutase
SubG1	Sub Gap 1 phase
tBID	Truncated BID
TMN	Tumour, metastasis, node staging
TNBC	Triple negative breast cancer
TNFR	Tumour necrosis factor receptor
TRAIL1	Tumor necrosis factor-related apoptosis-inducing ligand 1
Tris-HCl	Tris-Hydrochloric acid
Triton-X 100	Octylphenolpoly(ethyleneglycolether)$_x$

T-TBS	Tween Tris-buffered saline
μg	Microgram
μL	Microlitre
μm	Micrometer
μM	Micromolar
UPR	Unfolded Protein Response
WHO	World Health Organization
X	Times (fold)
XIAP	X-linked inhibitor of apoptosis protein
Z-VAD-fmk	Benzyloxycarbonyl-Val-Ala-Asp fluoromethylketone

Acknowledgements

First, a huge thank you to my supervisor Dr David Hoskin for all his support and guidance over the past few years. Your mentorship has meant so much to me and I feel that working in your lab has made me a better person as well as a better researcher. Thank you for putting up with my strange lab hours and for your calm optimism that kept me going through thick and thin.

A big thank you to my committee Dr Penny Barnes, Dr Karen Bedard and Dr Rob Liwski for all your help and advice. I also want to thank everyone in the Pathology department especially Dr Wenda Greer and Eileen Kaiser for all their help and support over the past few years.

To all the Hoskin labbers past, present and adopted, it has been an amazing ride! I can't believe how fast the years flew by. You guys made me excited to come to work every day and I feel so lucky to have worked in a lab full of such great people! I have learned so much (including some choice Islander phrases!) and had a wonderful time doing it! Thank you all for being there through the good, the bad and the hangry times. I couldn't have done it without your friendship, advice and support! A special thank you to those who were there at the start Dr Carolyn Doucette, Dr Ashley Hilchie, Dr Sue Furlong and Kim Sutton for showing me the ropes, I learned from the best!

I have been so lucky to be surrounded by such a great group of friends and I know I could never have done this without you guys! You kept my spirits up when experiments were not going my way, fed me when I became a hermit during thesis writing, and reminded me that there was a world outside of the lab that still needed exploring. You mean the world to me, thank you!

Finally, a huge thank you to my family for all their love and support! Thank you for always being there for me even when we were oceans and multiple time zones apart. I love you all.

CHAPTER 1: INTRODUCTION

1.1 Cancer Overview

Cancer is a collection of diseases that place an immense burden on society. In general, cancers are the first and second leading cause of death in Canada and the USA, respectively, and the lifetime risk of developing cancer is roughly 40 % (1–3). Cancers arise through the accumulation of DNA sequence mutations that lead to the deregulation of cellular growth and the invasion of neighbouring tissues and distant sites. Cancers are categorised on the basis of their specific cell and tissue type, and have been famously described by Hanahan and Weinberg (2011) to possess six specific hallmark capabilities: sustained proliferative signaling, evasion of growth suppression, resistance to death, angiogenesis, ability to invade and metastasise, and replicative immortality. In addition, there are two emerging hallmarks: deregulation of cellular energetics and immune evasion (4, 5).

Although the management of cancer has come a long way over the past decades, the high incidence of cancer along with the emergence of multi-drug resistant forms of the disease highlights the need for novel treatment strategies. This work focuses on ovarian and breast carcinomas, which are two important female cancers of epithelial origin that together comprise ~ 20 % of cancer-related deaths in the USA and Canada (1, 3), and the possible application of the anti-malarial agent artesunate (ART) in the management of these diseases.

1.2 Ovarian Cancer

Ovarian cancer is the fifth leading cause of cancer-related death in women and the most lethal gynecological malignancy, projected to kill 14,030 women in the United States in 2013 (1). Although the outlook for patients diagnosed with early stage ovarian cancer is encouraging (a 5-year survival rate of over 90 %), over 60 % of patients present with advanced metastatic disease, which has a 5-year survival rate below 30 % (1). The absence of effective screening methods for ovarian cancer along with the disease's non-specific symptoms often prevent early diagnosis (6).

The ovaries are composed of three main cell types: epithelial cells which form the outer layer of the ovaries, as well as line inclusion cysts and crypts, germ cells which are located inside the ovaries and develop to form the ova, and stromal cells which play an important structural role in the ovary and produce essential female hormones estrogen and progesterone. These three cell types are also the origin of the three most common ovarian tumours (7).

The majority of germ cell and stromal ovarian tumours are benign and, together, represent about 10 % of all malignant ovarian cancers (7). As these forms of ovarian cancer only represent an extremely small proportion of ovarian cancers, this chapter will focus on the most common and deadly type: epithelial ovarian cancer.

1.2.1 Epithelial Ovarian Carcinoma

Epithelial tumours are the most prevalent malignant ovarian tumour type representing over 85 % of all ovarian cancers (8). Ovarian tumours of epithelial origin are extremely heterogeneous and have been further subdivided into a number of histological subtypes. Recent research into these subtypes has revealed them to represent distinct diseases, differing significantly in their biology as well as their response to treatment (9, 10). Serous, mucinous, clear cell and endometrioid cancers represent the four major histological subtypes of epithelial ovarian carcinoma (EOC) defined by the World Health Organization (WHO) (8). Other subtypes include mixed carcinomas and undifferentiated carcinomas (8). There has been some controversy surrounding the classification of EOC. Recent improvements in genomic and pathologic techniques have led to the suggestion that many tumours previously identified as ovarian cancer may actually be metastases from another site, further complicating treatment of this disease (11–15).

1.2.1.1 Serous EOC

Serous EOC are the most prevalent form of metastatic ovarian cancer and also represent the subtype most commonly diagnosed at a later stage. Recently, tumours of this subtype have been further categorized into high grade, and the rarer low grade, serous EOC (16). High grade serous EOC is the most prevalent and deadly EOC (8, 16). They are typically quite aggressive and the majority of patients present with advanced disease, which has a 5 year survival of below 30 % (1, 16). BRCA1/2 and p53 mutations are more frequent in this form of EOC (16–19). Interestingly, persuasive recent evidence

suggests that the majority of these cancers may actually originate from the epithelium of distal fallopian tubes rather than from the ovary itself (13, 14, 20–23).

Unlike its high grade form, the majority of low grade serous EOC are thought to originate from non-metastatic ovarian epithelial tumours and they often share early genetic mutations (16). This form of serous cancer is far less common than the high grade variety and represents less than 5 % of all EOC (16, 24). Unlike high grade serous EOC, low grade serous EOC is less aggressive and typically slower growing. Even though low grade serous EOC usually presents as later stage disease, its prognosis is slightly better than high grade EOC (16).

1.2.1.2 Mucinous EOC

Mucinous cancers are the rarest of the EOC subtypes, comprising approximately 2-4 % of all EOC (11, 24, 25). In the past, mucinous EOC were believed to be much more prevalent, but recent diagnostic advances have shown that the majority of tumours previously classified as mucinous EOC are actually secondary metastatic lesions derived from intestinal and other cancers (11, 12, 15). Mucinous EOC are characterized by the presence of cellular mucin and are often associated with benign mucinous epithelia and/or mucin borderline tumours (8). These tumours are rarely bilateral and are often identified at an early stage (25, 26). Mucinous EOC are often less sensitive to platinum therapy, leading to an increased demand for alternate treatment strategies. Interestingly, recent evidence suggests that a significant subset of this ovarian cancer subtype over-express HER2, suggesting that herceptin may represent a possible treatment option for these tumours (27).

1.2.1.3 Endometrioid EOC

Endometrioid EOC have strong ties to endometriosis and represent approximately 10 % of all EOC (24, 28). As with mucinous EOC, endometrioid EOC is typically diagnosed at an early stage and carries a good prognosis (28, 29). Endometrioid EOC typically possesses similar features to endometrial epithelial cancers and endometrial atypical hyperplasia is believed to be a precursor for most of this subtype of ovarian cancer (29).

1.2.1.4 Clear Cell EOC

Clear cell EOC is named for its characteristic glycogen-rich clear, oxyphil, or hobnail cells comprises around 5-14 % of all EOC (9, 24, 30). Clear cell EOC often manifests as a large unilateral pelvic mass and diagnosis frequently occurs at an earlier stage than serous EOCs, often with over 50 % of clear cell EOC being diagnosed at stage I (9, 24, 31). Nevertheless, diagnosis with late stage clear cell EOC is associated with a poorer prognosis than other EOCs, possibly due in part to its resistance to platinum agents and propensity for recurrence following initial treatment (9, 31, 32). Clear cell EOC patients are often pooled with other EOC, receiving the same first line treatment.

1.2.2 EOC Staging and Treatment

Ovarian tumour staging is typically performed during surgery. Tumours are categorised into 1 of 4 stages, as described by the TMN and Federation Internationale de Gynecologie et d'Obstetrique (FIGO) classification systems, based on the extent of invasion, metastasis to the pleural cavity and presence of distant metastases. Stages defined by the FIGO are listed in Table 1 (adapted from (33)).

First-line treatment of ovarian cancer typically involves cytoreductive surgery consisting of an abdominal hysterectomy and bilateral salpingo-oophorectomy. Optimal tumor debulking resulting in less than 1 cm of residual disease is extremely important and provides a significant survival advantage (34). Surgery is commonly followed by a chemotherapeutic regimen, although chemotherapy can be omitted in the treatment of some low risk patients with early stage, low grade ovarian cancers (35, 36). In some cases, neoadjuvant chemotherapy can be applied followed by interim resection if abdominal bloating, ascites or other conditions prohibit initial surgical resection (37).

Over one-third of ovarian cancer patients with advanced disease develop ascites, which is the build up of fluid in the abdominal cavity. Ascites fluid contains many soluble factors, including cytokines, chemokines, angiogenic mediators and growth factors. Furthermore, ascites also contains a cellular fraction composed stromal and immune cells, as well as tumour cells present either in multicellular spheroids or as single cells (38). Unlike most cancers, ovarian cancer often spreads by direct extension to the surrounding peritoneal cavity. Cells are also shed into the peritoneal fluid or ascites and likely contribute to tumor cell dissemination (38).

Adjuvant chemotherapy is extremely important for the treatment of residual disease, especially in patients with malignant ascites. Chemotherapy usually consists of a cocktail containing a platinum-based agent and a taxane, typically carboplatin and paclitaxel, which are administered systemically (7, 37), although intraperitoneal administration of cisplatin has been recently recommended for certain patients (39). In the case of recurrent disease, treatment with carboplatin in combination with paclitaxel, docetaxel, gemcitabine, or liposomal doxorubicin are often recommended for platinum-sensitive tumours. Paclitaxel, docetaxel, gemcitabine, etoposide, topotecan or liposomal doxorubicin can be administered as single agents for the treatment of platinum-resistant disease (36, 39).

Table 1.1 Federation Internationale de Gynecologie et d'Obstetrique (FIGO) Staging For Ovarian Carcinoma (adapted from(33))

Stage I		Tumour limited to ovaries (one or both)
	IA	Tumour limited to one ovary; capsule intact, no tumour on ovarian surface. No malignant cells in ascites or peritoneal washings
	IB	Tumour limited to both ovaries; capsules intact, no tumour on ovarian surface. No malignant cells in ascites or peritoneal washings
	IC	Tumour limited to one or both ovaries with any of the following: capsule ruptured, tumour on ovarian surface, malignant cells in ascites or peritoneal washings
Stage II		Tumour involves one or both ovaries with pelvic extension
	IIA	Extension and/or implants on uterus and/or tube(s). No malignant cells in ascites or peritoneal washings
	IIB	Extension to and/or implants on other pelvic tissues. No malignant cells in ascites or peritoneal washings
	IIC	Pelvic extension and/or implants (T2a or T2b) with malignant cells in ascites or peritoneal washings
Stage III		Tumour involves one or both ovaries with microscopically confirmed peritoneal metastasis outside the pelvis
	IIIA	Microscopic peritoneal metastasis beyond pelvis (no macroscopic tumour)
	IIIB	Macroscopic peritoneal metastasis beyond pelvis 2 cm or less in greatest dimension
	IIIC	Peritoneal metastasis beyond pelvis more than 2 cm in greatest dimension and/or regional lymph node metastasis
Stage IV		Distant metastasis (excludes peritoneal metastasis)

The definitions of the T categories correspond to the stages accepted by the Federation Internationale de Gynecologie et d'Obstetrique (FIGO)

1.2.3 Limitations of Current Cancer Therapies

Although most patients initially exhibit a good response to primary treatment, relapses occur in the majority of patients with advanced ovarian cancer. Recurrent disease is often chemo-resistant and secondary treatment is typically palliative in nature (40, 41). The prevalence of recurrent disease and the high resulting morbidity highlights the need for the development of novel treatment modalities.

Ovarian cancer subtypes are genetically and pathologically diverse and differ greatly in their response to adjuvant chemotherapy. As the differences, both genetic and pathologic, between the subtypes continue to emerge there is an increasing demand for more individualized treatments, especially in the case of certain subtypes like clear cell EOC that are frequently resistant to platinum agents (9, 31, 32, 42). The identification of novel treatments with low toxicity profiles would be of great benefit to EOC patients, especially if these treatments could be used to sensitize cancer cells to current chemotherapy regimens in order to reduce the required dosage of the more toxic agents.

1.3 Breast Cancer

Breast cancer is the second leading cause of cancer-related death in women, who have a 1 in 8 lifetime chance of developing the disease. Breast cancer is projected to kill over 39,000 women and 2,000 men in the United States in 2013 (1). The last 30 years has seen significant improvements in the 5 year survival rate of this disease which is currently at 90 % for all stages combined (1). Nevertheless, the high incidence of this disease along with the prevalence of breast cancer recurrence highlights the need for new and better treatment options.

1.3.1 Breast Cancer Subtypes

Breast cancer is a very heterogeneous disease, comprised of a number of subtypes with different biologies and responses to treatment. Currently, breast cancers are categorised relative to their stage, histology, tumour grade, and molecular type. The combined results from these analyses determines the appropriate treatment regimen and prognosis (43).

1.3.1.1 Tumour Stage and Grade

Breast cancer staging is usually conducted using the TMN classification system, which places tumours into one of five stages based on size, invasiveness, lymph node involvement and presence of metastases (33). Tumour grade evaluates tumours relative to mitotic index, degree of tubule formation and nuclear polymorphism and uses this information to designate the level of tumour differentiation (44).

1.3.1.2 Breast Cancer Histology

WHO currently recognises over 18 histological types of breast cancer, of which the majority (40-75%) are classified as invasive ductal carcinomas (not otherwise specified) (IDC-NOS) (43). These tumours are a diverse group that lack sufficient distinctive characteristics to allow them to be categorised into a specific histological subtype (43). The second most pervasive type of breast cancer is invasive lobular carcinoma (5-15%). This subtype is often associated with lobular carcinoma *in situ* and tumour cells often appear disseminated in fibrous stroma either singly or in loose linear chords (8, 43). Other subtypes of breast cancer include inflammatory carcinoma, mucinous carcinoma, and tubular carcinoma; although the special histological subtypes are all relatively rare, each representing less than 5 % of breast cancers, the ability identify these different forms is important for delivering the appropriate treatment and determining prognosis (43, 45, 46).

1.3.1.3 Molecular Characterisation

Molecular characterisation and gene profiling by microarray analysis has led to the classification of 4 key breast cancer types: luminal A, luminal B, basal-like, and HER2-over-expressing (45, 47). Luminal A and B tumours are thought to originate from the inner, luminal layer, of the glandular breast epithelium and express characteristic luminal markers such as estrogen and progersterone receptors (ER and PR, respectively) (47–49). Luminal A tumours are the most common and are more likely to be associated with a lower histological grade and better prognosis than other breast cancer subtypes (49–51). Luminal B cancers also include HER2 over-expressing tumours and are often more aggressive with a higher grade than luminal A cancers, although prognosis for these cancers is better than for the HER2 over-expressing basal-like forms (49, 52). HER2-positive tumours either over-express the growth receptor or have increased gene copy numbers. This subtype is negative for hormone receptors (otherwise they are categorised

as luminal B). HER2 is a member of the human epidermal growth factor receptor family. Activation and heterodimerisation of HER2 with other family members regulates proliferation, differentiation and survival of cells. HER2 is over-expressed in 20-30 % of breast cancers, which leads to a proliferation and survival advantage in these cells and is associated with a poor prognosis (53). Basal-like tumours are characterised by increased expression of basal/myoepithelium cell markers, including cytokeratin 5/6 and 17, and, like HER2-over-expressing tumours, frequently contain p53 mutations (47, 54). Basal-like tumours are also more likely to develop in younger women and are often associated with BRCA1 mutations (48, 55, 56). These tumours are often triple-negative breast cancers (TNBC) (with low/no ER, PR and HER2 expression), although not all TNBC are of the basal type, nor are all basal-like tumours also TNBC (57). Recurrent TNBC tumors are especially hard to treat as they lack the receptors necessary for hormone- or HER2-targeted therapy and are often aggressive (55). Although diagnosis of breast cancer based upon these molecular subtypes has predictive value, these groups remain extremely heterogeneous and work is underway to further categorise these breast cancer subtypes. Recently, exciting advances in genomics, transcriptomics and proteomics have led to new classifications of breast cancer based on more extensive molecular profiling which may better predict clinical outcomes (58). These advances are greatly increasing the personalised nature of breast cancer management, although it will likely be challenging to integrate these genetic analyses into everyday clinical practice.

At this time, the extensive genetic analysis of tumour samples is not widely available and the immunohistochemical (IHC) assessment of biomarker expression (ER, PR, and HER2 status), as well as fluorescence in situ hybridization (FISH) analysis for HER2 amplification remain the most routinely used detection methods (59, 60). Biomarker status in conjunction with cancer histology, grade, and stage collectively contribute to our understanding of individual tumour types and play a vital role in the selection of the appropriate disease management strategy.

1.3.2 Breast Cancer Treatment

As mentioned above, the selection of the appropriate breast cancer treatment regimen is based on multiple factors that include tumour stage, grade, type, hormone and HER2 receptor expression, as well as individual patient considerations such as

menopausal status, co-morbidities and personal preferences (59, 61). Treatment typically consists of surgical resection with or without radiation and/or systemic therapy. Standard of care for early stage invasive carcinomas (stage I and II) consists of mastectomy or breast conservation surgery with adjuvant radiation followed by systemic therapy (59, 61). Options for systemic therapy depend on the hormonal and HER2 status of the tumour. TNBC tumours will exclusively receive chemotherapy, while tumours that are positive for hormone receptors or that over-express HER2 will receive endocrine therapy or trastuzumab (a monoclonal antibody that targets HER2), respectively, in addition to chemotherapy. The standard of care for systemic chemotherapy consists of an anthracycline (e.g. doxorubicin) in combination with a taxane (e.g. docetaxel), although regimens including cyclophosphamide, flurouricil, or cisplatin are also used (59, 61).

The standard of care for later stage invasive breast cancers that are inoperable involves induction chemotherapy which, if successful, can be followed by surgical resection and radiation therapy. Adjuvant endocrine and trastuzumab therapy is also recommended for patients presenting with hormone responsive or HER2-over-expressing cancers, respectively. Treatment for recurrent disease depends on the primary treatment, and may include mastectomy (if breast conservation surgery was initially performed), radiation, endocrine therapy and chemotherapy (36, 61). Treatment of systemic metastatic disease is palliative in nature and can involve surgery, radiation, trastuzumab, endocrine and chemotherapy, depending on the extent of metastasis and the goals of treatment. Use of other targeted therapies and the inclusion in clinical trial may also be an option (61, 62).

1.3.3 Limitations of Current Therapeutic Agents

Although there has been great improvement in the success of breast cancer management, breast cancer remains one of the leading causes of cancer related death in women (1). It is estimated that 10 to 20 % of patients will suffer disease recurrence within 5 to 10 years (63). Current treatment options are accompanied by significant adverse side effects that include fatigue, nausea and vomiting, neuro- and cardiotoxicities, myelosuppression, infertility, anemia, and an increased risk for secondary neoplasms (64, 65). For instance, long term use of tamoxifen is associated with an increased risk for endometrial cancers (62). All these factors negatively impact on

disease management by decreasing patient quality of life, regimen compliance, and limiting the maximum tolerated dose and number of treatment cycles.

The development of drug resistance to standard breast cancer treatment is also a major limiting factor in the management of breast cancer, especially in the case of recurrent disease (41, 66). Novel treatment options with fewer adverse side effects that are also active against chemoresistant forms of the disease would be of great benefit to the treatment of breast cancer.

1.4 Therapeutic Targets

1.4.1 Cell Proliferation

The process of cell division can be divided into mitosis and interphase. Interphase is the stage during which the cell prepares for division, while mitosis involves chromosomal separation and the physical partitioning of the parent and daughter cell. Interphase can be further subdivided into the Gap1 (G1), synthesis (S) and Gap2 (G2) phases (67). DNA replication occurs in the S phase, while preparation for the initiation of DNA synthesis and mitosis occurs during G1 and G2 phase, respectively. Cells must decide during early G1 whether to continue proliferating or to exit the cell cycle and enter a quiescent state (G_0). The restriction point (R) is the rubicon for this decision. Once cells pass this point they are committed to the cell cycle and are no longer affected by the presence or absence of growth stimuli (67, 68).

Progression through the cell cycle is regulated on a number of levels. Two key families of regulatory proteins are the cyclins and the cyclin-dependent kinases (CDKs), which associate to form heterodimeric complexes. The cyclins are the regulatory component required for the activation of the kinase activity of the catalytic CDK subunit. Once activated, the complexes initiate the phosphorylation of numerous substrates involved in cell cycle progression. Different CDK-cyclin complexes play distinct roles in the various stages of the cell cycle and, although CDK expression is relatively stable, cyclin expression varies depending on the cell cycle stage, helping to control when the different CDKs are active and to regulate the systematic progression of the cell cycle (67)(See Figure 1.4.1 for an overview). The CDK4/6-cyclin D and CDK2-cyclin E complexes play a vital role in the G1 to S phase transition. One of the key substrates

phosphorylated by CDK4/6-cyclin D during early G1 are the 'pocket proteins' which include the retinoblastoma protein (Rb) and its family members (69). Rb and its family members regulate the activity of the E2F family of transcription factors. The E2F family is composed transcriptional activators and repressor proteins. Rb-binding inhibits the activity of E2F1-3a, which activate transcription of a large number of target genes required for G1-S transition (69). E2F4-5 bind pocket proteins and actively repress the transcription of target genes. Phosphorylation by CDK4/6-cyclin D partially inactivates Rb family members and released E2F1-3 transcription factors initiate the expression of cyclin E (70). CDK2-cyclin E complexes subsequently catalyse the complete inactivation of the Rb family members, facilitating the transcription of numerous genes required for S phase entry by E2F1-3 (69–72).

In addition to cyclin binding, CDK activity is further controlled through phosphorylation, cellular localization of various activator and inhibitor molecules, and the expression of inhibitors. Maximal CDK activity requires the phosphorylation of a conserved tyrosine residue by the CDK activating kinase (CAK), which is composed of CDK7, cyclin H and Mat1 (73). Phosphorylation of inhibitory threonine and tyrosine residues by Wee1 and Myt1 suppresses CDK activity, an effect that is reversed by the CDC25 family of phosphatases (74). CDK/cyclin complex activity is also regulated through the expression of CDK inhibitor proteins (CKIs), which bind to and inhibit CDK kinase activity. The inhibitors of CDK4 (INK4) family p16ink4a, p15ink4b, p18ink4c and p10ink4d, bind to and inhibit CDK4,6, while the kinase inhibitor proteins (CIP/KIP) p21 waf1/cip1, p27kip1 and p57kip1 have a broader spectrum of activity and are able to inhibit the activity of all the CDK/cyclin complexes (67).

To prevent the replication of cells with damaged DNA, the cell cycle also contains a number of quality control checkpoints that are activated upon DNA damage or other internal or external stressors to induce temporary cell cycle arrest and, if the damage cannot be resolved, initiate apoptosis (75, 76). The checkpoints are located at key sites of cell cycle transition. The G1-S checkpoint prevents damaged DNA from being replicated. The G2 checkpoint prevents cells whose DNA was replicated incorrectly from entering mitosis. Checkpoints also exist within the S phase as well as within mitosis, which monitors spindle formation and chromosome segregation (67). The G1 and

G2 DNA damage checkpoints are the most relevant to this thesis. Briefly, DNA damage induces the activation of damage sensors ataxia telangiectasia mutated (ATM) and ataxia telangiectasia and Rad3-related (ATR) (76). These kinases then activate a number of substrates involved in DNA damage repair and checkpoint control, including Chk1/2 and p53. Chk kinases can inhibit CDK activity though the inhibition of the CDC25 family of phosphatases and the activation of Wee1 (76). p53, a well known tumour suppressor protein, activates proteins involved in DNA repair and cell cycle arrest, including p21waf1/cip1 (a CKI) and 14-3-3σ (involved in the export of cyclin B and CDC25 from the nucleus) (77).

1.4.1.1 The Cell Cycle and Cancer

Uncontrolled cell proliferation is a hallmark of cancer (4). Tumour cells employ a number of tactics to avoid cell cycle regulation and escape checkpoint-induced cell cycle arrest and apoptosis. Activation of mitogenic signaling pathways (e.g. Akt, myc, HER2 pathways), down-regulation of tumour suppressors (e.g. p53, Rb), and deregulation of the expression of certain cell cycle mediators are often observed in cancer cells (67). Interestingly, although CDK1 is the only essential mammalian CDK in most cell types (78), recent evidence suggests that different tumours may depend on the expression of specific CDKs (79). For instance, although cyclin D1-CDK4 activity is not required for mammary gland development or the development of myc-dependent breast tumours, cyclin D1-CDK4 is required for HER2-dependent breast tumour development (80). These differences in CDK dependencies may prove useful targets for future treatment of different cancers.

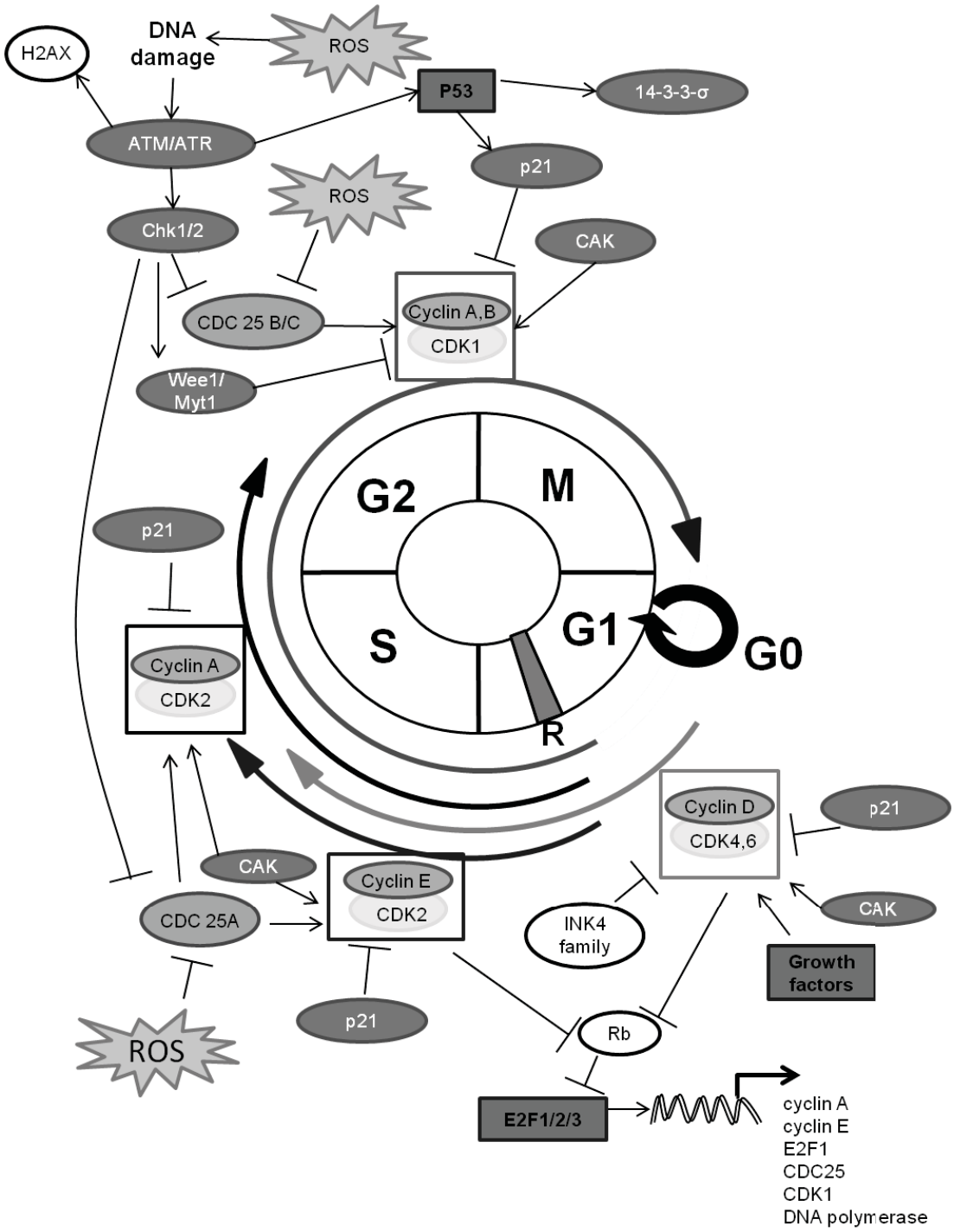

Figure 1.4.1 Overview of Some Important Regulators of the Cell Cycle.

1.4.2 Cell Death Pathways

Apoptosis and necrosis are two major forms of cell death that have distinct morphological features and cellular outcomes. Apoptosis leads to non-inflammatory cellular death through the partition of cellular contents into membrane-bound apoptotic bodies and their subsequent removal by phagocytes, while necrosis results in membrane lysis, the release of cellular contents, and the induction of inflammation (81–85). Other forms of cell death include autophagic cell death or "autosis" which can be repressed by the inhibition of autophagy and is associated with the absence of chromatin condensation and increased numbers of double membraned autophagosomes (81, 86). This section will focus on apoptosis and necrosis as these form of cell death are the most relevant to this thesis.

1.4.2.1 Apoptosis

Apoptosis is an active, programmed cell death pathway that is characterised by cell shrinkage, chromtin condensation, nuclear fragmentation, and apoptotic body formation (84, 85). The membranes of cells undergoing apoptosis remain intact and the cell is eventually broken up into many membrane-bound apoptotic bodies which are then removed by phagocytes, thus preventing the induction of inflammation (84, 85). In the absence of phagocytes (e.g. in cell cultures), or when phagocytosis is inefficient, apoptotic bodies eventually lose membrane integrity leading to the release of their membrane-bound contents, and a process known as secondary necrosis (84, 87).

Apoptosis can be initiated through the intrinsic/mitochondrial or extrinsic/death receptor pathways. Both pathways lead to the activation of caspases, which are key cysteine proteases that are important mediators of apoptosis (88). Caspases are initially produced as inactive zymogens and are activated upon proteolytic cleavage. Caspases can be divided into two distinct groups, initiator caspases (caspase 8, 9, and 10) and effector caspases (caspase 3, 6, and 7). Initiator caspases are upstream of effector caspases and participate in their activation (88). Active effector caspases cleave a variety of substrates to cause apoptosis. These substrates include numerous structural proteins, as well as poly (ADP-ribose) polymerase-1 (PARP-1), a protein involved in DNA repair, and the inhibitor of caspase-activated DNase (I(CAD)), the inhibitor of CAD, a protein involved in nuclear DNA fragmentation during apoptosis (88–90). Apoptosis is an active process

that requires ATP; thus lack of sufficient ATP can lead to a switch from apoptotic to necrotic cell death (91–93).

1.4.2.1.2 The Intrinsic / Mitochondrial Pathway

The intrinsic/mitochondrial pathway is initiated by the permeabilisation of the mitochondrial membrane. Although the mechanisms are not yet fully elucidated, the two principal non-exclusive models for permeabilisation involve the activation of the permeability transition pore complexes (PTPCs) and the B-cell leukemia/lymphoma 2 (Bcl-2) family proteins (94, 95). One model suggests that ROS or Ca^{2+} may activate the PTPCs in the inner mitochondrial membrane, leading loss of mitochondrial membrane potential, matrix swelling and mitochondrial outer membrane permeabilisation (MOMP). The result is the release of pro-apoptotic factors such as cytochrome c into the cytoplasm, which subsequently initiate the activation of the caspase cascade leading to apoptosis (described in more detail below) (94, 95).

The Bcl-2 family consists of both anti-apoptotic (e.g. Bcl-2, Bcl-X_L and Mcl-1) and pro-apoptotic members, (e.g. adaptor molecules Bax and Bak, and the Bcl-2 homology domain 3 (BH3)-only proteins Bim, Bad, tBid, NOXA). The BH3-only proteins share homology with the other Bcl-2 family members in the BH3 domain while Bax/ Bak and the anti-apoptotic proteins contain conserved BH domains 1-3 or 1-4, respectively (95, 96). Oligomerisation of the pro-apoptotic adaptor proteins results in the formation of mitochondrial outer membrane pores leading to MOMP, loss of mitochondrial transmembrane potential and the release of pro-apoptotic factors such as cytochrome c into the cytoplasm (94). Oligomerisation of Bak/Bax and pore formation is inhibited by the anti-apoptotic Bcl-2 members. BH3-only proteins promote apoptosis either through directly activating Bak and Bax (e.g. Bim, PUMA and tBID) or by binding to and inhibiting the activities of the anti-apoptotic family members (e.g. NOXA, Bad) (96, 97). Thus, the balance of pro- and anti-apoptotic factors determines whether or not apoptosis takes place. Interestingly, many cancers over-express anti-apoptotic proteins such as Bcl-2 in order to prevent mitochondrial-mediated apoptosis (98, 99). MOMP and loss of transmembrane potential either through membrane rupture or Bax/Bak-mediated pore formation is often considered a point of no return in the induction of cell death,

which can proceed by apoptosis or switch to necrosis depending on the situation (e.g. ATP availability) (91–93, 95).

Cytoplasmic cytochrome c induces the activation and oligomerisation of apoptosis-protease activating factor 1 (Apaf-1) to form the apoptosome, which then recruits and facilitates the activation of caspase 9. Active caspase 9 induces the activation of executioner caspases such as caspase 3, which subsequently cleave numerous cellular substrates (88). In addition to cytochrome c, several other pro-apoptotic factors are released from the mitochondria. These include second mitochondria-derived activator of caspase/direct IAP binding protein with low p*I* (Smac/DIABLO) and Omi which bind to and deactivate cytoplasmic inhibitor of apoptosis proteins (IAPs) (94, 100, 101). IAPs are anti-apoptotic proteins that bind caspases and inhibit their activation. Apoptosis-inducing factor (AIF) and endonuclease G (ENDOG) are also released from the mitochondria (94, 102). These proteins subsequently translocate to the nucleus and can mediate caspase-independent cell death. Interestingly, although its name suggests otherwise, AIF has also been connected to the induction of necrotic programmed cell death (aka necroptosis) (103).

1.4.2.1.3 The Extrinsic / Death Receptor Pathway

The extrinsic pathway of apoptosis is characterised by the ligand-stimulated activation of membrane-associated death receptors that are members of the tumour necrosis factor receptor (TNFR) family (e.g. Fas, TNFR1 and TNF-related apoptosis-inducing receptor 1 (TRAIL1)) (88, 104). Death receptor ligation promotes receptor trimerisation and the recruitment of adaptor molecules through their conserved cytoplasmic death domains, leading to the recruitment, oligomerisation and activation of caspase 8. Active caspase 8 can then trigger the activation of executioner caspases and/or it can initiate cross talk between the extrinsic and the mitochondrial apoptotic pathways by cleaving and activating BID to yield truncated Bid (tBid) (96). tBID translocates to the mitochondria to trigger mitochondrial membrane permeability by Bax/Bak, as described in the previous section (1.4.2.1.2).

1.4.2.2 Necrosis

Necrosis is a form of cell death characterised by cellular and organelle swelling, and membrane rupture. Necrosis is often defined in a negative capacity, since it is a mode

of cell death that lacks the hallmarks of other forms of cell death (81, 105). During necrosis, loss of cellular membrane integrity leads to the release of the cell's contents and the induction of inflammation (81). Until recently, necrosis was believed to be an accidental, uncontrolled form of cell death; however, new evidence suggests that some forms of necrosis, termed necroptosis, may be induced in a programmed fashion through signaling pathways (106–108).

1.4.2.2.1 Necroptosis

Multiple mechanisms and molecular pathways have been identified in the necroptotic cell program. The two main pathways under investigation are the TNFR1-stimulated pathway and a pathway mediated through alkylating DNA damage (103, 107, 109). Both pathways are caspase-independent and require the kinase activity of the receptor-interacting protein kinase 1 (RIPK1) since treatment with the RIPK1-inhibitor necrostatin-1 inhibits most forms of necroptosis (103, 107, 108). In the case of DNA-damage mediated necroptosis, PARP-1 activation leads to the release of mitochondrial AIF. AIF subsequently translocates to the nucleus where, in association with H2AX and the endonuclease cyclophilin A, it mediates cell death (103). TNFR1-stimulated necroptosis is activated following ligand binding, receptor trimerisation, internalisation and the recruitment of adaptor molecules, which include RIPK1 and RIPK3. Caspase 8 recruitment and activation subsequently leads to the induction of apoptosis; however, in the absence of functional caspase 8, which cleaves and deactivates RIPK1 and RIPK3, these proteins become activated and form the necrosome complex to mediate necroptotic cell death (107)

1.4.3 Oxidative Stress

Reactive oxygen species (ROS) possess paradoxical cellular effects as they can both stimulate cell proliferation and survival, as well as induce cell death. The factors that influence these differences in ROS activity are numerous and include ROS type, level and duration of the ROS-inducing insult, sub-cellular location, cell type and cellular environment (110–112).

ROS are highly reactive oxygen-containing molecules that include free radicals (contain an unpaired electron) such as the hydroxyl radical ($^{\bullet}OH$) and superoxide ($O_2^{\bullet-}$), as well as the uncharged hydrogen peroxide (H_2O_2) (113). Most ROS are unstable and

have a very short lifespan which leads to localised oxidation effects; however, the effects of H_2O_2 are farther reaching as it is more stable and diffusible (111). ROS arise from both exogenous and endogenous sources. Pollution and cigarette smoke are two examples of exogenous sources of ROS whereas $O_2^{\bullet-}$ production from the mitochondrion due to the reaction between oxygen and electrons leaked from the electron transport chain is a key source of endogenous ROS (111, 114, 115). ROS is also a by-product of oxidative protein folding in the ER (116). Furthermore, ROS can also be produced by the family of nicotine adenine dinucleotide phosphate (NADPH) oxidase (NOX) complexes, which produce $O_2^{\bullet-}$ or H_2O_2 depending on the NOX isoform (117, 118). Metals such as iron can also play an important role in the generation of ROS. For instance, H_2O_2 can be converted to the highly reactive $^{\bullet}OH$ radical through the iron-catalysed Fenton reaction (113).

Low levels of ROS play important physiological roles in healthy cells. However, ROS levels must be carefully regulated as they cause significant damage to DNA, lipids and proteins when their levels exceed the cell's anti-oxidative capacity. This condition is known as oxidative stress (91, 119). Cells are protected from excessive oxidative stress by thiol anti-oxidants such as reduced glutathione (GSH) and thioredoxin (which together with their oxidised counterparts play an important role in regulating the cell's redox status), as well as enzymatic anti-oxidants such as super oxide dismutases (SODs) that convert $O_2^{\bullet-}$ to H_2O_2, glutathione peroxidase which uses GSH to convert H_2O_2 to water and oxidised glutathione (GSSG), and catalase enzymes which catalyse the conversion of H_2O_2 to water and oxygen (113). Nevertheless, it is estimated that healthy cells still experience $1.5x10^5$ ROS-dependent mutagenic events per day (120–122). Although the majority of these mutations are efficiently repaired by the cell's DNA repair system, these constant attacks on the genome are believed to play an important role in the development of many pathologies, including cancer (111, 119).

1.4.3.1 ROS as Second Messengers

The ability of ROS to damage DNA, proteins and lipids has been known for decades, but it is only more recently that we have begun to appreciate the important role that ROS play as second messengers in cellular signalling (123, 124). ROS can influence the activation and/or signal transduction of multiple pathways including mitogenic

signalling, cell cycle regulation, and cell death, although our understanding of the mechanisms underlying these activities remains incomplete (123, 125). The effects of ROS on signalling are complex and are influenced by many different factors including the types of ROS involved, the intensity, duration, and localisation of the ROS stimulus, as well as the cell type and environment (110, 111, 126, 127). The oxidative capacity of ROS have been linked to their ability to inhibit the activities of cellular phosphatases, as well as activate certain tyrosine kinases and transcription factors such as activation protein-1 (AP-1) and nuclear factor kappa light chain enhancer of activated B cells (NFκB) (128–130). For instance, ROS oxidation contributes to the activation of c-Src, a protein tyrosine kinase involved in several cellular functions including cell adhesion and motility (131). Conversely, ROS can also oxidise and reversibly inhibit protein tyrosine phosphatases (PTP) which are also required for c-Src activity. As a result, ROS localisation and strength as well as the type and sensitivity of PTPs to oxidation, all play a role in c-Src activation (132, 133). Interestingly, growth factor receptor activation (such as the epidermal growth factor receptor (EGFR)) induces ROS production via the activation of NOX, in order to prevent phosphatase inhibition of mitogenic signalling through the mitogen-activated protein kinase (MAPK) pathway (119, 126). Nevertheless, although ROS deactivation of PTPs can increase cell proliferation and survival, it also has the ability to induce cell cycle arrest and cell death. As previously mentioned, the CDC25 family of phosphatases play a prominent role in cell cycle regulation (Figure 1.4.1) (67, 74). Deactivation of these important enzymes through the ROS-induced oxidation of cysteine residues in their active site inhibits their ability to remove inhibiting phosphates from CDKs and can lead to cell cycle arrest in the G1 or G2 phases of the cell cycle (CDC25A and CDC25B/C respectively) (74, 123). For example, Liu *et al.* (2012) have shown that vanadate treatment of PC-3 prostate cancer cells leads to G2/M cell cycle arrest induced by ROS-mediated CDC25C degradation (134). ROS activation of c-Jun N-terminal kinases (JNK) can also have a proliferation-promoting or pro-apoptotic effect on cell signalling depending on the length of stimulus. Activation of the tumor necrosis factor receptor (TNFR) leads to the activation of multiple signalling cascades, including JNK, in part via ROS-induced PTP oxidation. Research indicates that extended JNK activation leads to the initiation of apoptosis, while transient JNK activation induces

anti-apoptotic signals and increased proliferation through the activation of NFκB (135, 136).

1.4.3.2 Cytotoxic Effects of ROS

Although low, regulated, concentrations of ROS can act as second messengers in a number of important signalling pathways, robust, prolonged ROS exposure invariably damages DNA, proteins and lipids and can lead to cell death (119). Lipid peroxidation by ROS can damage cellular membranes and lead to cell death by apoptosis or necrosis, depending on the affected site and level of damage (91). For instance, ROS-induced lipid peroxidation of lysosomal membranes, likely mediated in part through lysosomal iron-catalysed Fenton reaction, can lead to membrane rupture and to the release of cell-death mediating proteases and lipases including cathepsins (137, 138). Furthermore, peroxidation of lipids can lead to the formation of additional reactive and highly mutagenic products (139).

As mentioned in the previous section, ROS are able to oxidise many different proteins. In most cases, oxidation caused by low levels of ROS is reversible and plays an important role in various signalling cascades (74, 124), but higher concentrations of ROS induce further protein oxidation that is irreversible (113). Prolonged ROS exposure can also alter signalling pathways. For example, as described above (section 1.4.3.1), prolonged JNK activation by ROS switches proliferative signals to apoptosis induction through the modulation of Bcl-2 family members, and may cause necrosis through less well defined mechanisms (135, 136, 140, 141)

ROS, especially the highly reactive $^{\bullet}OH$, can damage DNA through the formation of adducts and breaks. This activates the DNA damage response, inducing cell cycle arrest and, ultimately, cell death via apoptosis if the damage is too extensive for repair (113, 142). Mitochondrial DNA is especially sensitive to ROS-induced damage as it is not protected by histones and possesses limited repair mechanisms compared to nuclear DNA. Mitochondrial DNA is also exposed to continuous ROS attack due to its proximity to the electron transport chain (113). High ROS levels can damage mitochondrial membranes leading to MOMP and the release of pro-apoptotic factors such as cytochrome c (115, 143).

ROS can induce both apoptosis and necrosis, depending on ROS strength, localisation, and individual cell characteristics. Necrosis induction has been associated with higher ROS exposure, due in part to oxidant-induced depletion of ATP, which is required for energy-dependent apoptosis (91–93). Additionally, caspase activity can also be directly inhibited by ROS since essential cysteines in the active site of caspases are susceptible to oxidation. Therefore, if ROS levels are high enough in the cytoplasm, ROS-induced activation of caspase-mediated apoptosis may be delayed until ROS levels decrease and caspases can be reactivated. In this event, apoptosis proceeds via caspase-independent mechanisms such as AIF-mediated apoptosis, or, at even higher concentrations of ROS, cell death occurs via necrosis (144–146).

1.5 Artesunate (ART)

ART is a semi-synthetic derivative of artemisinin (qinghaosu), a natural compound from the Chinese herb Sweet Wormwood (*Artemisia annua L*) (147). Sweet Wormwood has been used for centuries in traditional Chinese medicine; descriptions of its use date back to 168 B.C. when it was recommended for treatment of hemorrhoids, and was later used for the treatment of fever, including fever caused by malaria (147, 148). More recently, artemisinin and its derivatives, which include ART, dihydroartemisinin (DHA), artemether, and arteether, have been employed as anti-malarial agents, showing good activity against *Plasmodium falciparum* and *P. vivax*, including multi-drug resistant strains of the parasite (147–149). First generation artemisinin derivatives were developed to address the insolubility of artemisinin and to increase treatment efficacy (148). Artemisinin and its derivatives are also cytotoxic to certain neoplastic cells (150, 151). Since the widespread use of these drugs as anti-malarial agents has been associated with few adverse effects (152, 153), the artemisinins such as ART may represent a promising new alternative to traditional treatments for cancer.

1.5.1 Basic Pharmacokinetic Properties of ART

ART is the most water soluble derivative of artemisinin and is currently the only artemisinin derivative that can be administered by intravenous (i.v.) injection (149, 154).

For the treatment of malaria, ART can be administered by oral, rectal, i.v. and intramuscular routes (149). ART is quickly absorbed, allowing for its detection in the blood within 15 min of administration. Once ingested, ART is rapidly converted to its primary active metabolite, DHA, through esterase-catalysed hydrolysis or first pass metabolism with an average half life of 20 to 40 min. The half-life of ART is less than 15 min when administered by the i.v. route (154, 155); however, peak plasma concentrations are achieved with i.v.-administered ART and concentrations of over 50 μM have been reported (155). DHA is detected quickly following ART administration and its estimated half-life is slightly longer; 0.5 to 1.5h h and 30 to 60 min for oral- and i.v.-administered ART, respectively (155).

A 4 mg/kg oral dose of ART for 3 d in combination with an additional anti-malarial agent with a longer half-life is recommended for the treatment of uncomplicated malaria. Administration of 2.4 mg/kg i.v. ART every 12 h for at least 24 h followed by combined modality ART treatment for 3 d is recommended for the management of severe malaria (149). DHA has recently become available as an oral formulation, although issues with thermal and chemical stability have hampered its use (149, 156, 157).

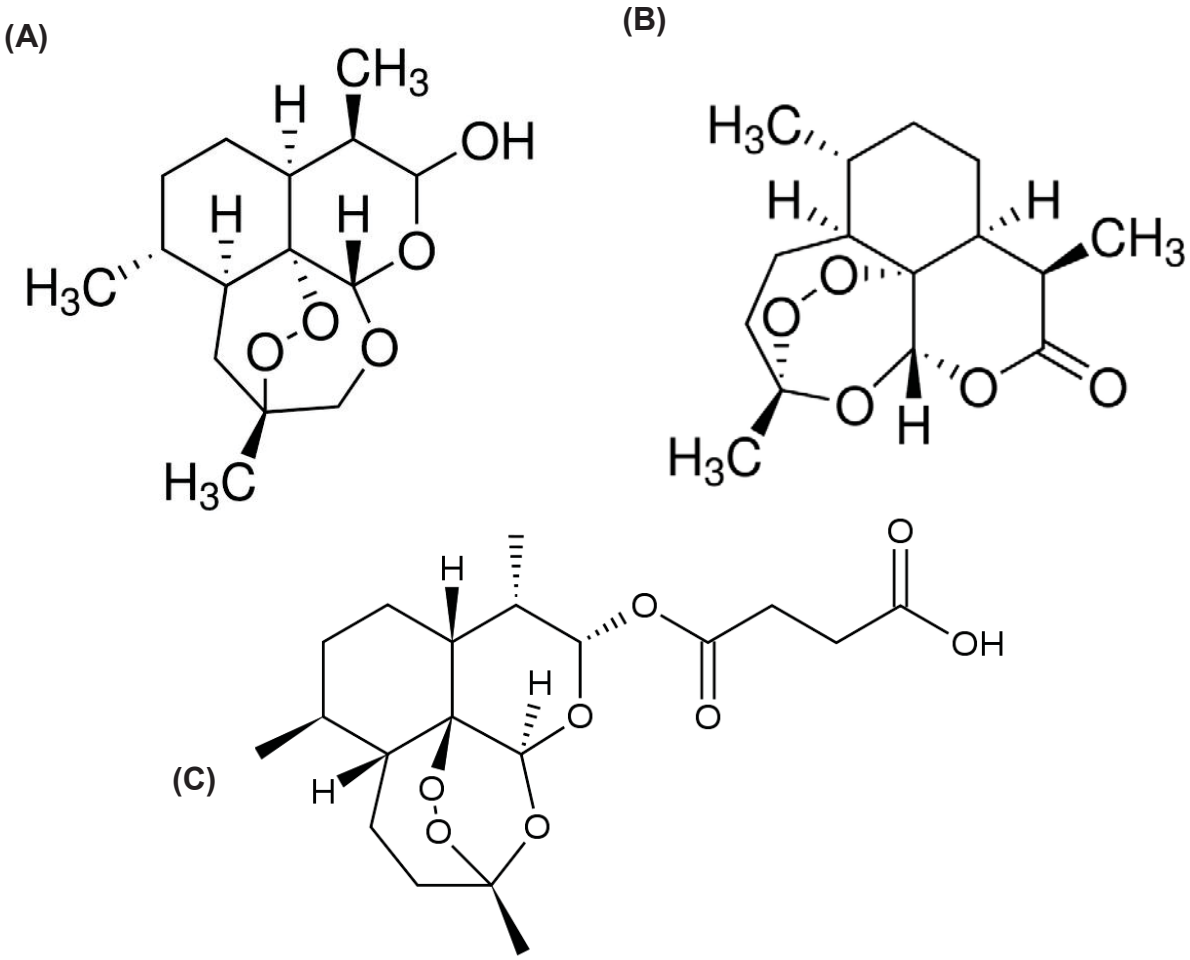

Figure 1.5.1 **Structure of Dihydroartemisinin (A), Artemisinin (B), and Artesunate (C).**

1.5.2 Anti-malarial Properties of ART

Artemisinin compounds (including ART) are potent anti-malarial agents with excellent activity against the erythrocytic stages of the malarial parasite life cycle (148, 158). Artemisinins rapidly reduce parasite burden in severe and uncomplicated forms of malaria, including disease caused by drug-resistant strains (158). Excellent efficacy along with the lack of significant adverse side effects have resulted in artemisinin-based combination therapies (ACT) being recommended as the standard of care by the World Health Organization (WHO) for the treatment of both uncomplicated and severe forms of malaria (149). Due to the short half-life of artemisinin compounds, monotherapy is discouraged and combined treatments comprised of an artemisinin compound and a longer lasting anti-malarial agent is required to prevent recrudescence and reduce the likelihood of the development of artemisinin-resistance (149, 154, 155).

Although artemisinin compounds, including ART, have been used in the treatment of malaria for several decades, the mechanisms underlying the anti-malarial activity of these compounds have yet to be fully elucidated and remain controversial (159, 160). The anti-malarial activity of ART and other artemisinins is believed to be dependent on the presence of an endoperoxide bridge (147, 159). Studies suggest that the bioactivation of the endoperoxide bridge occurs within the infected erythrocyte when artemisinin interacts with free cellular iron or heme from digested host hemoglobin in the parasitic food vacuole (159, 160). Bioactivation is predicted to result in the production of ROS and carbon-centred radicals that cause the alkylation of parasitic proteins such as heme and the inhibition of the *Plasmodium* orthologue of sarco/endoplasmic reticulum Ca^{2+} ATPase, resulting in parasite destruction (154, 159, 161)

1.5.3 Anti-cancer Properties of ART

In the early 1990's artemisinin and its derivatives were found to have activity against cancer cells, albeit at higher concentrations than are required for the treatment of malaria (150, 162–164). Since this discovery, there has been great interest in the activity of these compounds against different types of cancer due to the excellent safety profile of ART, DHA and other derivatives (150, 165–177).

Although artemisinin and its derivatives may share similar mechanisms of activity, the majority of the work reported in the literature has focused on the anti-cancer effects of ART and its primary active metabolite DHA; however, a role for other metabolites has not been conclusively rules out. Although this overview will focus on ART, as this is the artemisinin derivative investigated in this thesis, the DHA literature will also be described due to the close relationship between these two compounds.

The exact mechanisms underlying the anti-cancer activities of ART remain elusive; however, there is strong evidence to suggest that some of the mechanisms involved in its anti-malarial activity may also be involved in killing cancer cells. The artemisinin endoperoxide bridge is important for both anti-cancer and anti-malarial activities of ART and its analogues (154, 159, 178). The presence of iron and the production of ROS have also been widely associated with the anti-cancer activities of ART (138, 168, 179). To date, ART and its metabolite DHA have been tested against cancer types that include melanoma, leukemia, retinoblastoma, epidermoid carcinoma, and pancreatic, gastric, and cervical cancers, with encouraging results (168, 171, 179–184). Moreover, healthy cells appear to be significantly more resistant to ART and DHA compared to their cancerous counterparts, suggesting that ART and DHA may be selective for cancer cells (171, 178, 182, 185–187).

The literature suggests that ART and DHA have both anti-proliferative and cytotoxic effects on cancer cells. Anti-proliferative effects have been described in multiple cancer cell types including osteosarcoma, hepatoma, and epidermoid carcinoma, and ovarian, colon, and non-small cell lung carcinomas (166, 173, 180, 185, 187, 188). The stage of ART- and DHA-induced cell cycle arrest appears to be cell-type specific since arrest in G1, G2/M and simultaneous arrest at all cell cycle stages have been reported (165, 180, 182, 189–191). ART and DHA-induced changes in cell cycle regulatory protein expression have been determined for several cancer cell lines and are likely involved in the anti-proliferative effect (166, 171, 172, 180, 192, 193). In addition, ART- and DHA-induced alteration of several cell signaling pathways has also been reported. For example, ART inhibits the hyperactive Wnt/β-catenin pathway and decreases the expression of target genes *c-myc* and *survivin* in colorectal cancer cells (194). Down-regulation of c-myc expression in ART-treated myeloma and lymphoma

cells has also been reported (183). Moreover, ART causes EGFR expression and Akt activity to decrease in lung cancer cells (176), and DHA caused decreased translocation and DNA binding of NFκB in pancreatic cancer cells (165).

ART and DHA-induced apoptotic cell death has been described in numerous cancer cell lines, although death through oncosis (cytoplasmic swelling) rather than apoptosis has been noted for certain pancreatic and gastric cancer cell lines (138, 168, 169, 185, 195–198). At this time, the specific mechanisms that underlie ART-induced cancer cell death are under intense investigation. ART-induced activation of the intrinsic and extrinsic mitochondrial pathways have been suggested to be responsible for pro-apoptotic effects in different cancer cell lines (138, 169, 171, 172, 185, 191, 199). Recent findings suggest that ART-induced DNA damage may contribute to its cytotoxic effects. Berdelle *et al*. (2011) demonstrated that ART induces ROS-dependent DNA damage in human glioma cells. Importantly, the specific players involved in ART-induced cancer cell death appear to vary depending on the cell type being tested; thus ART- and DHA-induced apoptosis can be both dependent and independent of caspases, BID and p53 (200). ART appears to exert a very broad range of effects on cancer cells, suggesting the involvement of multiple pathways to achieve the same end point with the differences in cell genetics and treatment conditions likely determining the predominant pathway(s) of cell death.

In addition to direct anti-proliferative and cytotoxic effects of ART on cancer cells, anti-angiogenic and anti-metastatic activities have also been attributed to ART and are likely to contribute to its *in vivo* effects (190, 201–206).

1.5.3.1 Anti-cancer Activity of ART *in vivo*

A number of studies have investigated the effects of ART and DHA on murine xenograft tumours. Largely positive results have strongly supported the further development of ART as an anti-cancer agent (166, 171, 172, 179, 187, 192). For example, treatment of established pancreatic cancer xenografts with 50 and 100 mg/kg i.p. of ART inhibited tumour growth by 44 and 65 %, respectively, compared to controls. Moreover, ART did not affect the body weight of the tumour-bearing mice, whereas a similarly-effective treatment of gemcitabine reduced body weight by 25 % (179). Nevertheless, a recent study in which 23 dogs with different canine cancers were treated

with ART only saw limited benefit. Nevertheless, 1 dog did achieve a complete remission, and 7 others maintained stable disease for at least 4 weeks. Some treatment toxicity was observed, including gastrointestinal toxicities, fever and a decreased hematocrit value in some dogs (207).

Two case studies have described the use of ART in the treatment of metastatic uveal melanoma and laryngeal squamous cell carcinoma in humans. In both cases, ART was well tolerated by all the patients and significantly increased patient survival time (184, 208). Furthermore, a pilot study conducted in the Ivory Coast used artenimol-R (a hemi-succinate ester of DHA) to treat advanced cervical cancer and showed significant benefit. A 28 d course of treatment led to rapid improvement in clinical symptoms and an average 6 month remission in all 10 patients. In addition, patients survived for an average of 12 months, which is significantly longer than the 4 month survival typical of this disease. Artenimol-R was well tolerated and none of the patients experienced severe side effects (209).

Taken together, the results from animal studies and early human trials further support the continued investigation of ART as an anti-cancer therapy. Importantly, ART is currently in a phase 1 clinical trial for the treatment of advanced and metastatic breast cancer (www.clinicaltrials.gov identifier: NCT00764036). Nevertheless, a more detailed understanding of ART's mechanism of action on cancer cells is needed to optimise its potential clinical application.

1.5.3.2 Anti-ovarian Cancer Activity of ART

At the present time, little is known about the mechanism of action of ART on ovarian cancer cells. An early study examined the effect of ART on 55 different cancer cell lines, including 6 ovarian cancer cell lines. A combined IC_{50} of 13.55 +/- 8.09 μM was determined for the ovarian cancer cells (150). In a more recent study, artemisinin and several of its derivatives, including DHA and ART, were tested against OVCA-432 and SKOV-3 ovarian cancer cells (185). All derivatives showed growth-inhibitory activity although the effect of DHA was slightly better than that of the other artemisinin derivatives. DHA subsequently showed good activity against a panel of different ovarian cancer cell lines (185). Ovarian cancer cells that express wild-type p53 are more sensitive

to DHA with an average IC_{50} of ~5 μM, while mutant lines are more resistant with an IC_{50} of ~ 15 μM. Normal ovarian epithelial cells are resistant to DHA in comparison to cancer lines, with IC_{50} ~50 μM (185). Similarly, potent and selective growth-inhibitory activity was reported for both ART and DHA in A2780 and OVCAR-3 ovarian cancer cell lines whereas the non-malignant ovarian epithelial cell line IOSE144 was significantly more resistant to DHA and ART (IC_{50} of 106.03 and >500 μM for DHA and ART, respectively), which further supports the selectivity of ART and DHA for cancer cells (169). It is of note that, in contrast to the previous study by Jiao *et al*. (2007), p53 mutant OVCAR-3 cells (IC50 ~7 μM) were more sensitive to both ART and DHA than the p53 wild-type A2780 cell line (IC50 ~17 μM) (169). Further studies with a larger sample of ovarian cancer cell lines is therefore required to confirm the importance of p53 status on DHA sensitivity. Interestingly, Wu *et al*. (2012) recently reported an IC_{50} of 25-50 μM DHA for the HO8910PM ovarian cancer cell line, which is a significantly higher IC_{50} value than was previously determined in any other ovarian cancer cell line (190). Differences in the length of treatment, cell line and methodology could account for the discrepancy between this and other studies of DHA activity in ovarian cancer cells. Using the 36 cell line Oncotest panel that includes 3 ovarian cell lines, Kelter *et al*. (2007) determined that OVXF-1619L and OVCAR-32 ovarian cancer cells are very sensitive to ART (IC_{50} of 0.5 and 1.16 μM ART), whereas OVXL-899L cells are quite resistant to ART (IC_{50} 46.7 μM ART), suggesting that variability exists in the sensitivity of ovarian cancer cells to ART. Interestingly, the co-administration of iron with ART enhances the growth-inhibitory effects of ART on the OVCAR-3 cell line, but negatively affects its activity in other ovarian cancer cells (151). Taken together, the broad spectrum of activity and selectivity of DHA and ART for ovarian cancer cells strongly supports the potential use of these agents in the treatment of this deadly form of cancer.

DHA treatment of ovarian cancer cells causes a dose-dependent G2/M cell cycle arrest and apoptosis characterised by increased Bax and Bad expression and decreased Bcl-2 and Bcl-x_L expression (185). Chen *et al*. (2009) also demonstrated DHA-induced apoptosis in the two ovarian cancer cell lines that they examined (A2780 and OVCAR-3). In this case, apoptosis was characterised by decreased mitochondrial membrane potential, PARP-cleavage, decreased Bcl-2 and total BID and increased activity of caspases 3,9,

and 8. FAS and FADD were also increased in DHA-treated cells, suggesting that both the extrinsic and intrinsic apoptotic pathways may be involved in DHA-induced cell death (169). DHA treatment also significantly inhibited the growth of ovarian cancer xenografts in mice. Western blotting of tumour samples showed similar molecular changes to those observed *in vitro,* i.e. increased caspase 8 activation, as well as increased Bax and decreased Bcl-2 expression (169). Furthermore, DHA enhanced the activity of carboplatin both *in vitro* and *in vivo* (169). A more recent study has reported that DHA also decreases ovarian cancer cell adhesion, migration and invasion *in vitro* (190). DHA was further tested in an *in vivo* orthotopic model of ovarian cancer, and, although DHA did not significantly affect tumour size, it did significantly reduce tumour cell metastasis (190). However, it is important to note the anti-proliferative and cytotoxic effects of ART were not determined in these experiments.

In summary, DHA and ART appear to have a broad and selective spectrum of activity against ovarian cancer cells. Although the mechanism(s) involved in the activity of ART are poorly understood, studies using DHA have shown G2/M cell cycle arrest and apoptosis in several ovarian cancer cell lines. *In vivo* studies using mouse models of ovarian cancer have also supported the benefit of DHA treatment in ovarian cancer. Taken together, these data support the potential use of DHA and ART in the treatment of ovarian cancer. Further work is now required to better understand the mechanisms underlying ART's anti-cancer activity. Furthermore, since ART is the most soluble derivative of artemisinin and the only form that can be given i.v., it is important to show that ART has the same effects as DHA on ovarian cancer cells (149, 154).

1.5.3.3 Anti-breast Cancer Activity of ART

ART and DHA have been reported to inhibit the growth of breast cancer cell lines, including MCF-7, T47D, MDA-MB-231, MDA-MB-468, MDA-N, BT549, HTB-27, MAXF 401NL, and MDA-MB-435 cells (138, 150, 151, 186, 191). Although ART has good growth-inhibitory activity against most breast cancer cell lines, the highly metastatic MDA-MB-231 TNBC line is relatively ART-resistant (206, 210). ART also failed to show significant inhibitory effects in the growth of MDA-MB-231 xenografts in mice (206). Moreover, pre-treatment of MBA-MB-231 cells with ART resulted in the development of resistance towards further ART treatment. Resistance to ART is

characterised by increased expression of the AP-1 subunit c-jun and NFκB subunit p65, and a decrease in the Bax/Bcl-2 ratio. Interestingly, similar resistance to ART did not develop in the less metastatic MDA-MB-468 TNBC line, although a slight decrease in inhibitory activity was determined following the initial pre-treatment (206). Down-regulation of p65 and c-jun were reported following both the initial and secondary treatment of MDA-MB-468 cells with ART (206). These results suggest that some forms of breast cancer may not benefit from ART treatment. Further research is therefore warranted to determine the mechanism(s) behind breast cancer cell resistance to ART.

Mao *et al.* (2013) reported that DHA induced a G1 cell cycle arrest and apoptosis in T47D breast cancer cells. Apoptosis was characterised by the release of cytochrome c from mitochondria, cleavage of caspase 9 and BID, and an increase in the Bim/Bcl-2 ratio. Interestingly, caspase 8 expression was also increased but its activation was not described (191). DHA also shows good activity against MCF-7 breast cancer cells and has been reported to enhance the growth-inhibitory and cytotoxic effects of doxorubicin (210). In addition, additive effects were reported for combined ART and gemcitabine or oxaliplatin co-treatment of MCF-7 cells (189). ART monotherapy induces a G1 arrest at doses below 30 μM, whereas higher concentrations lead to broad spectrum arrest at all phases of the cell cycle. Cell cycle arrest was characterised by decreased cyclin D, CDK4 and p-Rb expression and increase p21 expression (189). Moreover, recent work using a holo-transferrin (HT)-conjugated form of DHA (4-(12-dihydroartemisininoxy) benzoic acid hydrazide) shows that conjugation enhances DHA-induced growth-inhibitory effects over 170-fold in MCF-7 cells while slightly decreasing DHA activity against normal breast epithelial cells (211).

ART causes apoptosis and necrosis in MCF-7 breast cancer cells through ROS-dependent permeabilisation of the mitochondrial membrane (138). Apoptosis was characterised by mitochondrial Bax clustering and cytochrome c release. Interestingly, neither BID nor cathepsins D, B, and L impacted on ART-induced death of MCF-7 cells. The cytotoxic activity of ART required functional lysosomes, and ART-induced ROS production and subsequent apoptosis could be inhibited with the endolysosomal iron chelator deferoxamine (DFO). The addition of HT enhanced ART-induced cell death, suggesting a role for lysosomal iron in the anti-breast cancer activity of ART. A similar

ROS- and iron-dependent effect was noted in ART-treated T47D and MDA-MB-231 breast cancer cells; however, no effect was seen on untransformed MCF-10A breast epithelial cells (138). The enhancement of ART-mediated killing of MCF-7 cells by HT conflicts with a previous report wherein the addition of iron II glycine sulfate decreased the growth-inhibitory activity of ART on MCF-7 cells (151); however, differences in the iron formulation and dosage could have contributed to the different outcomes. Furthermore, Hamacher-Brady *et al*. (2011) cultured MCF-7 cells in serum-free Krebs-Henseleit solution, (a basal salt solution containing defined levels of glucose), whereas Kelter *et al*. (2007) used FBS-supplemented DMEM. It is therefore conceivable that differences in nutrient availability impacted the cellular responses observed in these two studies. The enhancing effect of iron on breast cancer cell killing by DHA and ART has also been reported in other breast cancer cell lines, including HTB-27 and MAXF 401NL cells, respectively (151, 186).

A novel study that examined the effect of DHA on iron absorption determined that DHA causes iron depletion in MCF-7 breast cancer cells, which suggests that the involvement of iron in the activity of ART and DHA may not be limited to ROS induction (175). In this regard, DHA decreases the expression of iron homeostasis regulating proteins Steap3 and divalent metal transporter 1 (DMT1) in a ROS-independent manner in MCF-7 breast cancer cells and HepG2 hepatoma cells (175). In addition, DHA decreases surface CD71 expression in an abnormal lipid raft/ caveolae-mediated fashion. CD71 (aka transferrin receptor 1) binds HT and mediates iron uptake through receptor-mediated endocytosis (212). Steap3 is a ferrireductase that converts endosomal ferric iron to its ferrous form, while DMT1 transports ferrous iron into the cytoplasm (212, 213). CD71 expression is regulated by cellular iron levels (214) and is of special interest in cancer research as increased expression of this receptor is common in many neoplastic cells (214). Zhou *et al*. (2008) and Ba *et al*. (2012) examined the effect of ART and DHA on CD71 expression in HL60 leukemia and MCF-7/HepG2 cancer cells, respectively. Although they obtained conflicting results, both groups observed that DHA decreases surface CD71 expression. Furthermore, Ba *et al*. (2012) observed that the growth-inhibitory effects of DHA could be partially negated by siRNA-inhibition of CD71 expression, supporting a role for CD71 in the anti-neoplastic activity of DHA

(175). New evidence suggests that ART and its metabolite DHA may not only down-regulate CD71 expression, but that CD71 may also facilitate ART uptake. ART-internalisation and cytotoxicity in retinoblastoma cells is significantly inhibited when CD71 expression was repressed (182). Moreover, normal retinal pigment epithelial cells, which express only low levels of CD71 compared to the Rb cell line, are resistant to ART and internalise only a small amount of the drug (182). A correlation between cellular response to ART and CD71 expression has also been shown in a panel of 55 different cancer cell lines, which further supports the importance of CD71 in the anti-cancer activity of ART (151). Together, these findings suggest that CD71 may be involved in the cellular uptake of ART/DHA and play a role in the selective nature of these compounds for cancer cells. Furthermore, in addition to ROS-dependent cytotoxic activity, ART and its metabolite DHA may also exert anti-cancer effects through the depletion of cellular iron.

In summary, ART has both anti-proliferative and cytotoxic effects on breast cancer cells. Novel mechanisms of iron depletion and lysosome-dependent activity by ART and DHA have been recently described. However, it is important to note that the majority of the reports examining ART and DHA activity have used ER- and PR-positive breast cancer cell lines rather than TNBC or HER2-overexpressing cell lines (138, 175, 189, 191). Further research into the mechanisms by which ART inhibits the growth of HER2-overexpressing and TNBC lines is therefore necessary, given the evidence that effects can be cell type specific.

1.5.4 Safety of ART

ART has been used for many years in the treatment of malaria and large studies have not shown any significant adverse effects of ART treatment (152, 153). Common minor side effects include fever, nausea, diarrhea and vomiting. Neurologic toxicities have been a concern after ART and DHA were found to be cytotoxic for cultures of neuronal cells (215, 216). Some animal studies have reported neurologic issues following ART treatment; however, neurotoxicity has not been associated with the use of ART in humans (153, 217, 218). Furthermore, neurotoxicity in animal models is more closely associated with the oil-soluble artemether and arteether analogues (218). Embryotoxic effects of artemisinin compounds have been reported in cell culture and animal models,

although these effects have not been observed in humans (219–221). To date, clinical studies have not been large enough to detect rarer pregnancy-associated issues following treatment with artemisinin compounds. Further study is therefore warranted to ensure the safe use of these compounds during pregnancy (218). Artemisinin compounds are currently not recommended for the treatment of women in their first trimester of pregnancy (149).

1.6 Research Rationale and Objectives

Breast and ovarian cancers place a significant burden on society. In addition, novel treatments are needed to combat drug-resistant forms of breast and ovarian cancer. ART is a safe, well established, anti-malarial agent with potent anti-cancer activities that have potential for use in cancer treatment. Although there is currently great interest in the anti-cancer activities of ART, the mechanisms involved in its activity, especially in relation to its effects against breast and ovarian cancer cells remain poorly understood. An improved understanding the effect of ART on breast and ovarian cancer cells and its mechanisms of action will help to determine whether this compound has future use in the treatment of these cancers. In addition, a more complete understanding of the actions of ART on breast and ovarian cells will help to determine possible mechanisms of resistance and will aid in the development of optimal treatment strategies using ART as monotherapy or in combination with established chemotherapeutic agents. I hypothesise that the anti-cancer effects of ART are cell-type specific and are similar to those of DHA.

The objectives of this thesis are:

1) To determine the anti-proliferative and cytotoxic effects of ART on breast and ovarian cancer cells.
2) To investigate the mechanisms of action of ART in breast and ovarian cancer cells, including the effects of ART on cell death and proliferative pathways.

CHAPTER 2.0: MATERIALS AND METHODS

2.1 Reagents.

Artesunate (ART), propidium iodide (PI), 3-(4,5-Dimethylthiazol-2-yl)-2,5-diphenyltetrazolium bromide (MTT), reduced glutathione (GSH), aprotinin, bovine serum albumin (BSA), dimethyl sulfoxide (DMSO), leupeptin, β-mercaptoethanol (β-ME), nonidet P-40 (NP-40), pepstatin A, phenylarsine oxide (PAO), phenylmethylsulfonyl fluoride (PMSF), sodium fluoride (NaF), phosphate buffered saline (PBS), SB-366791, sodium deoxycholate, Triton X-100, phosphatase substrate, deferiprone (3-Hydroxy-1,2-dimethyl-4(1*H*)-pyridone) (DFE), necrostatin-1 (nec-1), Dulbecco's Modified Eagle's Medium (DMEM) D5796, DMEM D1145, Medium 199 and MCDB 105 medium were all purchased from Sigma-Aldrich Canada (Oakville, ON). DNase-free RNase A was purchased from Qiagen Inc. (Mississauga, ON). Cell trace Oregon Green® 488 and 5-(and-6)-chloromethyl-2',7'-dichlorodihydrofluorescein diacetate, acetyl ester (CM-H_2DCFDA) were purchased from Molecular Probes (Eugene, OR, USA). Annexin-V-FLUOS was purchased from Roche Diagnostics (Laval, QC). Bio-Rad protein assay dye reagent concentrate was purchased from BioRad (Hercules, CA). Fetal bovine serum (FBS), L-glutamine, 10,000 units/mL penicillin/10,000 μg/mL streptomycin, 1 M 4-(2-hydroxyethyl)-1-piperazineethanesulfonic acid (HEPES) buffer solution, 0.25% trypsin-EDTA, and B27 serum-free supplement were purchased from Invitrogen Canada Inc. (Burlington, ON). Sodium orthovanadate (Na_3VO_4) and calcium chloride ($CaCl_2$) were purchased from EMD Chemicals, Inc. (Gibbstown, NJ). Disodium hydrogen phosphate (Na_2HPO_4) and ethylene diamine tetraacetic acid (EDTA) were purchased from EM 46 Industries Inc. (Hawthorne, NY). Dithiothreitol (DTT), ethylene glycol tetraacetic acid (EGTA), paraformaldehyde (PFA), sodium chloride (NaCl), sodium dodecyl sulfate (SDS), Tris base and Tween-20 were purchased from Bio-Shop Canada Inc. (Burlington, ON). Basic fibroblast growth factor (bFGF) and epidermal growth factor (EGF) were both purchased from PrproTech (Dollard des Ormeaux, QC). Luminata™ Forte Western HRP Substrate was purchased from Millipore (Billerica, MA). DMSO was used as the vehicle for ART; ART stock was made up at 100 μM in DMSO and was stored in aliquots at -20°C until use.

2.2 Antibodies.

Anti-p21 (DCS22) mouse monoclonal antibody (mAb), anti-phospho (p)-Chk2 (Thr68) rabbit polyclonal antibody (pAb), anti-cyclin D3 (DCS83) mouse mAb, anti-CDK4 (DCS156) mouse mAb, anti-retinoblastoma protein (Rb) (4H1) mouse mAb, and anti-p-histone (γH2AX) (Ser139) rabbit mAb were purchased from Cell Signaling Technology Inc. (Beverly, MA). Poly(ADP-ribose) polymerase-1 (PARP-1) mouse mAb, bovine anti-goat IgG- horse-radish peroxidase (HRP), goat anti-mouse IgG-HRP, donkey anti-rabbit IgG-HRP, and anti-actin (I-19) goat pAb were all purchased from Santa Cruz Biotechnology (Santa Cruz, CA). Anti-cyclin B1 mouse mAb, anti-CDK1 (PSTAIR) rabbit pAb, anti-CDK2 (clone AN4.3) mouse mAb, anti-CDC25C (clone TC-15) mouse mAb, anti-cyclin A (clone BF 683) mouse mAb, anti-E2F-1 (clones KH20 and KH95) mouse mAb were purchased from Millipore. Anti-Smac/DIABLO (Y12) rabbit mAb was purchased from Epitomics (Burlingame, CA). Mouse anti-human CD71 (OKT9) fluorescein isothiocyanate (FITC) and its isotype control, mouse anti-human IGg1κ FITC were purchased from eBioscience (San Diego, CA). Mouse anti-human cytochrome c mAb was purchased from BD Biosciences (Mississauga, ON).

2.3 Cell Culture.

2.3.1 Culture of Cancer Cell Lines.

HEY1 and HEY2 ovarian cancer cell lines were subclones of HEY cells, which were a kind gift from Dr. M. Nachtigal (University of Manitoba, Winnipeg, MB). IGROV-1, OVCAR8 and OVCAR3 ovarian cancer cells and SK-BR-3 breast cancer cells were provided by Dr. G. Dellaire (Dalhousie University, Halifax, NS). TOV-21G, OV-90 and TOV-112D ovarian cancer cells were kindly gifted by Dr. Jules Dore from Memorial University of Newfoundland (St John's, NF). SKOV-3 ovarian cancer cells were a generous gift from Immunovaccine (Halifax, NS). MDA-MB-468 breast cancer cells and the ID8 mouse ovarian carcinoma cell line were a gift from Dr. P. Lee (Dalhousie University). TX400 MCF-7 cells and native MCF-7 human breast cancer cells were a kind gift from Dr Goralski (Dalhousie University). MDA-MB-231 human breast cancer cells were generously provided by Dr S. Drover (Memorial University of Newfoundland,

St John's, NL). The T47D human breast cancer cells were a gift from Dr J. Blay (University of Waterloo, Waterloo, ON).

All breast cancer lines, as well as SKOV-3, HEY, OVCAR8, IGROV-1, OVCAR3 and ID8 ovarian cells were grown in DMEM (D5796) supplemented with 10 % heat-inactivated (HI) (56°C for 30 min) FBS, 2 mM L-glutamine, 5 mM HEPES buffer (pH 7.4), 100 U/mL penicillin, and 100 µg/mL streptomycin; henceforth, referred to as complete DMEM (cDMEM). TX400 MC-F7 cell medium was supplemented with 400 ng/mL paclitaxel to maintain drug resistance. Cells were cultured for one passage without paclitaxel prior to use in experiments. TOV-21G, OV-90 and TOV-112D ovarian cancer cells were grown in a 1:1 ratio of Medium 199 : MCDB 105 medium, supplemented with 10 % HI FBS 2 mM L-glutamine, 1.5 g/L sodium bicarbonate, 5 mM HEPES buffer (pH 7.4), 100 U/mL penicillin, and 100 µg/mL streptomycin; henceforth, referred to as complete ovarian cancer cell medium (cOVM). Cells were propagated as required in T-75 mm^2 tissue culture flasks and cultured at 37°C in 10% or 5 % CO_2 humidified atmosphere for cells grown in cDMEM and cOVM respectively.

2.3.2 Ovarian Cancer Spheroid Culture.

Ovarian cancer cells were seeded at 8,000 cells/well into ultra low attachment Costar 6-well plates and spheroids were allowed to develop for 5 or 6 d (HEY1 and HEY2 lines, respectively) before use. Ovarian cancer spheroids were cultured in cDMEM and cells were fed every 72 h.

2.3.3 Breast Cancer Spheroid Culture.

MCF-7 spheroids were cultured in mammosphere medium (F12 medium supplemented with 20 ng/mL bFGF, 20 ng/mL EGF, 100 U/mL penicillin, 100 µg/mL streptomycin and 1x B27 serum-free supplement) at 37°C in a 10% CO_2 humidified atmosphere. MCF-7 cells were seeded at 30,000 cells/well into ultra low attachment Costar 6-well plates and spheroids were allowed to develop for 7 d prior to use. Spheroids were fed every 72 h.

2.4 Breast and Ovarian Cell Seeding and Harvesting.

After seeding, cells from all lines used were allowed to adhere to their respective plates/flasks overnight prior to treatment with ART and/or other agents.

2.4.1 Human Ovarian Cancer Cell Line Seeding.

All human ovarian cancer cell lines were seeded at the same densities. Unless otherwise indicated, 96-well plates were seeded at a density of 1,500 cells/well, 6-well plates were seeded at 20,000 cells/well and T75 flasks for western blot analysis were seeded at 250,000 cells/flask.

2.4.2 Murine Ovarian Cancer Cell Line Seeding.

Since the ID8 murine ovarian cancer cells proliferated at a significantly greater rate than their human counterparts, plates needed to be seeded at lower densities to avoid the problem of over-confluency. Unless otherwise indicated, 96-well plates were seeded at a density of 500 cells/well and 6-well plates were seeded at 10,000 cells/well.

2.4.3 Breast Cancer Cell Line Seeding.

For the MDA-MB-468 and MDA-MB-231 cell lines, unless otherwise indicated, 96-well plates were seeded at a density of 5,000 cells/well, 6-well plates were seeded at 50,000 cells/well and T75 flasks for western blot analysis were seeded at 700,000 cells/flask. For the SK-BR-3, MCF-7, TX400 MCF-7 and T47D cell lines, unless otherwise indicated, 96-well plates were seeded at a density of 10,000 cells/well, 6-well plates were seeded at 100,000 cells/well and T75 flasks for western blot analysis were seeded at 800,000 cells/flask.

2.4.4 Cell Harvesting.

Unless otherwise noted, both the non-adherent and adherent cells were harvested after ART treatment. Cell supernatant containing non-adherent cells was transferred to a tube and adherent cells were detached using TrypLE reagent for 3 min at 37°C. Detached cells were then added to the tube containing the culture supernatant. Cells were then centrifuged at 500 x *g* for 5 min and the supernatant was discarded. Cells were then washed and lysed or stained depending on the assay being used. All washes were by centrifugation at 500 x *g* for 5 min.

2.5 Flow cytometry.

Flow cytometry was performed on a FACSCalibur flow cytometer using Becton Dickinson (BD) CellQuest™ software (version 3.3; BD Biosciences, Mississauga, ON). A minimum of 10,000 live cell counts were acquired per sample with the exception of the following experiments: the cell death assay and analysis of changes in mitochondrial membrane stability, in which a total count of 10,000 cells (including those alive and dead) were acquired. In the case of cell cycle analysis event acquisition was decreased to a maximum of 70 cells/second and cells were gated to ensure that data was collected for 10,000 live, single cells (aggregated cells were excluded as they would confound cell cycle classification). Unless otherwise described, acquired data were analysed using FCS Express software (version 3.0; De Novo Software, Thornhill, ON).

2.6 MTT Assay.

Mitochondrial succinate dehydrogenase activity was used to assess cell growth and viability using a modified (3-(4,5-dimethylthiazol-2-yl)-2,5-diphenyltetrazolium bromide (MTT) assay (222). MTT is converted by mitochondrial succinate dehydrogenases to an insoluble purple formazan crystal. Differences in viable cell number are reflected in the amount of formazan produced, which can be quantified by colourometric analysis following solubilisation in DMSO.

Breast and ovarian cancer cells, seeded into 96-well plates, were treated with medium, vehicle or increasing concentrations of ART and incubated for the desired time. MTT was added to cultures to a final concentration of 0.5 μg/mL 2 h prior to cell harvesting for all cell lines with the exception of TOV-21G, OV-90 and TOV-112D cell lines, which were cultured with MTT for 4 h. Plates were centrifuged at 1,400 x *g* for 5 min, supernatant was discarded and formazan crystals were solubilised in 100 μL DMSO. Changes in well optical density (OD) were determined at 490 nm using a Asys Expert 96 Microplate Reader from Biochrom (Cambridge, UK). Changes in the % decrease in viable cell number are shown relative to the medium control.

2.6.1 Pre-treatment with holo-transferrin.

Breast cancer cells were treated for 1 h with 10 μM holo-transferrin (HT) or its vehicle (ddH_2O) at 37°C. Following treatment, HT-containing medium was removed and cells were treated with ART. Changes in cell number were assessed using the MTT assay as described above.

2.6.2 Combined Modality Treatments.

Breast cancer cells were pre-treated for 1 h with ART or its vehicle, then exposed to the desired concentrations of cisplatin, fluorouracil (FU), docetaxel, 4-hydroxycyclophosphamide (4-HC) or doxorubicin for 72 h. Changes in cell viability were assessed using the MTT assay as described above.

2.6.3 Combined Treatment of ART and Ionizing Radiation.

Breast cancer cells were seeded at 37,500 cells/well into 4-well plates (1.9 cm^2/well) and allowed to adhere overnight. Cells were treated for 1 h with ART or its vehicle, then exposed to 0-4 Gray (Gy) γ-irradiation using a GC-3000 ^{137}Cs source γ cell irradiator (MDS Nordion, Ottawa, ON). Following irradiation, plates were incubated at 37°C for 72 h. Changes in cell viability were assessed by MTT assay as described above; however, in this case, formazan crystals were solubilised in 0.45 mL DMSO (due to the increased well size) and 100 μL of the solution in quadruplicate was transferred to a 96-well flat-bottom plate for analysis at 490 nm as described above.

2.7 Acid Phosphatase Assay.

Cytoplasmic acid phosphatase activity was used to assess cell viability in the comparison of ART-treated TX400 MCF-7 and native MCF-7 cell lines since the increased expression of p-glycoprotein in the TX400 cells interfered with the use of MTT (223). MCF-7 and TX400 MCF-7 cells, seeded into 96-well plates, were treated with ART or its vehicle for the desired time. Following treatment, cells were washed in PBS, then incubated for 90 min at 37°C in a 1:1 ratio of 100 μL PBS and 100 μL phosphatase assay buffer (0.1 M sodium acetate pH 5.5, 1 μL/mL Triton X-100 and 4 mg/mL phosphatase substrate). Following the incubation, 10 μL 1 N sodium hydroxide (NaOH) was added to each well and OD was determined at 405 nm using an Asys Expert 96 Microplate Reader.

Changes in the % decrease in cellular acid phosphatase activity are shown relative to the medium control.

2.8 Acid Phosphatase Assay of Spheroids.

Following spheroid development, spheroids were treated with ART or vehicle for 72 or 96 h (for breast cancer and ovarian cancer spheroids, respectively). Following incubation, spheroids were washed in PBS and then resuspended in a 1:1 ratio (final volume 1 mL) of PBS and phosphatase solution (0.1 M sodium acetate pH 5.5, 0.1% Triton X-100, 4 mg/mL phosphatase substrate) and incubated for 90 min at 37°C in the dark. Following the incubation, 50 µM 1 N NaOH /mL was added to each tube, the solution was then centrifuged at 1000 x *g* for 5 min. The supernatant was transferred to a 96-well plate and the absorbance was determined at 405 nm using an Asys Expert 96 Microplate Reader. A phosphatase assay rather than an MTT assay was used for spheroid analysis as MTT would be unable to access the inner cells of the spheroids. As cells are lysed prior to the analysis of acid phosphatase activity, spheroids were disassociated and acid phosphatase activity could be determined for the entire spheroid cell population.

2.9 Annexin-V-FLUOS/PI Flow Cytometric Analysis.

Breast and ovarian cancer cells, seeded into 6-well plates, were treated with ART or its vehicle then incubated for the desired time. Following incubation, non-adherent and adherent cells were harvested and washed with PBS. Following washing, cells were stained with Annexin V-FLUOS (diluted as per the manufacturer's instructions) and PI (1 µg/mL) in 50 µL detection buffer (10 mM HEPES, 140 mM NaCl, and 5 mM $CaCl_2$) for 15 min at room temperature. Annexin-V-FLUOS is cell impermeable and binds phosphatidyl serine that has flipped from the inner to the outer leaflet of the cell membrane, a biochemical hallmark of apoptosis (81). The binding of fluorescent PI to DNA, indicates loss of cell membrane integrity. Following incubation, 250 µL of detection buffer was added to each tube prior to analysis. Early and late apoptotic cell death was detected by flow cytometry. Early apoptosis (%) represents the percentage of cells which stained positive for Annexin-V-FLUOS and negative for PI. Late

apoptosis/necrosis (%) represents the percentage of cells which stained positive for both Annexin-V-FLUOS and PI.

2.9.1 Importance of Iron on ART-induced Cell Death.

2.9.1.1 Effect of Increased Iron on ART-induced Cancer Cell Death.

To determine the effect of increased iron on ART-induced cell death, cells were pre-treated with 10 μM HT or its vehicle (ddH_2O) for 1 h. Following treatment, HT was removed and cells were treated with ART or its vehicle for 48 h, then harvested and analysed as described above.

2.9.1.2 Effect of Decreased Iron Availability on ART-induced Cancer Cell Death.

The iron chelator deferiprone (DFE) was used to evaluate the importance of iron in ART-induced apoptosis. Ovarian and breast cancer cells were pre-treated with DFE for 30 min prior to ART addition. Following 48 h ART-treatment, cells were subsequently harvested and analysed as described above. The final concentration of DFE was 12.5 μg/mL.

2.9.2 Importance of Caspase Activity on ART-induced Cytotoxicity.

To investigate whether ART-induced cell death is mediated through a caspase-dependent pathway, cells were pre-treated with Z-VAD-fmk, a pan-caspase inhibitor, or its vehicle (DMSO) for 1 h prior to ART addition. The final concentration of Z-VAD-fmk was 50 μM. Following treatment, cells were incubated, harvested, and analyzed as described above.

2.9.3 Importance of The Necroptotic Pathway in ART-induced Cytotoxicity.

To determine whether ART treatment induced necroptosis, breast and ovarian cancer cells were pre-treated for 1 h with necrostatin-1 (nec-1), a RIPK1 kinase inhibitor, prior to ART treatment for 48 h. The final concentration of nec-1 was 40 μM. Following treatment, the amount of cell death was determined as described above.

2.9.4 Importance of ROS in ART-induced Cancer Cell Death.

To determine the importance of ROS on ART-induced breast and ovarian cancer cell apoptosis, cells were pre-treated with GSH for 30 min prior to ART addition. Samples were then harvested and analysed as described above. The final concentration of GSH was 10 mM.

2.9.5 Oxygen Requirement for ART-induced Cancer Cell Death.

To examine the requirement of oxygen for ART-induced cancer cell death, MDA-MB-468 breast cancer cells were treated with ART then incubated under hypoxic conditions (0.5 % oxygen) in a C-Chamber hypoxic unit (BioSpherix, Lacona, NY), or under normoxic conditions for 48 h. In addition to the previous conditions, ART-treated cultures were also incubated first for 24 h under normoxic conditions than transferred to the hypoxic chamber for an additional 24 h. At the end of culture cell death was determined by Annexin-V-FLUOS and PI staining as detailed above.

2.10 Detection of ART-induced Caspase Activation.

Breast and ovarian cancer cells were seeded into 6-well plates and the following day cells were treated with ART or its vehicle. Following 48 h of treatment, cells were harvested and stained for 1 h at 37˚C with the fluorescent inhibitor of caspases (FLICA) reagent as per the manufacturer's instructions (Vybrant® FAM Poly Caspases Assay Kit, Invitrogen). Following staining, cells were washed as per the manufacturer's directions and changes in ART induced fluorescence were determined by flow cytometry.

2.11 Determination of Changes in Mitochondrial Membrane Stability.

Breast cancer cells were cultured in the presence of ART or its vehicle for the desired time. Following culture, cells and their culture supernatants were harvested and incubated for 15 min at room temperature with 40 nM 3,3′-dihexyloxacarbocyanine iodide ($DiOC_6$) in cDMEM before analysis by flow cytometry. Decreased $DiOC_6$ fluorescence signifies a loss of mitochondrial membrane stability.

2.11.1 Importance of ROS in ART-induced Changes in Mitochondrial Membrane Stability.

Breast cancer cells were pre-treated with GSH for 30 min prior to the addition of ART. Following culture, changes in mitochondrial membrane stability were assessed as described above.

2.12 Detection of Intracellular ROS production.

Breast and ovarian cancer cells were seeded at 100,000 cells/well into 6-well plates and allowed to adhere overnight. The following day adherent cells were washed with warm PBS and then stained in phenol-red- and serum-free DMEM supplemented with 2 mM L-glutamine, 5 mM HEPES buffer (pH 7.4), 100 U/mL penicillin, and 100 µg/mL streptomycin containing 5 µM CM-H_2DCFDA for 30 min in the dark. Once in the cell, CM-H_2DCFDA is cleaved by esterases and remains trapped within the cell, becoming highly fluorescent upon oxidation by ROS. Following the incubation, the staining solution was removed and cells were washed with warm PBS. For the remainder of the experiment, cell culture was performed in DMEM further supplemented with 1% HI FBS. To confirm the production of ROS, cells were pretreated with GSH for 30 min prior to the addition of ART or its vehicle and incubation for 8 or 24 h. H_2O_2 was used as a positive control. Cells and their culture supernatants were then harvested and resuspended in ice-cold PBS prior to analysis by flow cytometry. As changes in CM-H_2DCFDA-induced fluorescence were in the lower logarithmic range and ART possesses a low level of auto-fluorescence, unstained cells treated with ART or vehicle were also analysed to confirm that changes observed were due to increased ROS production rather than ART treatment. ART's auto-fluorescence levels were subtracted from CM-H_2DCFDA-treated cell fluorescence prior to further calculations. ROS production relative to the medium control was calculated using the following formula MCFS- AUTO/MCFM x 100 % where MCFS is the mean channel fluorescence of the sample, AUTO is the auto-fluorescence of ART and MCFM is the mean channel fluorescence of the medium control.

2.12.1 Effect of Increased Iron on ROS Production.

Following CM-H_2DCFDA staining, cells were pre-treated with 10 µM HT for 1 h. Following treatment, HT was removed and cells were treated with ART or its vehicle as described above.

2.13 Cell Proliferation Assay.

Cancer cells were seeded into 6-well plates and allowed to adhere overnight. The following day cells were stained with 1.25 μM Cell Trace Oregon Green® 488 for 45 min. Following staining, cells were washed 3x with cDMEM, then allowed to recover for 2-3 h. Baseline controls were harvested, fixed in 1% PFA and stored at 4°C until use. The remaining wells were treated with ART or its vehicle for 72 h prior analysis by flow cytometry. As Oregon Green® 488-stained cells divide, their fluorescence is halved, thus the number of cell divisions (n) was calculated using the mean channel fluorescence (MCF) of the sample (MCF_{sample}) and the MCF of the baseline control ($MCF_{baseline}$) as follows: $MCF_{baseline} = (2^n)(MCF_{sample})$.

2.13.1 Importance of ROS in the Anti-proliferative Activity of ART.

Cell Trace Oregon Green® 488-stained ovarian and breast cancer cells were pre-treated with GSH for 30 min prior to the addition of ART. The final concentration of GSH was 10 mM. Following culture, changes in the number of cell divisions were assessed as described above.

2.13.2 Importance of Iron in the Anti-proliferative Activity of ART.

Cell Trace Oregon Green® 488-stained ovarian cancer cells were pre-treated with DFE for 30 min prior to the addition of ART. The final concentration of DFE was 12.5 μg/mL. Following culture, changes in the number of cell divisions were assessed as described above.

2.14 ART Wash-out MTT Assay.

Ovarian cancer cells were treated with ART or its vehicle for 72 h in 96-well plates, then the first time point was analyzed by MTT assay. Supernatants from the remaining wells were removed and replaced with drug-free cDMEM. Following ART removal, the ability of the cancer cells to regain their proliferative capacity was evaluated by MTT assay every 48 h, over the course of 6 d. Medium and vehicle controls were used to control for confluence effects.

2.15 Cell Cycle Analysis.

Ovarian and breast cancer cells were serum starved for up to 24 h to synchronize their cell cycles to G0. Cells were then seeded in cDMEM into 6-well plates and allowed to adhere overnight. GSH was added to the cancer cells for 30 min prior to the addition of ART or vehicle and then cultured for another 48 h. The final concentration of GSH was 10 mM. Cells were harvested, washed in cold PBS and resuspended in 0.5 mL cold PBS. Ice cold 70 % ethanol was then added slowly drop by drop to a final volume of 5 mL, while the cells were vortexed continuously. Samples were then stored at -20°C for a minimum of 24 h. On the day of analysis, cells were washed in 5 mL PBS, then resuspended in PI solution (0.1% v/v Triton X-100 in PBS containing 0.2 mg/mL DNase-free RNase A and 0.02 mg/mL PI) and incubated for 30 min at room temperature before analysis by flow cytometry. Cellular DNA content is specific to the different phases of the cell cycle; cells in G0/G1 possess 1 copy of DNA, while cells in the G2 and S phase contain 2 copies or an intermediate amount, respectively. As PI, a fluorescent DNA intercalating agent, bound cells relative to their DNA content, the fluorescence level of stained cells could be used to determine their cell cycle stage. The DNA content of single, live cells was analyzed using ModFit LT 3.0 (Verity Software House, Topsham ME USA).

2.16 Analysis of CD71 Surface Expression.

Breast and ovarian cancer cells were treated with ART or vehicle for 24 h in 6-well plates. Following culture, cells were harvested using 10 mM EDTA, washed once in ice cold FACS buffer (0.2 % sodium azide and 1 % BSA in PBS), then stained for 1 h at 4˚C with mouse anti-human CD71 (OKT9) FITC or its isotype control (mouse anti-human IGg1κ FITC). Cells were then washed 3x in cold FACS buffer (0.2% sodium azide and 1% BSA in PBS), fixed in 1 % PFA and stored at 4˚C until fluorescence levels were determined by flow cytometry.

2.17 Colony Forming Assay.

A colony forming assay (CFA) was used to determine the effect of ART on the clonogenic ability of MDA-MB-468 breast cancer cells. Breast cancer cells were treated with ART or vehicle in T75 flasks and cultured for 24 h. Following treatment, cells and culture supernatant were harvested and the live cell number was ascertained. Equal numbers of cancer cells were then serially diluted and plated in fresh cDMEM into new 6-well plates. This was done in triplicate at concentrations of 2,000/1,000/500/250 cells/well. Plates were incubated 13-14 d to allow for the formation of colonies. Cells were fed as required. On the day of the harvest, medium was removed and colonies were washed with PBS. Colonies were then fixed and stained with 1 mL crystal violet (0.4% crystal violet in methanol) for 10 min. Crystal violet was then removed and wells were washed with dH_2O. Stained colonies containing >50 cells were counted.
Surviving fraction (SF) and plating efficiency (PE) were calculated as follows (224):
PE= # of colonies formed in the medium control / # of cells seeded
SF= (# of colonies formed after treatment) / (# of cells seeded * PE))* 100%

2.17.1 Combined Modality Colony Forming Assay

The CFA was conducted as described above with the exception that breast cancer cells were treated with a combination of ART and 0.1 μM cisplatin for 24 h. Cells were treated with ART 1 h prior to cisplatin addition.

2.18 SDS-PAGE and Western Blotting.

Ovarian and breast cancer cells were treated with ART or its vehicle in T75 flasks and cultured for the desired time. For the investigation of the effects of ROS on ART-induced changes in protein expression, GSH at a 10 mM final concentration was added 30 min prior to ART or vehicle treatment. Following incubation, cells were harvested, washed 2x with cold PBS, then lysed on ice for 30 min in 50 μL RIPA lysis buffer (1% NP-40, 0.5% sodium deoxycholate, 0.1% SDS, 20 mM Tris, 150 mM NaCl, 1 mM EDTA, 1 mM EGTA pH 7.5 with 5 μg/mL leupeptin, 5 μg/mL pepstatin, 10 μg/mL apotinin, 100 μM sodium orthovanadate, 1 mM DTT, 10 mM sodium fluoride, 10 μM phenylaesine oxide and 1 mM PMSF). Following lysis, samples were centrifuged at 14,000 x *g* at 4°C for 10

min. The protein concentration of cell lysates was determined using the Bio-Rad protein assay dye reagent as per the manufacturer's instructions. When isolating only the cytoplasmic cell fraction, digitonin lysis buffer (75 mM NaCl, 1 mM NaH_2PO_4, 8 mM Na_2HPO_4, 250 mM sucrose and 190 µg/mL digitonin with 5 µg/mL leupeptin, 5 µg/mL pepstatin, 10 µg/mL apotinin, 100 µM sodium orthovanadate, 1 mM DTT, 10 mM sodium fluoride and 10 µM phenylaesine oxide) was used in place of the RIPA lysis buffer. In this case, samples were only lysed on ice for 15 min. Following incubation samples were centrifuged at 1,000 x *g* 4°C for 5 min to remove unlysed cells. The cell lysate was then centrifuged at 14,000 x *g* at 4°C for 10 min and the protein concentration was determined using the Bio-Rad protein assay dye. Equal amounts of protein were resolved on 15, 12, or 7.5 % polyacrilamide gels (depending on desired protein size) for 1 h at 200 V. Following glycine SDS-PAGE, protein was transferred onto a nitrocellulose membrane using the iBlot transfer system (Invitrogen) as per the manufacturer's instructions. Membranes were blocked for 1 h or overnight in Tris buffered saline (200 mM Tris, 1.5 M NaCl pH 7.6) containing 0.05% Tween-20 (T-TBS) with 5 % w/v skim milk powder. Blots were then washed in T-TBS and incubated overnight at 4°C with the desired primary antibody in either 5 % w/v skim milk powder in T-TBS or 5% BSA in T-TBS depending on the manufacturers' specifications. Blots were then washed 5x in T-TBS and incubated with the appropriate secondary antibody (goat anti-mouse IgG-HRP or donkey anti-rabbit IgG-HRP) in 5 % w/v skim milk powder in T-TBS. After incubation, washing was repeated and protein bands were detected using Luminata™ Forte Western HRP Substrate followed by film exposure.

To confirm even protein loading, blots were reprobed with goat anti-actin antibody in 5 % skim milk powder and T-TBS for 1 h. Blots were washed as described above then incubated for 1 h with HRP-conjugated bovine anti-goat IgG antibody. Washing was repeated and protein bands were visualized as above.

2.19 Statistical Analysis.

Statistical analysis was performed using GraphPad InStat (GraphPad Software Inc. version 3.0).

CHAPTER 3: RESULTS

3.1 Results: Investigation of the Anti-ovarian Cancer Activity of ART.

3.1.1 ART Inhibits the Growth of a Panel of Ovarian Cancer Cell Lines in a Dose- and Time-dependent Manner.

An MTT assay was used to investigate the growth-inhibitory activity of ART against a panel of different ovarian cancer cell lines. Cell lines investigated included those differing in histological subtype and p53 tumour suppressor status (Table 3.1). ART elicited time- and dose-dependent decreases in viable cell number (indicating cytotoxic and/or anti-proliferative activity) compared to the vehicle control in all the ovarian cancer lines examined (Figure 3.1.1A). The concentration of ART that caused a half maximal inhibitory concentration (IC_{50}) in cancer cell number was calculated for each ovarian cancer cell line (Table 3.1). Values ranged from 0.51 +/- 0.03 μM (TOV-112D) to 31.89 +/- 1.62 μM (OV-90), with the majority of the cell lines exhibiting an IC_{50} below 10 μM. Furthermore, significant cancer cell inhibition was seen at ART doses as low as 1 μM in a majority of ovarian cancer cell lines tested. Sensitivity towards ART was not p53-dependent, although all the lines with higher IC_{50} values were p53 null or mutant. Interestingly, the SKOV-3 and OV-90 cells lines which were the least responsive to ART, also proliferated more slowly than the other ovarian cell lines that were investigated. A decreased growth rate would have made the anti-proliferative effect of ART less dramatic, and may play a role in the increased IC_{50} concentration seen by MTT assays between slow-growing and other ovarian cancer cell lines. Following 48 h culture with ART, visual assessment of HEY1 and HEY2 ovarian cancer cells revealed far lower numbers in ART-treated wells compared to those treated with vehicle (Figure 3.1.1B). Moreover, cells treated with 100 μM ART showed altered morphology consistent with cell death. Ovarian cancer is very heterogeneous and the different histological subtypes act as separate diseases. Therefore, ART's broad spectrum of activity against different ovarian cancer cell histological subtypes and towards ovarian cancer lines possessing platinum resistance recommends further research into its development as a possible treatment for different forms of ovarian cancer.

Table 3.1 Ovarian Cell Line Characteristics and ART IC_{50}

	p53 status (225)	**Histopathology**	**Prior treatment**	**ART IC50 (μM) at 72 h**
TOV-112D (226)	mut	Endometrioid	none	0.51 +/- 0.03
OVCAR8	mut	N/A	N/A	5.51 +/- 1.06
OVCAR3 (227)	mut	Ovarian adenocarcinoma	cisplatin, cyclophosphamide, adriamycin	14.95 +/- 6.38
SKOV-3 (228, 229)	null (although mut also reported)	Initially identified as an adenocarcinoma although recently reclassified as a clear	thiotepa	23.55 +/- 3.86
OV-90 (226)	mut	Serous adenocarcinoma	none	31.89 +/- 4.15
HEY1 [clone of the HEY cell line (230))	wt	Undifferentiated carcinoma	N/A	5.80 +/- 1.62
TOV-21G (226)	wt	Clear cell	none	6.11 +/- 0.64
HEY2 (clone of the HEY cell line (230))	wt	Undifferentiated carcinoma	N/A	7.34 +/- 0.56
IGROV1 (231)	conflicting reports	Ovarian carcinoma	cobalt therapy of cervix and vagina	8.82 +/- 1.18

wt - wild-type, mut- mutant, N/A-not available

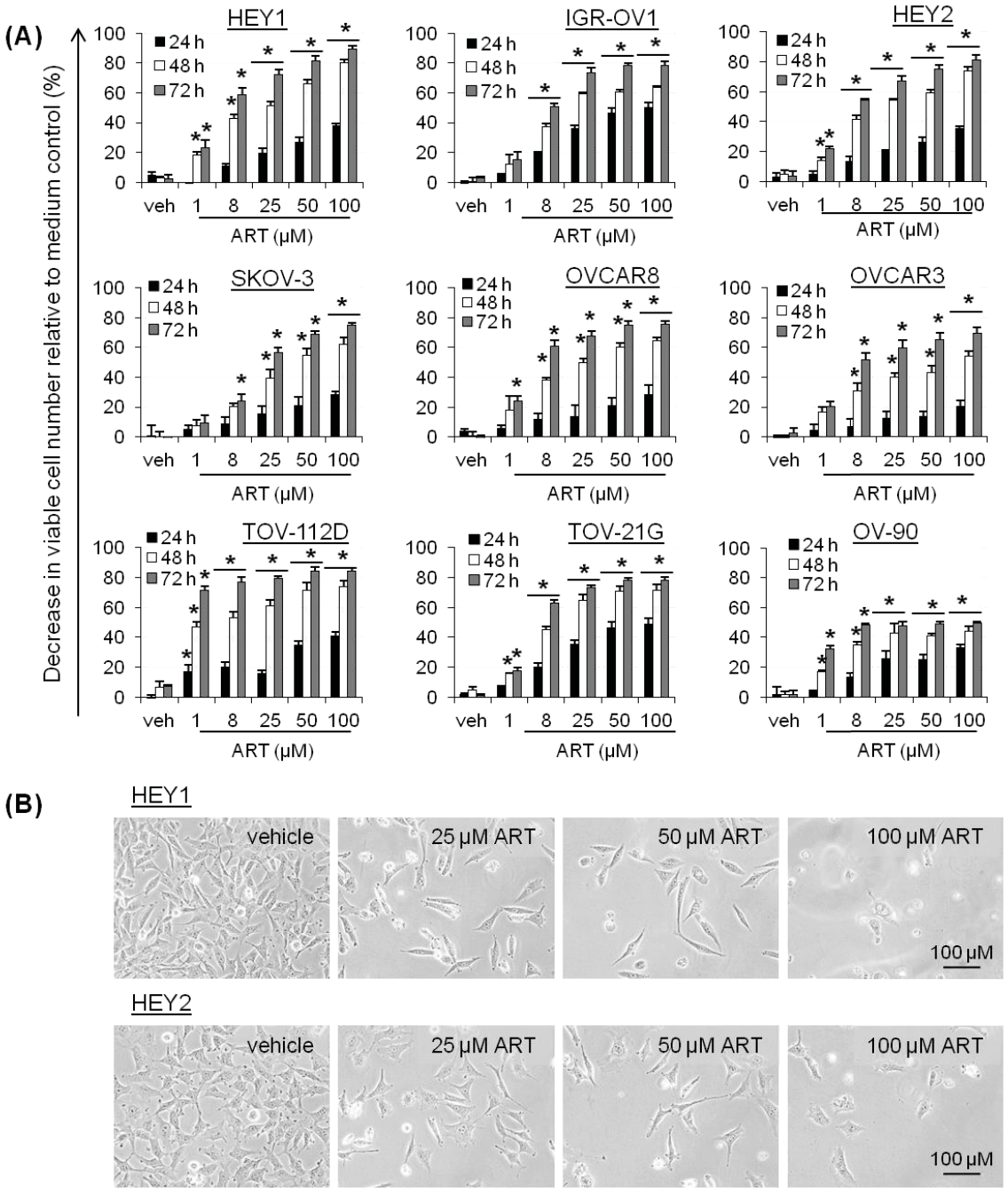

Figure 3.1.1 ART has a Potent Dose-dependent Inhibitory Effect on the Growth of Ovarian Cancer Cells. (A) Ovarian cancer lines were treated with ART or vehicle (veh) then cultured for the specified times. Following culture, changes in viable cell number were determined using an MTT assay. (B) HEY1 and HEY2 cells were treated with ART or vehicle for 24 h, then photographed. (B) Pictures are representative images from 3 independent experiments. (A) Data shown are the mean of at least 3 independent experiments ± SEM; * $p<0.05$ as compared to the vehicle, determined by a one-way ANOVA with a Tukey-Kramer post-test.

3.1.2 ART is Cytotoxic to Ovarian Cancer Cell Spheroids.

Vehicle-treated ovarian cancer spheroids were compact, cohesive and possessed clearly defined margins. Conversely, when cultured with ART, ovarian cancer spheroids became disrupted, and spheroids were smaller, more irregular, less compact and failed to exhibit the well defined borders present in vehicle control spheroids (Figure 3.1.2A). Moreover, a large number of single floating cells were seen in the ART-treated samples which were absent in vehicle wells. To verify changes in size and viability of ovarian cancer spheroid cells, an acid phosphatase assay was conducted to assess the number of viable cells in ART- and vehicle-treated samples. There was a strong, significant decrease in the number of viable cells in ART-treated spheroids compared to those treated with the vehicle (Figure 3.1.2B). ART-mediated inhibition of ovarian cancer cell growth was not as dramatic in the spheroid assay as it was in the MTT assays performed in 2D cultures. Nevertheless, ART retained strong activity in HEY1 and HEY2 ovarian spheroid cultures, demonstrating that the anti-ovarian cancer activity of ART can also be translated to a 3D culture system

3.1.3 Ovarian Cancer Cells Treated with Low Doses of ART Regrow Following ART Removal.

Wash-out assays were performed to assess the ability of ART-treated cells to recover following ART removal. Following 72 h of ART treatment, HEY1 and HEY2 ovarian cancer cells, or a population thereof, that were treated with lower concentrations of ART (10 and 25 μM) were able to regain their proliferative capacity within 144 h of ART removal, as determined by an MTT assay. By this time, the cell population treated with 10 μM ART reached the same level of growth as that of the vehicle control, while populations treated with 25 μM exhibited significant growth within this time period (Figure 3.1.3). Conversely, cells treated with higher concentrations of ART (50 and 100 μM) never recovered following ART removal. This suggests that higher concentrations of ART had a more severe and permanent effect on ovarian cancer cells than did treatments with lower doses of ART.

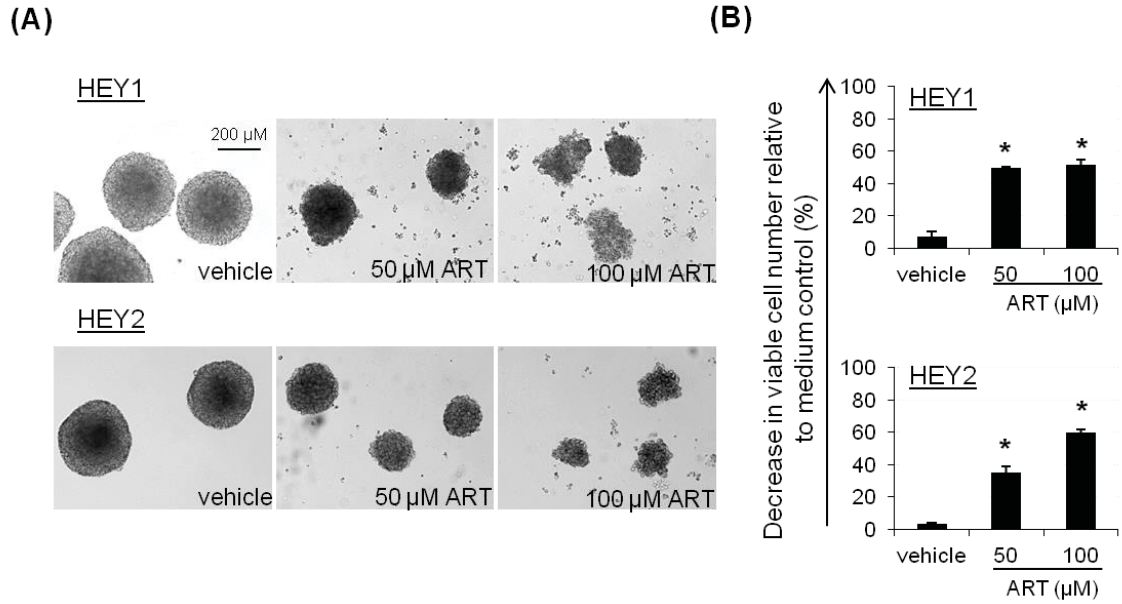

Figure 3.1.2 ART Maintains its Anti-cancer Activity in 3D Ovarian Cancer Cell Spheroids. (A,B) Ovarian cancer spheroids were grown for 5 or 6 d (HEY1 or HEY2 cells, respectively) in ultra low attachment plates, then treated with ART or vehicle for 72 h. Following culture, spheroids were photographed and changes in viable cell number were determined using an acid phosphatase assay. (A) Pictures depict a representative experiment. (B) Data shown are the mean of at least 3 independent experiments ± SEM; ++ $p<0.05$ as compared to the same dose at 0 h post wash, determined by a one-way ANOVA with a Tukey-Kramer post-test.

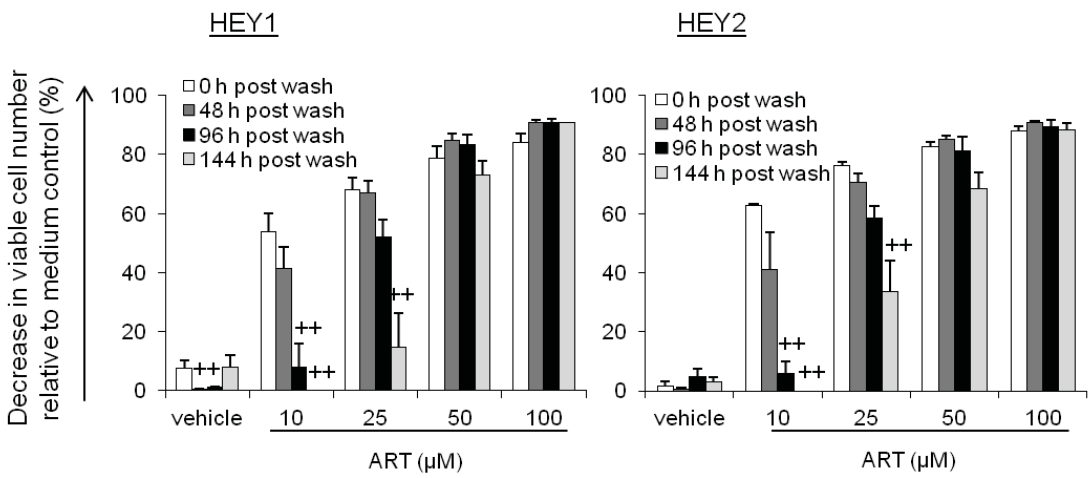

Figure 3.1.3 Ovarian Cancer Cells Treated with a Low Dose of ART Regain their Proliferative Capacity Following ART Removal. HEY1 and HEY2 ovarian cancer cells were treated with vehicle or ART for 72 h. Following culture, cell growth was assessed using an MTT assay or ART was replaced with drug-free cDMEM and cultured for an additional 48, 96, or 144 h. Cell growth was then determined by MTT assay. Medium and vehicle controls were maintained to prevent over confluence. Data shown are the mean of at least 3 independent experiments ± SEM;* $p<0.05$ as compared to the vehicle, determined by a one-way ANOVA with a Tukey-Kramer post-test.

3.1.4 ART Causes Dose-dependent Cell Death in Ovarian Cancer Cell Lines.

As the MTT assay cannot easily distinguish between cytotoxic and cytostatic effects, Annexin-V-FLUOS/PI staining was performed to determine the ability of ART to induce ovarian cancer cell apoptosis and/or necrosis. ART induced dose-dependent cancer cell death in all the cell lines tested after 48 h of treatment (Figure 3.1.4A,B). The sensitivity of cell lines to ART-treatment varied significantly and trends of cell death were slightly different than those observed with the MTT assay. TOV-21G cells appeared the most sensitive to ART, followed by TOV-112D, OVCAR8 and HEY1. Meanwhile, HEY2 and SKOV-3 cells were the most resistant to ART. Treatment with 50 and 100 μM ART elicited significant cytotoxicity in all the cell lines tested, while 25 μM ART was only cytotoxic towards the more sensitive lines (OVCAR8, TOV-21G, TOV-112D). Results from the Annexin-V-FLUOS/PI staining suggest that the pathways involved in ART-induced cell death differ between the ovarian cancer cell lines investigated. ART-treatment induced predominantly late apoptotic/necrotic cell death in the HEY1, HEY2 and OVCAR8 cell lines, whereas TOV-21G and TOV-112D displayed a significant increase in early apoptosis upon identical ART treatment.

3.1.5 The ID8 Murine Ovarian Cancer Cell Line is Killed by ART.

The sensitivity of murine ovarian cancer cells to ART were also investigated using the MTT assay and Annexin-V-FLUOS/PI staining. ART treatment significantly decreased cell growth in cultures of ID8 murine ovarian cancer cells in a time and dose-dependent manner (Figure 3.1.5A). ID8 cells were very sensitive to ART, as indicated by the IC_{50} of 3.54 +/- 0.67 μM. The Annexin-V-FLUOS/PI staining of ART-treated ID8 cells revealed that they were killed by ART in a dose-dependent manner (Figure 3.1.5B). As with the HEY1, HEY2, and OVCAR8 human ovarian cancer cell lines, ART-treatment led to predominantly necrotic cell death.

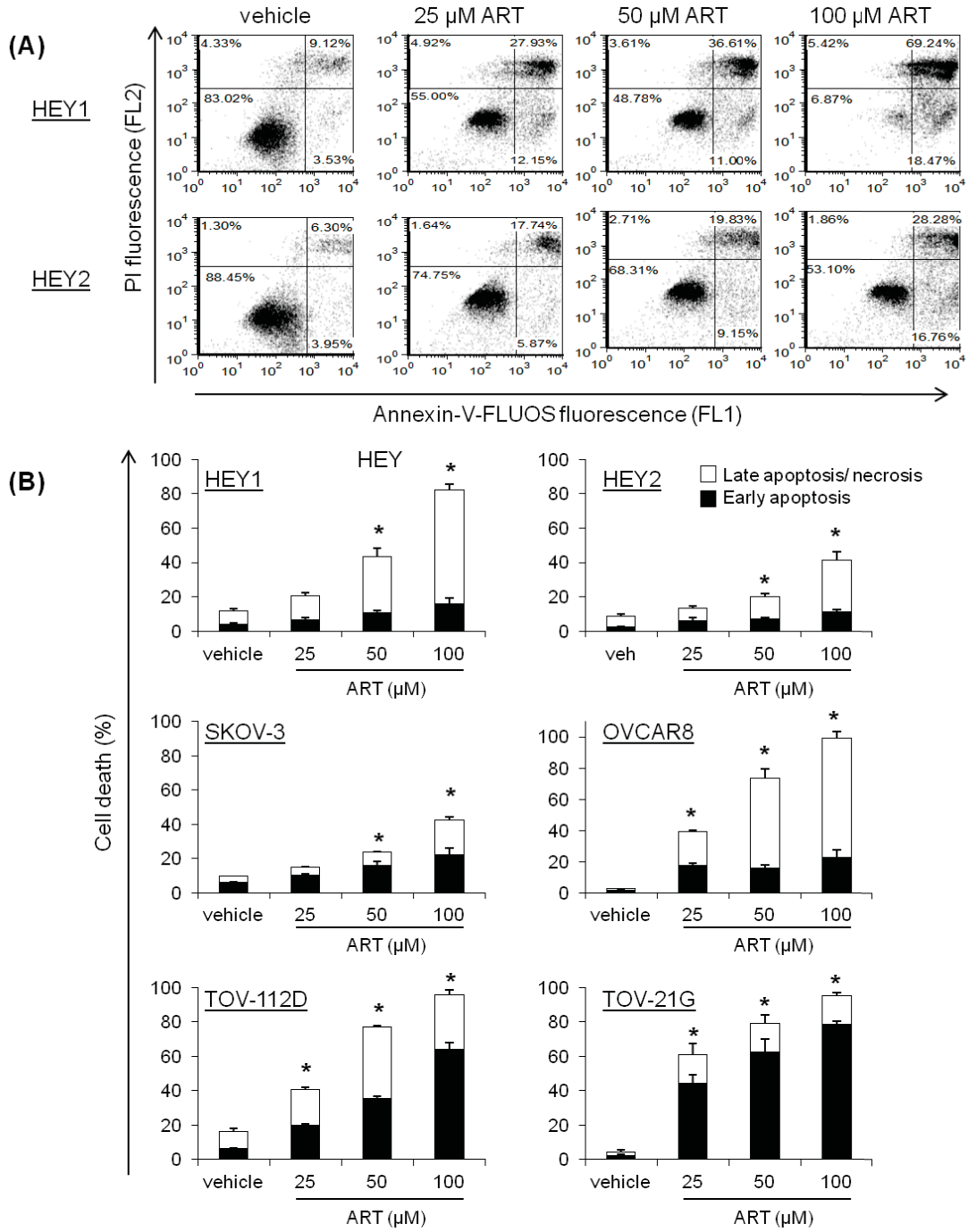

Figure 3.1.4 ART Induces Dose-dependent Cell Death in Ovarian Cancer Cell Lines. Ovarian cancer cells were treated with ART or vehicle (veh) for 48 h before levels of cell death were determined by Annexin-V-FLUOS/PI staining. (A) Histograms depict a representative experiment for the HEY1 and HEY2 cell lines. (B) Data shown are the mean of at least 3 independent experiments ± SEM; * $p<0.05$ as compared to the vehicle, determined by a one-way ANOVA with a Tukey-Kramer post-test.

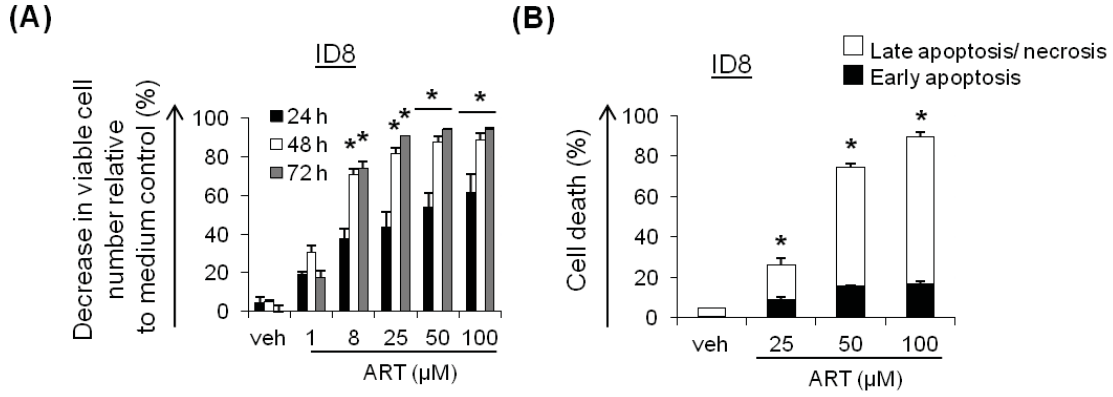

Figure 3.1.5 Murine Ovarian Cancer Cells are Sensitive to ART. (A) ID8 mouse ovarian cancer cells were cultured with ART or vehicle (veh) ART for the indicated time. Changes in viable cell number were determined using an MTT assay. (B) ID8 cells were treated with ART or vehicle for 48 h. The amount of cell death was subsequently assessed by Annexin-V-FLUOS/PI staining. (A,B) Data shown are the mean of at least 3 independent experiments ± SEM; * $p<0.05$ as compared to the vehicle, determined by a one-way ANOVA with a Tukey-Kramer post-test.

3.1.6 RIPK1 Inhibition Decreases ART-induced Cell Death in HEY1 and HEY2 Ovarian Cancer Cells.

RIPK1 is an important player in necroptosis (232). To confirm whether ART caused necroptotic cell death in HEY1 and HEY2 cell cultures, the Annexin-FLUOS/PI staining was repeated on cells treated with ART alone, or in combination with the RIPK1 inhibitor, necrostatin-1 (nec-1). RIPK1-inhibition decreased ART-induced cell death in both cell lines, indicating that ART causes necroptotic cell death of HEY1 and HEY2 cancer cells (Figure 3.1.6). As expected, nec-1 treatment only inhibited ART-induced necrotic cell death. Since nec-1 was unable to completely inhibit ART-induced cytotoxicity, this indicates that other cell death pathways are also involved in ART-mediated killing of ovarian cancer cells.

3.1.7 ART Induces ROS Production in Ovarian Cancer Cell Lines.

CM-H_2DCFDA staining was used to determine whether ART treatment induced the production of ROS in HEY1, HEY2 and SKOV-3 ovarian cancer cells. Flow cytometric analysis of stained cells revealed that ART induced a dose-dependent increase in intracellular ROS formation in all three of the ovarian cancer cell lines (Figure 3.1.7A,B). Treatment with lower concentrations of ART (10 μM) resulted in negligible ROS production while treatment with higher doses of ART (50-100 μM) resulted in a significant increase in intracellular ROS. Treatment of cells with the anti-oxidant GSH eliminated the ART-induced ROS production (Figure 3.1.7C).

ART treatment of SKOV-3 cells resulted in the lowest relative ROS production, while ART treatment of the HEY2 cells resulted in a significantly higher relative ROS production at 100 μM ART (as determined by a one-way ANOVA with a Tukey-Kramer post-test). ART-mediated relative ROS production in HEY1 cells was in-between that SKOV-3 and HEY2, but differences did not differ significantly from either cell line.

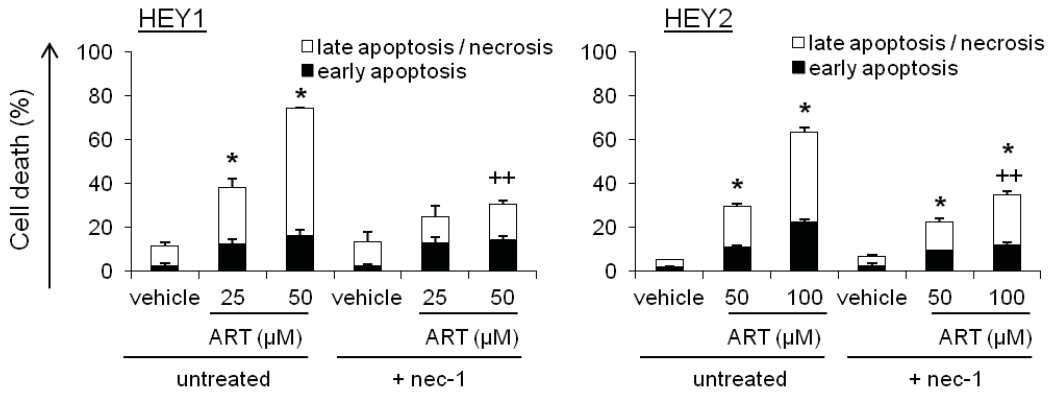

Figure 3.1.6 Inhibition of RIP1 Kinase Activity by Nec-1 Decreases ART-mediated Cytotoxicity in HEY1 and HEY2 Ovarian Cancer Cell Lines. Ovarian cancer cells were treated for 1 h with necrostatin-1 (nec-1), after which ART or vehicle was added to the culture. The final concentration of nec-1 was 40 μM. Following 48 h of culture, levels of cell death were determined using Annexin-V-FLUOS/PI staining. Data shown are the mean of at least 3 independent experiments ± SEM; * $p<0.05$ of total cell death as compared to the vehicle, determined by a one-way ANOVA with a Tukey-Kramer post-test; ++ $p<0.05$ as compared to the total cell death of the treatment in the absence of nec-1, determined by a one-way ANOVA with a Tukey-Kramer post-test.

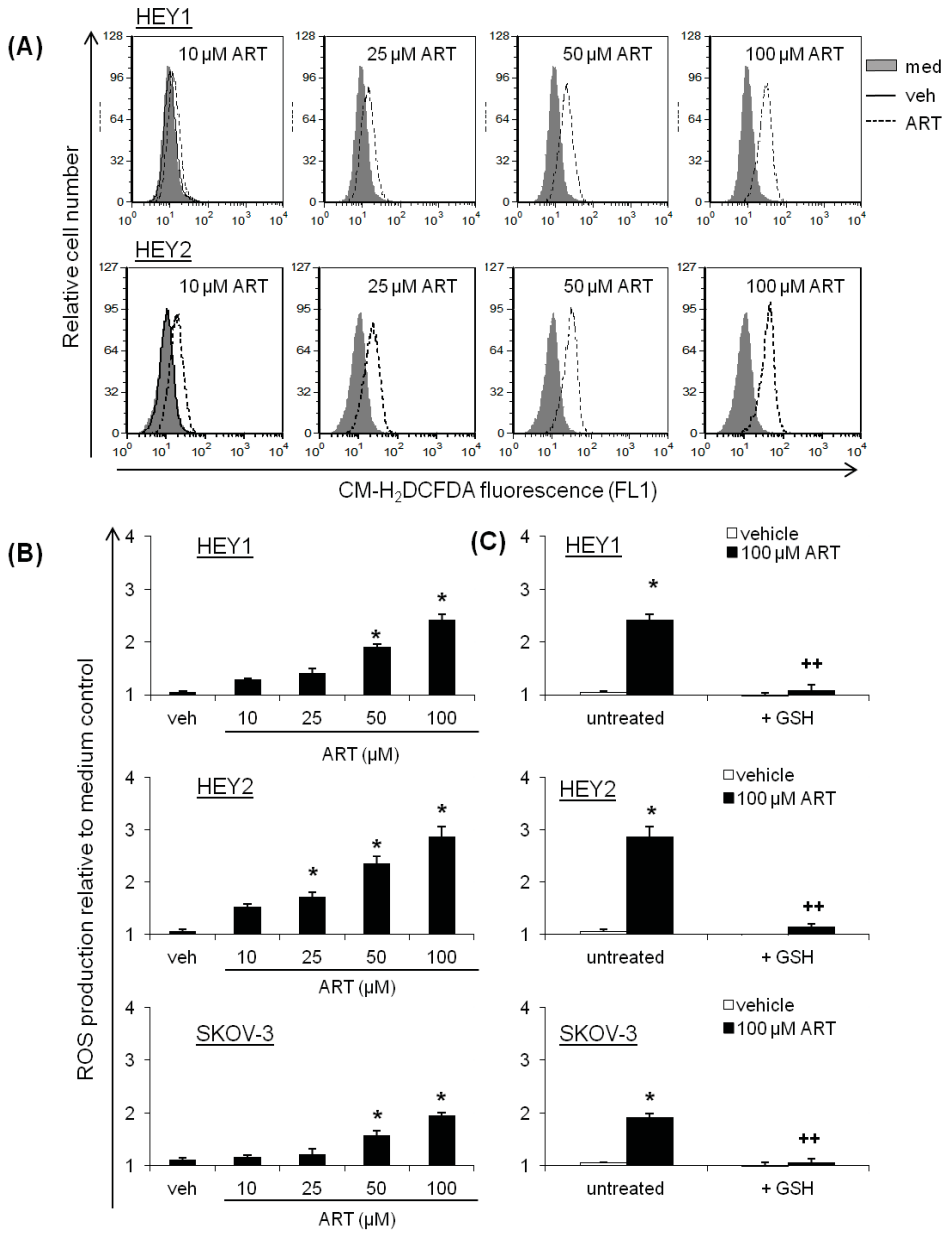

Figure 3.1.7 ART Treatment Induces Dose-dependent ROS Production in Ovarian Cancer Cells. Ovarian cancer cells were stained in phenol-red-free and serum-free DMEM containing 5 μM CM-H_2DCFDA for 30 min in the dark. The staining solution was then removed and cells were washed with warm PBS. Cells were then treated for 24 h with ART or vehicle (veh) (C) in the presence or absence of 10 mM GSH (GSH was added 30 min prior to ART treatment) in phenol-red-free DMEM supplemented with 1% HI FBS. H_2O_2 was used as a positive control. ART-induced increases in fluorescence indicating increased ROS production were determined by flow cytometry. (A) Histograms depict a representative experiment using the HEY1 and HEY2 cell lines. (B,C) Data shown had ART background fluorescence subtracted and are the mean of at least 3 independent experiments ± SEM; * $p<0.05$ as compared to the vehicle, determined by a one-way ANOVA with a Tukey-Kramer post-test.

3.1.8 ART Causes ROS-dependent Cell Death in Ovarian Cancer Cell Lines.

To investigate the importance of ART-mediated ROS production on the cytotoxic activity of ART in a panel of ovarian cancer cells, the Annexin-V-FLUOS/PI apoptosis assay was repeated and ovarian cancer cells were cultured with ART in the presence or absence of GSH. Treatment of the cells with GSH significantly decreased ART-induced cytotoxicity in all lines tested, indicating that ROS play an important role in ART-induced ovarian cancer cell death (Figure 3.1.8A).

In addition to the human ovarian cancer cell lines, the ID8 murine ovarian cancer cell line showed a similar dependency on ROS for ART-mediated cell death, although GSH treatment in conjunction with ART did not inhibit ART-induced cell death as dramatically as in the human cell lines (Figure 3.1.8B). In fact, cell death associated with 25 μM ART treatment was slightly increased in the presence of GSH.

3.1.9 ART-induced Ovarian Cancer Cell Death Requires Iron and is Enhanced by HT Treatment.

As iron aids in the production of ROS via the Fenton reaction (233), the importance of iron in ART-mediated cell death was investigated in HEY1, HEY2 and SKOV-3 ovarian cancer cells. Iron loading of the cancer cells with HT significantly increased ART-induced cell death in HEY1 and SKOV-3 ovarian cancer cell lines. A similar trend was observed for HEY2 ovarian cancer cells, although differences did not reach statistical significance (Figure 3.1.9). Combined treatment of HEY1, HEY2 and SKOV-3 cells with ART and the iron chelator deferiprone (DFE) significantly diminished ART-induced cell death in all cell lines tested. Together, these results underline the importance of iron in the anti-ovarian cancer activity of ART.

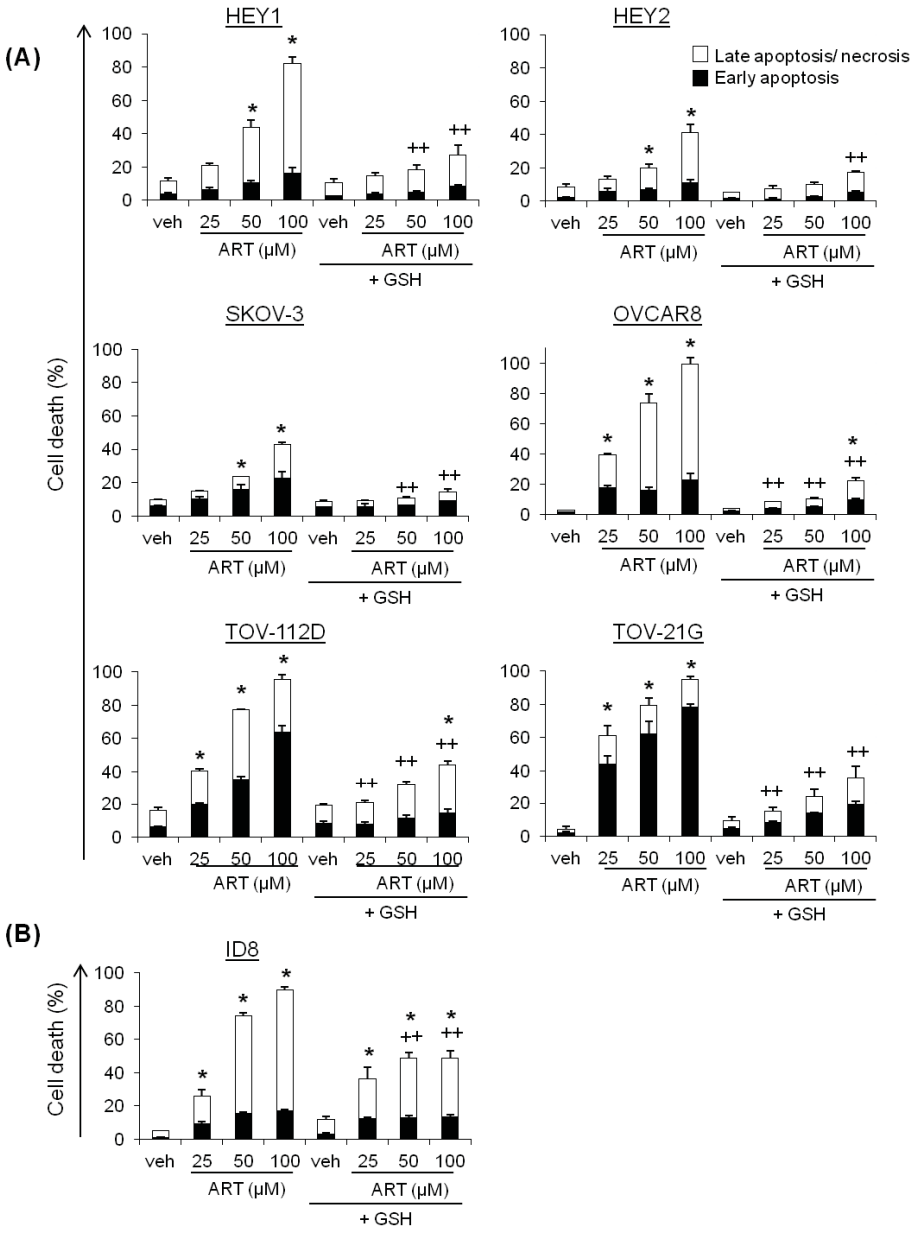

Figure 3.1.8 ART Induces ROS-dependent Cell Death in Ovarian Cancer Cell Lines. Human ovarian cancer cells (A) or murine ID8 ovarian cancer cells (B) were treated with ART or vehicle in the presence or absence of 10 mM GSH, then cultured for 48 h before levels of cell death were determined using Annexin-V-FLUOS/PI staining. Cells were treated with GSH 30 min prior to ART addition. (A,B) Data shown are the mean of at least 3 independent experiments ± SEM; * $p<0.05$ of cell death as compared to the vehicle, determined by a one-way ANOVA with a Tukey-Kramer post-test; ++ $p<0.05$ as compared to cell death of the treatment in the absence of GSH, determined by a one-way ANOVA with a Tukey-Kramer post-test.

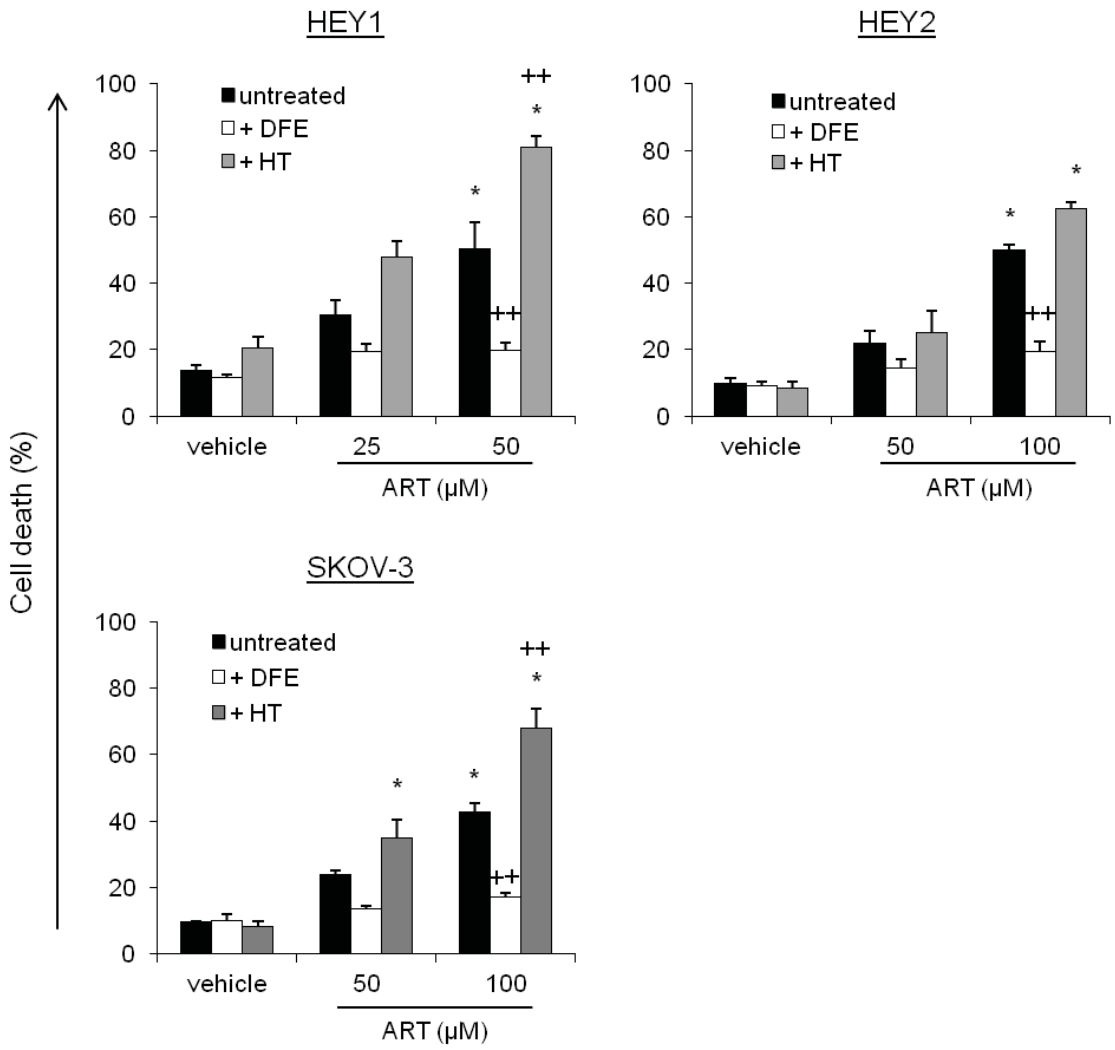

Figure 3.1.9 Iron is Involved in ART-mediated Cytotoxicity in Ovarian Cancer Cells. Ovarian cancer cells were pre-treated with 10 μM holo-transferrin (HT), as an iron source, for 1 h, following which HT was removed and cells were treated with ART or vehicle. Following culture the amount of cell death was determined using Annexin-V-FLUOS/PI staining. To determine the effect of iron removal on ART-activity, ovarian cancer cells were treated with ART or vehicle for 48 h in the presence or absence of 12.5 μg/mL μM deferiprone (DFE), an iron chelator. DFE was added 30 min prior to ART treatment. Following culture the amount of cell death was determined using Annexin-V-FLUOS/PI staining. Data shown are the mean of at least 3 independent experiments ± SEM;* $p<0.05$ as compared to the vehicle, determined by a one-way ANOVA with a Tukey-Kramer post-test.

3.1.10 Caspases are Involved but are Not Essential for the Majority of ART-induced Cancer Cell Death.

A pan-caspase activation assay was used to determine whether ART treatment resulted in caspase activation in HEY1 and HEY2 ovarian cancer cells. ART induced dose- and time-dependent increases in caspases activity after 48 h of culture (Figure 3.1.10 A,B). As expected, caspase activation was greater in the HEY1 line, which was more sensitive to ART-treatment. To determine the importance of activated caspases for ART-mediated cell death, ovarian cancer cells treated with ART alone or in combination with the pan-caspase inhibitor Z-VAD-fmk were stained with Annexin-V-FLUOS/PI. Interestingly, although ART-induced cell death was significantly inhibited in the presence of Z-VAD-fmk, ART maintained a significant cytotoxic effect, implying that additional cell death pathways are involved in ART-induced killing of ovarian cancer cells (Figure 3.1.10B). These results are in agreement with my finding that ART induces necroptotic cell death in the HEY1 and HEY2 ovarian cancer cell lines.

3.1.11 ART Does Not Affect Surface CD71 Expression in Ovarian Cancer Cells.

Recent evidence suggests that ART may enter tumour cells using CD71, also known as transferrin receptor1 (232). To examine the effect of ART on CD71 expression by ovarian cancer cells, changes in CD71 surface expression were determined following 24 h of cell culture in the presence of ART. CD71 was expressed by both HEY1 and HEY2 cells, although the HEY2 line expressed significantly higher levels (Figure 3.1.11B). ART treatment induced a slight, but not significant, decrease in surface CD71 expression by HEY2 cells, while there was little change in ART-treated HEY1 cells (Figure 3.1.11A,B).

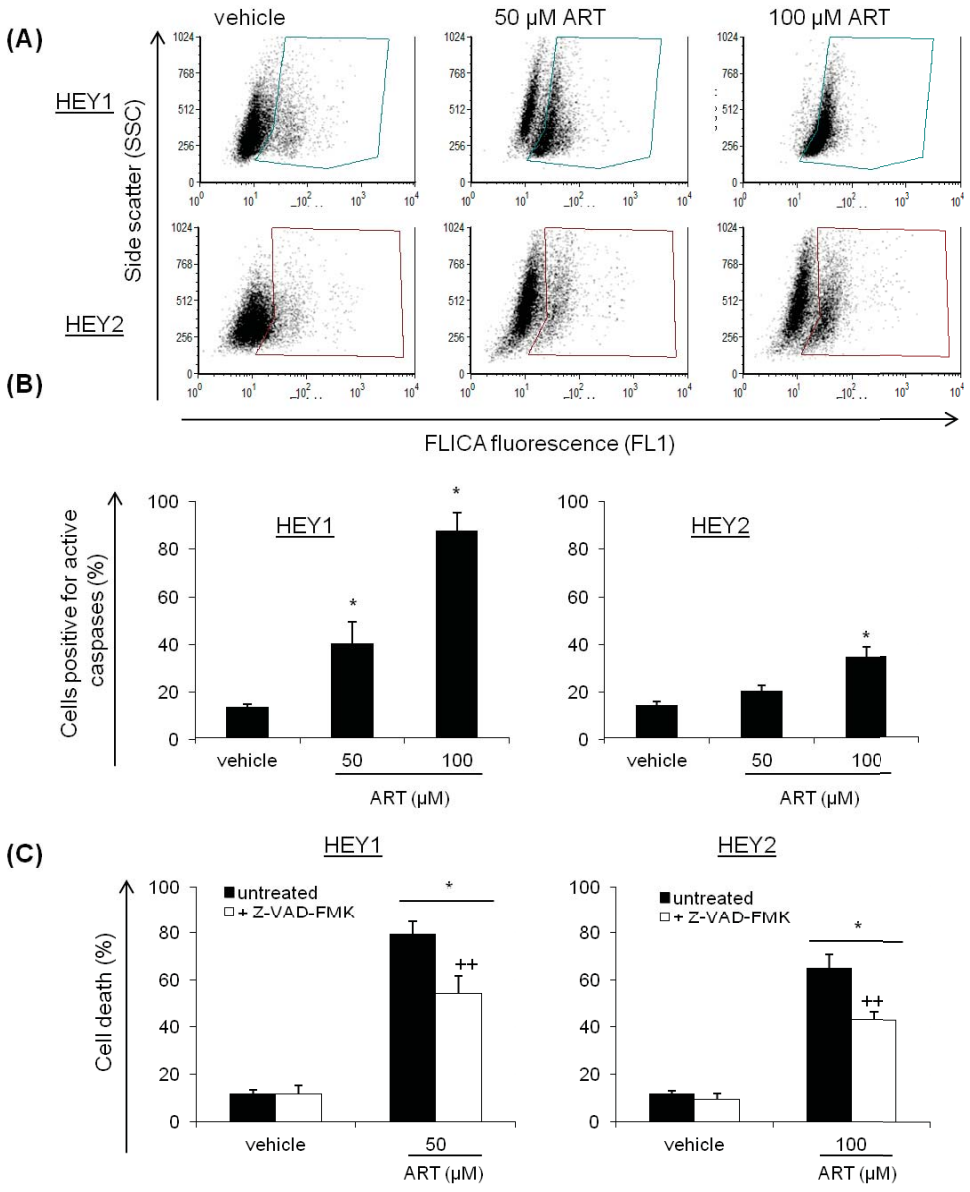

Figure 3.1.10 Caspases are Involved but are Not Essential for ART-mediated Ovarian Cancer Cell Death. (A,B) HEY1 and HEY2 cells were treated with ART or vehicle (veh) for 48 h. Following culture, cells were harvested and stained for 1 h at 37˚C with the fluorescent inhibitor of caspases (FLICA) reagent. Cells were then washed and changes in fluorescence were determined by flow cytometry. (C) Ovarian cancer cells were treated with ART or vehicle in the presence or absence of 50 μM of the Z-VAD-fmk pan-caspase inhibitor for 72 h. Z-VAD-fmk was added to cells 1 h prior to ART. Changes in the amount of cell death were determined using Annexin-V-FLUOS/PI staining. (A) Dot plots depict a representative experiment. (B,C) Data shown are the mean of at least 3 independent experiments ± SEM;* $p<0.05$ as compared to the vehicle, determined by a one-way ANOVA with a Tukey-Kramer post-test; ++ $p<0.05$ as compared to the total cell death of the treatment in the absence of Z-VAD-fmk, determined by a one-way ANOVA with a Tukey-Kramer post-test.

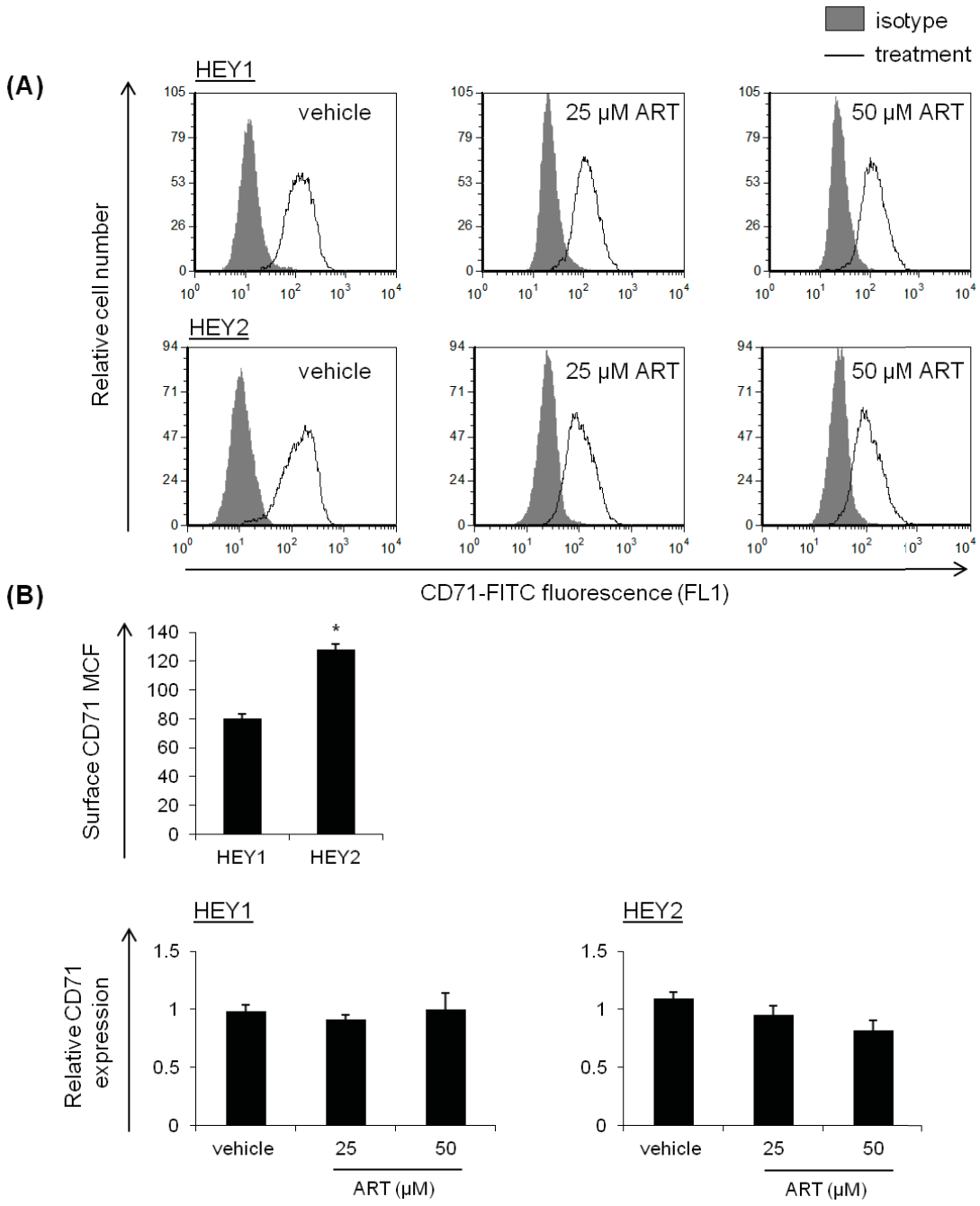

Figure 3.1.11 ART Does Not Affect Surface Expression of CD71 on HEY1 or HEY2 Cells. Ovarian cancer cells were treated with ART or vehicle for 24 h, after which cells were harvested using EDTA, washed and stained for 1 h at 4˚C with mouse anti-human CD-71 (OKT9) FITC or its isotype control (mouse anti-human IGg1κ FITC). Cells were then washed 3x and fixed in 1 % PFA. Mean channel fluorescence (MCF) was subsequently determined by flow cytometry. (A) Histograms depict a representative experiment. (B) Data shown are the mean of at least 3 independent experiments ± SEM; * $p<0.05$ as compared to the vehicle, determined by a two-tailed unpaired t-test.

3.1.12 ART has an Anti-proliferative Effect on Ovarian Cancer Cells.

Although Annexin-V-FLUOS/PI staining of ART-treated ovarian cancer cell lines demonstrated significant ROS-dependent cytotoxicity at higher doses of ART, little cell death was present when less than 25 μM ART was used. However, MTT assays showed significant decreases in viable cell number at doses as low as 1 μM ART. Since MTT assays cannot discriminate between cytotoxic and cytostatic effects, the discrepancy in results obtained using these two assays, suggests that ART also possesses anti-proliferative activity.

An Oregon Green 488 cell proliferation assay was conducted to determine the effect of ART on ovarian cancer cell cycle progression. At all doses examined, ART treatment strongly inhibited HEY1 and HEY2 cancer cell proliferation compared to vehicle-treated cells (Figure 3.1.12A). Furthermore, ART-induced inhibition of HEY1 and HEY2 cancer cell proliferation was not ROS-dependent as the presence of GSH did not affect the anti-proliferative activity of ART. However, dose-dependent inhibition of cell proliferation by ART was not as apparent in GSH-treated cells (Figure 3.1.12B).

Interestingly, in the presence of the iron chelator DFE, both vehicle- and ART-treated HEY1 and HEY2 cells showed similar levels of proliferation, which were below those of control cells cultured in the absence of DFE (Figure 3.1.12C).

3.1.13 ART Induces Cell Cycle Arrest in Ovarian Cancer Cells

To further understand the effect of ART on ovarian cancer cell proliferation, cell cycle analysis was performed. Cell cycle analysis demonstrated that ART-treated cells arrested in the G1 and G2/M phases of the cell cycle, depending on the dose of ART that was administered. Lower doses of ART induced a G1 phase arrest while higher doses resulted in cells arresting in the G2/M phase (Figure 3.1.13A,B). Decreases in the percentage of the cell population in S phase were consistent with the increased percentage of cells in either G1 or G2/M phase. Dose-dependent cell cycle arrest was more dramatic in the HEY2 cells, but the trend was still present in the HEY1 ovarian cancer cells. The low sub G1 peak (Figure 3.1.13 C) was consistent with a necrotic form of cell death.

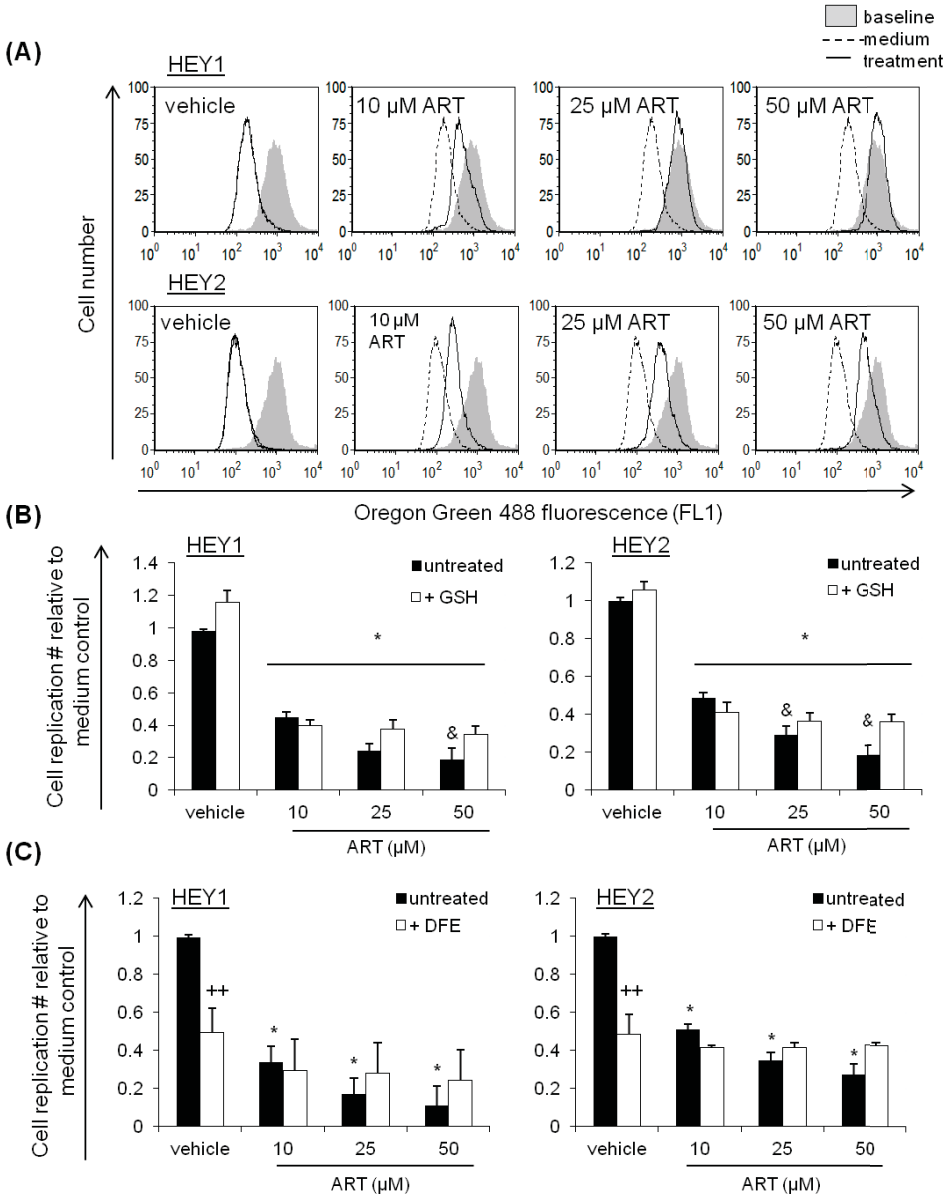

Figure 3.1.12 The Anti-proliferative Activity of ART is Not ROS-dependent. HEY1 and HEY2 ovarian cancer cells were stained with Oregon Green 488 dye, then treated with ART (A) in the presence or absence of 10 mM reduced glutathione (GSH) (B) or 12.5 μg/mL deferiprone (DFE) (C). Both GSH and DFE were added to the cells 30 min prior to ART. A sample of Oregon green 488-stained ovarian cancer cells were fixed in 1% PFA and stored at 4˚C at the time of ART treatment for use as a baseline control. Following 72 h of culture, cell proliferation represented by decreased Oregon Green 488 fluorescence, as determined by flow cytometry. (A) Histograms depict a representative experiment. (B,C) Data shown are the mean of at least 3 independent experiments ± SEM;* $p<0.05$ as compared to the vehicle, determined by a one-way ANOVA with a Tukey-Kramer post-test; ++ $p<0.05$ as compared to the treatment in the absence of GSH/DFE, determined by a one-way ANOVA with a Tukey-Kramer post-test, & $p<0.05$ as compared to the 10 μM ART treatment, determined by a one-way ANOVA with a Tukey-Kramer post-test.

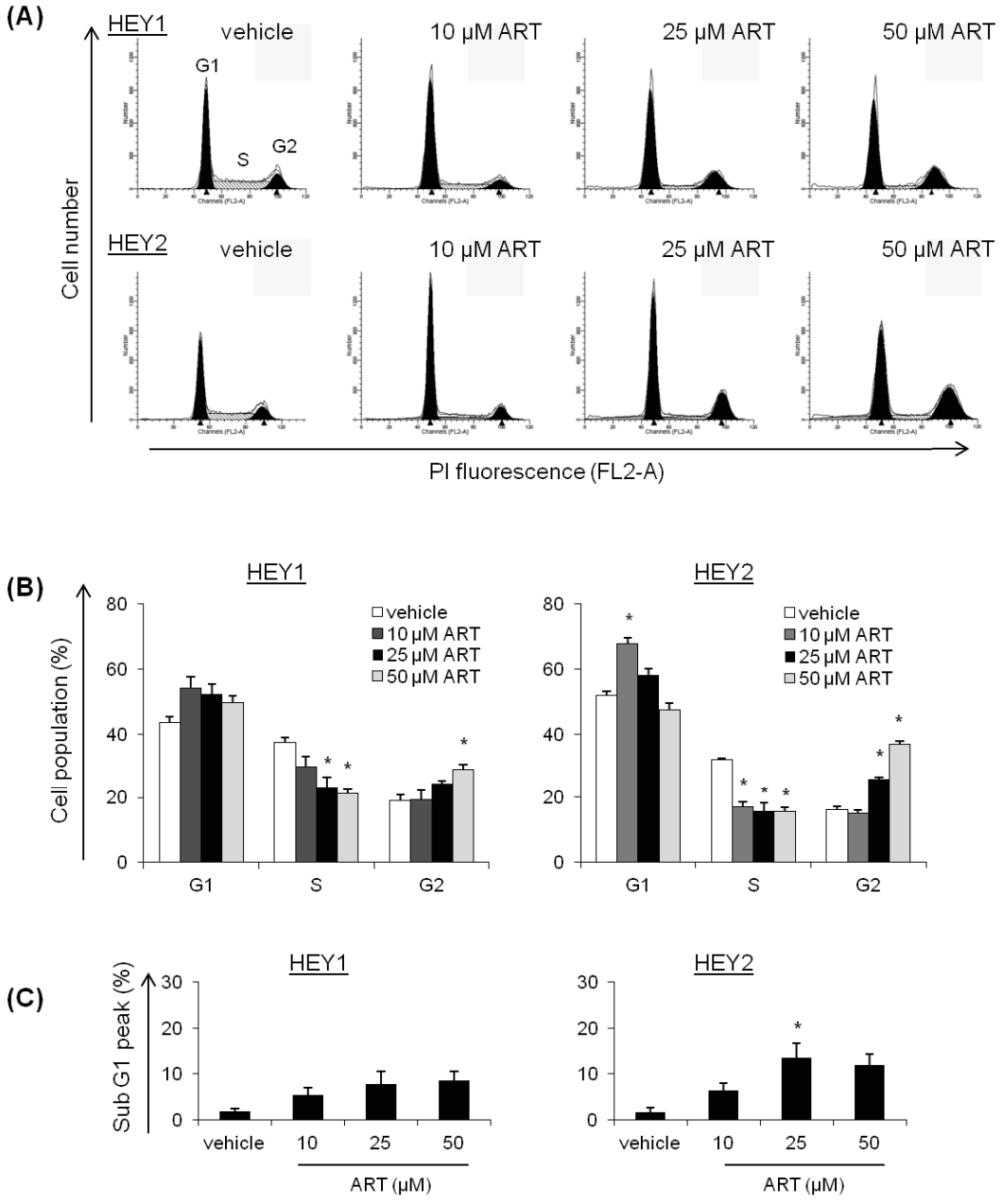

Figure 3.1.13 ART Induces Dose-dependent G2/M Cell Cycle Arrest in Ovarian Cancer Cells. (A,B,C) Ovarian cancer cells were treated with ART or vehicle for 48 h. Following culture, cells were fixed and permeabilised in ethanol, then stored for a minimum of 24 h at -20˚C. Cells were then washed and stained with PI, after which, DNA content was determined by flow cytometry. (A) Histograms depict a representative experiment. (B,C) Data shown are the mean of at least 3 independent experiments ± SEM;* $p<0.05$ as compared to the vehicle, determined by a one-way ANOVA with a Tukey-Kramer post-test.

3.1.14 ART Affects the Expression of Cell Cycle Regulatory Proteins in Ovarian Cancer Cells.

To investigate the molecular mechanisms behind the ability of ART to inhibit ovarian cancer cell cycle proliferation, western blotting was used to determine the effect of ART on the expression of a panel of cell cycle regulatory proteins (Figure 3.1.14). Consistent with previously observed ability of ART to induce cancer cell cycle arrest, ART treatment resulted in decreased levels of cell cycle regulatory proteins involved in different stages of cell cycle progression. The expression of cyclins D3, A and B were down-regulated in ART-treated cells along with their complimentary CDKs (CDK4, 2, and 1). Rb and the transcription factor E2F-1, important players in the G1/S transition, were also strongly down-regulated. CDC25C, a member of the CDC25 phosphatase family involved in the dephosphorylation and activation of CDK1, was also down-regulated. Increased activation of the Chk2 kinase, an important player in the DNA damage response and an inhibitor of the CDC25 phosphatases, was up-regulated in both ovarian cancer lines. In addition, the protein levels of tumour suppressor p21 WAF1/CIP1 were up-regulated in both cell lines, and increases in the expression of this CDK inhibitor likely played a role in ART-induced cell cycle arrest. Changes in ART-induced protein expression were very similar between the HEY1 and HEY2 cell lines. Most changes were visible at 24 h post ART-treatment, although changes in certain protein levels, especially CDC25C, Rb and CDK1 were more pronounced after 48 h of ART treatment.

3.1.15 ART-induced G2/M Cell Cycle Arrest in Ovarian Cancer Cells is ROS-dependent.

Ovarian cancer cells were treated with ART alone or in combination with GSH to further characterise the role of ROS in ART-induced cell cycle arrest. Interestingly, the ART-induced, dose-dependent G2/M cell cycle arrest seen in ovarian cancer cells was lost in the presence of GSH and cells arrested instead in the G1 phase (Figure 3.1.15). Taken together, these results indicate that that ROS are involved in the ART-induced G2/M phase arrest seen with 50 μM ART treatment, but not the G1 arrest achieved with lower doses of ART.

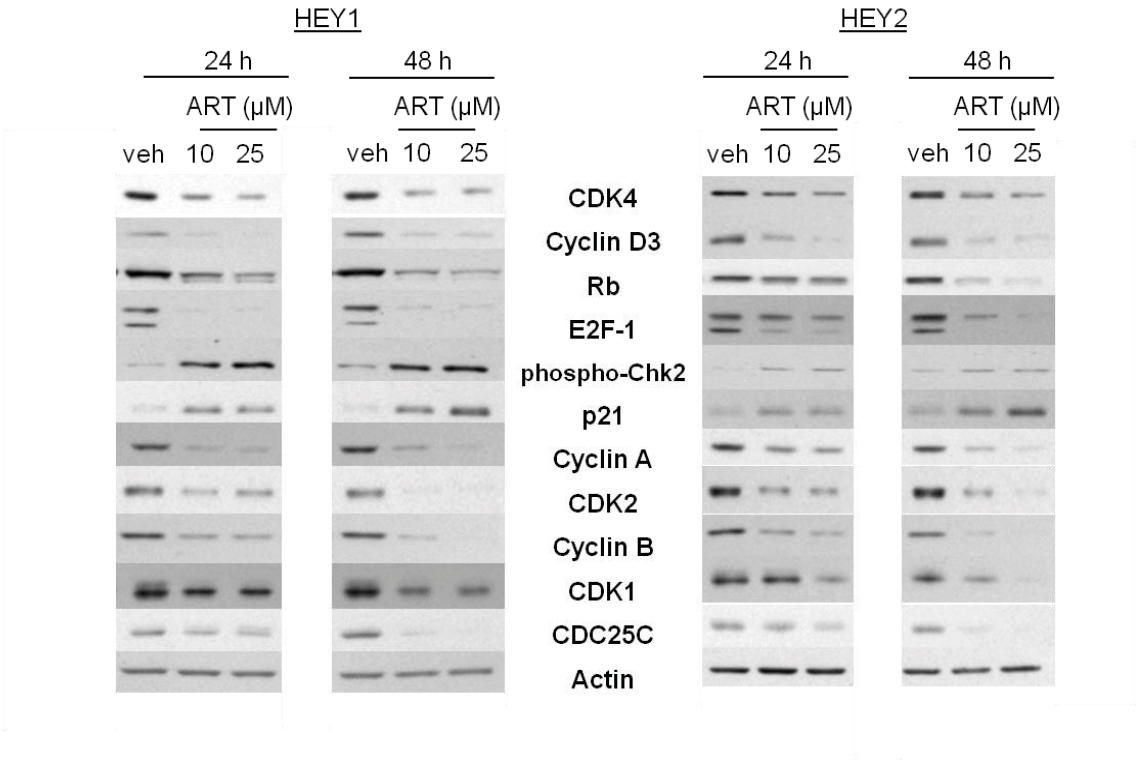

Figure 3.1.14 ART Treatment Alters the Expression of Cell Cycle Regulatory Proteins. HEY1 and HEY2 ovarian cells were treated with ART or vehicle (veh) for 24 or 48 h, cells were subsequently lysed and cell cycle regulatory protein levels were determined by western blotting. Actin expression levels were determined for each blot to confirm equal protein loading. (A,C) Blots depict representative experiments and a representative actin (n=3).

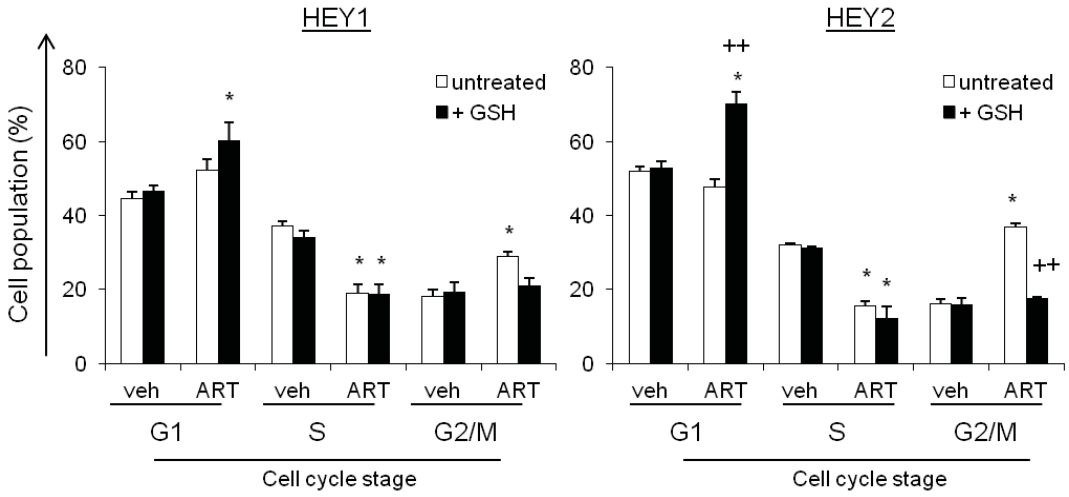

Figure 3.1.15 ART-induced G2/M Cell Cycle Arrest is ROS-dependent in Ovarian Cancer Cells. Ovarian cancer cells were treated with 50 µM ART or vehicle in the absence or presence of 10 mM of GSH, for 48 h. GSH was added 30 in prior to ART. Following culture, cells were fixed and permeabilised in ethanol, then stored for a minimum of 24 h at -20˚C. Cells were then washed and stained with PI, after which, DNA content was determined by flow cytometry. Data shown are the mean of at least 3 independent experiments ± SEM;* $p<0.05$ as compared to the vehicle, determined by a one-way ANOVA with a Tukey-Kramer post-test; ++ $p<0.05$ as compared to the treatment in the absence of GSH, determined by a one-way ANOVA with a Tukey-Kramer post-test.

3.1.16 ART-induces ROS-dependent DNA Damage.

Western blotting for γH2AX was used to determine whether ART caused double-strand DNA breaks. After 48 h, γH2AX was detected in the total cell lysate of HEY2 cells treated with 50 μM ART but was absent in the lysate of cells treated with a lower dose of ART (10 μM) (Figure 3.1.16A). γH2AX was not detected in HEY2 cells treated with both ART and GSH, indicating that ART-induced DNA damage is ROS-dependent. These results suggest that the increased oxidative stress induced though the treatment of ovarian cells with higher concentrations of ART may lead to DNA damage and the activation of the G2/M DNA damage checkpoint. Meanwhile, in the absence of oxidative stress either through the co-treatment of cancer cells with GSH or the administration of ART at low doses, DNA damage does not occur and instead, there is ROS-independent G1 cell cycle arrest.

3.1.17 ART-induced ROS Production Regulates the Expression of CDC25C and Cyclin B.

As the inhibition of ROS by GSH prevented ART-induced G2/M arrest, lysates from cells treated with ART in the presence or absence of GSH were examined by western blotting to determine the role of ROS in CDC25C and cyclin B expression in ART-treated cells, two important players in the G2/M phase of the cell cycle. The HEY2 cell line was selected for this analysis as the ART-induced ROS- and dose-dependent changes in the phase of cell cycle arrest were more pronounced in this line than in HEY1 ovarian cancer cells. A higher concentration of ART (50 μM) was used since higher doses of ART were associated with cell death and G2/M cell cycle arrest. In the presence of GSH, 50 μM ART-induced down-regulation of Cyclin B and CDC25C expression was significantly diminished. No significant differences were present in cells treated with 10 μM ART in the presence or absence of GSH (Figure 3.1.16B).

(A)

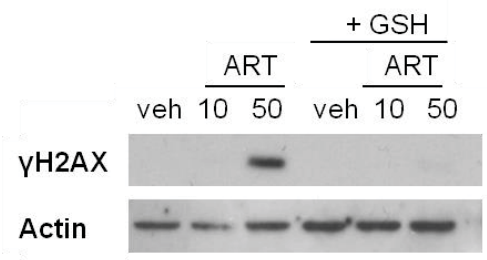

(B)

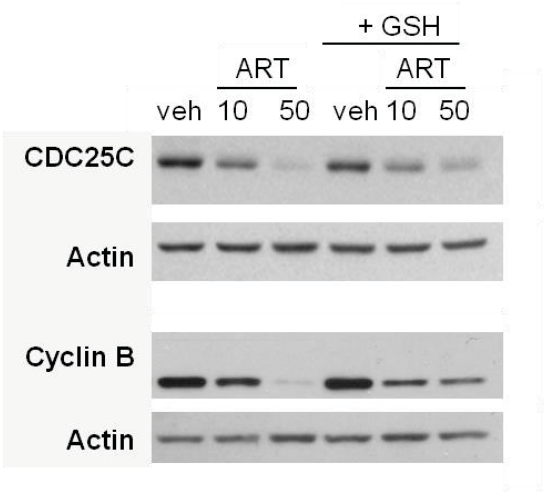

Figure 3.1.16 ART-induced ROS Production Causes DNA Damage and Modulates the Expression of CDC25C and Cyclin B Cell Cycle Regulatory Proteins. HEY2 cells were treated with ART or vehicle (veh) in the absence or presence of 10 mM GSH for 48 h. Cells were subsequently lysed and protein levels were examined by western blotting. Actin expression levels were determined for each blot to confirm equal protein loading. (A,C) Blots depict representative experiments (n=3).

3.2 Results: Investigation of the Anti-breast Cancer Activity of ART.

3.2.1 ART Inhibits the Growth of a Panel of Breast Cancer Cells Including a Paclitaxel-resistant Cell Line.

To determine whether the activity of ART encompassed a wide variety of breast cancer types, ART was tested against a panel of 5 different breast cancer cell lines: MCF-7 (ER-positive, caspase 3-negative, p53-wildtype), MDA-MB-468 (ER-negative, PR-negative HER2-negative, Rb-null, p53-mutant), MDA-MB-231 (ER-negative, PR-negative, HER2-negative, p53-mutant), T47D (ER-positive, p53-mutant), SK-BR-3 (ER-negative, p53-mutant, HER2–over-expressing). ART demonstrated dose- and time-dependent inhibitory activity against all 5 breast cancer cell lines, although the potency of its activity differed between the various cell lines (Figure 3.2.1A). The MDA-MB-468 and T47D breast cancer cell lines were the most sensitive to ART. ART also exhibited excellent inhibitory effects against SK-BR-3 cells after 48 and 72 h culture. MDA-MB-231 and MCF-7 breast cancer cell lines were also sensitive to ART, although to a lesser degree than the other three cell lines. The p53-status of the cell lines did not appear to affect ART-induced growth inhibition. ART-mediated inhibitory activity was also tested against the paclitaxel-resistant TX400 MCF-7 cell line, a variant of the MCF-7 line that over-expresses p-glycoprotein. As the increased p-glycoprotein expression associated with paclitaxel resistance in TX400 MCF-7 cells is known to interfere with the MTT assay (223), ART-induced growth inhibitory activity was determined using the acid phosphatase assay. ART showed good activity against the TX400 paclitaxel-resistant MCF-7 cells, although its potency was slightly lower than that observed for the parental cell line (Figure 3.2.1B). Confirmation of TX400 MCF-7 resistance to paclitaxel is shown in Appendix 1.

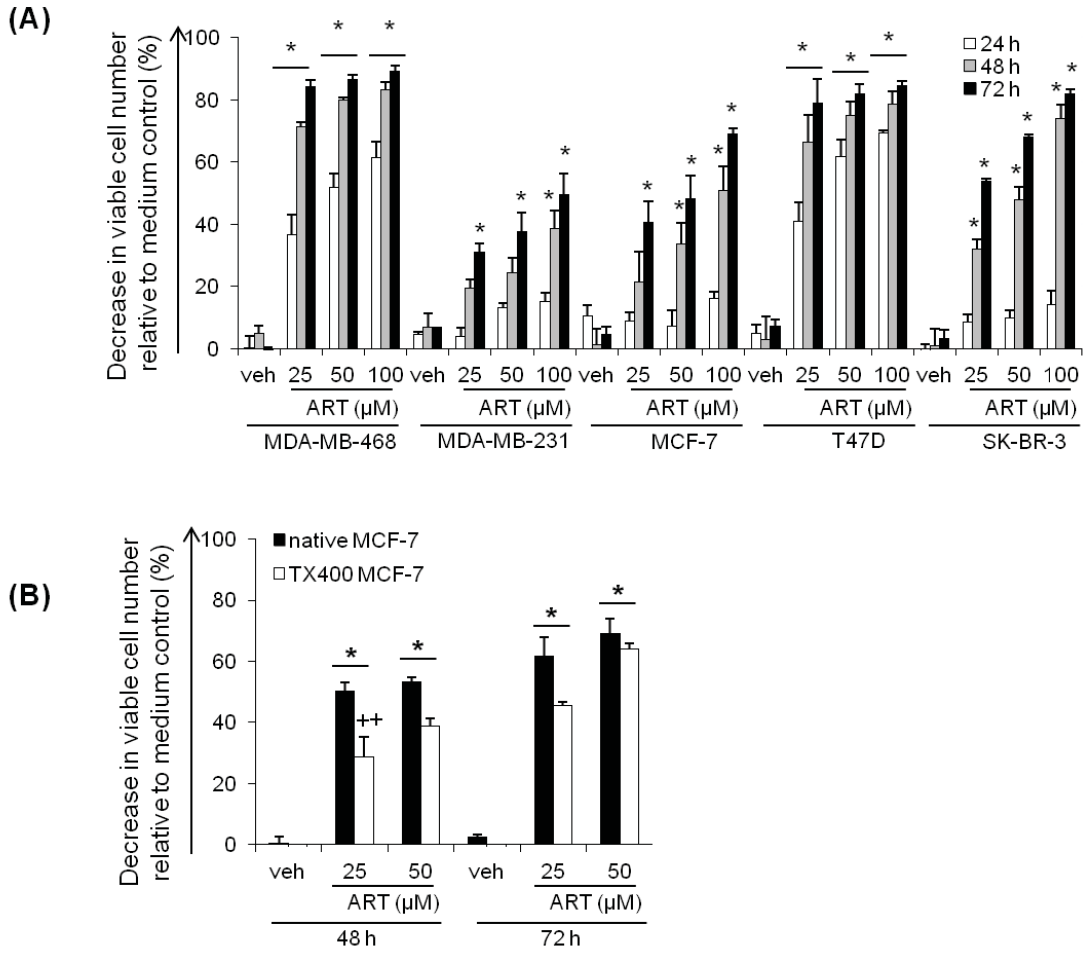

Figure 3.2.1 ART has a Potent Dose-dependent Inhibitory Effect on Breast Cancer Cell Growth (A) Breast cancer cell lines were treated with ART or vehicle (veh) then cultured for the specified times. Following culture, changes in viable cell number were determined using an MTT assay. (B) Parental and mutant TX400 MCF-7 breast cancer cell lines were treated with ART or vehicle, then cultured for the indicated times. Following culture, changes in viable cell number were determined using an acid phosphatase assay. (A,B) Data shown are the mean of at least 3 independent experiments ± SEM; * $p<0.05$ as compared to the vehicle, determined by a one-way ANOVA with a Tukey-Kramer post-test.

3.2.2 ART Maintains its Anti-breast Cancer Activity in 3D Cultures.

Visual assessment showed that MCF-7 spheroids treated with vehicle were compact and possessed clear, well defined margins. In contrast, ART-treated spheroids were smaller, less compact and irregular in shape. Furthermore, ART-treated cultures contained a significant number of single floating cells (Figure 3.2.2A). An acid phosphatase assay confirmed that ART-treatment led to a significant decrease in the number of viable MCF-7 cells contained in the spheroids in comparison to the vehicle-treated control (Figure 3.2.2B), indicating that ART was able to maintain its cytotoxic activity in a 3D culture system.

3.2.3 The Colony-forming Capacity of MDA-MB-468 Breast Cancer Cells is Reduced Following ART Treatment.

To further evaluate the ability of ART to inhibit the growth of breast cancer cells, the clonogenic activity of MDA-MB-468 breast cancer cells was determined following a 24 h treatment with ART. The clonogenic assay showed that higher concentrations of ART (25 and 50 μM) effectively inhibited the colony forming ability of surviving cells. Meanwhile, 5 μM ART, which showed significant inhibitory activity in the MTT assay did not affect the ability of surviving cells to form colonies (Figure 3.2.3 A,B).

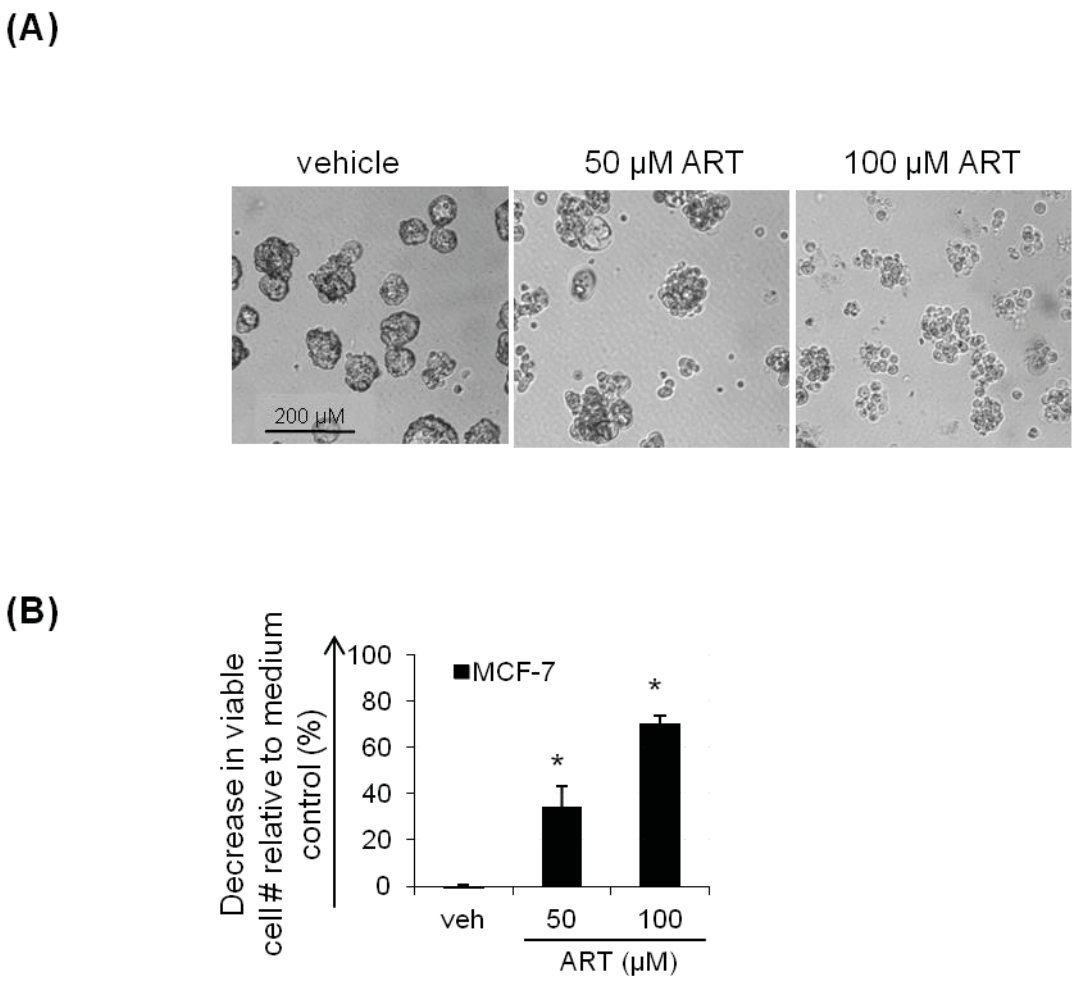

Figure 3.2.2 ART has an Anti-cancer Effect on MCF-7 Breast Cancer Spheroids. (A,B) MCF-7 spheroids were grown for 7 d in ultra low attachment plates, then treated with ART or vehicle for 72 h. Following culture, spheroids were photographed and changes in viable cell number were determined using an acid phosphatase assay. (A) Pictures depict results from a representative experiment. (A,B) Data shown are the mean of at least 3 independent experiments ± SEM; * $p<0.05$ as compared to the vehicle, determined by a one-way ANOVA with a Tukey-Kramer post-test.

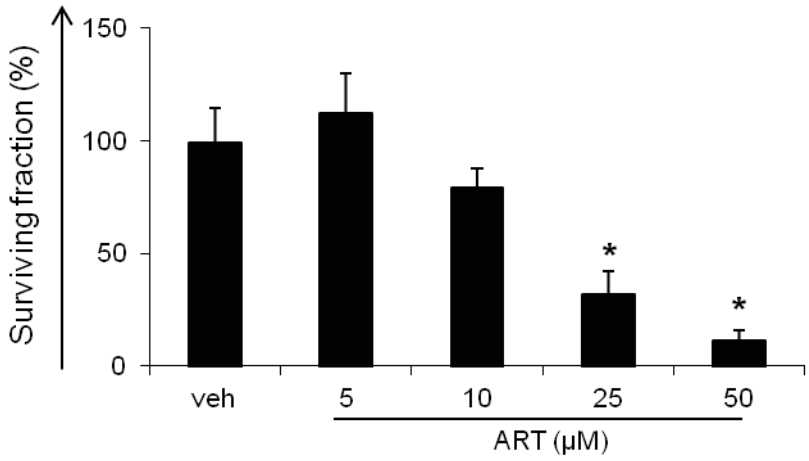

Figure 3.2.3 ART Inhibits the Colony-forming Capacity of MDA-MB-468 Breast Cancer Cells. MDA-MB-468 breast cancer cells were treated with ART or vehicle (veh) for 24 h. Following culture, cells were counted and equal numbers of cells were serially diluted and seeded in triplicate into 6-well plates. Colonies were cultured for ~14 d, then plates were washed, fixed and stained with crystal violet. Data shown are the mean of at least 3 independent experiments ± SEM; * $p<0.05$ as compared to the vehicle, determined by a one-way ANOVA with a Tukey-Kramer post-test.

3.2.4 ART Induces Apoptosis in MDA-MB-468 and SK-BR-3 Breast Cancer Cells.

Since the MTT assay cannot easily differentiate between anti-proliferative and cytotoxic activity, the ability of ART to induce apoptosis and/or necrosis in breast cancer cells was evaluated by Annexin-V-FLUOS/PI staining. Both MDA-MB-468 and SK-BR-3 cells treated with ART exhibited a dose- and time-dependent increase in early apoptosis, indicated by an increase in Annexin-V-FLUOS staining, as well as some late apoptotic/necrotic staining (indicated by staining with both Annexin-V-FLUOS and PI), compared to vehicle controls (Figure 3.2.4A,B). Apoptosis appeared to be the main mechanism of cytotoxicity because the majority of ART-treated cells stained positive for just Annexin-V-FLUOS.

Although ART-treatment resulted in significant breast cancer cell death, results were not as dramatic as those observed at the same time and dose in the MTT assay, suggesting that ART may also possess anti-proliferative activity in breast cancer cell culture. In accordance with the MTT assay results, ART demonstrated slightly better cytotoxic activity in following Annexin-V-FLUOS/PI staining towards the MDA-MB-468 cells compared to the SK-BR-3 line. Cell death occurred earlier in the MDA-MB-468 cells, although ART did show excellent cytotoxicity in both cell lines after 48 and 72 h culture.

3.2.5 RIPK1 Activity Does Not Significantly Contribute to the Cytotoxic Effects of ART Against Breast Cancer Cells.

To determine whether necoptosis was activated by ART and was involved in ART-induced breast cancer cell death, MDA-MB-468 breast cancer cells were treated with ART alone or in combination with the RIPK1 inhibitor nec-1. Nec-1- treatment in combination with ART had negligible effects on the breast cancer cells, confirming the importance of apoptosis rather than necrosis in ART-induced cell death (Figure 3.2.5). Nec-1 treatment did have a slight effect on cells treated with 50 μM ART, leading to a slight, yet significant, decrease in total ART-mediated cell death, although significance was not reached when statistics were calculated separately for early and late apoptosis.

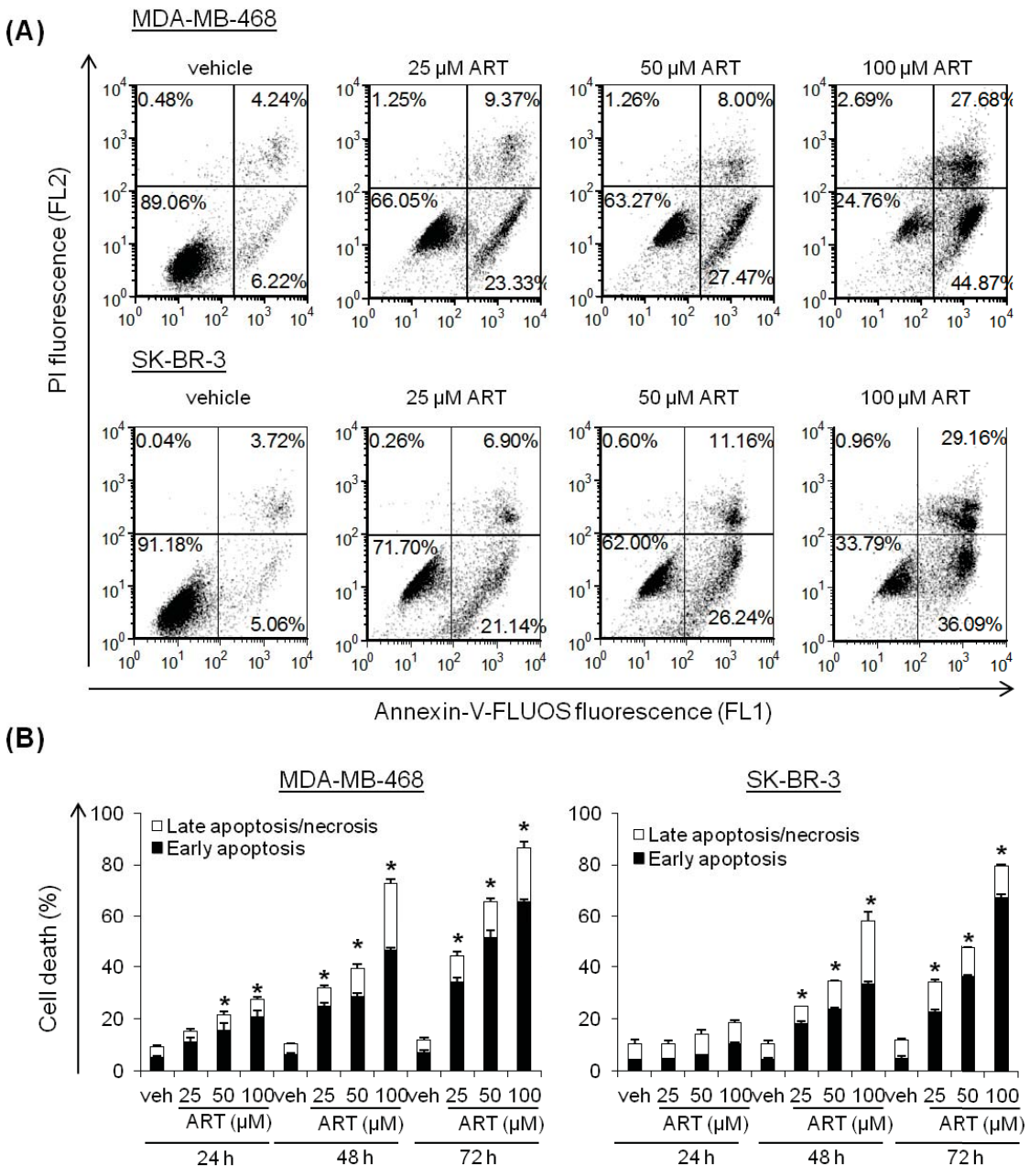

Figure 3.2.4 ART Causes Dose- and Time-dependent Apoptosis in Breast Cancer Cells. MDA-MB-468 and SK-BR-3 breast cancer cells were treated with ART or vehicle (veh), then cultured for the indicated times. Following culture, the amount of cell death was determined by Annexin-V-FLUOS/PI staining. (A) Histograms depict a representative experiment at 48 h. (B) Data shown are the mean of at least 3 independent experiments ± SEM; * $p<0.05$ as compared to the total cell death of the vehicle, determined by a one-way ANOVA with a Tukey-Kramer post-test.

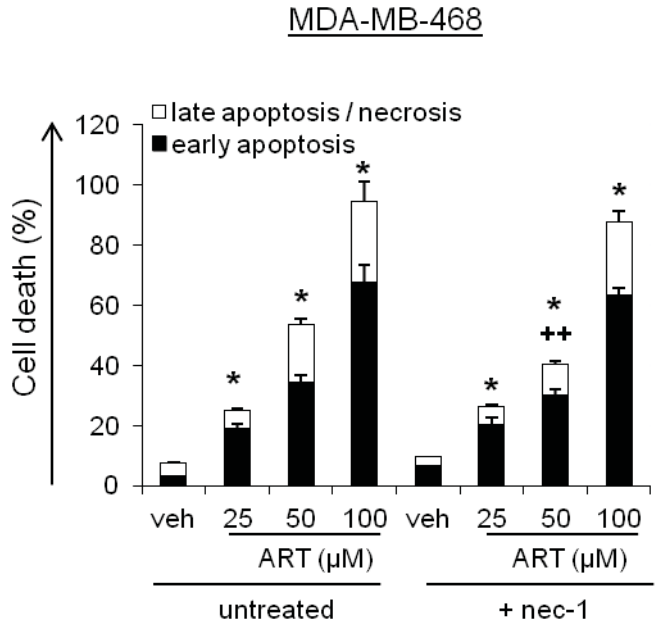

Figure 3.2.5 ART Fails to Cause Necroptotic Cell Death in MDA-MB-468 Breast Cancer Cells. MDA-MB-468 breast cancer cells were treated with ART in the presence or absence of 40 μM necrostatin (nec-1), which was added 30 min prior to ART. Following culture, the amount of cell death was determined by Annexin-V-FLUOS/PI staining. Data shown are the mean of at least 3 independent experiments ± SEM; * $p<0.05$ as compared to the total cell death of the vehicle, determined by a one-way ANOVA with a Tukey-Kramer post-test; ++ $p<0.05$ as compared to the total cell death of the treatment in the absence of nec-1, determined by a one-way ANOVA with a Tukey-Kramer post-test.

3.2.6 ART-induced Apoptosis in Breast Cancer Cells is Caspase-dependent and Characterised by PARP-1 Cleavage.

To confirm the importance of caspases in ART-mediated breast cancer cell apoptosis, caspase activation was assayed using the fluorescent labeled inhibitor of caspases (FLICA) probe which binds active caspases, leading to increased cellular fluorescence. ART-treated MDA-MB-468 and SK-BR-3 breast cancer cells had higher numbers of cells containing activated caspases than those treated with vehicle, indicating that ART induces caspase activation in these breast cancer cell lines (Figure 3.2.6A).

Since caspase activation alone does not prove that ART-induced apoptosis was caspase-dependent, breast cancer cells were treated with ART in the presence or absence of Z-VAD-fmk, which is a pan-caspase inhibitor. Z-VAD-fmk-treatment significantly decreased ART-induced total cell death (early apoptosis + late apoptosis/necrosis) in both MDA-MB-468 and SK-BR-3 breast cancer cells, indicating that ART-induced cytotoxicity is caspase-dependent in these breast cancer cell lines (Figure 3.2.6B). Culture of breast cancer cells in the presence of Z-VAD-fmk brought ART-induced early apoptosis back to baseline levels in both the SK-BR-3 and MDA-MB-468 cells. However, Z-VAD-fmk did not change the levels of late apoptotic/necrotic cell death for either ART-treated cell line. Consistent with caspase-dependent apoptotic cell death, ART caused PARP-1 cleavage in the SK-BR-3 and MDA-MB-468 breast cancer cell lines (Figure 3.2.4C). These results confirm that ART-induced apoptosis is caspase-dependent, but additional caspase-independent pathways leading to necrosis are also activated upon ART treatment.

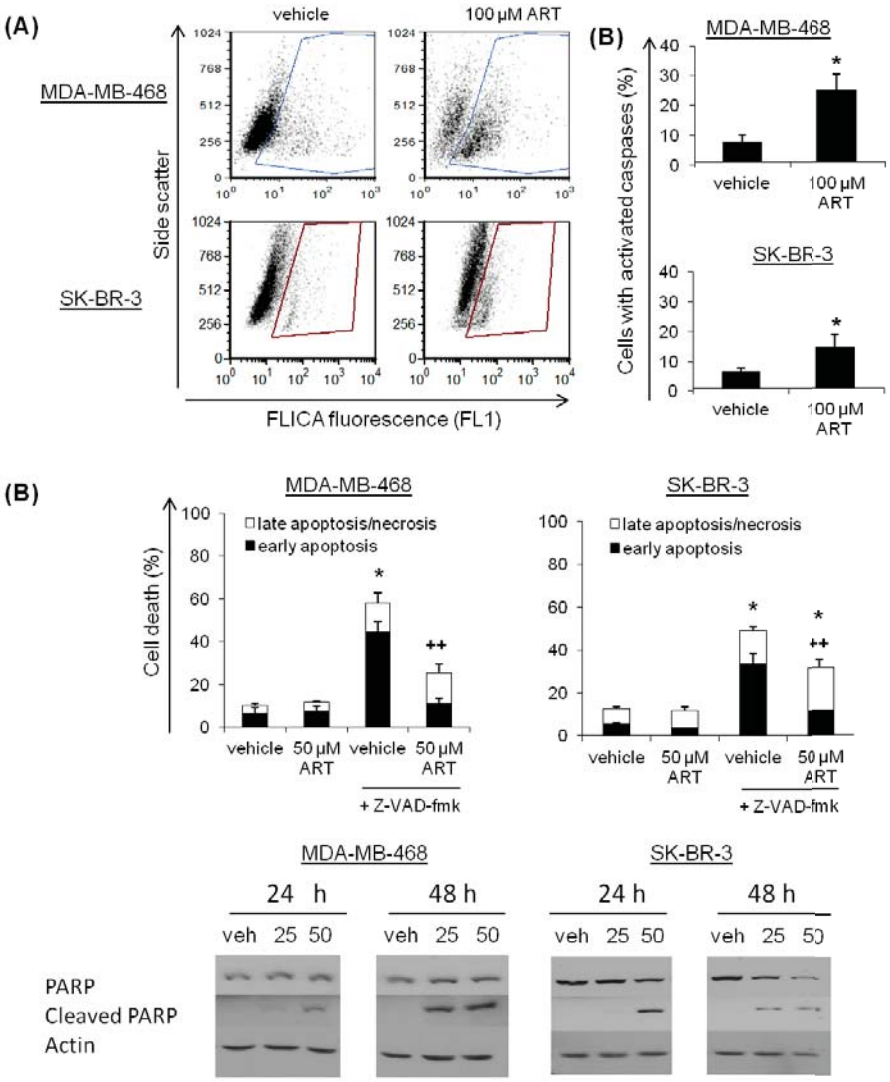

Figure 3.2.6 ART-induced Breast Cancer Cell Apoptosis is Caspase-dependent. (A,B) MDA-MB-468 and SK-BR-3 breast cancer cells were treated with ART or vehicle for 24 or 48 h, respectively. Following culture, cells were harvested and stained for 1 h at 37˚C with the fluorescent inhibitor of caspases (FLICA) reagent. Cells were then washed and changes in fluorescence were determined by flow cytometry. (C) Breast cancer cells were treated with ART or vehicle in the presence or absence of 50 µM of the pan-caspase inhibitor Z-VAD-fmk for 72 h. Z-VAD-fmk was added to cells 1 h prior to ART. Changes in the level of cell death were determined by Annexin-V-FLUOS/PI staining. (D) Breast cancer cells were treated with ART or its vehicle (veh) for the desired time. Following culture, cells were harvested and the total protein was collected and analyzed for PARP-1 cleavage by western blotting. (A) Dot plots depict results from a representative experiment. (B,C) Data shown are the mean of at least 3 independent experiments ± SEM; * $p<0.05$ as compared to the vehicle, determined by a one-way ANOVA with a Tukey-Kramer post-test; ++ $p<0.05$ as compared to the total cell death of the treatment in the absence of Z-VAD-fmk, determined by a one-way ANOVA with a Tukey-Kramer post-test. (D) Blots depict results from a representative experiment (n=3).

3.2.7 ART Induces the Production of ROS which is Required for ART-mediated MDA-MB-468 and SK-BR-3 Breast Cancer Cell Apoptosis.

CM-H_2DCFDA staining of ART-treated breast cancer cell lines revealed that ART induced significant ROS production following 24 h culture (Figure 3.2.7A,B). Treatment of cells with GSH inhibited ART-induced ROS production, confirming that GSH can effectively inhibit ROS generation. Interestingly, relative ROS production was higher in MDA-MB-468 cells than in SK-BR-3 cells, which may account for the increased sensitivity of MDA-MB-468 cells to ART-induced cell death at the 24 h time point. To determine the importance of ART-induced ROS production in breast cancer cell apoptosis, cells were treated with ART in the presence or absence of GSH. GSH treatment significantly inhibited ART-induced cell death, demonstrating the importance of ROS in ART-mediated killing of breast cancer cells (Figure 3.2.7C). Nevertheless, GSH was unable to completely prevent the cytotoxic activity of ART, indicating that other pathways that do not require ROS may also contribute to the cytotoxic activity of ART.

3.2.8 ART-induced Apoptosis is Iron-dependent.

The iron-catalysed Fenton reaction is often involved in ROS production (233). To gauge the importance of iron in ART-induced ROS production, CM-H_2DCFDA-stained breast cancer cells were loaded with iron in the form of HT prior to ART treatment. Pre-treatment with HT significantly enhanced ART-induced ROS production in MDA-MB-468 breast cancer cells following 8 h of culture (Figure 3.2.8A). A similar trend was also observed for the SK-BR-3 cell line. Furthermore, HT pre-treatment also enhanced the growth inhibitory effect of ART in an MTT assay (Figure 3.2.8B). The increase in ART-mediated growth inhibition was most apparent at 24 h at the highest concentrations of ART administered (25 and 50 μM ART for MDA-MB-468 and SK-BR-3 cells, respectively). Breast cancer cells that were treated with ART in the presence of the iron chelator deferiprone (DFE) showed reduced apoptosis (Figure 3.2.8C). Taken together, these data demonstrates a role for iron in ART-induced ROS production and breast cancer cell killing.

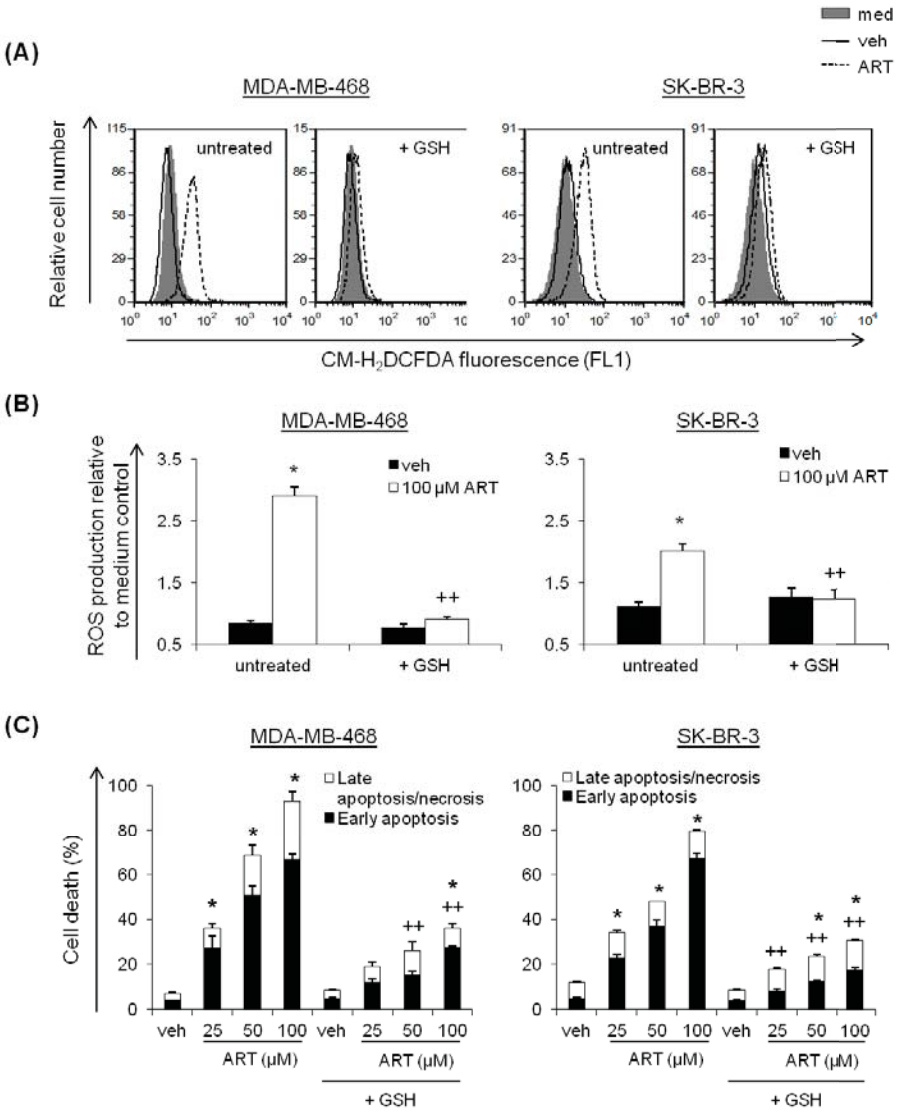

Figure 3.2.7 ART-induced ROS Production is Involved in Apoptosis Induction in Breast Cancer Cells. (A,B) MDA-MB-468 and SK-BR-3 breast cancer cells were stained with 5 µM CM-H_2DCFDA, then cultured with ART or vehicle (veh) in the presence or absence of 10 mM reduced glutathione (GSH) for 24 h. GSH was added 30 min prior to ART. H_2O_2 was used as a positive control. Following culture, ROS production, represented by increased cellular fluorescence, was determined by flow cytometry. (C) Breast cancer cells were cultured for 72 h with ART or vehicle (veh) in the presence or absence of 10 mM GSH. GSH was added 30 min prior to ART. Following culture, the amount of cell death was determined using the Annexin-V-FLUOS/PI assay. (A) Histograms depict results from a representative experiment. (B) Data shown had ART background fluorescence subtracted. (B,C) Data shown are the mean of at least 3 independent experiments ± SEM; * $p<0.05$ as compared to the vehicle, determined by a one-way ANOVA with a Tukey-Kramer post-test, ++ $p<0.05$ as compared to the treatment in the absence of GSH, determined by a one-way ANOVA with a Tukey-Kramer post-test.

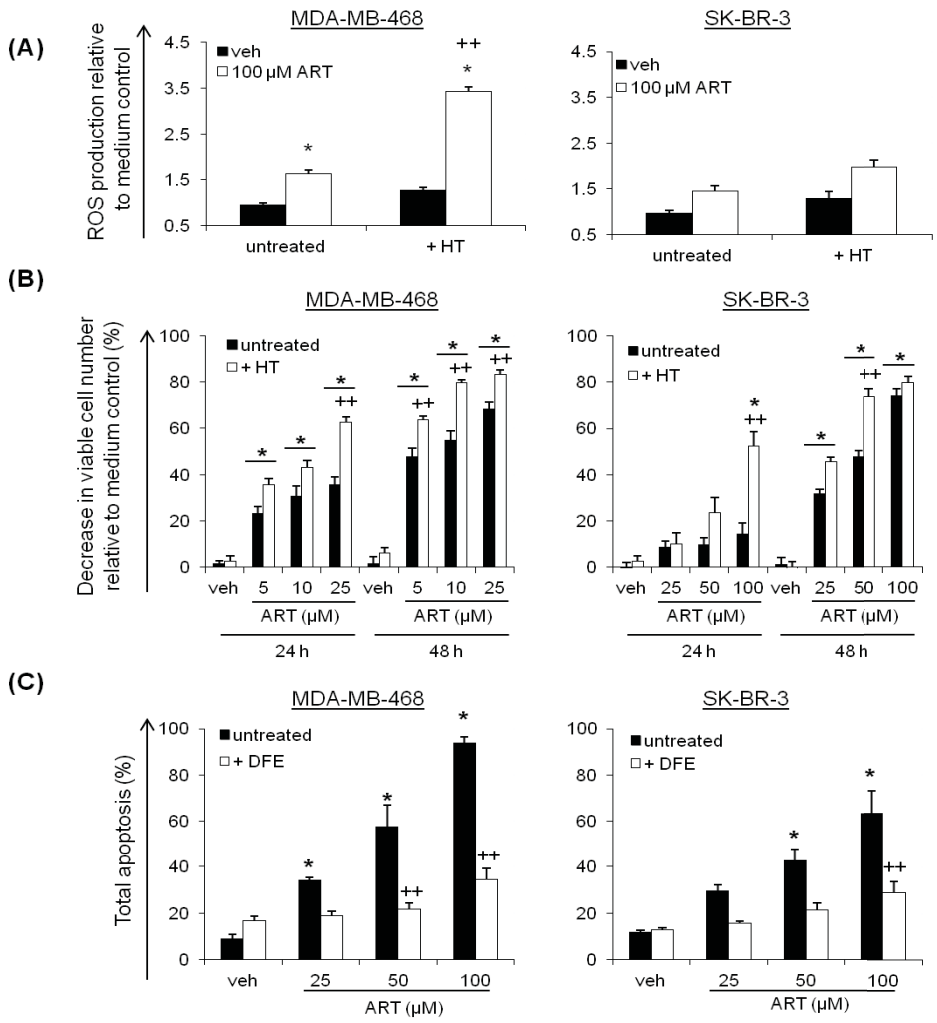

Figure 3.2.8 Iron is Required for ART-induced Apoptosis and Iron Pre-treatment Enhances ROS Production and Sensitises Breast Cancer Cells to ART. (A) MDA-MB-468 and SK-BR-3 breast cancer cells were stained with 5 µM CM-H_2DCFDA, following which, cells were treated for 1 h with 10 µM holo-transferrin (HT). HT-containing medium was then removed and cells were treated with ART or vehicle (veh) for 8 h. Following culture, ROS production, represented by increased cellular fluorescence, was determined by flow cytometry. (B) Breast cancer cells were treated with 10 µM HT for 1 h. HT was then removed and cells were treated with ART or vehicle and cultured for 24 or 48 h. Changes in viable cell number were determined using the MTT assay. (C) Breast cancer cells were cultured for 48 h with ART or vehicle in the presence or absence of 12.5 µg/mL deferiprone (DFE), which was added 30 min prior to ART. Following culture, the amount of cell death was determined by Annexin-V-FLUOS/PI staining. (A) Data shown had ART background fluorescence subtracted. (A,B) Data shown are the mean of at least 3 independent experiments ± SEM; * $p<0.05$ as compared to the vehicle, determined by a one-way ANOVA with a Tukey-Kramer post-test; ++ $p<0.05$ as compared to the treatment in the absence of HT/DFE, determined by a one-way ANOVA with a Tukey-Kramer post-test.

3.2.9 ART-induced ROS-dependent DNA Damage.

AR-induced double strand DNA breaks in MDA-MB-468 and SK-BR-3 breast cancer cells were demonstrated by the presence of phosphorylated Ser139 on H2AX (γH2AX) (Figure 3.2.9). DNA damage was ROS-dependent since phosphorylation of Ser139 was not observed in the presence of GSH.

3.2.10 Oxygen is Required for ART-induced Apoptosis.

The effect of ART treatment in the presence or absence of oxygen was examined using a hypoxia chamber. There was a significant decrease in ART-induced cell death in MDA-MB-468 cells that were incubated for 48 h under hypoxic conditions compared to those incubated in normoxia, indicating that oxygen is required for ART-mediated cytotoxicity (Figure 3.2.10). Moreover, ART-treated cells that were incubated under normoxic conditions for 24 h then transferred to the hypoxic chamber and cultivated for an additional 24 h maintained their sensitivity towards ART, suggesting that the presence of oxygen is only essential for the first 24 h following ART treatment.

3.2.11 ART Induces Dose-dependent Mitochondrial Membrane Destabilization in Breast Cancer Cells.

To further investigate the ability of ART to promote apoptosis, ART-treated breast cancer cells were stained with $DiOC_6$ to determine whether the integrity of breast cancer cell mitochondria was affected by ART. ART treatment induced a decrease in the fluorescence in both MDA-MB-468 and SK-BR-3 cells, indicating mitochondrial membrane permeabilisation (Figure 3.2.11A,B). ART-induced changes to the mitochondrial membrane were both dose- and time-dependent.

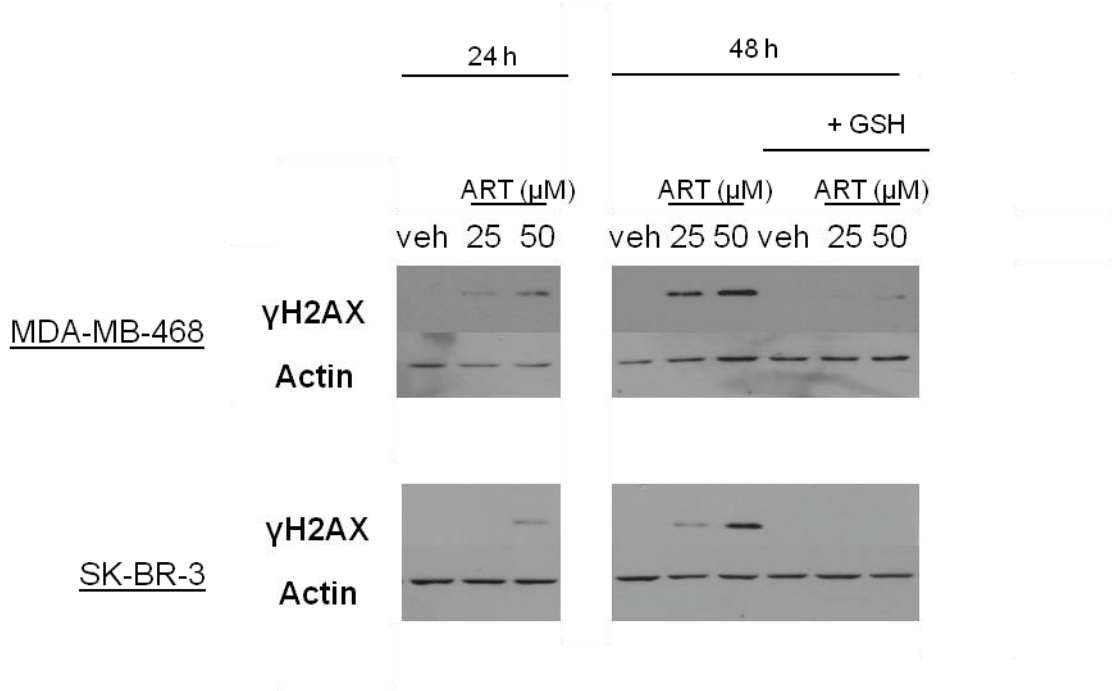

Figure 3.2.9 ART Induces ROS-dependent DNA Damage in Breast Cancer Cells. MDA-MB-468 and SK-BR-3 breast cancer cells were cultured for the indicated times with ART or its vehicle (veh) in the presence or absence of 10 mM GSH, which was added 30 min prior to ART. Following culture, cells were harvested and the total protein was collected and analyzed by western blotting. Blots depict results from a representative experiment (n=2).

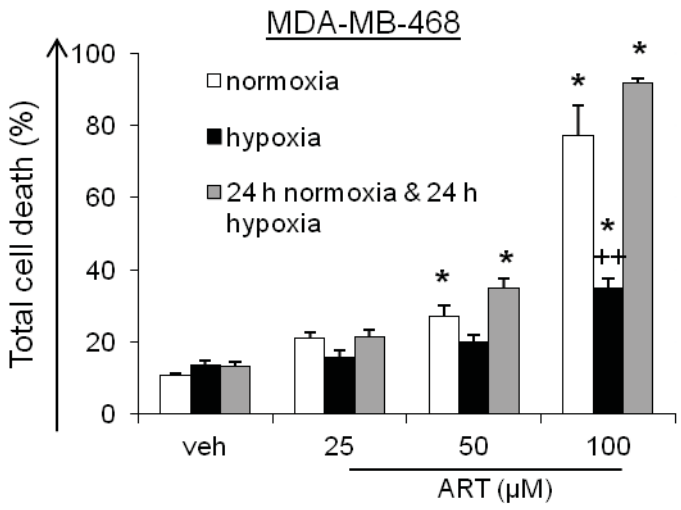

Figure 3.2.10 Oxygen is Required for ART-mediated Apoptosis in MDA-MB-468 Breast Cancer Cells. MDA-MB-468 breast cancer cells were treated with ART or vehicle (veh), then cultured for 48 h under conditions of normoxia and/or hypoxia. Cells cultured under combinational conditions were cultured under normoxic conditions for 24 h following ART-treatment, then were cultured for an additional 24 h under hypoxic conditions. Data shown are the mean of at least 3 independent experiments ± SEM;* $p<0.05$ as compared to the vehicle, determined by a one-way ANOVA with a Tukey-Kramer post-test; ++ $p<0.05$ as compared to the normoxic treatment, determined by a one-way ANOVA with a Tukey-Kramer post-test.

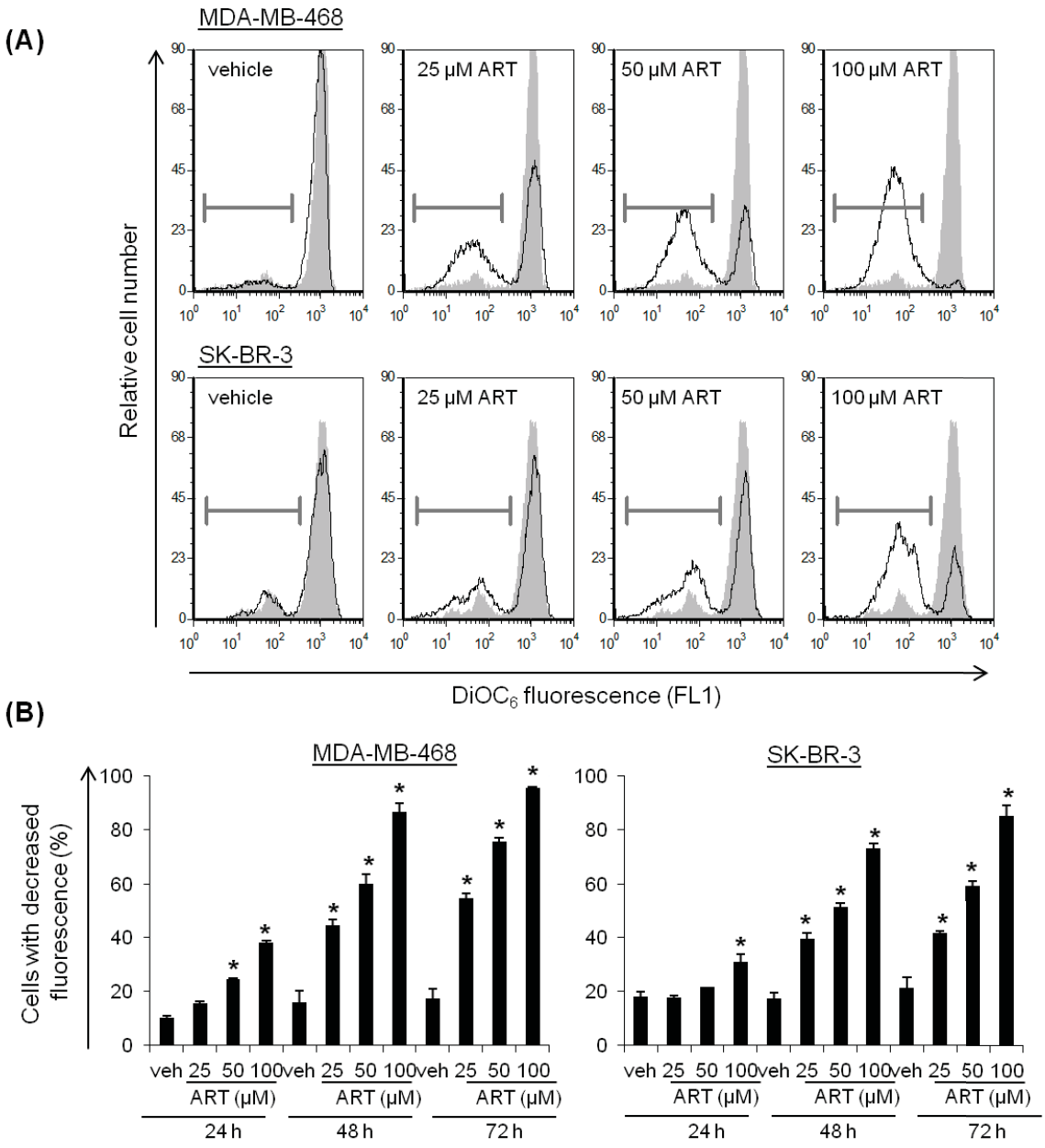

Figure 3.2.11 ART-induced Apoptosis is Characterised by Mitochondrial Membrane Destabilisation. MDA-MB-468 and SK-BR-3 breast cancer cells were treated with ART or vehicle (veh) for the indicated times, then stained with 40 nM $DiOC_6$ for 15 min before analysis by flow cytometry. (A) Histograms depict results from a representative experiment at 48 h. (B) Data shown are the mean of at least 3 independent experiments ± SEM;* $p<0.05$ as compared to the vehicle, determined by a one-way ANOVA with a Tukey-Kramer post-test.

3.2.12 ART-induced Mitochondrial Membrane Destabilization is Characterised by the Release of Cytochrome c and Smac/DIABLO.

Western blotting was used to determine whether pro-apoptotic factors normally sequestered in the mitochondria were released upon ART treatment. The plasma membrane of ART-treated MDA-MB-468 and SK-BR-3 breast cancer cells was selectively permeabilised and the cytoplasmic cellular fraction was collected. Western blot analysis of the cytoplasmic fraction of ART-treated cells showed an increase in cellular cytochrome c and Smac/DIABLO, proteins normally sequestered in the mitochondria of healthy cells (Figure 3.2.12). Cytochrome c and Smac/DIABLO release corroborate the results obtained by $DiOC_6$ staining, and confirm that ART causes mitochondrial membrane destabilization in breast cancer cells.

3.2.13 ART Induces ROS-dependent Mitochondrial Membrane Destabilization in MDA-MB-468 and SK-BR-3 Breast Cancer Cell Lines.

Since ROS were required for ART-induced breast cancer cell apoptosis, the requirement for ROS was also determined for the destabilising effects of ART on the mitochondrial membrane. ART was unable to affect mitochondrial membrane stability in the presence of GSH, suggesting that ROS production is up-stream of the mitochondria (Figure 3.13).

3.2.14 ART-treatment of MDA-MB-468 and SK-BR-3 Breast Cancer Cells Leads to a Decrease in the Surface Expression of CD71.

It has been suggested that the CD71 receptor may be involved in the anti-cancer activity of ART (175, 182). Both MDA-MB-468 and SK-BR-3 breast cancer cells expressed similar levels of surface CD71 (Figure 3.2.14B). Interestingly, 50 μM of ART significantly decreased the expression of CD71 in both breast cancer cell lines after 24 h of culture (Figure 3.2.14A,B).

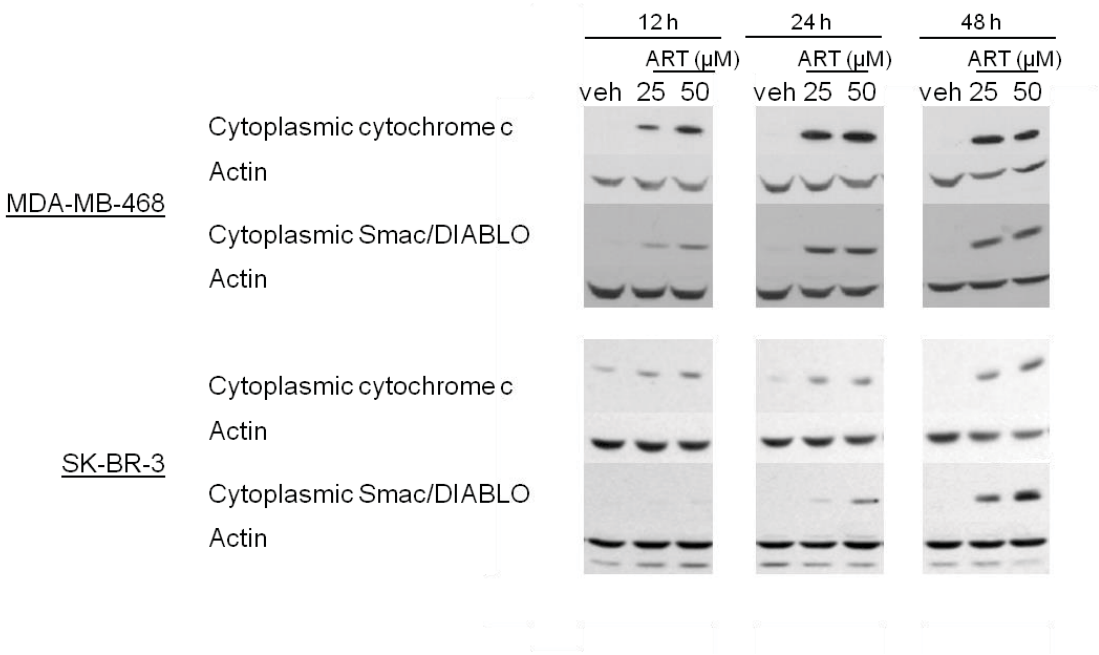

Figure 3.2.12 ART-mediated Mitochondrial Membrane Destabilisation is Characterised by the Release of Cytochrome c and Smac/DIABLO. MDA-MB-468 and SK-BR-3 breast cancer cells were cultured with ART of vehicle (veh) for 24 or 48 h. Following culture, cells were washed and lysed using cytoplasmic membrane-specific digitonin lysis buffer before analysis by western blotting. Blots depict results from a representative experiment (n=3).

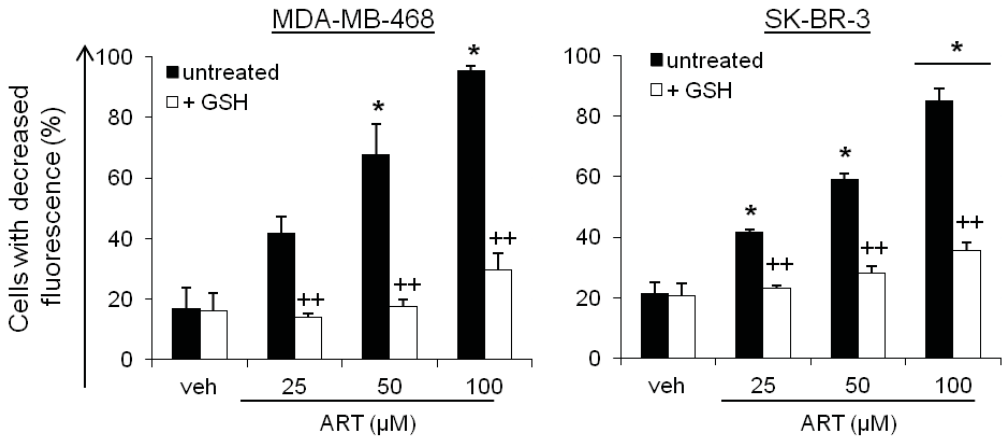

Figure 3.2.13 ART-mediated Mitochondrial Membrane Destabilisation is ROS-dependent. MDA-MB-468 and SK-BR-3 breast cancer cells were treated with ART or vehicle (veh) in the presence or absence of 10 mM GSH for 72 h. GSH was added 30 min prior to ART. Following culture, cells were stained with 40 nM $DiOC_6$ for 15 min, then analysed by flow cytometry. Data shown are the mean of at least 3 independent experiments ± SEM; * $p<0.05$ as compared to the vehicle, determined by a one-way ANOVA with a Tukey-Kramer post-test; ++ $p<0.05$ as compared to the treatment in the absence of GSH, determined by a one-way ANOVA with a Tukey-Kramer post-test.

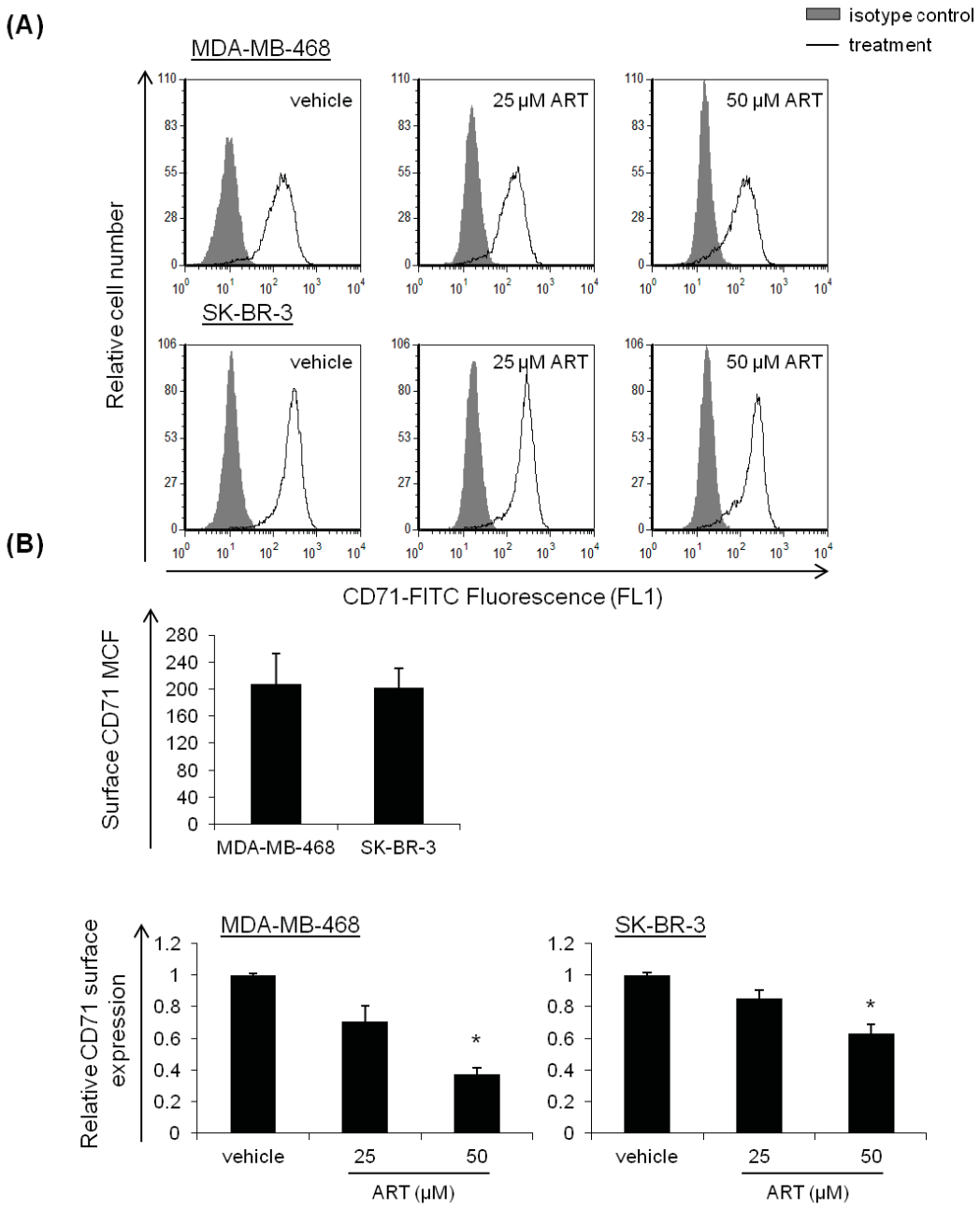

Figure 3.2.14 ART Decreases Surface Expression of CD71 in Breast Cancer Cells. MDA-MB-468 and SK-BR-3 breast cancer cells were treated with ART or vehicle, then cultured for 24 h. Following culture, cells were harvested using EDTA, washed and stained for 1 h at 4˚C with mouse anti-human CD71 (OKT9) FITC or its isotype control (mouse anti-human IGg1κ FITC). Cells were then washed and fixed in 1 % PFA. Mean channel fluorescence (MCF) was subsequently determined by flow cytometry. (A) Histograms depict results from a representative experiment. (B) Data shown are the mean of at least 3 independent experiments ± SEM; * $p<0.05$ as compared to the vehicle, determined by a one-way ANOVA with a Tukey-Kramer post-test.

3.2.15 ART Inhibits MDA-MB-468 and SK-BR-3 Breast Cancer Cell Proliferation.

To investigate the effect of ART on breast cancer cell replication, MDA-MB-468 and SK-BR-3 breast cancer cells were stained with Oregon Green 488 dye. Cells treated with ART possessed a higher fluorescence than cells treated with the vehicle, indicating that they had gone through fewer cycles of division (Figure 3.2.15A). Vehicle-treated cells underwent an average of 3 or 2 rounds of replication (MDA-MB-468 and SK-BR-3, respectively) while cells treated with ART only replicated once (Figure 3.2.15A,B). The addition of GSH did not increase the proliferation of ART-treated breast cancer cells, indicating that, unlike the cytotoxic activity, ART-induced anti-proliferative effects are ROS-independent (Figure 3.2.15B).

3.2.16 ART Alters the Expression of Key Cell Cycle Regulatory Proteins in Breast Cancer Cells.

To gain a better understanding, on the molecular level, of how ART affected breast cancer cell proliferation, western blotting was used to determine changes in the expression of key cell cycle regulatory proteins. ART-treatment had a broad impact on the expression of cycle proteins involved in all stages of the cell cycle (Figure 3.2.16). There was a a significant decrease in the level of E2F-1, as well as an increase in the CDK inhibitor p21WAF1/CIP1 protein levels. Protein levels of Cyclin D3, CDC25C, CDK2, CDK4 and CDK1 were also decreased in both cell lines after ART treatment. Decreased levels of cyclin A and cyclin B were also observed in ART-treated SK-BR-3 cells, although these changes were minimal in the MDA-MB-468 cell line. Rb expression was decreased following a 24 h exposure to ART, but changes were minimal at 48 h. Since, MDA-MB-468 cells lack the Rb protein, ART-induced changes could not be assessed in this cell line.

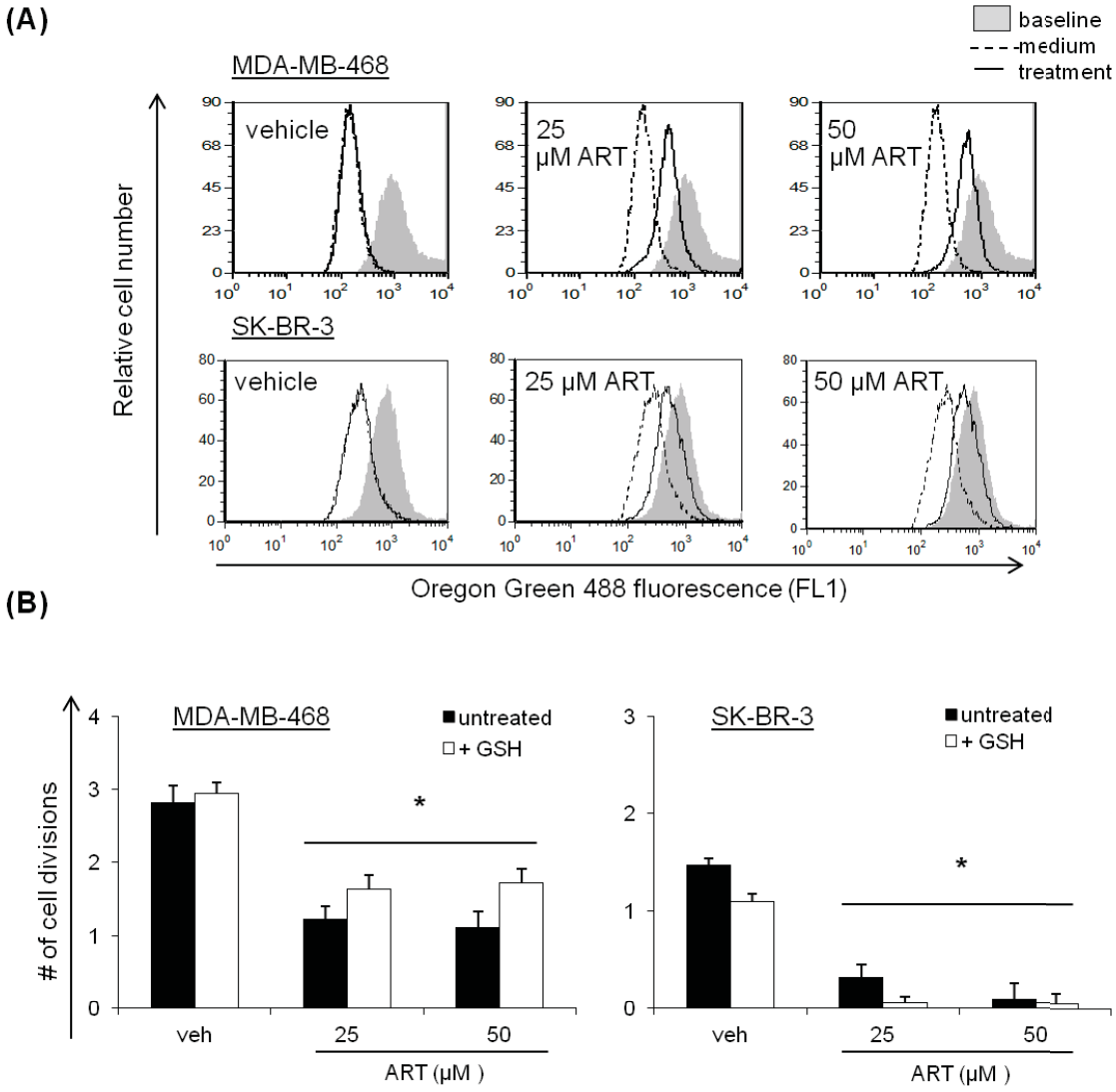

Figure 3.2.15 ART has a ROS-independent Anti-proliferative Effect on MDA-MB-468 and SK-BR-3 Breast Cancer Cells. (A,B) MDA-MB-468 and SK-BR-3 breast cancer cells were stained with Oregon Green 488 dye. Cells were then cultured for 72 h with ART or vehicle (veh) in the presence or absence of 10 mM GSH, which was added 30 min prior to ART. Cell fluorescence was subsequently determined by flow cytometry. (A) Histograms depict results from a representative experiment. (B) Data shown are the mean of at least 3 independent experiments ± SEM; *p< 0.05 as compared to respective vehicle controls, determined by a one-way ANOVA with a Tukey-Kramer post-test.

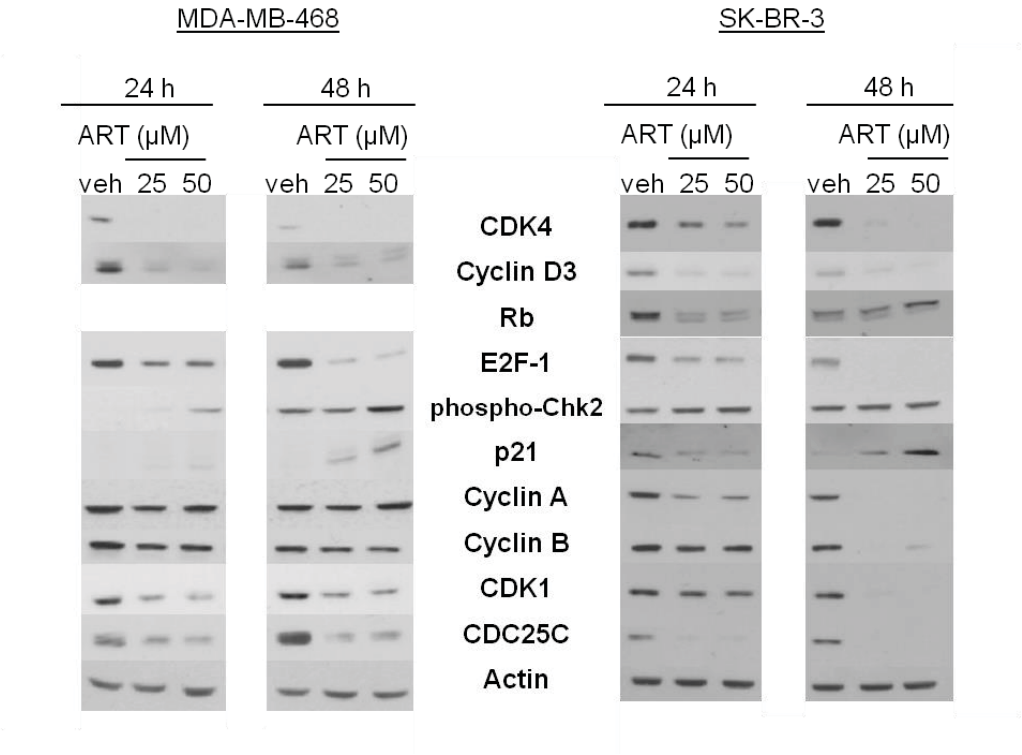

Figure 3.2.16 ART Modulates the Expression of Key Cell Cycle Regulatory Proteins in Breast Cancer Cells. MDA-MB-468 and SK-BR-3 breast cancer cells were treated with ART or its vehicle (veh) for the indicated times. Following culture, cells were harvested and the total protein was collected and analysed by western blotting. Blots depict results from a representative experiment and a representative actin (n=3).

3.2.17 MDA-MB-468 and SK-BR-3 Breast Cancer Cells Treated with ART Arrest in the G2/M and G1 Phases of the Cell Cycle, Respectively.

To determine whether the anti-proliferative activity of ART resulted in a cell cycle block, PI was used to determine the distribution of cells in the different stages of the cell cycle following exposure to ART. ART-treated MDA-MB-468 cells displayed a marked increase in the fraction of cells present in the G2/M phase of the cell cycle compared to those treated with vehicle (Figure 3.2.17A,B). There was a corresponding decrease in the number of cells present in G1. Meanwhile, SK-BR-3 cells arrested in the G1 phase, although there was also a significant increase in the number of cells in G2/M following 50 μM ART treatment compared to vehicle-treated cells. Both cell lines showed an ART-induced increase in the sub G1 peak (Figure 3.2.17C) consistent with the induction of apoptosis by ART.

3.2.18 ART-induced MDA-MB-468 G2/M Cell Cycle Arrest is ROS-dependent.

Interestingly, although the anti-proliferative activity of ART was not influenced by ROS production, treatment of MDA-MB-468 breast cancer cells with GSH in combination with ART impacted the phase of the cell cycle at which the cells arrested. Instead of a G2/M arrest, ART treatment in the presence of GSH led to an increase in the number of cells in the G1 phase of the cell cycle, and a corresponding decrease in the G2/M population (Figure 3.2.18). The slight increase in the number of cells present in the G2/M phase in the ART-treated SK-BR-3 cells was lost in the presence of GSH, which also resulted in an increase in number of cells in the G1 phase. These results suggest that ART can induce cell cycle arrest by two distinct mechanisms, one that requires ROS and results in a G2/M arrest, and another that is ROS-independent and leads to cells arresting in the G1 phase of the cell cycle.

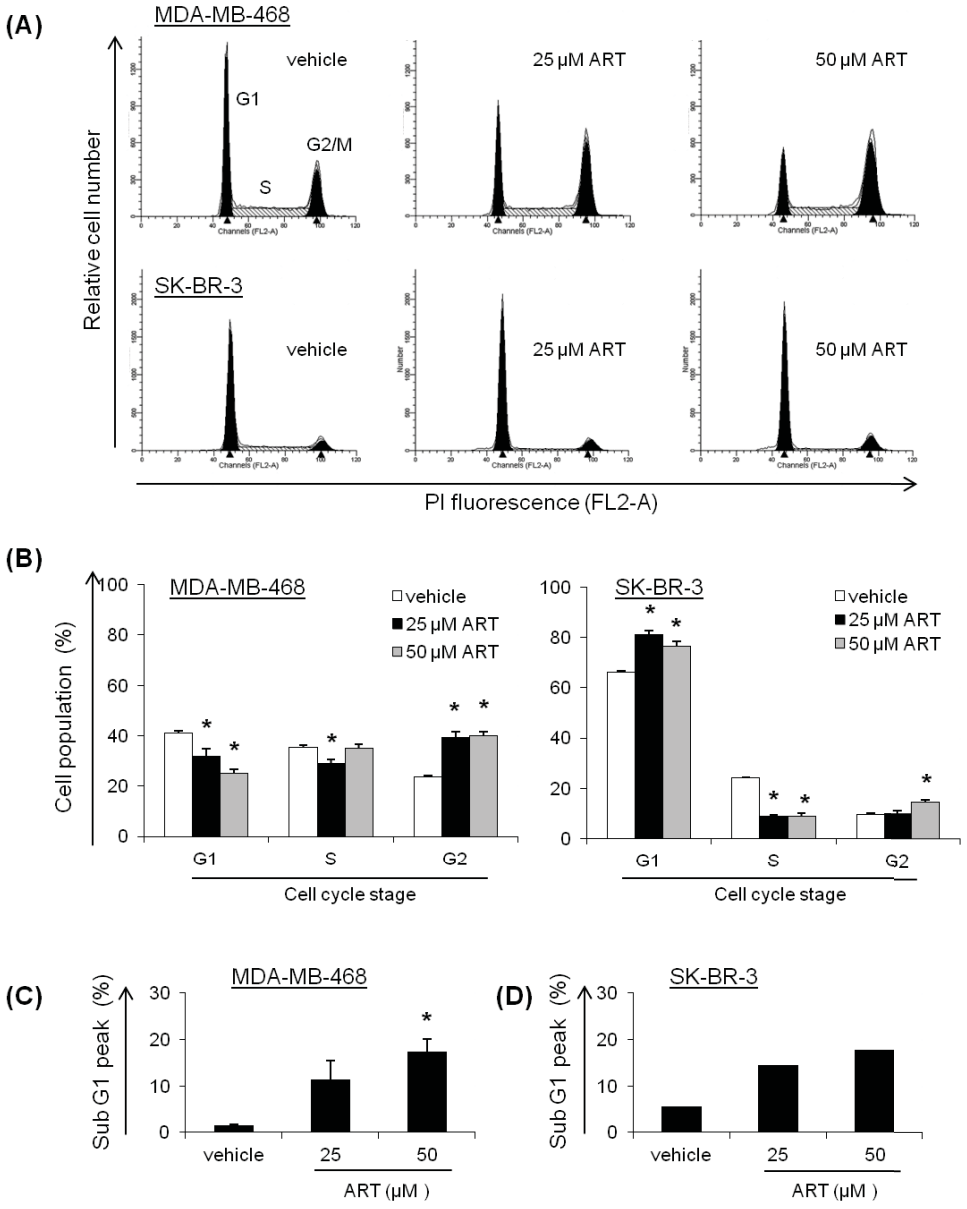

Figure 3.2.17 ART Induces G2/M Cell Cycle Arrest in MDA-MB-468 Breast Cancer Cells and G1 and G2/M Arrest in SK-BR-3 Cells. (A,B,C) MDA-MB-468 and SK-BR-3 breast cancer cells were cultured with ART or vehicle for 48 h. Cells were then permeabilised, fixed in ethanol, and stored at -20˚C for at least 24 h. Cells were subsequently washed and stained with PI for 30 min prior to analysis by flow cytometry. (A,D) Histograms and bar chart depict results from a representative experiment. Histograms do not show the sub G1 peak. (B,C) Data shown are the mean of at least 3 independent experiments ± SEM; *p< 0.05 as compared to the vehicle control, determined by a one-way ANOVA with a Tukey-Kramer post-test.

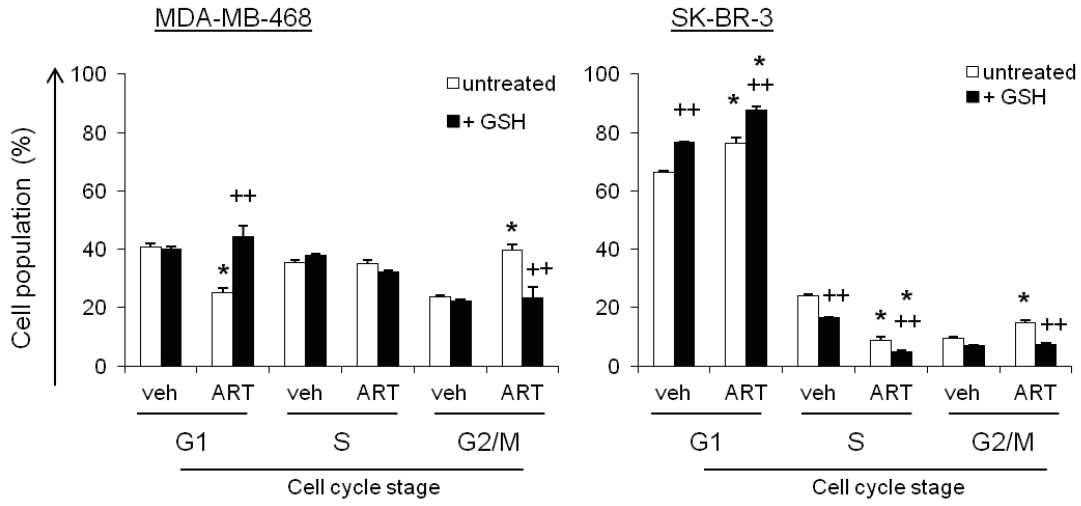

Figure 3.2.18 ART-induced G2/M Cell Cycle Arrest is ROS-dependent. MDA-MB-468 and SK-BR-3 breast cancer cells were cultured with 50 µM ART or vehicle (veh) in the absence or presence of 10 mM GSH for 48 h. GSH was added 30 min prior to ART. Following culture, cells were permeabilised and fixed in ethanol, then stored at -20˚C for at least 24 h. Cells were subsequently washed and stained with PI for 30 min prior to analysis by flow cytometry. Data shown are the mean of at least 3 independent experiments ± SEM; *$p< 0.05$ as compared to the respective vehicle control; ++ $p<0.05$ as compared to the treatment in the absence of GSH, determined by a one-way ANOVA with a Tukey-Kramer post-test.

3.2.19 Low Doses of ART Enhance the Effect of Radiation Therapy on MDA-MB-468 Breast Cancer Cells.

Treatment of MDA-MB-468 cells with very low concentrations of ART enhanced the growth-inhibitory effect of radiation therapy, suggesting that ART may have value as a radio-sensitising agent in the treatment of breast cancer (Figure 3.2.19).

3.2.20 Low Doses of ART Sensitises MDA-MB-468 Breast Cancer Cells to Chemotherapeutic Agents.

Chemotherapy is usually administered as a cocktail of anti-cancer agents. To determine whether ART could be effectively combined with standard chemotherapeutic drugs, cells were treated with low doses of ART for 1 h and then exposed to a panel of drugs typically used in the treatment of breast cancer. Low doses of ART were able to significantly lower the EC_{50} values of all the standard chemotherapeutic agents tested, suggesting potential use for ART in combined modality treatment of breast cancer (Figure 3.2.20).

3.2.21 Treatment of MDA-MB-468 with a Sub-cytotoxic Level of ART Sensitises Breast Cancer Cells to Cisplatin.

To further explore the potential of ART as an addition to current chemotherapy regimens, a colony forming assay was performed using a combination of cisplatin and ART. Unlike in the MTT assay, 5 μM ART treatment showed little effect on the clonal growth of MDA-MB-468 breast cancer cells after 24 h treatment. However, when combined with cisplatin, ART significantly decreased the colony forming ability of breast cancer cells compared to cisplatin treatment alone (Figure 3.2.21). The ability of ART to enhance the effect of growth inhibitory cisplatin on breast MDA-MB-468 breast cancer cells is consistent with the results from the MTT assay and indicates that further study examining the combination of cisplatin and ART is warranted.

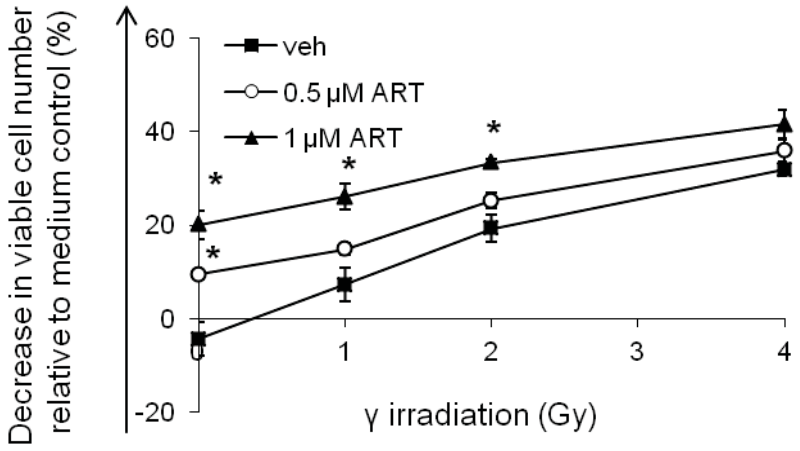

Figure 3.2.19 Low Doses of ART Enhances the Effect of Radiation Treatment on MDA-MB-468 Breast Cancer Cells. MDA-MB-468 breast cancer cells were cultured with ART or vehicle for 1 h, then exposed γ-irradiation. Breast cancer cells were subsequently cultured for 72 h, then changes in viable cell number were determined using an MTT assay. Data shown are the mean of at least 3 independent experiments ± SEM; *$p < 0.05$ as compared to respective treatment in the absence of ART, determined by a one-way ANOVA with a Tukey-Kramer post-test.

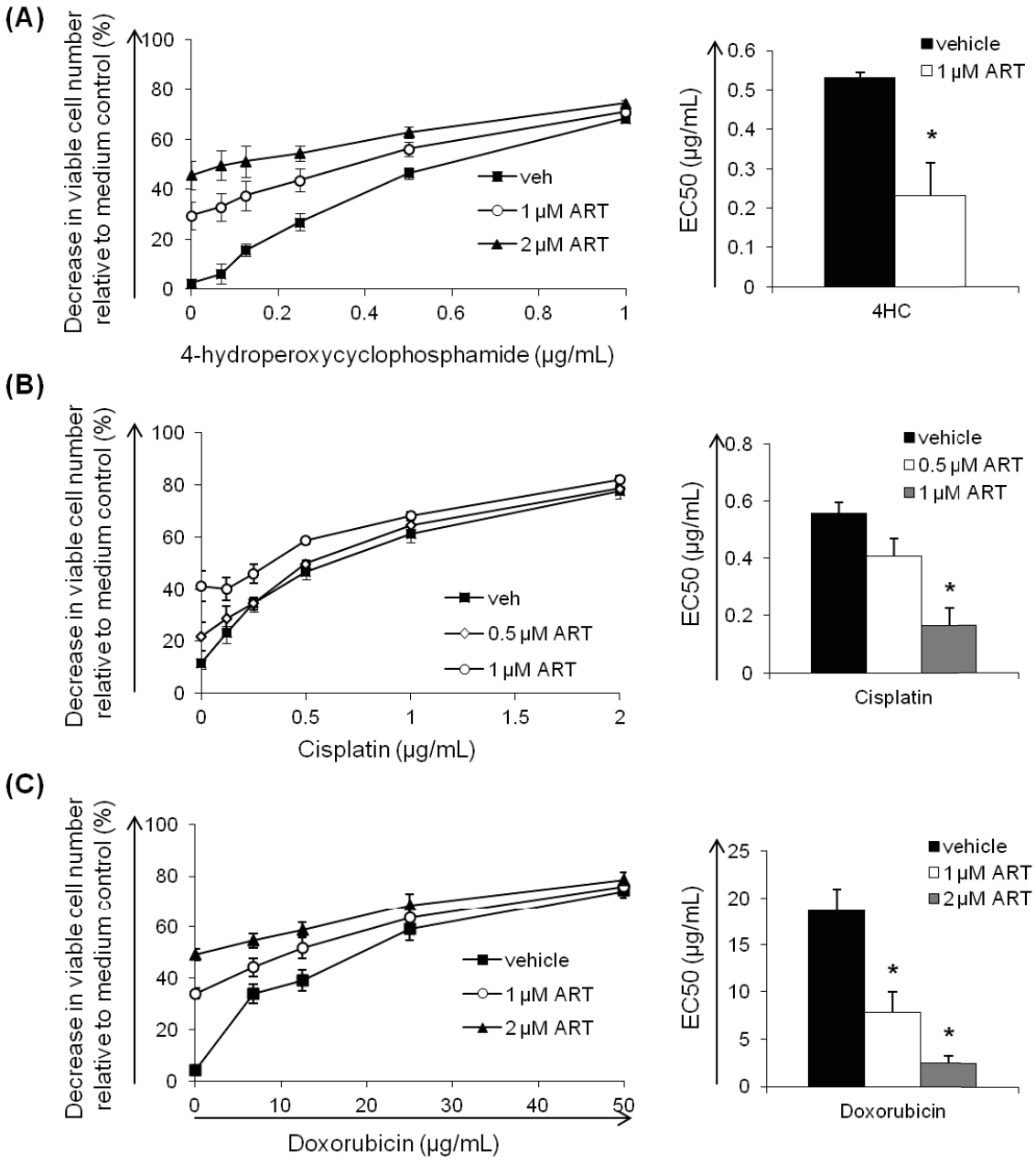
(A)
Decrease in viable cell number relative to medium control (%)
100
80
60
40
20
0
0
0.2
0.4
0.6
0.8
1
veh
1 μM ART
2 μM ART
4-hydroperoxycyclophosphamide (μg/mL)
EC50 (μg/mL)
0.6
0.5
0.4
0.3
0.2
0.1
0
vehicle
1 μM ART
*
4HC
(B)
Decrease in viable cell number relative to medium control (%)
100
80
60
40
20
0
0
0.5
1
1.5
2
veh
0.5 μM ART
1 μM ART
Cisplatin (μg/mL)
EC50 (μg/mL)
0.8
0.6
0.4
0.2
0
vehicle
0.5 μM ART
1 μM ART
*
Cisplatin
(C)
Decrease in viable cell number relative to medium control (%)
100
80
60
40
20
0
0
10
20
30
40
50
vehicle
1 μM ART
2 μM ART
Doxorubicin (μg/mL)
EC50 (μg/mL)
25
20
15
10
5
0
vehicle
1 μM ART
2 μM ART
*
*
Doxorubicin

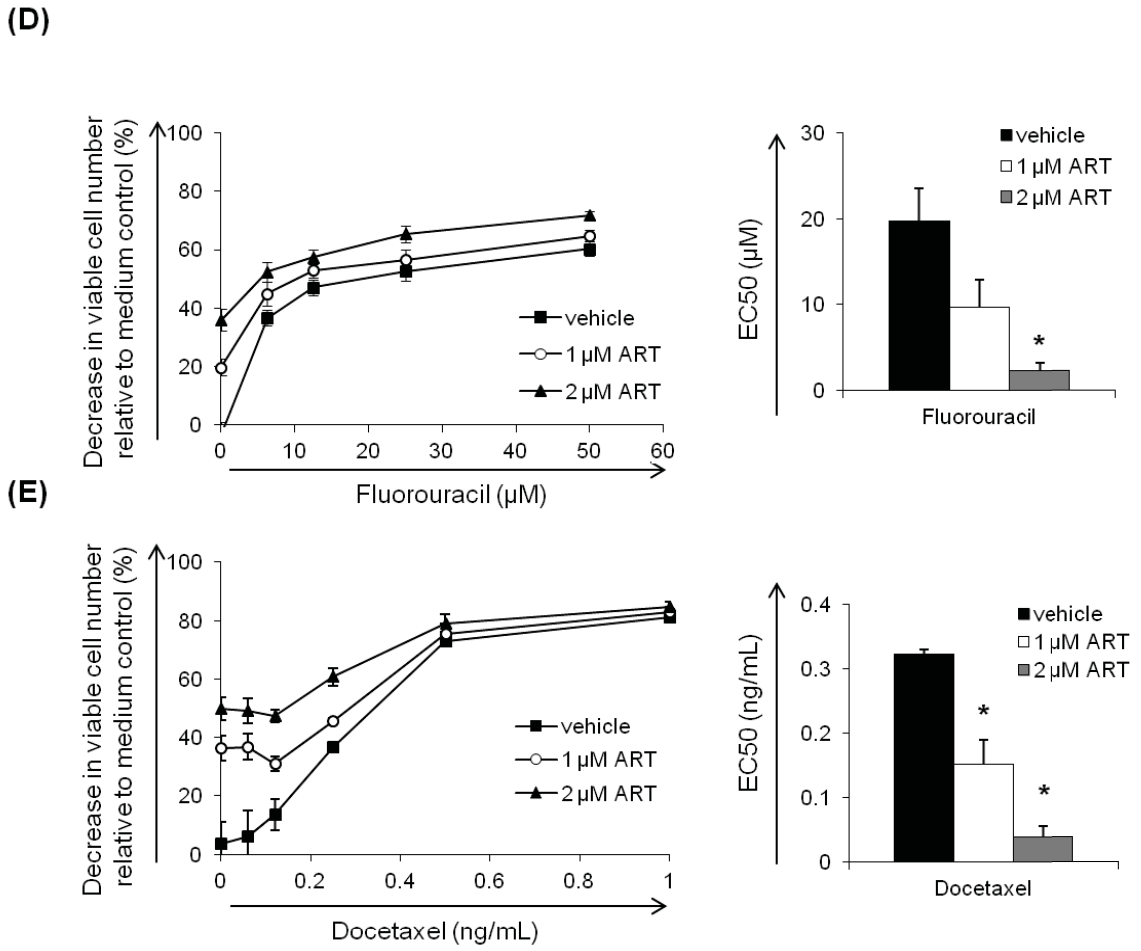

Figure 3.2.20 ART Enhances MDA-MB-468 Breast Cancer Cell Growth Inhibition by a Panel of Chemotherapeutic Agents. MDA-MB-468 cells were cultured for 72 h with (A) 4-hydroperoxycyclophosphamide, (B) cisplatin, (C) doxorubicin, (D) fluorouracil, or (E) docetaxel in the presence or absence of ART or its vehicle. Following culture, changes in viable cell number were determined using an MTT assay. Data shown are the mean of at least 3 independent experiments ± SEM; *$p < 0.05$ as compared to respective EC50 concentration in the absence of ART, determined by a one-way ANOVA with a Tukey-Kramer post-test.

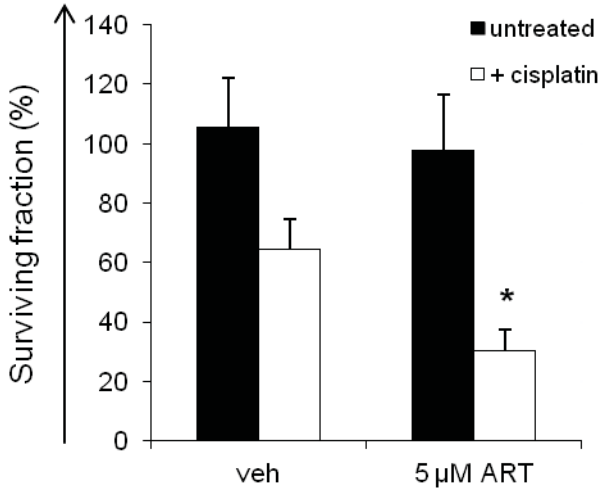

Figure 3.2.21 ART Enhances the Inhibitory Effects of Cisplatin on the Clonogenic Survival of MDA-MB-468 Breast Cancer Cells. MDA-MB-468 breast cancer cells were cultured for 24 h with ART or vehicle (veh) in the presence or absence of 0.1 µM cisplatin. ART was added 1 h prior to cisplatin. Following culture, cells were counted and equal numbers of cells were serially diluted and seeded in triplicate into 6-well plates. Cells were cultured for ~14 d, then plates were washed, and colonies were fixed and stained with crystal violet. Data shown are the mean of at least 3 independent experiments ± SEM; * $p<0.05$ as compared to cisplatin treatment in the absence of ART, determined by an unpaired, two-tailed t test.

CHAPTER 4: DISCUSSION

The high incidence of breast cancer along with the lethality of ovarian cancer place a huge burden on society, since these diseases are predicted to cause 20 % of all cancer deaths in women from the USA in 2013 (1). As a result, there is great need for the development of novel agents for the treatment of ovarian and breast cancer, especially for the management of relapsed disease. The present study investigates the anti-proliferative and cytotoxic effects of the anti-malarial drug ART in ovarian and breast cancer cell lines. Furthermore, this work explores the mechanisms that underlie these two distinct growth inhibitory activities of ART.

4.1 ART Inhibits the Growth of Ovarian and Breast Cancer Cell Lines.

The activities of ART and its primary active metabolite DHA have been investigated in numerous cancers, including leukemia, lymphoma, retinoblastoma, osteosarcoma, epidermoid carcinoma, and lung, hepatocellular, pancreatic, gastic, and cervical cancers (166, 168, 171, 179–183, 187, 198, 234). However, only a few studies have examined the effect of ART on breast and ovarian cancer cells (138, 151, 169, 185, 206).

Here, I examined the growth-inhibitory activity of ART against 9 different ovarian cancer cell lines which differ in histological subtype, p53 status, and resistance to traditional chemotherapeutic agents (Table 3.1.1). ART demonstrated excellent growth-inhibitory activity against all the ovarian cancer cell lines tested. In accordance with other reports for ART and DHA (150, 169, 185), the half maximal inhibitory concentration (IC_{50}) of ART was in the low micromolar range for the panel of ovarian cancer cell lines. IC_{50} values calculated for each line in this study varied from 0.51 - 31.89 μM.

I also evaluated, 6 different breast cancer lines with different molecular characteristics for ART-sensitivity. Again, ART showed excellent growth-inhibitory activity against all the cell lines tested, although ART-sensitivity of breast cancer cell lines was more heterogeneous than was observed for the ovarian cancer cell lines. Moreover, ART maintained significant inhibitory activity towards a paclitaxel-resistant breast cancer cell line which over-expressed p-glycoprotein, supporting the potential use of ART in the treatment of chemo-resistant disease. These positive results are in

accordance with other studies which also found ART to possess excellent growth-inhibitory activity against breast cancer cell lines (138, 150, 151).

The potent growth inhibitory effects of ART against panels of ovarian and breast cancer cell lines provides support for its potential as an anti-breast and anti-ovarian cancer agent. Nevertheless, breast and ovarian cancers are very heterogeneous and ART was only analysed against one or two representative lines from the different genetic/histological backgrounds. As the effect of ART on a representative line is insufficient to predict its effect on a genetic/histological type of breast or ovarian cancer, further testing against a larger number of clinical samples and cell lines is required to determine whether a specific type of breast or ovarian cancer would benefit more from ART treatment.

The p53 status of different ovarian and breast cancer cell lines did not impact sensitivity to ART. The p53-independence seen here is in contrast to a previous study that examined the anti-cancer effects of DHA in ovarian cancer cells. Previously, Jiao *et al.* (2007) found that p53 wild-type ovarian cancer cells had increased sensitivity to DHA compared to p53 mutant or null cell lines. Sensitivity to ART observed with the ovarian cancer cell lines used in this study and that of Jiao *et al.* (2007) were similar, although IC_{50} concentrations were determined for different treatment time points, i.e. 48 h for Jiao *et al.* (2007) and 72 h in the present study. Furthermore, ovarian cancer cell lines are often unstable (235), this in addition to the fact that a number of the ovarian cancer cell lines examined did not overlap, could have led to different conclusions on the importance of wild-type p53. Moreover, since Jiao *et al.* (2007) utilised DHA rather than ART, it is possible that other metabolites of ART may have affected ovarian cancer growth, resulting in different treatment outcomes.

To determine whether ART-treated cells were able to recover their ability to replicate following ART removal, I performed a wash-out assay and a colony forming assay on ART-treated ovarian and breast cancer cells, respectively. Interestingly, both assays showed that ART induced similar effects in breast and ovarian cancer cells. The response of the ovarian and breast cancer cells following ART removal was dependent on the concentration of ART that was administered. While high concentrations of ART permanently inhibited ovarian cancer cell growth and survival, cells treated with lower

doses of ART, or a population thereof, were able to recover their proliferative capacity following ART removal, indicating that cells treated with lower concentrations of ART remained viable.

Many of the previous studies that examined the effect of artemisinin derivatives on ovarian and breast cancer cell lines used DHA rather than ART (185, 191, 236). Although DHA is the active metabolite of ART, ART is the most soluble artemisinin derivative, and the one that is currently recommended for i.v. therapy, a treatment route frequently employed in the management of breast and ovarian cancer (149, 154). For this reason, I believe it is important to determine the activity of ART as well as to DHA in ovarian and breast cancer cell lines, as additional ART metabolites may contribute to its growth inhibitory activity.

4.2 ART Maintains its Inhibitory Activity in Ovarian and Breast Cancer Spheroid Cultures.

The peritoneal cavity is the primary route of tumour cell dissemination in the early stages of metastatic ovarian cancer (38). As ovarian cancer progresses, tumour cells are shed from the ovary surface and disseminate throughout the abdominal cavity as single cells or clusters of cells (spheroids) in the acites or peritoneal fluid. Using this route, cells are able to seed the surfaces of the peritoneal cavity and adjacent organs (237, 238). Interestingly, *in vitro* studies have shown spheroids to be less sensitive to certain chemotherapeutic agents than cells grown in 2D culture. In general, multicellular tumour spheroids are a more complex *in vitro* cancer model that better represent the primary solid tumour than 2D monolayers (239–241). 3D culture affects intracellular adhesions and as a result spheroids develop a more heterogeneous cell population with expression profiles that differ from their monolayer culture counterparts (239, 240). Increased resistance of spheroids to chemotherapy may play a role in the high incidence of disease recurrence seen in ovarian cancers, making spheroids an important target in the treatment of advanced disease (38, 238, 242–244). Ovarian cancer cells grown as tumour spheroids are more representative of tumour cells present in malignant ascites and their 3D structures results in similar oxygen and nutrient gradients (38). Therefore, the ability of ART to exert cytotoxic activity against HEY1 and HEY2 ovarian cancer spheroids is

extremely encouraging, and suggests that ART may be of benefit to patients with advanced disease, especially if administered by the intra-peritoneal route. ART also demonstrated strong cytotoxic activity against MCF-7 breast cancer spheroids. Consequently, the potent actions of ART in both breast and ovarian spheroid cultures is evidence that ART will be effective against the primary cancer lesion. It is noteworthy that the inhibitory activity of ART on tumour spheroids was not as dramatic as it was in 2D cultures. These differences could be due in part to increased resistance to ART of cells in spheroid culture due to the activation of survival-promoting signaling pathways or decreased drug accessibility spheroid cells compared to those grown as a monolayer. It is also plausible that decreased proliferation rates of cells in spheroid culture as well as differences between the acid phosphatase and MTT assays could also have contributed to the disparity in effectiveness of ART.

To the author's knowledge, this is the first example of any artemisinin derivative being tested in an *in vitro* 3D culture system in any cancer model. These experiments represent a starting point for future investigation into the effects of ART on ovarian and breast cancer cell spheroids. Spheroid models could be used to assess the effectiveness of ART in combination with established chemotherapeutic agents. In addition, it would be interesting to investigate the effects of ART on cellular adhesion molecules since ART effectively disrupted the structure of both the ovarian and breast cancer spheroids.

In regards to ovarian cancer, further research, including experiments investigating the effects of ART on clinical isolates of spheroids from the peritoneal ascites of ovarian cancer patients, would further support the potential of ART for use in the treatment of advanced ovarian cancers. In addition, studies of the pharmacokinetics of ART and its metabolites following intra-peritoneal delivery, which has not been studied previously, would help to determine the feasibility of this treatment route.

4.3 ART is Cytotoxic to Breast and Ovarian Cancer Cells.

In accordance with other cancer models, this study found that ART killed breast and ovarian cancer cell lines. Apoptosis and necrosis are two of the primary pathways which mediate cell death (105). To date, the majority of studies investigating ART-induced cytotoxicity have described apoptosis as the primary route of cell death, although

recently, DHA/ART-induced oncosis-like cell death, characterised by cell swelling and membrane lysis, has been described in pancreatic and gastric cancer cell lines. Necrotic cell death was also reported following ART-treatment of glioblastoma cells (142, 168, 179, 180, 187, 245, 246).

4.3.1 ART is Cytotoxic to Ovarian Cancer Cell Lines

In the present study, ART demonstrated a dose-dependent cytotoxic effect on 6 different ovarian cancer cell lines. Significant cytotoxicity was typically present at ART concentrations of 50 and 100 μM, although cytotoxic activity was also observed at 25 μM in the more sensitive cell lines. Interestingly, the mechanisms of ART-induced cancer cell death were cell-line specific. ART induced predominantly late apoptotic/necrotic cell death in the HEY1, HEY2 and OVCAR8 cell lines, whereas TOV-21G and TOV-112D displayed a significant increase in early apoptosis upon identical ART treatment. As phagocytes are not present to remove apoptotic bodies, late apoptotic cells lose membrane integrity and cannot be differentiated from their necrotic counterparts (84). Nevertheless, one would expect increased early apoptosis in conjunction with late apoptosis/necrosis, especially at less toxic doses. Therefore, the absence of early apoptotic cells upon ART treatment suggests that ART may be triggering necrosis rather than apoptosis in the HEY1, HEY2 and OVCAR8 cell lines.

RIP1K is a key player in programmed necrosis, also known as necroptosis (106). Inhibition of RIP1K activity with necrostatin-1 led to a significant decrease in ART-induced cell death in the HEY1 and HEY2 cell cultures, demonstrating that these cells die in part through the necroptotic pathway. This is the first report of necroptosis activation by any artemisinin derivative and this work represents a starting point for further research into the mechanisms underlying the ability of ART to activate the necroptotic pathway. As only a portion some cancer cell lines tested with ART died by necrosis, it would be interesting to understand the mechanisms that determine whether a cell dies through the apoptotic pathway or necroptotic pathway. Moreover, it would be of interest to determine whether necroptosis is also involved in the oncosis-like cell death observed in ART-treated pancreatic and gastric cancer cells (179, 245).

Cancer cells can use different strategies to increase their resistance to chemotherapy-induced apoptosis; for instance, many ovarian cancers have decreased

apoptosome activity which can cause chemoresistance (247). Cancer cells also up-regulate anti-apoptotic proteins and/or down regulate pro-apoptotic factors such as Bcl-2 and Bax, respectively (98, 99). It is therefore conceivable that, in certain cell lines, defects in apoptosis signalling may lead to necroptotic rather than apoptotic cell death upon ART treatment. Alternatively, differences in ATP concentration could also have impacted on the method of ART-induced-cell death. I observed that ART induced double-strand DNA breaks in HEY2 ovarian cancer cells (described in detail in Section 4.4). Furthermore, ART-induced oxidative DNA damage has also been reported in glioblastoma cells (142). As ATP is required for apoptosis, it has been suggested that decreased ATP levels induced through sustained activation of DNA repair mechanisms could have resulted in ART-induced necrotic cell death (142). ART-induced DNA damage could also have led to AIF-mediated necroptotic cell death (103). Cell-type specific differences, for example, in the sensitivity of cells to ART-induced DNA damage, could have impacted on the effect of ART on ATP levels or AIF release and influenced the mechanism of cell death.

The ability of ART to trigger different cell death programs warrants further research, as this may contribute to its broad spectrum of activity, including cancer cell lines that are resistant to other established therapeutic agents. Further research is required to determine whether the cell-type specific cell death mechanisms induced by ART *in vitro* translate to *in vivo* models of ovarian cancer.

DHA-induced cell death has been previously examined in ovarian cancer cell lines (185, 236), Jiao *et al.* (2007) described DHA-induced apoptosis in OVCA-420 ovarian cancer cells, whereas Chen *et al*. (2009) found that DHA induces apoptosis in OVCAR3 and A2780 ovarian cancer cell lines. In both cases, apoptosis was characterised by increased Bax and decreased Bcl-2 expression. ART-induced apoptosis in OVCAR3 and A2780 ovarian cancer cells was also characterised by an increase in cleaved PARP-1, caspase activation, Fas and FADD expression and increased mitochondrial membrane permeability (236). Furthermore, DHA inhibited tumour growth and induced similar changes in the Bax/Bcl-2 ratio in xenografts of ovarian cancer in immune-deficient mice (169). As the present study demonstrated the cell line-specificity of ART-mediated cell death mechanisms in ovarian cancer cells, this likely accounts for the difference in the

mechanism of cell death observed between my study and those by Chen *et al*. (2009) and Jiao *at al*. (2007). Nevertheless, it is possible that the different artemisinin derivative used could also have affected treatment outcomes. Interestingly, significant late apoptosis/necrosis was also present in the OVCAR3 and A2780 cells treated with 25 and 50 μM DHA, suggesting that DHA-induced necroptosis may also contributed to the death of these cancer cell lines (169).

Although apoptosis has been associated with ART- and DHA-mediated killing of different cancer cell types, the importance of caspases is still debated and appears to be cell type specific. For example, some studies have reported caspase-dependent cell death caused by ART and DHA (172, 178, 181, 248) while others have described caspase-independent cell death (179, 196, 245). However, few of these studies used a caspase inhibitor to confirm a functional role for caspases. In the present study, although ART-treatment led to significant caspase activation, the pan-caspase inhibitor only slightly reduced ART-mediated cytotoxicity, indicating that caspases contribute only marginally to the killing of HEY1 and HEY2 ovarian cancer cells by ART. In contrast, inhibition of RIP1K activity by necrostatin-1 led to a more significant decrease in ART-induced cell death. Caspase-independent cell death is consistent with my findings that ART-induced cell death occurs primarily by necroptosis in the HEY1 and HEY2 ovarian cancer cell lines. These results suggest that ART activates both apoptotic and necroptotic pathways in ovarian cancer cells and it is likely that a number of factors determine which cell death pathway is ultimately prevails. Future research investigating the caspase-dependence of ART-induced cytotoxicity in the TOV-21G and TOV-112D cell lines that died through ART-mediated apoptosis is warranted to further explore the cell-specific cytotoxic activities of ART on ovarian cancer cell lines. ART treatment has also been associated with the induction of senescence and autophagic cell death in other cancer cell types (171, 249). Although preliminary data suggests that ART is not inducing senescence in the HEY1 and HEY2 ovarian cancer cell lines (data not shown), further study is required to investigate the possibility of a role, for autophagy and senescence in ART-induced ovarian cancer cell death.

4.3.2 ART induces breast cancer cell apoptosis

ART-induced cytotoxicity was further explored in MDA-MB-468 and SK-BR-3 breast cancer cell lines. These lines were selected because they were sensitive to ART and represented two important classes of breast cancer, TNBC (MDA-MB-468) and HER-2 over-expressing breast cancer (SK-BR-3). ART caused apoptosis in both cells lines in a dose-and time-dependent manner. In accordance with the MTT data, the effect of ART on SK-BR-3 cells was delayed compared to MDA-MB-468 cells and significant cytotoxicity was only seen following 48 h culture. Apoptosis in ART-treated breast cancer cells was characterised by loss of mitochondrial membrane potential and subsequent release of cytochrome c and Smac/DIABLO into the cytoplasm. Increased mitochondrial permeability was an early event as mitochondrial Smac/DIABLO was present in the cytosol as early as 12 h following ART treatment. Unlike the effect of ART on ovarian cancer cell lines, ART-induced cell death in breast cancer cells was caspase-dependent and characterised by PARP-1 cleavage. Breast cancer cell death was not dependent upon RIP1K activity, which is in agreement with activation of an apoptotic cell death program. Nevertheless, as in the ovarian cancer cells, ART does appear to activate both necrotic and apoptotic programs as caspase inhibition only reduced the apoptotic fraction of the SK-BR-3 cells, resulting in reduced, but still significant death by necrosis. The effect of ART on senescence and autophagy in the SK-BR-3 and MDA-MB-468 cell lines was not investigated as part of this thesis. It is possible that these forms of cell death/stasis may have contributed to the effects of ART on the breast cancer cells. Further research is warranted to explore the importance of these mechanisms in ART-induced anti-breast cancer activity.

Caspase-dependent apoptosis associated with mitochondrial disruption observed in this study is consistent with previous reports that ART-induced apoptosis in MDA-MB-468 and MDA-MB-231 breast cancer cell lines (206). Additionally, apoptosis characterised by changes in Bcl-2 family member expression/activation along with increased mitochondrial membrane permeability and caspase activation has also been described for ART and DHA in MCF-7 and T47D breast cancer cells, respectively (138, 191). Interestingly, ART treatment also induces significant necrotic cell death in MCF-7 breast cancer cells, suggesting that, as in the ovarian cancer cell lines, the cell death

program activated by ART in breast cancer cells may be cell-line specific. However, since the analysis of the apoptotic-promoting effects of ART on MCF-7 cells were conducted in a serum-free Krebs-Henseleit solution, a basal salt solution containing defined levels of glucose, it is conceivable that these culture conditions may alter MCF-7 cell sensitivity to ART(138).

The present study is the first to examine the effect of a caspase inhibitor on ART-induced apoptosis of breast cancer cells and the first to show ART-mediated activation of the mitochondrial pathway of apoptosis which involves cytochrome c and smac/DIABLO release and PARP-1 cleavage in TNBC and HER-2 over-expressing breast cancer cells. Currently, there are more treatment options for ER-positive breast cancers, which have a better prognosis than ER-negative breast cancers (46, 250). Because there are fewer options for the treatment of recurrent TNBC, I believe it is important to investigate the efficacy of ART against this breast cancer cell type.

4.4 ART-mediated Cell Death is ROS and Iron-dependent.

Although the exact mechanisms behind the anti-malarial activity of ART remain elusive, the heme-dependent production of carbon-centred radicals and ROS is believed to play an important role in the ability of ART to kill malarial parasites (154, 159, 160). Similar mechanisms have also been associated with the anti-cancer activities of ART, but the importance of ROS and iron have yet to be determined for ART-mediated inhibition of ovarian cancer cell growth. Moreover, only limited studies have investigated this aspect of ART activity in breast cancer lines (138, 151, 211). Ferrous iron or heme-catalysed cleavage of the endoperoxide is hypothesised to result in the production of carbon-centred radicals and ROS which cause cancer cell death (160, 178). As iron is essential for cell proliferation, cancer cells often maintain higher iron levels than their normal counterparts (212). It has been suggested that the increased level of cellular iron in cancer cells may sensitise them to ART-induced cell death (159).

In this study, ART induced dose-dependent intracellular ROS production in HEY1, HEY2 and SKOV-3 ovarian cancer cells, which was inhibited in the presence of the ROS scavenger GSH. ART treatment of breast cancer cells similarly induced ROS production in SK-BR-3 and MDA-MB-468 breast cancer cell lines. Furthermore, pre-

treatment of MDA-MB-468 breast cancer cells with HT enhanced ART-mediated ROS production. Lower relative ROS production was present in SK-BR-3 cells 24 h following ART treatment, which may have contributed to the lower cytotoxicity observed for this breast cancer cell line at this time point compared to MDA-MB-468 cells.

It is notable that ROS production in the ovarian cancer cell lines was dose-dependent, and higher ROS production correlated with increased cell death. Negligible ROS production was observed when ovarian cancer cells were treated with less than 25 μM ART, doses that also showed little cytotoxic activity but were still effective at inhibiting growth in the MTT assay. Therefore, it stands to reason that lower doses of ART may elicit anti-proliferative effects that are ROS-independent.

The presence of GSH almost completely negated ART-induced cell killing of 6 different ovarian cancer and 2 breast cancer cell lines, suggesting that the dose-dependent cytotoxicity of ART is due largely to the generation of ROS. These results are in-line with the ability of GSH to inhibit ART-mediated ROS production in the CM-H_2DCFDA assay. My finding that ART-induced ROS production is important for inhibition of breast and ovarian cancer cell growth is in agreement with studies performed in other cancer cell types, including glioblastoma, leukemia, and lung cancer (142, 168, 198). Importantly, GSH also inhibited ART-induced mitochondrial membrane depolarisation, indicating that ROS production occurs upstream of its effects on the mitochondria.

Increased oxidative stress can damage cellular proteins and membranes, as well as cellular and mitochondrial DNA (111). In the present study, I have shown for the first time, that cytotoxic doses of ART cause double-strand DNA breaks in breast and ovarian cancer cells, as represented by the phosphorylation of ser139 of H2AX. DNA breaks were not apparent when ART was used in combination with GSH, nor at ART concentrations that did not cause substantial ROS production in ovarian cancer cells. Taken together, these data suggest that DNA damage was ROS-dependent. It therefore is conceivable that ART-induced DNA damage, leading to activation of the DNA damage response could play a role in causing cell cycle arrest and, ultimately, cell death. These results are in agreement with those of previous studies which showed ART-induced DNA oxidation in glioblastoma and Chinese hamster ovary cell lines (142, 251). It is of note that cells defective in homologous recombination due to the inactivation of DNA repair

genes, including BRCA2, are more sensitive to ART than are the parental cell line (251). Since BRCA2 mutations are associated with familial breast and ovarian cancer syndromes (252), this could represent a population of patients who would receive a greater benefit from ART-treatment.

As previously mentioned, ferrous iron and/or heme is believed to be needed for the activation of the ART endoperoxide bridge (253). In addition, combined treatment with ART and iron (e.g., as iron (II) glycine sulphate or HT) is associated with increased cytotoxic activity of ART in numerous cancer cell types (142, 151, 186, 254, 255). Nevertheless, not all cell lines responded well to the combination of ART and iron, in that ART activity was unchanged or decreased in certain cell lines including MCF-7 breast cancer cells (151). Since iron is required for cellular proliferation, addition of exogenous iron may have led to increased proliferation of certain cell lines which could have affected the IC_{50} of ART (151, 256).

In agreement with other studies, iron supplementation in the form of pre-treatment with HT significantly increased ART-induced cell death in HEY1 and SKOV-3 ovarian cancer cell lines. Furthermore, iron chelation using DFE significantly inhibited the cytotoxic activity of ART, underlining the importance of iron in ART killing of ovarian cancer cell lines. Similar effects were also observed for the SK-BR-3 and MDA-MB-468 breast cancer cell lines. Since HT pre-treatment enhanced ART-induced ROS production in MDA-MB-468 cells, it is likely that the increases in cell death observed in HT pre-treated cell cultures were due to increased ROS production. Iron-dependent cytotoxicity that I observed is in agreement with the finding that lysosomal iron is involved in ART-mediated anti-breast cancer cell activity (138). These results promote the combination of iron and ART for the treatment of ovarian and breast cancers, although it must be taken into consideration that not all ovarian and breast cancer cell types may benefit from the addition of iron to ART treatment. It is noteworthy that the beneficial effects of HT pre-treatment were only observed in ovarian cancer cells stained with Annexin-V-FLUOS/PI, whereas only a small enhancing effect was observed on growth-inhibition in an MTT assay (e.g. for HEY1 cells treated with 50 μM ART; Annexin-V-FLUOS/PI staining: 30.69 % enhancement of cell death with HT, MTT assay: 10.77 % enhancement of growth inhibition). It is possible that that the rapid cell growth of the HEY1 and HEY2

ovarian cancers cells along with the potent inhibitory activity of ART, masked that effects of iron supplementation on ART-induced cytotoxicity in the MTT assay.

Although all the ovarian and breast cancer cell lines tested in this study were sensitive to ART, the degree of sensitivity varied. Multiple factors are likely to influence the effectiveness of ART, including the level of certain glutathione-related enzymes, expression of anti-oxidant genes, and molecules involved in iron homeostasis such as the CD71 transferrin receptor (151, 257, 258). The significant difference in ART-sensitivity between the HEY1 and HEY2 clones was especially interesting; although HEY2 cells expressed higher levels of CD71 and ART-treatment led to the production of higher ROS in these cells, they were much less sensitive to ART than the HEY1 cell line. It is possible that differences in the anti-oxidant capacity of the cell line could account for the divergence in sensitivity observed, further characterisation of these two cell lines is warranted and could provide new insights into factors that influence ART sensitivity in ovarian cancer cells.

Since iron plays an essential role in the anti-cancer activity of ART, the propensity for anaemia in cancer patients may have an impact on clinical application of ART. Many factors can contribute to the development of anaemia, including effects by the tumour itself and side effects of different chemotherapy regimens (259). The type of anaemia and underlying cause of the disease could affect the efficacy of ART treatment in cancer patients. Further study both *in vitro* and *in vivo* is therefore required to determine if anaemic patients could benefit from ART treatment, as well as what form of iron supplementation would be the most effective in amplifying ART-mediated anti-cancer activities.

4.5 Oxygen is Required for ART-induced Breast Cancer Cell Death.

Incubation of breast cancer cells with ART under different oxygen conditions revealed, for the first time, that hypoxia inhibited the cytotoxic activity of ART in breast cancer cell cells. Hypoxia is a common feature of solid tumours and is a negative prognostic factor in many cancer types (260). My results suggest that cancer cells in hypoxic regions of a tumour may not respond as well to ART treatment. Interestingly, exposure to hypoxic conditions following 24 h of ART treatment under normoxic

conditions did not result in breast cancer cell resistance to ART. Since significant ROS production was evident at 24 h post-ART treatment and mitochondrial membrane permeability was evident 12 h following ART treatment, it is likely that ART-induced cell death was already well underway by the time the cells were exposed to hypoxia.

Hypoxia-induced chemoresistance is associated, in part, with the hypoxia-induced stabilisation and activation of the hypoxia-inducible factor 1α (HIF-1α) transcription factor. HIF-1α is involved in many key biological pathways and is up-regulated in many different cancers (261). Inhibition of DNA damage and apoptosis, as well as the up-regulation of drug efflux pumps have all been associated with HIF-1α-induced drug-resistance (261). It is therefore conceivable that culture under hypoxic conditions resulted in cellular changes that led to decreased effectiveness of ART in breast cancer cells. Moreover, a recent study in MDA-MB-231 breast cancer cells demonstrated that hypoxic conditions caused decreased intracellular ROS production (262), which would affect ART-induced ROS-dependent cell death. Conversely, Huang *et al*. (2007) examined the activity of ART in glioma cells under hypoxic conditions and found that ART caused decreased HIF-1α expression whereas, under normoxic conditions, another study found that ART activates HIF-1α expression (175, 263). Further research is clearly required to clarify these contradictory results. Knock-down of HIF-1α expression by siRNA prior to ART treatment and hypoxic culture could determine whether HIF-1α is involved in ART resistance of hypoxic breast cancer cells. Hypoxia may also decrease or inhibit the production of ROS by ART, which could be tested by measuring the level of different ROS. Additional experimentation investigating the changes in sensitivity to ART elicited by hypoxia are important, as these results could have a significant clinical impact on the potential of ART as a treatment for solid tumours with significant hypoxic regions.

4.6 ART Causes Decreased Ovarian Cancer Cell Proliferation.

Although the anti-proliferative effect of ART on certain cancer cells is well established, the mechanisms underlying this effect remain elusive. In the present study, ART-induced inhibition of cell growth was observed at concentrations as low as 1 μM in breast and ovarian cancer cells, which is significantly less than the dose needed for cytotoxic activity of ART. Here, I showed for the first time that the potent anti-

proliferative effect of ART was ROS-independent in both breast and ovarian cells, suggesting that mechanisms behind this anti-proliferative activity are distinct from those involved in cytotoxic effects. Nevertheless, although ART was able to inhibit cell proliferation in the presence of GSH, growth inhibition at 25 μM and 50 μM ART was not as dramatic as when ovarian cancer cells were treated with ART alone. It is therefore possible that in the presence of ROS, cells treated with 50 μM ART may arrest earlier than cells treated with ART in the presence of GSH.

Recent studies have shown that ART and DHA can decrease the surface level of CD71 in cancer cells and ART-induced iron depletion has been suggested to play a role in its anti-cancer activity (175, 182, 195). Moreover, CD71-mediated endocytosis has been suggested as a possible route for ART entry into cancer cells (182). CD71 mediates the cellular import of iron through receptor mediated endocytosis of HT (212). Since iron is important for cell proliferation, cancer cells often express higher levels of CD71 than untransformed cells (214, 264). I investigated the effect of ART on the surface expression of CD71 on breast and ovarian cancer cells. Although both breast and ovarian cancer cells expressed CD71, only the breast cancer cell lines showed a decrease in the surface expression of this receptor following ART-treatment. These results suggest that CD71 internalisation may not be essential for ART-induced activity in ovarian cancer cells; however, it is possible that ART-treatment could have increased CD71 expression, which could have masked ART-induced changes. In a previous study, although treatment with a anti-CD71 mAb inhibited the enhancement of ART activity induced by the addition of iron, it did not affect the growth inhibitory effect of ART alone (254). Therefore, it is likely that mechanisms other than CD71-mediated endocytosis mediate ART entry into cancer cells and the importance of the ART-induced decrease in breast cancer CD71 expression shown in this thesis is currently unclear.

Since ART-induced cell death was enhanced by the addition of exogenous iron and inhibited by iron depletion in breast and ovarian cancer cells, it seems unlikely that the ROS-dependent cytotoxic activity of ART was due to iron deprivation. Nevertheless, ART shows potent anti-proliferative activity in the presence of GSH, which could involve iron deprivation. In fact, treatment with an iron chelator had an anti-proliferative effect in the presence or absence of ART. Ba *et al*. (2012) found that low doses of ART

decreased the expression of other important players in iron homeostasis, including Steap3 (a ferrireductase that converts ferric to ferrous iron) and DMT1 (which transports endocytic iron to the cytoplasm) (212, 213). Further investigation is needed to determine whether iron supply deprivation is involved in the activity of ART on breast and ovarian cancer cells.

4.7 ART-Treatment Causes Cell Cycle Arrest.

Cell cycle analysis and western blotting of key cell cycle regulatory proteins was used to further examine the anti-proliferative effects of ART in breast and ovarian cancer cells. Interestingly, the phase at which ART-induced cell cycle arrest occurred was dose-dependent in ovarian cancer cells. A low dose of ART (10 μM) induced G1 phase cell cycle arrest, whereas, a higher dose (50 μM) led to arrest in the G2/M phase. These results are in line with a previous study in which DHA caused dose-dependent G2/M cell cycle arrest in OVCA-420 ovarian cancer cells (185). In addition, MDA-MB-468 cells arrested in the G2/M phase, whereas SK-BR-3 cells arrested in G1, with a slight increase in the number of cells in G2/M at 50 μM ART. G1 phase cell cycle arrest has been observed in DHA-treated T47D breast cancer cells (191).

G2/M and G1 cell cycle arrest caused by ART and DHA have been documented in different cancer cell types, including osteosarcoma, ovarian, and liver cancer (G2/M arrest) and retinoblastoma, epidermoid, liver, gastric, colorectal, breast, and pancreatic cancers (G1 arrest) (165, 166, 171, 172, 180, 182, 185, 187, 191, 194, 199). A non-specific arrest induced by ART at all phases of the cell cycle has also been reported (189). An investigation of 7 different cell lines derived from 6 different cancer types showed that four of these cells lines (leukemia, glioma, colorectal, and small cell lung carcinoma) arrested in the G2/M phase following ART-treatment (167). Although ART-treated HCT-116 colorectal cancer cells were observed to arrest in G2/M by Steinbrueck *et al.* (2010), another study showed arrest in G1 following DHA treatment (167, 265). Collectively, these results suggest that ART- and DHA-induced cell cycle arrest is likely tissue-specific, and may be additionally influenced by the artemisinin derivative used, as well as the dosage and timing of treatment.

I found that ART modulated the expression of several key cell cycle regulatory proteins in breast and ovarian cancer cells. This effect likely plays an important role in the anti-proliferative activity of ART. The effect of ART on cell cycle regulatory protein expression was similar between the breast and ovarian cancer cell lines. ART may, therefore, cause cell cycle arrest by a similar mechanism in breast and ovarian cancer cells. ART induced decreased expression of CDK4, cyclin D3, E2F-1, cyclin A, cyclin B, CDK2 (only examined in the ovarian cancer cell lines), CDK1, and CDC25C, and increased expression of p21Waf1/Cip1 and phospho-Chk2. Nevertheless, slight differences in the effects of ART were noted when different cell lines were compared. For instance, MDA-MB-468 breast cancer cells failed to demonstrate changes in cyclin A or cyclin B expression after ART treatment, whereas no changes in phospho-Chk2 were observed in SK-BR-3 cells. Decreased Rb expression was also induced by ART treatment of ovarian cancer cell lines. Moreover, Rb-null MDA-MB-468 breast cancer cells were sensitive to ART, suggesting that modulation of Rb expression may not be an important determinant of ART action on breast cancer cells. This result is in agreement with the potent anti-cancer activity of ART and DHA against Hep3B hepatocellular carcinoma cells that also lack Rb (166). Since Rb expression is often lost in breast cancer cells (266, 267), the Rb-independent activity of ART is an advantage that would allow for a broad spectrum of activity against breast cancer cells. In line with the current study, ART and DHA-induced cell cycle arrest has been associated with changes in cell cycle regulatory protein expression by other cancer cell types, including osteosarcoma, gastric, hepatocellular, and epidermoid cancers (166, 171, 180, 187).

As mentioned earlier, two recent studies suggest that the anti-cancer effects of ART may be due to iron depletion (175, 182). Cells that are deprived of iron undergo G1/S phase arrest and there is decreased expression of cell cycle regulators including cyclin A, cyclin B, cyclin D1-3, CDK2 and CDK4 by cancer cells in the presence of iron chelators (268–270). It is therefore possible that ART-mediated iron deprivation may be involved in its anti-proliferative effects; however increased p21Waf1/Cip1 protein expression is not normally observed in iron-deprived cells (268, 271). Further research is required to determine the importance of iron depletion in the anti-proliferative activity of ART in breast and ovarian cancer cells.

The E2F transcription factors play an important role in many cellular processes, including the G1-S transition. E2F-1 activity is positively regulated by cyclin D/CDK4/6 and cyclin E/CDK2 heterodimers which phosphorylate Rb, releasing E2F-1 to induce the expression of numerous genes that are required for cell cycle progression and DNA replication (71). In line with the present study, artemisinin, from which ART is derived, was recently shown to induce G1 cell cycle arrest and inhibit the expression of E2F-1, CDK4, cyclin D1, cyclin E and CDK2 cell cycle regulatory proteins in MCF-7 breast cancer cells. Over a 10-fold increase in artemisinin concentration was required compared to ART to elicit similar decreases in cell cycle regulatory protein expression (e.g. 200-300 μM artemisinin compared to 10-25 μM ART). In addition, artemisinin did not induce increased p21Waf1/Cip1 expression (272), whereas I observed increased p21Waf1/Cip1 expression in ART-treated breast and ovarian cancer cells. Nevertheless, down-regulation of E2F-1 expression plays an important role in the anti-proliferative activity of artemisinin. E2F-1 regulates the expression of numerous proteins that include cyclin E, DNA polymerase and CDK2, as well as its own expression in a positive-feedback loop (70). Constitutive E2F-1 expression in MCF-7 cells inhibited artemisinin-induced G1 arrest and down-regulation of CDK2 and cyclin E expression, implicating down-regulation of E2F-1 by artemisinin as an important mechanism of its anti-proliferative activity (272). ART-induced down-regulation of E2F-1 may also be of similar importance for ART-mediated anti-proliferative activity. Moreover, as E2F-1 regulates numerous target genes involved in many different key biological pathways, including cell cycle regulation, DNA replication, cell cycle checkpoint regulation, well as DNA damage repair and apoptosis (71, 273), ART-induced down-regulation of E2F-1 expression could have a broad impact on cancer cell growth. Further investigation is required to determine the importance of ART-mediated E2F-1 inhibition with regard to its anti-proliferative effects on breast and ovarian cancer cells, as well as the growth of normal breast and ovarian epithelial cells.

In a study of 77 ovarian cancer patients, E2F-1 levels were increased in ovarian cancers compared to normal controls, and E2F-1 expression correlated with tumour grade (273). E2F-1 expression is also increased in invasive ductal breast carcinoma relative to normal breast tissue and, as in ovarian tumours, increased E2F-1 expression is associated

with higher histological grade and advanced disease (274). E2F-1 therefore appears to play an important role in cancer cell proliferation. It is conceivable that ART-induced down-regulation of this transcription factor in breast and ovarian cancer cells may be of clinical value. Finally, since breast cancer cells that lack hormone receptors often express higher levels of E2F-1 (274), ART-induced inhibition of E2F-1 may be particularly well suited for the treatment of TNBC.

4.8 ART-mediated G2/M Cell Cycle Arrest is ROS-dependent.

To further characterise the anti-proliferative effects of ART in breast and ovarian cancer cells, the role of ROS in ART-mediated cell cycle arrest was investigated. This study was the first to investigate the impact of ROS on ART-induced cell cycle arrest in breast and ovarian cancer cells, as well as the role of ROS on modulation of cell cycle protein expression by ART. Interestingly, in the presence of GSH, ART-induced G2/M cell cycle arrest was inhibited in both ovarian and breast cancer cells, indicating that G2/M cell cycle arrest was dependent on ROS production. Moreover, in place of G2/M arrest, cells treated with GSH and ART arrested in the G1 phase of the cell cycle. Therefore, although ROS did not influence the overall anti-proliferative activity of ART, the phase at which cell cycle arrest occurred was dependent on ROS.

In ovarian cancer cells, ROS-dependent G2/M cell cycle arrest was induced by 25 and 50 μM ART but not with 10 μM ART, which is in line with ROS production and ROS-dependent cell death in ART-treated ovarian cancer cells. As ART-mediated DNA damage was also ROS-dependent it is possible that DNA damage could have activated the DNA damage response, leading to G2/M cell cycle arrest and cell death. It is interesting that SK-BR-3 breast cancer cells were the only cell line in this study that did not show a strong G2/M cell cycle arrest as a result of 50 μM ART treatment. It is possible that the differences were cell type specific, as a G1 arrest was also observed for DHA-treated T47D breast cancer cells (191). It is also possible that the kinetics of ART action were different in Sk-BR-3 cells. Inhibition of cell growth and apoptosis-induction were only observed after SK-BR-3 cells were treated with ART for 48 h, whereas these effects were seen after 24 h for MDA-MB-468 cells. In addition, the amount of ROS

produced by ART-treatment in SK-BR-3 cells was significantly less than that produced by the same concentration of ART in MDA-MB-468 breast cancer cells after 24 h.

The role of ROS in ART-induced modulation of cell cycle protein expression was investigated in the HEY2 ovarian cancer cell line. Interestingly, down-regulation of cyclin B and CDC25C by ART was lessened when ART was administered in combination with GSH. Cyclin B and CDC25C play an important role in the G2/M cell cycle phase since both are required for CDK1-mediated cell cycle cell cycle progression in G2 (67). In a recent study, vanadate, an oxoanion under investigation for its anti-diabetic activities, induced G2/M cell cycle arrest through ROS-mediated degradation of CDC25C in PC-3 prostate cancer cells (134). It is conceivable that ART causes CDC25C degradation and G2/M cell cycle arrest through a similar mechanism. Further research is required to understand the mechanisms behind ROS-dependent cyclin B and CDC25C inhibition in ART-treated ovarian cancer cells and to determine whether the activation of the DNA damage response by ART-induced double-strand DNA breaks is involved in ROS-dependent G2/M cell cycle arrest in breast and ovarian cancer cells.

4.9 ART Enhances The Inhibitory Effects of Ionizing Radiation and Established Chemotherapeutic Agents on the Growth of Breast Cancer Cells.

Combined modality treatments are the standard of care in the management of breast and ovarian cancer (35, 36, 62). The administration of multiple agents with different mechanisms of activity, as well as different toxicity profiles, helps to increase treatment efficacy while limiting adverse side effects. Nevertheless, current treatment regimens result in significant toxicities that limit the maximum tolerated dose and negatively affect treatment adherence and patient quality of life (64, 65). In the present study, ART was found to possess both anti-proliferative and cytotoxic activity against breast and ovarian cancer cell lines. As ART is well tolerated in malarial patients, ART may have value as an addition to current treatments of cancer (152, 218). However, few studies have investigated the combined effects of ART or DHA and established chemotherapy agents in breast cancer (189, 210). I therefore performed preliminary studies to investigate the ability of low doses of ART to enhance the anti-cancer effects

of ionizing radiation and established chemotherapeutic agents in MDA-MB-468 breast cancer cells.

The addition of low doses of ART prior to γ-irradiation treatment resulted in enhanced growth inhibition of MDA-MB-468 breast cancer cells. The ability of ART to induce G2/M arrest in breast cancer cells, which is the most radio-sensitive phase of the cell cycle, may have contributed to the beneficial effect of ART treatment prior to irradiation of breast cancer cells (275). These results are encouraging, and suggest that ART may have promise as an adjunct to radiation therapy. However, radiation therapy induces ROS-dependent oxidative damage which can have immediate, as well as delayed effects on cancer cells (275). Since the MTT assay only assesses changes occurring within a 72 h period, it is not possible to determine later effects of combined treatment using this assay. MTT is also unable to detect cells which survive a number of proliferation cycles before losing their reproductive integrity. The clonogenic assay is the 'gold standard' for evaluating cell death following ionizing radiation as it measures the effect of the treatment on the ability of cancer cells to maintain long-term replicative activity (224). In this assay, treated cells are plated in low numbers and their ability to form large multicellular colonies is evaluated after several weeks. Following the analysis of multiple treatment doses, a survival curve can be produced to evaluate the effects of different treatment concentrations on cancer cell survival (224). Further investigation of the effects of ART pretreatment on breast cancer cell-susceptibility to ionizing radiation using the clonogenic assay will allow for a better evaluation of the combined effects of these two treatments. Analysis of the mechanisms behind the radio-enhancing activity of ART, along with investigation of the effects of combined modality treatment in an animal model should then be conducted.

The potential for ART to increase the effectiveness of radiation therapy in breast cancer cells is supported by reports that ART and DHA sensitise radiation non-small cell lung cancer, glioma and cervical cancers cells to ionizing (173, 198, 276–278). Moreover, enhanced inhibition of tumour growth following combined treatment of ART and local radiation has also been described in an xenograft model of non-small-cell lung cancer, further supporting the potential of use ART as a radio-enhancing agent (173).

In addition to the effects of ART on radiation therapy, I also investigated the ability of ART to enhance the inhibition of breast cancer cell growth by 5 established chemotherapeutic agents (doxorubicin, cisplatin, docetaxel, fluorouracil and 4-hydroperoxycyclophosphamide, a metabolite of cyclophosphamide) used in the treatment of breast cancer (59, 61). In preliminary studies using the MTT assay, exposure to low doses of ART significantly reduced the EC_{50} concentrations of all five chemotherapeutic agents. These results support the possible application of ART in combined modality treatment of breast cancer. Further experiments using a greater range of ART concentrations in combination with these chemotherapeutic agents are now required to allow for the calculation of the combination index, to determine whether the effect is additive or synergistic (279).

The anti-breast cancer effects mediated by cisplatin in combination with ART were also investigated using a clonogenic assay. A 5 μM concentration of ART, which alone had no effect on the replicative ability of MDA-MB-468 breast cancer cells, significantly reduced the survival fraction of cells treated with ART and cisplatin. To the author's knowledge, this is the first report of the combined effects of ART and cisplatin in breast cancer cells, and these results, in addition to results from the MTT assay, argue for the possible use of ART in combined modality treatment of breast cancer.

The ability of ART and DHA to enhance the activity of established chemotherapeutic agents against other cancer types has been reported previously (166, 189, 210, 280, 281). The effect of DHA-treatment in combination with doxorubicin has been documented in breast cancer cell lines that include MCF-7, T47D and MDA-MB-231 cells (210). Calculation of the combination index revealed synergistic anti-proliferative effects between ART and doxorubicin for certain cell line and dosage combinations. Furthermore, combined treatment enhances apoptosis and caspase activation in MCF-7 cells. Interestingly, artemisinin, (the parental compound of ART and DHA) induces doxorubicin-resistance in colon cancer cells through the up-regulation of p-glycoprotein, resulting in decreased cellular uptake of doxorubicin (280). In contrast to artemisinin, DHA did not affect doxorubicin accumulation in the breast cancer cells (210). Nevertheless, further study is needed to determine whether these different effects are due to differences in the cancer cell lines or the specific drug activity. Additive effects

between ART and gemcitabine and oxaliplatin have also been reported in MCF-7 breast cancer cells and HCT116 colon cancer cells. DHA and, to a lesser extent ART, enhanced gemcitabine activity *in vitro* and *in vivo* in hepatoma cells (166, 189). The combination of DHA and carboplatin is also effective in a xenograft model of ovarian cancer. Similar results were also obtained with cyclophosphamide and cisplatin in a lung cancer model (169, 281). Taken together, ART shows potential for use in combined modality treatment in the management of breast and other cancers. Since ART has few adverse side effects in the treatment of malaria patients, its addition to breast cancer chemotherapy may benefit patients by lowering the required dose of more toxic conventional chemotherapeutic drugs.

4.10 Advantages and Limitations of ART as an Anti-Cancer Agent

ART has been used for many years in the successful treatment of malaria (147, 148). Water-soluble ART can be administered through multiple routes, including oral and i.v routes, and has been used to treat of millions of malaria patients with few toxic side effects (149, 152, 153). ART has now been shown to possess a broad spectrum of activity against many different cancer cell types, including cancer cells that are resistant to established chemotherapeutic agents (150, 151, 168, 282). Furthermore, selectivity of ART for cancer cells over normal cells has also been reported (171, 182, 185–187, 253). ART, and its primary metabolite DHA have both anti-proliferative and cytotoxic effects on cancer cells *in vitro* and *in vivo* (150, 151, 179, 184, 208, 209). Nevertheless, treatment of cancer cells appears to require a higher dose of ART than is required for the management of malaria. In addition, higher doses of ART would likely be required to achieve a similar ART level in distal tumour tissue to that attained in the parasitised red blood cells of malaria patients. Adverse side effects not observed in ART treatment of malaria are therefore possible with increased dosage and long term use that would be required for cancer treatment; hence, further research is needed (159, 160, 163, 218). Furthermore, the short half-life of ART could impede its use in cancer therapy and would require more frequent administration (154, 155). In addition, as

Nevertheless, the potent anti-cancer activity of ART, along with its reliable and safe use in malaria patients, recommends further investigation of this agent for translation to the clinic for the treatment of cancer.

4.11 Study Limitations and Future Directions

4.11.1 *In vivo* studies

The use of cell culture systems to examine the effects of ART on breast and ovarian cancer cell lines provides an inexpensive and rapid method to evaluate multiple parameters involved in ART's activities, including its effects on cancer cell proliferation and survival as well as the biochemical pathways underlying this activity. This approach also allowed me to test ART against breast and ovarian cancer cell lines with known genetic backgrounds to better understand its spectrum of activity. The *in vitro* studies described in this thesis show that ART has a potent inhibitory effect on the proliferation and survival of breast and ovarian cancer cells. Nevertheless, to have significant value as a therapeutic agent ART also needs to be selective for cancer cells. Experiments examining the effect of ART on the growth and viability of normal breast and ovarian cells are therefore required.

ART-induced growth inhibition of breast and ovarian cancer cell lines was determined using the MTT assay, which analysed changes in the mitochondrial activity of cells treated in the absence or presence of ART (222). Recent evidence suggests that mitochondrial metabolism is high in senescent cells (283) and this could influence results obtained from the MTT assay leading to an underestimation of ART activity, if ART were able to induce senescence in the breast and ovarian cancer cells used in this study. Nevertheless, preliminary results suggest that senescence is not induced in ART-treated HEY1 and HEY2 ovarian cancer cell lines (data not shown).

Although *in vitro* systems facilitate the study of mechanisms involved in the anti-cancer effects of ART, in reality, cancers develop in the extremely complex environment that is the human body. Nevertheless, the strong inhibitory activity of ART on growth of spheroid cultures of ovarian and breast cancer cells is very encouraging as this culture system is more representative of some aspects of tumours *in situ* (238, 239, 241, 284, 285). However, *in vivo,* tumour cells interact with the immune system, as well with other

cells of the tumour microenvironment and are exposed to adverse oxygenation and pH conditions. It is therefore important to confirm the mechanisms seen *in vitro* in animal models of breast and ovarian cancer. The next objective of this project will be to evaluate the effects of ART on ovarian and breast cancer xenografts grown in immune-deficient mice. Western blotting of tumour samples for ART-induced changes in the expression of cell cycle regulatory proteins and proteins involved in apoptosis/necroptosis will further validate the mechanisms of action that were observed *in vitro*.

4.11.2 Continued Investigation of ART-mediated Anti-cancer Mechanisms

This thesis has shown that ART exerts potent anti-proliferative effects at low μM concentrations that are well below those required to induce cell death. In the present study, I showed that the anti-proliferative effect of ART on breast and ovarian cancer cells was ROS-independent and involved changes in the expression of key cell cycle regulatory proteins. As lower concentrations of ART will be easier to obtain *in vivo* and less likely to induce adverse side effects, I believe it is important to further investigate the mechanisms behind this anti-proliferative activity. Recent studies have implicated iron deprivation as a possible mechanism of ART and DHA activity (175, 182). Further research in this area is therefore warranted in breast and ovarian cancer models. Furthermore, it is important to continue to explore ART-induced changes in cell cycle regulatory protein expression and their contribution to the anti-proliferative and cytotoxic effects of ART.

4.11.3 Novel Drug Delivery Platforms

The short half-life of ART is a significant limitation for the translation of this anti-malarial drug to the clinic for the treatment of cancer (154). As a significantly higher concentration of ART is required for the treatment of cancer cells, compared to the dose needed to manage malaria, and solid tumours are not as accessible as the malaria-parasitised red blood cells, novel strategies are required to maximise the amount of ART that reaches cancer cells. One possible strategy is to develop novel delivery platforms based on nanoparticles and liposomal packaging (286). In fact, liposome nanoparticles able to release novel artemisinin dimers in areas of decreased pH are currently under investigation (287). Development of novel synthetic endoperoxides, as well as DHA and

artemisinin dimers with more potent anti-cancer activity is also in progress (177, 288, 289).

4.11.4 Combined Modality Treatments

Preliminary experiments presented in this study have demonstrated the value of ART as a potential addition to novel or established combined modality treatments of breast cancer. The effect of combined treatment with ART and radiation or chemotherapeutic drugs should now be confirmed using a large panel of breast cancer cell lines, including breast cancer cells with different hormone receptor status and genetic backgrounds. MTT and colony-forming assays should be used to determine the short and long term effects of ART combinatorial treatments on breast cancer cell proliferation, viability, and survival in order to calculate the combinational index. Western blotting, flow cytometry, and microarray analysis can also be performed to determine the biochemical pathways affected by ART combination therapy, including the expression and activity of pro- and anti-apoptotic proteins. Lastly, the anti-cancer effects of combinational ART therapy should be validated in an *in vivo* model of breast cancer. Screening of potential ART combinations could be initially performed in zebrafish embryos implanted with breast cancer xenografts (290). The high throughput nature of the zebrafish system will allow for the identification of the most potent treatment combinations, as well as the screening of these combinations against a variety of different breast cancer cell types. The most promising ART combinations could then be further validated in murine models of breast cancer.

4.11.5 Continued Studies of Ovarian Tumour Spheroids

The present study was the first to determine the potent inhibitory effect of ART on breast and ovarian cancer spheroids. As ovarian cancer cells often disseminate through the peritoneal cavity in the form of spheroids, and spheroid cultures have been associated with a more chemoresistant phenotype *in vitro*, I believe the strong inhibitory activity of ART towards the HEY1 and HEY2 ovarian cancer spheroids described in this study makes ART an exciting potential candidate for the treatment of ovarian cancers (237, 238, 244). To further explore the scope of the effects of ART on tumour spheroids, ART should be tested on clinical spheroid isolates from the peritoneal ascites of ovarian cancer

patients. Western blotting and mRNA analysis for ART-induced changes in the expression of adhesion molecules, as well as cell cycle and apoptosis regulatory proteins, would further our understanding of the effects of ART on ovarian cancer spheroids. Furthermore, as ART showed excellent activity towards the murine ID8 ovarian cancer cell line, the ability of ART to inhibit ovarian cancer cell growth, spheroid formation and peritoneal metastasis could be determined in a syngeneic mouse model of ovarian cancer (291). Good activity in this *in vivo* model would provide strong support for the further investigation of ART as a possible treatment for ovarian cancer.

4.12 Conclusions

In summary, my thesis research has established that ART, like DHA, has potent anti-proliferative and cytotoxic effects on breast and ovarian cancer cells. At concentrations above 25 μM, ART induced apoptotic and/or necrotic cell death in the breast cancer and ovarian cancer cell lines. Apoptotic cell death was caspase-dependent and involved increased mitochondrial membrane permeability and PARP cleavage in breast cancer cells. Necrotic cell death of HEY1 and HEY2 ovarian cancer cells involved RIP1K. Cell death was dependent on ART-induced ROS production and required the presence of iron. Moreover, iron supplementation increased ART-induced ROS production in breast cancer cells. ROS-dependent cell death was characterised by G2/M cell cycle arrest and DNA damage in the majority of the cell lines tested.

The anti-proliferative activity of ART was observed at concentrations as low as 1 μM. This effect was ROS-independent. In the absence of ROS, ART caused cell cycle arrest in the G1 phase in both ovarian and breast cancer cells. Cell cycle arrest was characterised by ART-induced alterations in the expression of key cell cycle regulatory proteins (a summary of significant finds can be seen in Table 4.1).

My research has increased our knowledge of the multimodal activity of ART on breast and ovarian cancer cells and highlights novel and important differences in the anti-proliferative and cytotoxic effects of ART. Furthermore, my thesis has elucidated the underlying mechanisms of action of ART and shown them to be similar in breast and ovarian cancer cells. Understanding how ART affects cancer cells will be important in its

further development as an anti-cancer agent, particularly for the treatment of breast and ovarian cancer.

Table 4.1 Summary of ART Activity in Breast and Ovarian Cancer Cell Lines.

	Ovarian cancer			Breast cancer	
	HEY1	**HEY2**	**SKOV-3**	**MDA-MB-468**	**SK-BR-3**
Cytotoxic activity					
Main method of cell death	Necroptosis	necroptosis	necrosis/ apoptosis	apoptosis	apoptosis
Caspase activation	Yes	yes	nd	yes	yes
Caspase-dependence	Slight	slight	nd	significant	significant
RIPK1-dependent	Yes	yes	nd	no	no
ROS-dependent	Yes	yes	yes	yes	yes
Iron-dependent	Yes	yes	yes	yes	yes
Effect of HT pre-treatment on anti-cancer activity	Increased	slightly increased	increased	increased	increased
Mitochondrial membrane permeabilisation	Nd	nd	nd	yes, ROS-dependent	yes, ROS-dependent
DNA damage	yes, ROS-dependent	yes, ROS-dependent	nd	yes, ROS-dependent	yes, ROS-dependent
ROS production	Yes	yes	yes	yes	yes
Effect of HT on ROS production	Nd	nd	nd	increased	increased
Decreased surface CD71	No	no	nd	yes	yes
Anti-proliferative activity					
ROS-dependent	No	no	nd	no	no
Phase of cell cycle arrest	dose dependent G1 (10μM ART) G2/M (50 μM ART)	dose dependent G1 (10μMART) G2/M (50 μM ART)	nd	G2/M	G1
Phase of cell cycle arrest in the presence of GSH	G1	G1	nd	G1	G1
Cell cycle regulatory proteins affected	↓CDK4, ↓CDK2, ↓CDK1, ↓E2F-1 ↓cyclin D3, ↓Rb ↓cyclin B, ↓cyclin A ↓CDC25C ↑p-Chk2, ↑p21Waf1/Cip1	↓CDK4,↓CDK2 ↓CDK1, ↓E2F-1 ↓cyclin D3, ↓Rb ↓cyclin B ↓cyclin A ↓CDC25C ↑p-Chk2, ↑p21Waf1/Cip1	nd	↓CDK4 ↓CDK1 ↓CDC25C ↓cyclin D3 ↑p-Chk2, ↑p21Waf1/Cip1 ↓E2F-1	↓CDK4 ↓CDK1 ↓E2F-1, ↓CDC25C ↓cyclin D3, ↓cyclin A, ↓cyclin B ↑p-Chk2, ↑p21Waf1/Cip1

REFERENCES

1. Siegel, R., D. Naishadham, and A. Jemal. 2013. Cancer statistics, 2013. *CA A Cancer J. Clin.* 63: 11–30.

2. Canada, S. 2012. Table102-0561 - Leading causes of death, total population, by age group and sex, Canada, annual. *CANISM (database)*.

3. Canadian Cancer Society's Advisory Committee on Cancer Statistics. 2013. *Canadian Cancer Statistics Special topic : Liver cancer*,. Toronto, ON; 1–114.

4. Hanahan, D., and R. Weinberg. 2011. Hallmarks of Cancer: The Next Generation. *Cell* 144: 646–674.

5. Hanahan, D., and R. A. Weinberg. 2000. The hallmarks of cancer. *Cell* 100: 57–70.

6. Lutz, A. M., J. K. Willmann, C. W. Drescher, P. Ray, F. V Cochran, N. Urban, and S. S. Gambhir. 2011. Early diagnosis of ovarian carcinoma: is a solution in sight? *Radiology* 259: 329–345.

7. Romero, I., and R. C. Bast. 2012. Minireview: human ovarian cancer: biology, current management, and paths to personalizing therapy. *Endocrinology* 153: 1593–602.

8. Tavassoli, F. A., and P. (Eds) Devilee. 2003. *World Health Organisation Classification of Tumors. Pathology and Genetics of Cancer. Tumors of the Breast and Female Genital Organs.*,. IARC Press, Llyon; 113–202.

9. Chan, J. K., D. Teoh, J. M. Hu, J. Y. Shin, K. Osann, and D. S. Kapp. 2008. Do clear cell ovarian carcinomas have poorer prognosis compared to other epithelial cell types? A study of 1411 clear cell ovarian cancers. *Gynecol. Oncol.* 109: 370–6.

10. Vaughan, S., J. Coward, R. Bast, A. Berchuck, J. Berek, J. Brenton, G. Coukos, C. Crum, R. Drapkin, D. Etemadmoghadam, M. Friedlander, and H. Gabra. 2011. Rethinking ovarian cancer: recommendations for improving outcomes. *Nat. Rev. Cancer* 11: 719–725.

11. Seidman, J. D., R. J. Kurman, and B. M. Ronnett. 2003. Primary and metastatic mucinous adenocarcinomas in the ovaries: incidence in routine practice with a new approach to improve intraoperative diagnosis. *Am. J. Surg. Pathol.* 27: 985–93.

12. Yemelyanova, A. V, R. Vang, K. Judson, L. Wu, and B. M. Ronnett. 2008. Distinction of primary and metastatic mucinous tumors involving the ovary: analysis of size and laterality data by primary site with reevaluation of an algorithm for tumor classification. *Am. J. Surg. Pathol.* 32: 128–38.

13. Kindelberger, D. W., Y. Lee, A. Miron, M. S. Hirsch, C. Feltmate, F. Medeiros, M. J. Callahan, E. O. Garner, R. W. Gordon, C. Birch, R. S. Berkowitz, M. G. Muto, and C. P. Crum. 2007. Intraepithelial carcinoma of the fimbria and pelvic serous carcinoma: Evidence for a causal relationship. *Am. J. Surg. Pathol.* 31: 161–9.

14. Przybycin, C. G., R. J. Kurman, B. M. Ronnett, I.-M. Shih, and R. Vang. 2010. Are all pelvic (nonuterine) serous carcinomas of tubal origin? *Am. J. Surg. Pathol.* 34: 1407–16.

15. Lee, K. R., and R. H. Young. 2003. The distinction between primary and metastatic mucinous carcinomas of the ovary: gross and histologic findings in 50 cases. *Am. J. Surg. Pathol.* 27: 281–92.

16. Vang, R., I. Shih, and R. Kurman. 2009. Ovarian low-grade and high-grade serous carcinoma: pathogenesis, clinicopathologic and molecular biologic features, and diagnostic problems. *Adv. Anat. Pathol.* 16: 267–282.

17. Zhang, S., R. Royer, S. Li, J. R. McLaughlin, B. Rosen, H. a Risch, I. Fan, L. Bradley, P. Shaw, and S. Narod. 2011. Frequencies of BRCA1 and BRCA2 mutations among 1,342 unselected patients with invasive ovarian cancer. *Gynecol. Oncol.* 121: 353–7.

18. Kuo, K., B. Guan, Y. Feng, T. Mao, X. Chen, N. Jinawath, Y. Wang, R. J. Kurman, I.-M. Shih, and T.-L. Wang. 2009. Analysis of DNA copy number alterations in ovarian serous tumors identifies new molecular genetic changes in low-grade and high-grade carcinomas. *Cancer Res.* 69: 4036–42.

19. Salani, R., R. J. Kurman, R. Giuntoli, G. Gardner, R. Bristow, T. Wang, and I. Shih. 2008. Assessment of TP53 mutation using purified tissue samples of ovarian serous carcinomas reveals a higher mutation rate than previously reported and does not correlate with drug resistance. *Int. J. Gynecol. Cancer* 18: 487–91.

20. Erickson, B. K., M. G. Conner, and C. N. Landen. 2013. The role of the fallopian tube in the origin of ovarian cancer. *Am. J. Obstet. Gynecol.* 209: 409–14.

21. Salvador, S., A. Rempel, R. A. Soslow, B. Gilks, D. Huntsman, and D. Miller. 2008. Chromosomal instability in fallopian tube precursor lesions of serous carcinoma and frequent monoclonality of synchronous ovarian and fallopian tube mucosal serous carcinoma. *Gynecol. Oncol.* 110: 408–17.

22. Salvador, S., B. Gilks, M. Köbel, D. Huntsman, B. Rosen, and D. Miller. 2009. The fallopian tube: primary site of most pelvic high-grade serous carcinomas. *Int. J. Gynecol. Cancer* 19: 58–64.

23. George, S. H., J. Greenaway, A. Milea, V. Clary, S. Shaw, M. Sharma, C. Virtanen, and P. A. Shaw. 2011. Identification of abrogated pathways in fallopian tube epithelium from BRCA1 mutation carriers. *J. Pathol.* 225: 106–17.

24. Köbel, M., S. E. Kalloger, D. G. Huntsman, J. L. Santos, K. D. Swenerton, J. D. Seidman, and C. B. Gilks. 2010. Differences in tumor type in low-stage versus high-stage ovarian carcinomas. *Int. J. Gynecol. Pathol.* 29: 203–11.

25. Hart, W. R. 2005. Mucinous Tumors of the Ovary : A Review. *Int. J. Gynecol. Pathol.* 78: 4–25.

26. Lee, K. R., and R. E. Scully. 2000. Mucinous tumors of the ovary: a clinicopathologic study of 196 borderline tumors (of intestinal type) and carcinomas, including an evaluation of 11 cases with "pseudomyxoma peritonei". *Am. J. Surg. Pathol.* 24: 1447–64.

27. McAlpine, J. N., K. C. Wiegand, R. Vang, B. . Ronnett, A. Adamiak, M. Köbel, S. E. Kalloger, K. D. Swenerton, D. G. Huntsman, C. B. Gilks, and D. M. Miller. 2009. HER2 overexpression and amplification is present in a subset of ovarian mucinous carcinomas and can be targeted with trastuzumab therapy. *BMC Cancer* 9: 433.

28. Prat, J. 2012. Ovarian carcinomas: five distinct diseases with different origins, genetic alterations, and clinicopathological features. *Virchows Arch.* 460: 237–49.

29. Gurung, A., T. Hung, J. Morin, and C. B. Gilks. 2013. Molecular abnormalities in ovarian carcinoma: clinical, morphological and therapeutic correlates. *Histopathology* 62: 59–70.

30. Anglesio, M. S., M. S. Carey, M. Köbel, H. Mackay, and D. G. Huntsman. 2011. Clear cell carcinoma of the ovary: a report from the first Ovarian Clear Cell Symposium, June 24th, 2010. *Gynecol. Oncol.* 121: 407–15.

31. Kamura, T., D. Ph, J. Kigawa, N. Terakawa, Y. Kikuchi, and T. Kita. 2000. Clinical characteristics of clear cell carcinoma of the ovary a distinct histologic type with poor prognosis and resistance to platinum- based chemotherapy. *Cancer* 88: 2584–2589.

32. Lee, Y., T. Kim, M. Kim, H. Kim, T. Song, M. Kyu, C. Hun, J. Lee, D. Bae, and B. Kim. 2011. Prognosis of ovarian clear cell carcinoma compared to other histological subtypes : A meta-analysis. *Gynecol. Oncol.* 122: 541–547.

33. Greene, F. L., A. Trotti, A. G. Fritz, C. C. Compton, D. R. Byrd, and S. B. Edge (Eds). 2010. *AJCC Cancer Staging Handbook - 7th Ed.*, 7th ed. American Joint Committee on Cancer., Chicago, IL.

34. Bristow, R. E., R. S. Tomacruz, D. K. Armstrong, E. L. Trimble, and F. J. Montz. 2002. Survival effect of maximal cytoreductive surgery for advanced ovarian carcinoma during the platinum era: a meta-analysis. *J. Clin. Oncol.* 20: 1248–59.

35. Raja, F., N. Chopra, and J. Ledermann. 2012. Optimal first-line treatment in ovarian cancer. *Ann. Oncol.* 23 Suppl 1: x118–27.

36. National Cancer Institute. National Cancer Institute: PDQ® Ovarian Epithelial Cancer Treatment. http://www.cancer.gov/cancertopics/pdq/treatment/ovarianepithelial/HealthProfessional. .

37. Hennessy, B. T., R. L. Coleman, and M. Markman. 2009. Ovarian cancer. *Lancet* 374: 1371–1382.

38. Ahmed, N., and K. L. Stenvers. 2013. Getting to know ovarian cancer ascites: opportunities for targeted therapy-based translational research. *Front. Oncol.* 3: 256.

39. Morgan, R. J., R. D. Alvarez, D. K. Armstrong, R. A. Burger, L.-M. Chen, L. Copeland, M. A. Crispens, D. M. Gershenson, H. J. Gray, A. Hakam, L. J. Havrilesky, C. Johnston, S. Lele, L. Martin, U. A. Matulonis, D. M. O'Malley, R. T. Penson, M. A. Powell, S. W. Remmenga, P. Sabbatini, J. T. Santoso, J. C. Schink, N. Teng, T. L. Werner, M. A. Dwyer, and M. Hughes. 2013. Ovarian cancer, version 2.2013. *J. Natl. Compr. Canc. Netw.* 11: 1199–209.

40. Cannistra, S. A. 2004. Cancer of the ovary. *N. Engl. J. Med.* 351: 2519–29.

41. Eckstein, N. 2011. Platinum resistance in breast and ovarian cancer cell lines. *J. Exp. Clin. Cancer Res.* 30: 91.

42. Karst, A. M., and R. Drapkin. 2010. Ovarian cancer pathogenesis: a model in evolution. *J. Oncol.* 2010: 932371.

43. Lakhani, S. R., I. O. Ellis, S. J. Schnitt, P. H. Tan, M. J. van de Vijver, and (Eds). 2012. *WHO classification of tumours of the breast.*,. IARC Press, Lyon.

44. Elston, C. W., and I. O. Ellis. 1991. Pathological prognostic factors in breast cancer. I. The value of histological grade in breast cancer: experience from a large study with long-term follow-up. *Histopathology* 19: 403–10.

45. Gannon, L. M., M. B. Cotter, and C. M. Quinn. 2013. The classification of invasive carcinoma of the breast. *Expert Rev. Anticancer Ther.* 13: 941–54.

46. Engebraaten, O., H. K. Moen Vollan, and A. L. Børresen-Dale. 2013. Triple-negative breast cancer and the need for new therapeutic targets. *Am. J. Pathol.* 183: 1064–1074.

47. Sørlie, T., C. M. Perou, R. Tibshirani, T. Aas, S. Geisler, H. Johnsen, T. Hastie, M. B. Eisen, M. van de Rijn, S. S. Jeffrey, T. Thorsen, H. Quist, J. C. Matese, P. O. Brown, D. Botstein, P. E. Lønning, and A. L. Børresen-Dale. 2001. Gene expression patterns of breast carcinomas distinguish tumor subclasses with clinical implications. *Proc. Natl. Acad. Sci. U. S. A.* 98: 10869–74.

48. Sorlie, T., R. Tibshirani, J. Parker, T. Hastie, J. S. Marron, A. Nobel, S. Deng, H. Johnsen, R. Pesich, S. Geisler, J. Demeter, C. M. Perou, P. E. Lønning, P. O. Brown, A.-L. Børresen-Dale, and D. Botstein. 2003. Repeated observation of breast tumor subtypes in independent gene expression data sets. *Proc. Natl. Acad. Sci. U. S. A.* 100: 8418–23.

49. Hu, Z., C. Fan, D. S. Oh, J. S. Marron, X. He, B. F. Qaqish, C. Livasy, L. A. Carey, E. Reynolds, L. Dressler, A. Nobel, J. Parker, M. G. Ewend, L. R. Sawyer, J. Wu, Y. Liu, R. Nanda, M. Tretiakova, A. Ruiz Orrico, D. Dreher, J. P. Palazzo, L. Perreard, E. Nelson, M. Mone, H. Hansen, M. Mullins, J. F. Quackenbush, M. J. Ellis, O. I. Olopade, P. S. Bernard, and C. M. Perou. 2006. The molecular portraits of breast tumors are conserved across microarray platforms. *BMC Genomics* 7: 96.

50. Yang, X. R., M. E. Sherman, D. L. Rimm, J. Lissowska, L. a Brinton, B. Peplonska, S. M. Hewitt, W. F. Anderson, N. Szeszenia-Dabrowska, A. Bardin-Mikolajczak, W. Zatonski, R. Cartun, D. Mandich, G. Rymkiewicz, M. Ligaj, S. Lukaszek, R. Kordek, and M. García-Closas. 2007. Differences in risk factors for breast cancer molecular subtypes in a population-based study. *Cancer Epidemiol. Biomarkers Prev.* 16: 439–43.

51. Nguyen, P. L., A. G. Taghian, M. S. Katz, A. Niemierko, R. F. Abi Raad, W. L. Boon, J. R. Bellon, J. S. Wong, B. L. Smith, and J. R. Harris. 2008. Breast cancer subtype approximated by estrogen receptor, progesterone receptor, and HER-2 is associated with local and distant recurrence after breast-conserving therapy. *J. Clin. Oncol.* 26: 2373–8.

52. Carey, L. A., E. C. Dees, L. Sawyer, L. Gatti, D. T. Moore, F. Collichio, D. W. Ollila, C. I. Sartor, M. L. Graham, and C. M. Perou. 2007. The triple negative paradox: primary tumor chemosensitivity of breast cancer subtypes. *Clin. Cancer Res.* 13: 2329–34.

53. Davoli, A., B. A. Hocevar, and T. L. Brown. 2010. Progression and treatment of HER2-positive breast cancer. *Cancer Chemother. Pharmacol.* 65: 611–23.

54. Nielsen, T. O., F. D. Hsu, K. Jensen, M. Cheang, G. Karaca, Z. Hu, T. Hernandez-Boussard, C. Livasy, D. Cowan, L. Dressler, L. A. Akslen, J. Ragaz, A. M. Gown, C. B. Gilks, M. van de Rijn, and C. M. Perou. 2004. Immunohistochemical and clinical characterization of the basal-like subtype of invasive breast carcinoma. *Clin. Cancer Res.* 10: 5367–74.

55. Carey, L., E. Winer, G. Viale, D. Cameron, and L. Gianni. 2010. Triple-negative breast cancer: disease entity or title of convenience? *Nat. Rev. Clin. Oncol.* 7: 683–92.

56. Easton, D. F., D. Ford, D. T. Bishop, and C. Linkage. 1995. Breast and Ovarian Cancer Incidence in BRCA I -Mutation Carriers. *Am. J. Hum. Genet.* 579: 265–271.

57. Pazaiti, A., and I. S. Fentiman. 2011. Basal phenotype breast cancer: implications for treatment and prognosis. *Womens. Health (Lond. Engl).* 7: 181–202.

58. Dawson, S. J., O. M. Rueda, S. Aparicio, and C. Caldas. 2013. A new genome-driven integrated classification of breast cancer and its implications. *EMBO J.* 32: 617–28.

59. BC Cancer Agency. Cancer management guidelines. http://www.bccancer.bc.ca/HPI/CancerManagementGuidelines/Breast/1Demographicsandriskfactors.htm.

60. Nofech-Mozes, S., E. T. Vella, S. Dhesy-Thind, and W. M. Hanna. 2012. Cancer care ontario guideline recommendations for hormone receptor testing in breast cancer. *Clin. Oncol. (R. Coll. Radiol).* 24: 684–96.

61. Maughan, K. L., M. A. Lutterbie, and P. S. Ham. 2010. Treatment of breast cancer. *Am. Fam. Physician* 81: 1339–46.

62. National Cancer Institute. National Cancer Institute: PDQ® Breast Cancer Treatment. http://www.cancer.gov/cancertopics/pdq/treatment/breast/healthprofessional. .

63. Brewster, A. M., G. N. Hortobagyi, K. R. Broglio, S.-W. Kau, C. A. Santa-Maria, B. Arun, A. U. Buzdar, D. J. Booser, V. Valero, M. Bondy, and F. J. Esteva. 2008. Residual risk of breast cancer recurrence 5 years after adjuvant therapy. *J. Natl. Cancer Inst.* 100: 1179–83.

64. Shapiro, C. L., and A. Recht. 2001. Side effects of adjuvant treatment of breast cancer. *N. Engl. J. Med.* 344: 1997–2008.

65. Kayl, A. E., and C. A. Meyers. 2006. Side-effects of chemotherapy and quality of life in ovarian and breast cancer patients. *Curr. Opin. Obstet. Gynecol.* 18: 24–8.

66. Murray, S., E. Briasoulis, H. Linardou, D. Bafaloukos, and C. Papadimitriou. 2012. Taxane resistance in breast cancer: Mechanisms, predictive biomarkers and circumvention strategies. *Cancer Treat. Rev.* 38: 890–903.

67. Vermeulen, K., D. R. Van Bockstaele, and Z. N. Berneman. 2003. The cell cycle: a review of regulation, deregulation and therapeutic targets in cancer. *Cell Prolif.* 36: 131–49.

68. Massagué, J. 2004. G1 cell-cycle control and cancer. *Nature* 432: 298–306.

69. Cam, H., and B. D. Dynlacht. 2003. Emerging roles for E2F: Beyond the G1/S transition and DNA replication. *Cancer Cell* 3: 311–316.

70. Harbour, J. W., R. X. Luo, A. Dei Santi, A. A. Postigo, and D. C. Dean. 1999. Cdk phosphorylation triggers sequential intramolecular interactions that progressively block Rb functions as cells move through G1. *Cell* 98: 859–69.

71. Bracken, A. P., M. Ciro, A. Cocito, and K. Helin. 2004. E2F target genes: unraveling the biology. *Trends Biochem. Sci.* 29: 409–17.

72. Lundberg, A. S., and R. A. Weinberg. 1998. Functional inactivation of the retinoblastoma protein requires sequential modification by at least two distinct cyclin-cdk complexes. *Mol. Cell. Biol.* 18: 753–61.

73. Lolli, G., and L. N. Johnson. 2005. CAK-cyclin-dependent activating kinase: a key kinase in cell cycle control and a target for drugs? *Cell Cycle* 4: 572–577.

74. Rudolph, J. 2005. Redox regulation of the Cdc25 phosphatases. *Antioxid. Redox Signal.* 7: 761–767.

75. Lu, J. J. J., S. M. M. Chen, J. Ding, and L.-H. H. Meng. 2012. Characterization of dihydroartemisinin-resistant colon carcinoma HCT116/R cell line. *Mol. Cell. Biochem.* 360: 329–337.

76. Medema, R. H. and L. Macůrek. 2012. Checkpoint control and cancer. *Oncogene* 31: 2601–13.

77. Vousden, K. H., and C. Prives. 2009. Blinded by the Light: The Growing Complexity of p53. *Cell* 137: 413–431.

78. Santamaría, D., C. Barrière, A. Cerqueira, S. Hunt, C. Tardy, K. Newton, J. F. Cáceres, P. Dubus, M. Malumbres, and M. Barbacid. 2007. Cdk1 is sufficient to drive the mammalian cell cycle. *Nature* 448: 811–5.

79. Malumbres, M., and M. Barbacid. 2009. Cell cycle, CDKs and cancer: a changing paradigm. *Nat. Rev. Cancer* 9: 153–66.

80. Yu, Q., E. Sicinska, Y. Geng, M. Ahnström, A. Zagozdzon, Y. Kong, H. Gardner, H. Kiyokawa, L. N. Harris, O. Stål, and P. Sicinski. 2006. Requirement for CDK4 kinase function in breast cancer. *Cancer Cell* 9: 23–32.

81. Kroemer, G., L. Galluzzi, P. Vandenabeele, J. Abrams, E. S. Alnemri, E. H. Baehrecke, M. V Blagosklonny, W. S. El-Deiry, P. Golstein, D. R. Green, M. Hengartner, R. a Knight, S. Kumar, S. a Lipton, W. Malorni, G. Nuñez, M. E. Peter, J. Tschopp, J. Yuan, M. Piacentini, B. Zhivotovsky, and G. Melino. 2009. Classification of cell death: recommendations of the Nomenclature Committee on Cell Death 2009. *Cell Death Differ.* 16: 3–11.

82. Ouyang, L., Z. Shi, S. Zhao, F. T. Wang, T. T. Zhou, B. Liu, and J. K. Bao. 2012. Programmed cell death pathways in cancer: a review of apoptosis, autophagy and programmed necrosis. *Cell Prolif.* 45: 487–98.

83. Leist, M., and P. Nicotera. 1997. The shape of cell death. *Biochem. Biophys. Res. Commun.* 236: 1–9.

84. Saraste, A. 1999. Morphologic criteria and detection of apoptosis. *Herz* 24: 189–95.

85. Kerr, J. F. R., A. H. Wyllie, and A. R. Currie. 1972. Apoptosis : a basic biological phenomenon with wide-ranging implications in tissue kinetics. *Br. J. Cancer* 26: 239–257.

86. Liu, Y., S. Shoji-Kawata, R. M. Sumpter, Y. Wei, V. Ginet, L. Zhang, B. Posner, K. a Tran, D. R. Green, R. J. Xavier, S. Y. Shaw, P. G. H. Clarke, J. Puyal, and B. Levine. 2013. Autosis is a Na+,K+-ATPase-regulated form of cell death triggered by autophagy-inducing peptides, starvation, and hypoxia-ischemia. *Proc. Natl. Acad. Sci. U. S. A.* 110: 20364–71.

87. Silva, M. T. 2010. Secondary necrosis: The natural outcome of the complete apoptotic program. *FEBS Lett.* 584: 4491–4499.

88. Hengartner, M. O. 2000. The biochemistry of apoptosis. *Nature* 407: 770–6.

89. Enari, M., H. Sakahira, H. Yokoyama, K. Okawa, A. Iwamatsu, and S. Nagata. 1998. A caspase-activated DNase that degrades DNA during apoptosis. *Nature* 393: 43–50.

90. Chaitanya, G. V., A. J. Steven, and P. P. Babu. 2010. PARP-1 cleavage fragments: signatures of cell-death proteases in neurodegeneration. *Cell Commun. Signal.* 8: 31.

91. Ozben, T. 2007. Oxidative Stress and Apoptosis : Impact on Cancer Therapy. *J. Pharm. Sci.* 96: 2181–2196.

92. Lee, Y. J., and E. Shacter. 1999. Oxidative stress inhibits apoptosis in human lymphoma cells. *J. Biol. Chem.* 274: 19792–8.

93. Lelli, J. L., L. L. Becks, M. I. Dabrowska, and D. B. Hinshaw. 1998. ATP converts necrosis to apoptosis in oxidant-injured endothelial cells. *Free Radic. Biol. Med.* 25: 694–702.

94. Garrido, C., L. Galluzzi, M. Brunet, P. E. Puig, C. Didelot, and G. Kroemer. 2006. Mechanisms of cytochrome c release from mitochondria. *Cell Death Differ.* 13: 1423–33.

95. Green, D. R., and G. Kroemer. 2004. The pathophysiology of mitochondrial cell death. *Science* 305: 626–9.

96. Kim, H., M. Rafiuddin-Shah, H. C. Tu, J. R. Jeffers, G. P. Zambetti, J. J. D. Hsieh, and E. H.-Y. Cheng. 2006. Hierarchical regulation of mitochondrion-dependent apoptosis by BCL-2 subfamilies. *Nat. Cell Biol.* 8: 1348–58.

97. Kim, H., H. C. Tu, D. Ren, O. Takeuchi, J. R. Jeffers, G. P. Zambetti, J. J. D. Hsieh, and E. H.-Y. Cheng. 2009. Stepwise activation of BAX and BAK by tBID, BIM, and PUMA initiates mitochondrial apoptosis. *Mol. Cell* 36: 487–99.

98. Cory, S., and J. M. Adams. 2002. The Bcl2 family: regulators of the cellular life-or-death switch. *Nat. Rev. Cancer* 2: 647–56.

99. Reed, J. C. 1997. Bcl-2 family proteins: regulators of apoptosis and chemoresistance in hematologic malignancies. *Semin. Hematol.* 34: 9–19.

100. Du, C., M. Fang, Y. Li, L. Li, and X. Wang. 2000. Smac, a Mitochondrial Protein that Promotes Cytochrome c–Dependent Caspase Activation by Eliminating IAP Inhibition. *Cell* 102: 33–42.

101. Hegde, R., S. M. Srinivasula, Z. Zhang, R. Wassell, R. Mukattash, L. Cilenti, G. DuBois, Y. Lazebnik, A. S. Zervos, T. Fernandes-Alnemri, and E. S. Alnemri. 2002. Identification of Omi/HtrA2 as a mitochondrial apoptotic serine protease that disrupts inhibitor of apoptosis protein-caspase interaction. *J. Biol. Chem.* 277: 432–8.

102. Kroemer, G., and S. J. Martin. 2005. Caspase-independent cell death. *Nat. Med.* 11: 725–30.

103. Delavallée, L., L. Cabon, P. Galán-Malo, H. K. Lorenzo, and S. A. Susin. 2011. AIF-mediated caspase-independent necroptosis: a new chance for targeted therapeutics. *IUBMB Life* 63: 221–32.

104. Sprick, M. R., M. A. Weigand, E. Rieser, C. T. Rauch, P. Juo, J. Blenis, P. H. Krammer, and H. Walczak. 2000. FADD/MORT1 and Caspase-8 Are Recruited to TRAIL Receptors 1 and 2 and Are Essential for Apoptosis Mediated by TRAIL Receptor 2. *Immunity* 12: 599–609.

105. Duprez, L., E. Wirawan, T. Vanden Berghe, and P. Vandenabeele. 2009. Major cell death pathways at a glance. *Microbes Infect.* 11: 1050–62.

106. Yu, X., Q. Deng, A. M. Bode, Z. Dong, and Y. Cao. 2013. The role of necroptosis, an alternative form of cell death, in cancer therapy. *Expert Rev. Anticancer Ther.* 13: 883–93.

107. Vandenabeele, P., L. Galluzzi, T. Vanden Berghe, and G. Kroemer. 2010. Molecular mechanisms of necroptosis: an ordered cellular explosion. *Nat. Rev. Mol. Cell Biol.* 11: 700–14.

108. Degterev, A., Z. Huang, M. Boyce, Y. Li, P. Jagtap, N. Mizushima, G. D. Cuny, T. J. Mitchison, M. A. Moskowitz, and J. Yuan. 2005. Chemical inhibitor of nonapoptotic cell death with therapeutic potential for ischemic brain injury. *Nat. Chem. Biol.* 1: 112–9.

109. Baritaud, M., L. Cabon, L. Delavallée, P. Galán-Malo, M.-E. Gilles, M.-N. Brunelle-Navas, and S. a Susin. 2012. AIF-mediated caspase-independent necroptosis requires ATM and DNA-PK-induced histone H2AX Ser139 phosphorylation. *Cell Death Dis.* 3: e390.

110. Panieri, E., V. Gogvadze, E. Norberg, R. Venkatesh, S. Orrenius, and B. Zhivotovsky. 2013. Reactive oxygen species generated in different compartments induce cell death, survival, or senescence. *Free Radic. Biol. Med.* 57: 176–87.

111. Valko, M., D. Leibfritz, J. Moncol, M. T. D. Cronin, M. Mazur, and J. Telser. 2007. Free radicals and antioxidants in normal physiological functions and human disease. *Int. J. Biochem. Cell Biol.* 39: 44–84.

112. Kietzmann, T. 2010. Intracellular redox compartments: mechanisms and significances. *Antioxid. Redox Signal.* 13: 395–8.

113. Valko, M., C. J. Rhodes, J. Moncol, M. Izakovic, and M. Mazur. 2006. Free radicals, metals and antioxidants in oxidative stress-induced cancer. *Chem. Biol. Interact.* 160: 1–40.

114. Cadenas, E., and K. J. Davies. 2000. Mitochondrial free radical generation, oxidative stress, and aging. *Free Radic. Biol. Med.* 29: 222–30.

115. Kowaltowski, A. J., and A. E. Vercesi. 1999. Mitochondrial damage induced by conditions of oxidative stress. *Free Radic. Biol. Med.* 26: 463–471.

116. Malhotra, J. D., and R. J. Kaufman. 2007. Endoplasmic reticulum stress and oxidative stress: a vicious cycle or a double-edged sword? *Antioxid. Redox Signal.* 9: 2277–93.

117. Takac, I., K. Schröder, L. Zhang, B. Lardy, N. Anilkumar, J. D. Lambeth, A. M. Shah, F. Morel, and R. P. Brandes. 2011. The E-loop is involved in hydrogen peroxide formation by the NADPH oxidase Nox4. *J. Biol. Chem.* 286: 13304–13.

118. Bartosz, G. 2009. Reactive oxygen species: destroyers or messengers? *Biochem. Pharmacol.* 77: 1303–15.

119. Vera-Ramirez, L., P. Sanchez-Rovira, M. C. Ramirez-Tortosa, C. L. Ramirez-Tortosa, S. Granados-Principal, J. A. Lorente, and J. L. Quiles. 2011. Free radicals in breast carcinogenesis, breast cancer progression and cancer stem cells. Biological bases to develop oxidative-based therapies. *Crit. Rev. Oncol. Hematol.* 80: 347–68.

120. Beckman, K. B. 1997. Oxidative Decay of DNA. *J. Biol. Chem.* 272: 19633–19636.

121. Nakae, D., Y. Mizumoto, E. Kobayashi, O. Noguchi, and Y. Konishi. 1995. Improved genomic / nuclear DNA extraction for 8- hydroxydeoxyguanosine analysis of small amounts of rat liver tissue. *Cancer Lett.* 97: 233–239.

122. Nakajima, M., T. Takeuchi, and K. Morimoto. 1996. Determination of 8-hydroxydeoxyguanosine in human cells under oxygen-free conditions. *Carcinogenesis* 17: 787–91.

123. Verbon, E. H., J. A. Post, and J. Boonstra. 2012. The influence of reactive oxygen species on cell cycle progression in mammalian cells. *Gene* 511: 1–6.

124. Tonks, N. K. 2005. Redox redux: revisiting PTPs and the control of cell signaling. *Cell* 121: 667–70.

125. Circu, M. L., and T. Y. Aw. 2010. Reactive oxygen species, cellular redox systems, and apoptosis. *Free Radic. Biol. Med.* 48: 749–62.

126. Chen, K., M. T. Kirber, H. Xiao, Y. Yang, and J. F. Keaney. 2008. Regulation of ROS signal transduction by NADPH oxidase 4 localization. *J. Cell Biol.* 181: 1129–39.

127. Wallace, D. F., L. Summerville, P. E. Lusby, and V. N. Subramaniam. 2005. Prohepcidin localises to the Golgi compartment and secretory pathway in hepatocytes. *J. Hepatol.* 43: 720–728.

128. Chiu, W. C., C. Chen, T. S. Lee, Z. Chen, P. H. Ke, and A. N. Chiang. 2010. Oxidative stress enhances AP-1 and NF-κB-mediated regulation of β(2)-glycoprotein I gene expression in hepatoma cells. *J. Cell. Biochem.* 111: 988–98.

129. Chaum, E., J. Yin, H. Yang, F. Thomas, and J. C. Lang. 2009. Quantitative AP-1 gene regulation by oxidative stress in the human retinal pigment epithelium. *J. Cell. Biochem.* 108: 1280–91.

130. Karin, M., T. Takahashi, P. Kapahi, M. Delhase, Y. Chen, C. Makris, D. Rothwarf, V. Baud, G. Natoli, F. Guido, and N. Li. 2001. Oxidative stress and gene expression: the AP-1 and NF-kappaB connections. *Biofactors* 15: 87–9.

131. Giannoni, E., F. Buricchi, G. Raugei, G. Ramponi, and P. Chiarugi. 2005. Intracellular reactive oxygen species activate src tyrosine kinase during cell adhesion and anchorage-dependent cell growth. *Mol. Cell. Biol.* 25: 6391–6403.

132. Giannoni, E., and P. Chiarugi. 2013. Redox circuitries driving Src regulation. *Antioxid. Redox Signal.* in press.

133. Singh, D. K., D. Kumar, Z. Siddiqui, S. K. Basu, V. Kumar, and K. V. S. Rao. 2005. The strength of receptor signaling is centrally controlled through a cooperative loop between Ca2+ and an oxidant signal. *Cell* 121: 281–93.

134. Liu, T. T., Y. J. Liu, Q. Wang, X. G. Yang, and K. Wang. 2012. Reactive-oxygen-species-mediated Cdc25C degradation results in differential antiproliferative activities of vanadate, tungstate, and molybdate in the PC-3 human prostate cancer cell line. *J. Biol. Inorg. Chem.* 17: 311–20.

135. Kamata, H., S. I. Honda, S. Maeda, L. Chang, H. Hirata, and M. Karin. 2005. Reactive oxygen species promote TNFalpha-induced death and sustained JNK activation by inhibiting MAP kinase phosphatases. *Cell* 120: 649–61.

136. Shen, H. M., and Z. Liu. 2006. JNK signaling pathway is a key modulator in cell death mediated by reactive oxygen and nitrogen species. *Free Radic. Biol. Med.* 40: 928–39.

137. Johansson, A. C., H. Appelqvist, C. Nilsson, K. Kågedal, K. Roberg, and K. Ollinger. 2010. Regulation of apoptosis-associated lysosomal membrane permeabilization. *Apoptosis* 15: 527–40.

138. Hamacher-Brady, A., H. A. Stein, S. Turschner, I. Toegel, R. Mora, N. Jennewein, T. Efferth, R. Eils, and N. R. Brady. 2011. Artesunate activates mitochondrial apoptosis in breast cancer cells via iron-catalyzed lysosomal reactive oxygen species production. *J. Biol. Chem.* 286: 6587–6601.

139. De Bont, R. 2004. Endogenous DNA damage in humans: a review of quantitative data. *Mutagenesis* 19: 169–185.

140. Tsuruta, F., J. Sunayama, Y. Mori, S. Hattori, S. Shimizu, Y. Tsujimoto, K. Yoshioka, N. Masuyama, and Y. Gotoh. 2004. JNK promotes Bax translocation to mitochondria through phosphorylation of 14-3-3 proteins. *EMBO J.* 23: 1889–99.

141. Yamamoto, K., H. Ichijo, and S. J. Korsmeyer. 1999. BCL-2 is phosphorylated and inactivated by an ASK1/Jun N-terminal protein kinase pathway normally activated at G(2)/M. *Mol. Cell. Biol.* 19: 8469–78.

142. Berdelle, N., T. Nikolova, S. Quiros, T. Efferth, and B. Kaina. 2011. Artesunate induces oxidative DNA damage, sustained DNA double-strand breaks, and the ATM/ATR damage response in cancer cells. *Mol. Cancer Ther.* 10: 2224–2233.

143. Kowaltowski, A. J., N. C. de Souza-Pinto, R. F. Castilho, and A. E. Vercesi. 2009. Mitochondria and reactive oxygen species. *Free Radic. Biol. Med.* 47: 333–43.

144. Borutaite, V., and G. C. Brown. 2001. Caspases are reversibly inactivated by hydrogen peroxide. *FEBS Lett.* 500: 114–8.

145. Samali, A., H. Nordgren, B. Zhivotovsky, E. Peterson, and S. Orrenius. 1999. A comparative study of apoptosis and necrosis in HepG2 cells: oxidant-induced caspase inactivation leads to necrosis. *Biochem. Biophys. Res. Commun.* 255: 6–11.

146. Hampton, M. B., and S. Orrenius. 1997. Dual regulation of caspase activity by hydrogen peroxide: implications for apoptosis. *FEBS Lett.* 414: 552–556.

147. Klayman, D. L. 1985. Qinghaosu (artemisinin): an antimalarial drug from China. *Science* 228: 1049–1055.

148. Li, Y., and Y. Wu. 2003. An over four millennium story behind qinghaosu (artemisinin)-a fantastic antimalarial drug from a traditional Chinese herb. *Curr. Med. Chem.* 10: 2197–2230.

149. WHO. 2010. *Guidlines for the treatment of malaria: second edition.*, 2nd ed. Geneva.

150. Efferth, T., H. Dunstan, A. Sauerbrey, H. Miyachi, and C. R. Chitambar. 2001. The anti-malarial artesunate is also active against cancer. *Int. J. Oncol.* 18: 767–773.

151. Kelter, G., D. Steinbach, and V. Konkimalla. 2007. Role of transferrin receptor and the ABC transporters ABCB6 and ABCB7 for resistance and differentiation of tumor cells towards artesunate. *PLoS One* 2: e798.

152. Adjuik, M., A. Babiker, P. Garner, P. Olliaro, W. Taylor, and N. White. 2004. Artesunate combinations for treatment of malaria: meta-analysis. *Lancet* 363: 9–17.

153. Simpson, J. A., T. Agbenyega, K. I. Barnes, G. Di Perri, P. Folb, M. Gomes, S. Krishna, S. Krudsood, S. Looareesuwan, S. Mansor, H. McIlleron, R. Miller, M. Molyneux, J. Mwenechanya, V. Navaratnam, F. Nosten, P. Olliaro, L. Pang, I. Ribeiro, M. Tembo, M. van Vugt, S. Ward, K. Weerasuriya, K. Win, and N. J. White. 2006. Population pharmacokinetics of artesunate and dihydroartemisinin following intra-rectal dosing of artesunate in malaria patients. *PLoS Med.* 3: e444.

154. Gautam, A., T. Ahmed, V. Batra, and J. Paliwal. 2009. Pharmacokinetics and pharmacodynamics of endoperoxide antimalarials. *Curr. Drug Metab.* 10: 289–306.

155. Morris, C. A., S. Duparc, I. Borghini-Fuhrer, D. Jung, C.-S. Shin, and L. Fleckenstein. 2011. Review of the clinical pharmacokinetics of artesunate and its active metabolite dihydroartemisinin following intravenous, intramuscular, oral or rectal administration. *Malar. J.* 10: 263.

156. Meshnick, S. R., A. Thomas, A. Ranz, C. M. Xu, and H. Z. Pan. 1991. Artemisinin (qinghaosu): the role of intracellular hemin in its mechanism of antimalarial action. *Mol. Biochem. Parasitol.* 49: 181–9.

157. Jansen, F. H. 2010. The pharmaceutical death-ride of dihydroartemisinin. *Malar. J.* 9: 212.

158. Rosenthal, P. J. 2008. Artesunate for the treatment of severe falciparum malaria. *N. Engl. J. Med.* 358: 1829–1836.

159. O'Neill, P. M., V. E. Barton, and S. a Ward. 2010. The molecular mechanism of action of artemisinin--the debate continues. *Molecules* 15: 1705–21.

160. Efferth, T. 2007. Willmar schwabe award 2006 : antiplasmodial and antitumor activity of artemisinin ± from bench to bedside. *Planta Med.* 73: 299–309.

161. Shandilya, A., S. Chacko, B. Jayaram, and I. Ghosh. 2013. A plausible mechanism for the antimalarial activity of artemisinin: a computational approach. *Sci. Rep.* 3: 2513.

162. Woerdenbag, H. J., T. A. Moskal, N. Pras, and T. M. Malingre. 1993. Cytotoxicity of artemisinin-related endoperoxides to ehrlich acites tumor cells. *J. Nat. Prod.* 56: 849–856.

163. Ferreira, I. D., D. Lopes, A. Martinelli, C. Ferreira, V. E. do Rosário, and P. Cravo. 2007. In vitro assessment of artesunate, artemether and amodiaquine susceptibility and molecular analysis of putative resistance-associated mutations of Plasmodium falciparum from São Tomé and Príncipe. *Trop. Med. Int. Health* 12: 353–62.

164. Pattanaik, S., D. Hota, S. Prabhakar, P. Kharbanda, and P. Pandhi. 2009. Pharmacokinetic interaction of single dose of piperine with steady-state carbamazepine in epilepsy patients. *Phytother. Res.* 23: 1281–1286.

165. Chen, H., B. Sun, S. Wang, S. Pan, Y. Gao, X. Bai, and D. Xue. 2010. Growth inhibitory effects of dihydroartemisinin on pancreatic cancer cells: involvement of cell cycle arrest and inactivation of nuclear factor-kappaB. *J. Cancer Res. Clin. Oncol.* 136: 897–903.

166. Hou, J., D. Wang, R. Zhang, and H. Wang. 2008. Experimental therapy of hepatoma with artemisinin and its derivatives: in vitro and in vivo activity, chemosensitization, and mechanisms of action. *Clin. Cancer Res.* 14: 5519–5530.

167. Steinbrueck, L., G. Pereira, and T. Efferth. 2010. Effects of artesunate on cytokinesis and G2/M cell cycle progression of tumour cells and budding yeast. *Cancer Genomics Proteomics* 7: 337–346.

168. Efferth, T., M. Giaisi, A. Merling, P. H. Krammer, and M. Li-Weber. 2007. Artesunate induces ROS-mediated apoptosis in doxorubicin-resistant T leukemia cells. *PLoS One* 2: e693.

169. Chen, T., M. Li, R. Zhang, and H. Wang. 2009. Dihydroartemisinin induces apoptosis and sensitizes human ovarian cancer cells to carboplatin therapy. *J. Cell. Mol. Med.* 13: 1358–1370.

170. Wang, S. J., B. Sun, Z. X. Cheng, H. X. Zhou, Y. Gao, R. Kong, H. Chen, H. C. Jiang, S.-H. Pan, D.-B. Xue, and X.-W. Bai. 2011. Dihydroartemisinin inhibits angiogenesis in pancreatic cancer by targeting the NF-κB pathway. *Cancer Chemother. Pharmacol.* 68: 1421–30.

171. Sun, H., X. Meng, J. Han, Z. Zhang, B. Wang, X. Bai, and X. Zhang. 2013. Anti-cancer activity of DHA on gastric cancer-an in vitro and in vivo study. *Tumour Biol.* in press.

172. Zhang, C. Z., H. Zhang, J. Yun, G. G. Chen, and P. B. S. Lai. 2012. Dihydroartemisinin exhibits antitumor activity toward hepatocellular carcinoma in vitro and in vivo. *Biochem. Pharmacol.* 83: 1278–89.

173. Zhao, Y., W. Jiang, B. Li, Q. Yao, J. Dong, Y. Cen, X. Pan, J. Li, J. Zheng, X. Pang, and H. Zhou. 2011. Artesunate enhances radiosensitivity of human non-small cell lung cancer A549 cells via increasing NO production to induce cell cycle arrest at G2/M phase. *Int. Immunopharmacol.* 11: 2039–2046.

174. Morrissey, C., B. Gallis, J. W. Solazzi, B. J. Kim, R. Gulati, F. Vakar-Lopez, D. R. Goodlett, R. L. Vessella, and T. Sasaki. 2010. Effect of artemisinin derivatives on apoptosis and cell cycle in prostate cancer cells. *Anticancer. Drugs* 21: 423–32.

175. Ba, Q., N. Zhou, J. Duan, T. Chen, M. Hao, X. Yang, J. Li, J. Yin, R. Chu, and H. Wang. 2012. Dihydroartemisinin exerts its anticancer activity through depleting cellular iron via transferrin receptor-1. *PLoS One* 7: e42703.

176. Ma, H., Q. Yao, A. Zhang, S. Lin, X. Wang, L. Wu, J. Sun, Z. Chen, and X. Hospital. 2011. The effects of artesunate on the expression of EGFR and ABCG2 in A549 human lung cancer cells and a xenograft model. *Molecules* 16: 10556–10569.

177. Nam, W., J. Tak, J. Ryu, M. Jung, and J. Yook. 2007. Effects of artemisinin and its derivatives on growth inhibition and apoptosis of oral cancer cells. *Head Neck* 10.1002: 335–340.

178. Mercer, A. E., J. L. Maggs, X.-M. Sun, G. M. Cohen, J. Chadwick, P. M. O'Neill, and B. K. Park. 2007. Evidence for the involvement of carbon-centered radicals in the induction of apoptotic cell death by artemisinin compounds. *J. Biol. Chem.* 282: 9372–82.

179. Du, J. H., H. D. Zhang, Z. J. Ma, and K. M. Ji. 2010. Artesunate induces oncosis-like cell death in vitro and has antitumor activity against pancreatic cancer xenografts in vivo. *Cancer Chemother. Pharmacol.* 65: 895–902.

180. Jiang, Z., J. Chai, H. H. Chuang, S. Li, T. Wang, Y. Cheng, W. Chen, and D. Zhou. 2012. Artesunate induces G0/G1 cell cycle arrest and iron-mediated mitochondrial apoptosis in A431 human epidermoid carcinoma cells. *Anticancer. Drugs* 23: 606–613.

181. Thanaketpaisarn, O., P. Waiwut, H. Sakurai, and I. Saiki. 2011. Artesunate enhances TRAIL-induced apoptosis in human cervical carcinoma cells through inhibition of the NF-kappaB and PI3K/Akt signaling pathways. *Int. J. Oncol.* 39: 279–285.

182. Zhao, F., H. Wang, P. Kunda, X. Chen, Q. Liu, and T. Liu. 2013. Artesunate exerts specific cytotoxicity in retinoblastoma cells via CD71. *Oncol. Rep.* 30: 1473–1482.

183. Holien, T., O. E. Olsen, K. Misund, H. Hella, A. Waage, T. Baade, A. Sundan, and M. Medicine. 2013. Lymphoma and myeloma cells are highly sensitive to growth arrest and apoptosis induced by artesunate. *Eur. J. Haematol.* 91: 339–346.

184. Berger, T. G., D. Dieckmann, T. Efferth, E. S. Schultz, J. Funk, A. Baur, and G. Schuler. 2005. Artesunate in the treatment of metastatic uveal melanoma - first experiences. *Oncol. Rep.* 14: 1599–1603.

185. Jiao, Y., C. M. Ge, Q. H. Meng, J. P. Cao, J. Tong, and S. J. Fan. 2007. Dihydroartemisinin is an inhibitor of ovarian cancer cell growth. *Acta Pharmacol. Sin.* 28: 1045–1056.

186. Singh, N. P., and H. Lai. 2001. Selective toxicity of dihydroartemisinin and holotransferrin toward human breast cancer cells. *Life Sci.* 70: 49–56.

187. Xu, Q., Z. X. Li, H. Q. Peng, Z. W. Sun, R. L. Cheng, Z. M. Ye, and W. X. Li. 2011. Artesunate inhibits growth and induces apoptosis in human osteosarcoma HOS cell line in vitro and in vivo. *J. Zhejiang Univ.* 12: 247–255.

188. Han, P., Y. Luan, Y. Liu, Z. Yu, J. Li, Z. Sun, G. Chen, and B. Cui. 2013. Small interfering RNA targeting Rac1 sensitizes colon cancer to dihydroartemisinin-induced cell cycle arrest and inhibited cell migration by suppressing NFκB activity. *Mol. Cell. Biochem.* 379: 171–80.

189. Liu, W. M., A. M. Gravett, and A. G. Dalgleish. 2011. The antimalarial agent artesunate possesses anticancer properties that can be enhanced by combination strategies. *Int. J. cancer* 128: 1471–1480.

190. Wu, B., K. Hu, S. Li, J. Zhu, L. Gu, H. Shen, B. D. Hambly, S. Bao, and W. Di. 2012. Dihydroartiminisin inhibits the growth and metastasis of epithelial ovarian cancer. *Oncol. Rep.* 27: 101–108.

191. Mao, H., H. Gu, X. Qu, J. Sun, B. Song, W. Gao, J. Liu, and Q. Shao. 2013. Involvement of the mitochondrial pathway and Bim/Bcl-2 balance in dihydroartemisinin-induced apoptosis in human breast cancer in vitro. *Int. J. Mol. Med.* 31: 213–8.

192. Chen, H., B. Sun, S. Pan, H. Jiang, and X. Sun. 2009. Dihydroartemisinin inhibits growth of pancreatic cancer cells in vitro and in vivo. *Anticancer. Drugs* 20: 131–40.

193. Efferth, T., A. Sauerbrey, A. Olbrich, E. Gebhart, P. Rauch, H. O. Weber, J. G. Hengstler, M. E. Halatsch, M. Volm, K. D. Tew, D. D. Ross, and J. O. Funk. 2003. Molecular modes of action of artesunate in tumor cell lines. *Mol. Pharmacol.* 64: 382–394.

194. Li, L. N., H. D. Zhang, S. J. Yuan, Z. Y. Tian, L. Wang, and Z. X. Sun. 2007. Artesunate attenuates the growth of human colorectal carcinoma and inhibits hyperactive Wnt/beta-catenin pathway. *Int. J. cancer* 121: 1360–1365.

195. Zhou, H. J., Z. Wang, and A. Li. 2008. Dihydroartemisinin induces apoptosis in human leukemia cells HL60 via downregulation of transferrin receptor expression. *Anticancer. Drugs* 19: 247–55.

196. Zhou, C., W. Pan, X. P. Wang, and T. S. Chen. 2012. Artesunate induces apoptosis via a Bak-mediated caspase-independent intrinsic pathway in human lung adenocarcinoma cells. *J. Cell. Physiol.* 227: 3778–3786.

197. Nam, W., J. Tak, J. K. Ryu, M. Jung, J. I. Yook, H. J. Kim, and I. H. Cha. 2007. Effects of artemisinin and its derivatives on growth inhibition and apoptosis of oral cancer cells. *Head Neck* 29: 335–340.

198. Chen, T., M. Chen, and J. Chen. 2013. Ionizing radiation potentiates dihydroartemisinin-induced apoptosis of A549 cells via a caspase-8-dependent pathway. *PLoS One* 8: e59827.

199. Ji, Y., Y. C. Zhang, L.-B. Pei, L. L. Shi, J. L. Yan, and X.-H. Ma. 2011. Anti-tumor effects of dihydroartemisinin on human osteosarcoma. *Mol. Cell. Biochem.* 351: 99–108.

200. Handrick, R., T. Ontikatze, K.-D. Bauer, F. Freier, A. Rübel, J. Dürig, C. Belka, and V. Jendrossek. 2010. Dihydroartemisinin induces apoptosis by a Bak-dependent intrinsic pathway. *Mol. Cancer Ther.* 9: 2497–510.

201. Chen, H., H. Zhou, and X. Fang. 2003. Inhibition of human cancer cell line growth and human umbilical vein endothelial cell angiogenesis by artemisinin derivatives in vitro. *Pharmacol. Res.* 48: 231–236.

202. Zhou, H. J., W. Q. Wang, G. D. Wu, J. Lee, and A. Li. 2007. Artesunate inhibits angiogenesis and downregulates vascular endothelial growth factor expression in chronic myeloid leukemia K562 cells. *Vascul. Pharmacol.* 47: 131–138.

203. Chen, H., L. Shi, X. Yang, S. Li, X. Guo, and L. Pan. 2010. Artesunate inhibiting angiogenesis induced by human myeloma RPMI8226 cells. *Int. J. Hematol.* 92: 587–597.

204. Huan-huan, C., Y. Li-li, and L. Shang-bin. 2004. Artesunate reduces chicken chorioallantoic membrane neovascularisation and exhibits antiangiogenic and apoptotic activity on human microvascular dermal endothelial cell. *Cancer Lett.* 211: 163–173.

205. Rasheed, S. A., T. Efferth, I. A. Asangani, and H. Allgayer. 2010. First evidence that the antimalarial drug artesunate inhibits invasion and in vivo metastasis in lung cancer by targeting essential extracellular proteases. *Int. J. Cancer* 127: 1475–1485.

206. Bachmeier, B., I. Fichtner, P. H. Killian, E. Kronski, U. Pfeffer, and T. Efferth. 2011. Development of resistance towards artesunate in MDA-MB-231 human breast cancer cells. *PLoS One* 6: e20550.

207. Rutteman, G. R., S. A. Erich, J. A. Mol, B. Spee, G. Grinwis, L. Fleckenstein, C. A. London, and T. Efferth. 2013. Safety and efficacy field study of artesunate for dogs with non-resectable tumours. *Anticancer Res.* 33: 1819–1828.

208. Singh, N., and K. Verma. 2002. Case report of a laryngeal squamous cell carcinoma treated with artesunate. *Arch. Oncol.* 10: 279–280.

209. Jansen, F. H., I. Adoubi, K. C. J C, T. DE Cnodder, N. Jansen, A. Tschulakow, and T. Efferth. 2011. First study of oral Artenimol-R in advanced cervical cancer: clinical benefit, tolerability and tumor markers. *Anticancer Res.* 31: 4417–22.

210. Wu, G. S., J. J. Lu, J. J. Guo, M. Q. Huang, L. Gan, X.-P. Chen, and Y. T. Wang. 2013. Synergistic anti-cancer activity of the combination of dihydroartemisinin and doxorubicin in breast cancer cells. *Pharmacol. Rep.* 65: 453–9.

211. Xie, W., P. Yang, X. Zeng, H. Wang, H. Cai, and J. Cai. 2010. Visual characterization of targeted effect of holo-transferrin-tagged dihydroartemisinin on human breast cancer cells. *Chinese Sci. Bull.* 55: 2390–2395.

212. Torti, S. V, and F. M. Torti. 2013. Iron and cancer: more ore to be mined. *Nat. Rev. Cancer* 13: 342–355.

213. Ohgami, R. S., D. R. Campagna, E. L. Greer, B. Antiochos, A. McDonald, J. Chen, J. J. Sharp, Y. Fujiwara, J. E. Barker, and M. D. Fleming. 2005. Identification of a ferrireductase required for efficient transferrin-dependent iron uptake in erythroid cells. *Nat. Genet.* 37: 1264–1269.

214. Daniels, T. R., T. Delgado, J. A. Rodriguez, G. Helguera, and M. L. Penichet. 2006. The transferrin receptor part I: Biology and targeting with cytotoxic antibodies for the treatment of cancer. *Clin. Immunol.* 121: 144–158.

215. McLean, W. G., and S. A. Ward. 1998. In vitro neurotoxicity of artemisinin derivatives. *Med. Trop. (Mars).* 58: 28–31.

216. Smith, S. L., C. J. Sadler, C. C. Dodd, G. Edwards, S. A. Ward, B. K. Park, and W. G. McLean. 2001. The role of glutathione in the neurotoxicity of artemisinin derivatives in vitro. *Biochem. Pharmacol.* 61: 409–416.

217. Kissinger, E., T. T. Hien, N. T. Hung, N. D. Nam, N. L. Tuyen, B. V Dinh, C. Mann, N. H. Phu, P. P. Loc, J. a Simpson, N. J. White, and J. J. Farrar. 2000. Clinical and neurophysiological study of the effects of multiple doses of artemisinin on brain-stem function in Vietnamese patients. *Am. J. Trop. Med. Hyg.* 63: 48–55.

218. Efferth, T., and B. Kaina. 2010. Toxicity of the antimalarial artemisinin and its dervatives. *Crit. Rev. Toxicol.* 40: 405–21.

219. Clark, R. L., A. Arima, N. Makori, Y. Nakata, F. Bernard, W. Gristwood, A. Harrell, T. E. K. White, and P. J. Wier. 2008. Artesunate: developmental toxicity and toxicokinetics in monkeys. *Birth Defects Res. B. Dev. Reprod. Toxicol.* 83: 418–34.

220. Clark, R. L., T. E. K. White, S. A Clode, I. Gaunt, P. Winstanley, and S. A. Ward. 2004. Developmental toxicity of artesunate and an artesunate combination in the rat and rabbit. *Birth Defects Res. B. Dev. Reprod. Toxicol.* 71: 380–94.

221. White, T. E. K., P. B. Bushdid, S. Ritter, S. B. Laffan, and R. L. Clark. 2006. Artesunate-induced depletion of embryonic erythroblasts precedes embryolethality and teratogenicity in vivo. *Birth Defects Res. B. Dev. Reprod. Toxicol.* 77: 413–29.

222. Mosmann, T. 1983. Rapid colorometric assay for cellular growth and survival: application to proliferation and cytotoxic assays. *J Immunol Meth.* 65: 55–63.

223. Vellonen, K.-S., P. Honkakoski, and A. Urtti. 2004. Substrates and inhibitors of efflux proteins interfere with the MTT assay in cells and may lead to underestimation of drug toxicity. *Eur. J. Pharm. Sci.* 23: 181–8.

224. Franken, N. a P., H. M. Rodermond, J. Stap, J. Haveman, and C. van Bree. 2006. Clonogenic assay of cells in vitro. *Nat. Protoc.* 1: 2315–9.

225. Petitjean, A., E. Mathe, S. Kato, C. Ishioka, S. V. Tavtigian, P. Hainaut, and M. Olivier. 2007. Impact of mutant p53 functional properties on TP53 mutation patterns and tumor phenotype: lessons from recent developments in the IARC TP53 database. *Hum Mutat.* 28: 622–9.

226. Provencher, D. M., H. Lounis, L. Champoux, M. Tetrault, E. N. Manderson, J. C. Wang, P. Eydoux, R. Savoie, P. N. Tonin, and A. M. Mes-Masson. 2000. Characterization of four novel epithelial ovarian cancer cell lines. *Vitr. Cell. Dev. Biol.* 36: 357–361.

227. Hamilton, T. C., R. C. Young, W. M. Mckoy, K. R. Grotzinger, J. A. Green, E. W. Chu, J. Whang-peng, A. M. Rogan, W. R. Green, and R. F. Ozols. 1983. Characterization

of a human ovarian carcinoma cell line (NIH : OVCAR-3) with androgen and estrogen Receptors with androgen and estrogen receptors. *Cancer Res.* 43: 5379–5389.

228. Shaw, T. J., M. K. Senterman, K. Dawson, C. A. Crane, and B. C. Vanderhyden. 2004. Characterization of intraperitoneal, orthotopic, and metastatic xenograft models of human ovarian cancer. *Mol. Ther.* 10: 1032–1042.

229. Fogh, J. 1975. *Human tumor cells in vitro*,. Plenum Press, New York.

230. Buick, R. N., R. Pullano, J. M. Trent, and R. Rullano. 1985. Comparative Properties of Five Human Ovarian Adenocarcinoma Cell Lines. 3668–3676.

231. Bénard, J., J. Da Silva, M. De Blois, J. Bã, P. Boyer, P. Duvillard, E. Chiric, and G. Riou. 1985. Characterization of a Human Ovarian Adenocarcinoma Line , IGROV1 , in Tissue Culture and in Nude Mice. *Cancer Res.* 45: 4970–4979.

232. Vanlangenakker, N., T. Vanden Berghe, and P. Vandenabeele. 2012. Many stimuli pull the necrotic trigger, an overview. *Cell Death Differ.* 19: 75–86.

233. Halliwell, B. 2001. Free radicals and other reactive species in disease. *Encycl. life Sci.* 1–7.

234. Chaijaroenkul, W., V. Viyanant, W. Mahavorasirikul, and K. Na-Bangchang. 2011. Cytotoxic activity of artemisinin derivatives against cholangiocarcinoma (CL-6) and hepatocarcinoma (Hep-G2) cell lines. *Asian Pac. J. Cancer Prev.* 12: 55–59.

235. Orth, K., J. Hung, a Gazdar, a Bowcock, J. M. Mathis, and J. Sambrook. 1994. Genetic instability in human ovarian cancer cell lines. *Proc. Natl. Acad. Sci. U. S. A.* 91: 9495–9.

236. Chen, T., M. Li, R. Zhang, and H. Wang. 2009. Dihydroartemisinin induces apoptosis and sensitizes human ovarian cancer cells to carboplatin therapy. *J. Cell. Mol. Med.* 13: 1358–1370.

237. Naora, H., and D. J. Montell. 2005. Ovarian cancer metastasis: integrating insights from disparate model organisms. *Nat. Rev. Cancer* 5: 355–66.

238. Shield, K., M. L. Ackland, N. Ahmed, and G. E. Rice. 2009. Multicellular spheroids in ovarian cancer metastases: Biology and pathology. *Gynecol. Oncol.* 113: 143–8.

239. Kenny, P., G. Lee, C. Myers, and R. Neve. 2007. The morphologies of breast cancer cell lines in three-dimensional assays correlate with their profiles of gene expression. *Mol. Oncol.* 1: 84–96.

240. Smart, C. E., B. J. Morrison, J. M. Saunus, A. C. Vargas, P. Keith, L. Reid, L. Wockner, M. A. Amiri, D. Sarkar, P. T. Simpson, C. Clarke, C. W. Schmidt, B. a

Reynolds, S. R. Lakhani, and J. A. Lopez. 2013. In vitro analysis of breast cancer cell line tumourspheres and primary human breast epithelia mammospheres demonstrates inter- and intrasphere heterogeneity. *PLoS One* 8: e64388.

241. Mayer, B., G. Klement, M. Kaneko, S. Man, S. Jothy, J. Rak, and R. S. Kerbel. 2001. Multicellular gastric cancer spheroids recapitulate growth pattern and differentiation phenotype of human gastric carcinomas. *Gastroenterology* 121: 839–52.

242. Makhija, S., D. D. Taylor, R. K. Gibb, and C. Gerçel-Taylor. 1999. Taxol-induced bcl-2 phosphorylation in ovarian cancer cell monolayer and spheroids. *Int. J. Oncol.* 14: 515–21.

243. Desoize, B., and J. Jardillier. 2000. Multicellular resistance: a paradigm for clinical resistance? *Crit. Rev. Oncol. Hematol.* 36: 193–207.

244. Frankel, A., R. Buckman, and R. S. Kerbel. 1997. Abrogation of taxol-induced G 2 - M arrest and apoptosis in human ovarian cancer cells grown as multicellular tumor spheroids abrogation of taxol-induced G2- M arrest and apoptosis in human ovarian cancer cells grown as multicellular tumor spheroids. *Cancer Res.* 57: 2388–2393.

245. Zhou, X., W. Sun, W. Wang, K. Chen, J. Zheng, M.-D. Lu, P.-H. Li, and Z. Zheng. 2013. Artesunate inhibits the growth of gastric cancer cells through the mechanism of promoting oncosis both in vitro and in vivo. *Anticancer. Drugs* 24: 920–7.

246. Li, S., F. Xue, Z. Cheng, X. Yang, S. Wang, F. Geng, and L. Pan. 2009. Effect of artesunate on inhibiting proliferation and inducing apoptosis of SP2/0 myeloma cells through affecting NFkappaB p65. *Int. J. Hematol.* 90: 513–521.

247. Liu, J., A. Opipari, L. Tan, Y. Jiang, and Y. Zhang. 2002. Dysfunctional apoptosome activation in ovarian cancer: implications for chemoresistance. *Cancer Res.* 62: 924–931.

248. Gao, N., A. Budhraja, S. Cheng, E.-H. Liu, C. Huang, J. Chen, Z. Yang, D. Chen, Z. Zhang, and X. Shi. 2011. Interruption of the MEK/ERK signaling cascade promotes dihydroartemisinin-induced apoptosis in vitro and in vivo. *Apoptosis* 16: 511–23.

249. Du, X.-X., Y.-J. Li, C.-L. Wu, J.-H. Zhou, Y. Han, H. Sui, X.-L. Wei, L. Liu, P. Huang, H.-H. Yuan, T.-T. Zhang, W.-J. Zhang, R. Xie, X.-H. Lang, D.-X. Jia, and Y.-X. Bai. 2013. Initiation of apoptosis, cell cycle arrest and autophagy of esophageal cancer cells by dihydroartemisinin. *Biomed. Pharmacother.* 67: 417–24.

250. Foulkes, W., I. Smith, and J. S. Reis-filho. 2010. Triple-negative breast cancer. *N. Engl. J. Med.* 363: 1938–1948.

251. Li, P. C. H., E. Lam, W. P. Roos, M. Z. M. Z. Zdzienicka, B. Kaina, and T. Efferth. 2008. Artesunate derived from traditional Chinese medicine induces DNA damage and repair. *Cancer Res.* 68: 4347–4351.

252. Prat, J., A. Ribé, and A. Gallardo. 2005. Hereditary ovarian cancer. *Hum. Pathol.* 36: 861–870.

253. Mercer, A. E., I. M. Copple, J. L. Maggs, P. M. O'Neill, and B. K. Park. 2011. The role of heme and the mitochondrion in the chemical and molecular mechanisms of mammalian cell death induced by the artemisinin antimalarials. *J. Biol. Chem.* 286: 987–996.

254. Efferth, T., A. Benakis, M. R. Romero, M. Tomicic, R. Rauh, D. Steinbach, R. Hafer, T. Stamminger, F. Oesch, B. Kaina, and M. Marschall. 2004. Enhancement of cytotoxicity of artemisinins toward cancer cells by ferrous iron. *Free Radic. Biol. Med.* 37: 998–1009.

255. Bhat, T., and R. Singh. 2008. Tumor angiogenesis--a potential target in cancer chemoprevention. *Food Chem. Toxicol.* 46: 1334–1345.

256. Bystrom, L. M., M. L. Guzman, and S. Rivella. 2013. Iron and reactive oxygen species: friends or foes of cancer cells? *Antioxid. Redox Signal.* in press.

257. Efferth, T., M. Briehl, and M. Tome. 2003. Role of antioxidant genes for the activity of artesunate against tumor cells. *Int. J. Oncol.* 23: 1231–1235.

258. Efferth, T., and M. Volm. 2005. Glutathione-related enzymes contribute to resistance of tumor cells and low toxicity in normal organs to artesunate. *In Vivo (Brooklyn).* 232: 225–232.

259. Janis, M. 2012. Iron deficiency anemia in cancer patients. *Oncol. Hematol. Rev.* 8: 74–80.

260. Vaupel, P., and A. Mayer. 2007. Hypoxia in cancer: significance and impact on clinical outcome. *Cancer Metastasis Rev.* 26: 225–239.

261. Rohwer, N., and T. Cramer. 2011. Hypoxia-mediated drug resistance: novel insights on the functional interaction of HIFs and cell death pathways. *Drug Resist. Updat.* 14: 191–201.

262. Karlenius, T. C., F. Shah, G. Di, F. M. Clarke, and K. F. Tonissen. 2012. Biochemical and Biophysical Research Communications Cycling hypoxia up-regulates thioredoxin levels in human MDA-MB-231 breast cancer cells. *Biochem. Biophys. Res. Commun.* 419: 350–355.

263. Huang, X. J., Z. Q. Ma, W. P. Zhang, Y. B. Lu, and E. Q. Wei. 2007. Dihydroartemisinin exerts cytotoxic effects and inhibits hypoxia inducible factor-1alpha activation in C6 glioma cells. *J. Pharm. Pharmacol.* 59: 849–856.

264. Högemann-Savellano, D., E. Bos, C. Blondet, F. Sato, T. Abe, L. Josephson, R. Weissleder, J. Gaudet, D. Sgroi, P. J. Peters, and J. P. Basilion. The transferrin receptor: a potential molecular imaging marker for human cancer. *Neoplasia* 5: 495–506.

265. Lu, J. J., S. M. Chen, X. W. Zhang, J. Ding, and L. H. Meng. 2011. The anti-cancer activity of dihydroartemisinin is associated with induction of iron-dependent endoplasmic reticulum stress in colorectal carcinoma HCT116 cells. *Invest. New Drugs* 29: 1276–83.

266. Fernández, P. L., P. Jares, M. J. Rey, E. Campo, and A. Cardesa. 1998. Cell cycle regulators and their abnormalities in breast cancer. *Mol. Pathol.* 51: 305–309.

267. Pietiläinen, T., P. Lipponen, S. Aaltomaa, M. Eskelinen, V. M. Kosma, and K. Syrjänen. 1995. Expression of retinoblastoma gene protein (Rb) in breast cancer as related to established prognostic factors and survival. *Eur. J. Cancer* 31A: 329–33.

268. Le, N. T. V, and D. R. Richardson. 2002. The role of iron in cell cycle progression and the proliferation of neoplastic cells. *Biochim. Biophys. Acta* 1603: 31–46.

269. Somers-Edgar, T. J., M. J. Scandlyn, E. C. Stuart, M. J. Le Nedelec, S. P. Valentine, and R. J. Rosengren. 2008. The combination of epigallocatechin gallate and curcumin suppresses ER alpha-breast cancer cell growth in vitro and in vivo. *Int. J. Cancer* 122: 1966–1971.

270. Kulp, K. S., S. L. Green, and P. R. Vulliet. 1996. Iron deprivation inhibits cyclin-dependent kinase activity and decreases cyclin D/CDK4 protein levels in asynchronous MDA-MB-453 human breast cancer cells. *Exp. Cell Res.* 229: 60–8.

271. Fu, D., and D. R. Richardson. 2007. Iron chelation and regulation of the cell cycle: 2 mechanisms of posttranscriptional regulation of the universal cyclin-dependent kinase inhibitor p21CIP1/WAF1 by iron depletion. *Blood* 110: 752–761.

272. Tin, A. S., S. N. Sundar, K. Q. Tran, A. H. Park, K. M. Poindexter, and G. L. Firestone. 2012. Antiproliferative effects of artemisinin on human breast cancer cells requires the downregulated expression of the E2F1 transcription factor and loss of E2F1-target cell cycle genes. *Anticancer. Drugs* 23: 370–379.

273. Reimer, D., S. Sadr, A. Wiedemair, G. Goebel, N. Concin, G. Hofstetter, C. Marth, and A. G. Zeimet. 2006. Expression of the E2F family of transcription factors and its clinical relevance in ovarian cancer. *Ann. N. Y. Acad. Sci.* 1091: 270–281.

274. Zhang, S. Y., S. C. Liu, L. F. Al-saleem, and A. J. P. Klein-szanto. 2000. E2F-1 : a proliferative marker of breast neoplasia. *Cancer Epidemiol. biomarkers Prev.* 9: 395–401.

275. Pawlik, T. M., and K. Keyomarsi. 2004. Role of cell cycle in mediating sensitivity to radiotherapy. *Int. J. Radiat. Oncol. Biol. Phys.* 59: 928–42.

276. Reichert, S., V. Reinboldt, S. Hehlgans, T. Efferth, C. Rodel, and F. Rodel. 2012. A radiosensitizing effect of artesunate in glioblastoma cells is associated with a diminished expression of the inhibitor of apoptosis protein survivin. *Radiother. Oncol.* 103: 394–401.

277. Luo, J., X. Chen, G. Chen, X. Zhou, X. Lu, Y. Ling, S. Zhang, W. Zhu, and J. Cao. 2013. Dihydroartemisinin induces radiosensitivity in cervical cancer cells by modulating cell cycle progression. *Saudi Med. J.* 34: 254–260.

278. Garg, A. K., T. A. Buchholz, and B. B. Aggarwal. 2005. Chemosensitization and radiosensitization of tumors by plant polyphenols. *Antioxid. Redox Signal.* 7: 1630–1647.

279. Chou, T. 2010. Drug combination studies and their synergy quantification using the Chou-Talalay method. *Cancer Res.* 70: 440–446.

280. Riganti, C., S. Doublier, D. Viarisio, E. Miraglia, G. Pescarmona, D. Ghigo, and A. Bosia. 2009. Artemisinin induces doxorubicin resistance in human colon cancer cells via calcium-dependent activation of HIF-1alpha and P-glycoprotein overexpression. *Br. J. Pharmacol.* 156: 1054–66.

281. Zhou, H., J. Zhang, A. Li, Z. Wang, and X. Lou. 2010. Dihydroartemisinin improves the efficiency of chemotherapeutics in lung carcinomas in vivo and inhibits murine Lewis lung carcinoma cell line growth in vitro. *Cancer Chemother. Pharmacol.* 66: 21–9.

282. Michaelis, M., M. C. Kleinschmidt, S. Barth, F. Rothweiler, J. Geiler, R. Breitling, B. Mayer, H. Deubzer, O. Witt, J. Kreuter, H. W. Doerr, J. Cinatl, and J. Cinatl Jr. 2010. Anti-cancer effects of artesunate in a panel of chemoresistant neuroblastoma cell lines. *Biochem. Pharmacol.* 79: 130–136.

283. Salama, R., M. Sadaie, M. Hoare, and M. Narita. 2014. Cellular senescence and its effector programs. *Genes Dev.* 28: 99–114.

284. Puiffe, M.-L., C. Le Page, A. Filali-Mouhim, M. Zietarska, V. Ouellet, P. N. Tonin, M. Chevrette, D. M. Provencher, and A.-M. Mes-Masson. 2007. Characterization of ovarian cancer ascites on cell invasion, proliferation, spheroid formation, and gene Expression in an in vitro model of epithelial ovarian cancer. *Neoplasia* 9: 820–829.

285. Kunz-Schughart, L. A. 1999. Multicellular tumor spheroids: intermediates between monolayer culture and in vivo tumor. *Cell Biol. Int.* 23: 157–61.

286. Sanna, V., G. Pintus, A. Roggio, S. Punzoni, A. Posadino, A. Arca, S. Marceddu, P. Bandiera, S. Uzzau, and M. Sechi. 2011. Targeted biocompatible nanoparticles for the delivery of (-)-epigallocatechin 3-gallate to prostate cancer cells. *J. Med. Chem.* 54: 1321–1332.

287. Zhang, Y. J., B. Gallis, M. Taya, S. Wang, R. J. Y. Ho, and T. Sasaki. 2013. pH-responsive artemisinin derivatives and lipid nanoparticle formulations inhibit growth of breast cancer cells in vitro and induce down-regulation of HER family members. *PLoS One* 8: e59086.

288. Gong, Y., B. M. Gallis, D. R. Goodlett, Y. Yang, H. Lu, E. Lacoste, H. Lai, and T. Sasaki. 2013. Effects of transferrin conjugates of artemisinin and artemisinin dimer on breast cancer cell lines. *Anticancer Res.* 33: 123–32.

289. Stockwin, L. H., B. Han, S. X. Yu, M. G. Hollingshead, M. a ElSohly, W. Gul, D. Slade, A. M. Galal, D. L. Newton, and M. a Bumke. 2009. Artemisinin dimer anticancer activity correlates with heme-catalyzed reactive oxygen species generation and endoplasmic reticulum stress induction. *Int. J. cancer* 125: 1266–75.

290. Corkery, D. P., G. Dellaire, and J. N. Berman. 2011. Leukaemia xenotransplantation in zebrafish--chemotherapy response assay in vivo. *Br. J. Haematol.* 153: 786–9.

291. Roby, K. F., C. C. Taylor, J. P. Sweetwood, Y. Cheng, J. L. Pace, O. Tawfik, D. L. Persons, P. G. Smith, and P. F. Terranova. 2000. Development of a syngeneic mouse model for events related to ovarian cancer. *Carcinogenesis* 21: 585–591.

Appendix 1 Confirmation of TX400 MCF-7 Paclitaxel-resistance.